Université de Montréal

Nouveaux complexes pinces POCOP, NHCCOP, PIMCOP et PIMIOCOP, et complexes cyclométallés de Ni^{II} : Synthèse, Caractérisation et Réactivité.

par : Boris Vabre

Département de chimie

Faculté des arts et des sciences

Thèse présentée à la Faculté des études supérieures et postdoctorales en vue de l'obtention du grade de Philosophiæ Doctor (Ph.D.) en chimie.

Juillet 2014

Résumé

Cette thèse traite de la chimie des complexes pinces de Ni(II) ainsi que des complexes cyclométallés de Ni(II) comportant au moins un motif phosphinite. Elle se divise en trois parties. La première concerne la synthèse, la caractérisation, le mécanisme de formation et la réactivité des complexes pinces de Ni(II) à base de ligand de type POCOP 1,3-(i-$Pr_2PO)_2C_6H_4$. De nouveaux ligands de type R-(POCOP) = $\kappa^P,\kappa^C,\kappa^P$-{$R_n$-2,6-($R'_2PO)_2C_6H_{4-n}$}; R_n = 4-OMe, 4-Me, 4-CO_2Me, 3-OMe, 3-CO_2Me, 3,5-t-Bu_2 ; R' = i-Pr, t-Bu ont été synthétisés suite à l'addition de chlorophosphine $ClPR'_2$ à une solution de résorcinol ou dérivés en présence de base. La synthèse des complexes R-(POCOP)Ni(Br) s'effectue à partir du ligand correspondant en présence de base, et de $\{NiBr_2(NC^iPr)\}_n$. Ce nouveau précurseur de nickel est synthétisé à partir de brome de nickel métallique dans l'isobutyronitrile. Il est stable sous atmosphère inerte et sa solubilité dans les solvants polaires permet d'étudier les synthèses des complexes en milieu homogène. Le mécanisme de formation des complexes portant des ligand pinces ($PC_{sp3}P$) 1,3-(i-$Pr_2PCH_2CH_2)_2CH_2$, ($POC_{sp3}OP$) 1,3-(i-$Pr_2POCH_2)_2CH_2$, ($PC_{sp2}P$) 1,3-(i-$Pr_2PCH_2)_2C_6H_4$, R_n-($POC_{sp2}OP$) 1,3-(i-$Pr_2PO)_2C_6H_{4-n}$ via nickellation du lien C-H a été investigué avec une méthode de réaction de compétition. Cette étape a été déterminée comme étant de nature électrophile. Les complexes résultants ont été complètement caractérisés. Une corrélation a notamment été effectuée entre le déplacement chimique du C_{ipso} en spectroscopie RMN ^{13}C et le potentiel d'oxydation E_{ox} en voltamétrie cyclique. Une nouvelle méthode de synthèse directe verte "one pot" a été mise en place. En faisant réagir à 75 °C un mélange hétérogène de

résorcinol, de chlorodiisopropylphosphine et de nickel métallique en poudre, on obtient le complexes pince (POCOP)Ni(Cl) avec des rendements allant jusqu'à 93%. La réactivité de ces complexes POCOP a été investiguée pour des réactions de fluorination et trifluorométhylation des halogénures d'alkyle. La synthèse du (POCOP)Ni(F) a lieu à partir de précurseur (POCOP)Ni(X) (X=Br, Cl), en présence d'un large excès de fluorure d'argent AgF. Ce complexe catalyse la fluorination du bromure de benzyle et peut être converti en (POCOP)Ni(CF_3) en présence de réactif du Ruppert, Me_3SiCF_3. La réaction entre (POCOP)Ni(CF_3) et le bromure de benzyle dans les solvants aromatiques mène à la conversion totale du complexe en (POCOP)Ni(Br) et à l'inattendue benzylation du solvant aromatique utilisé.

La seconde partie concerne la synthèse des nouveaux complexes non symétriques à base de ligands comportant un motif imidazolo-phosphine (PIMCOP) 3-[2-(R_2P)-$C_3H_2N_2$]-(R_2PO)-C_6H_3, imidazoliophosphine (PIMIOCOP) 3-[2-(R_2P)-3-(CH_3)-$C_3H_2N_2$]-(R_2PO)-C_6H_3] et carbène N-hétérocyclique (NHCCOP). La double déprotonation du 3-hydroxyphenyl-imidazole suivi de l'addition de deux équivalents de chlorodiphenylphosphine mène à l'obtention du ligand PIMCOP 3-[3-(CH_3)-$C_3H_2N_2$]-(R_2PO)-C_6H_3. L'étape de nickellation a lieu comme dans le cas des composés (POCOP)Ni. La méthylation du motif imidazole du (PIMCOP)Ni(Br) par le triflate de méthyle MeOTf, donne le dérivé (PIMIOCOP)Ni(Br). Ce dernier est converti en (NHCCOP)Ni(Br) après l'addition de chlorure de tétraéthylamonium NEt_4Cl. Les analogues *i*-Pr_2P de ces complexes sont synthétisés en remplaçant $ClPPh_2$ par $ClPiPr_2$. On obtient les espèces cationiques [(PIMCOP)Ni($NCCH_3$)][OTf], [(PIMIOCOP)Ni($NCCH_3$)][OTf]$_2$ et

[(NHCCOP)Ni($NCCH_3$)][OTf] suite à l'addition en solution dans l'acétonitrile de triflate d'argent AgOTf. Ces espèces ont été utilisés comme catalyseurs pour la synthèse d'amidine à partir de benzonitrile et de diverse amines aliphatiques.

Enfin des complexes orthonickellés *trans*-Ni[(κ^2-*P*,*C*-P(OC_6H_4)-(^{i}Pr_2)(^{i}Pr_2P(OC_6H_5))]Br à base de phosphinite ont été synthétisés et caractérisés. Les ligands sont synthétisés par réaction d'un phénol et de chlorodiisopropylphosphine en présence de base. L'ajout de {$NiBr_2$(NC^iPr)}$_n$ et de triéthylamine permet l'orthométallation via une étape de nickellation C-H. Un intermédiaire *trans*-[$NiBr_2${P^iPr_2(OC_6H_5)}$_2$] de cette réaction a été isolé. Le complexe dimère peut réagir avec des espèces électrophiles mener à l'ortho-fonctionnalisation de la phosphinite.

Mots-clés: nickel (II), complexes pinces, complexes de type POCOP, complexes de type PIMCOP, complexes de type PIMIOCOP, complexes de type NHCCOP, nickellation C-H, fluorination, trifluoromethylation, cyclométallation, synthèse des amidines, fonctionnalisation C-H.

Abstract

This thesis describes the chemistry of Ni (II) pincer and cyclonickelated complexes bearing at least one phosphinite moiety. The content is divided into three parts. A first study concerns the synthesis, the characterization, the mechanism of formation and the reactivity of nickel complexes bearing a ligand POCOP (1,3-(*i*-$Pr_2PO)_2C_6H_4$). New ligands R-(POCOP) = $\kappa^P,\kappa^C,\kappa^P$-{$R_n$-2,6-($R'_2PO)_2C_6H_{3-n}$}; R_n = 4-OMe, 4-Me, 4-CO_2Me, 3-OMe, 3-CO_2Me, 3,5-*t*-Bu_2 ; R' = *i*-Pr, *t*-Bu have been synthesized by addition of chlorophosphine in presence of base in a resorcinol or derivatives solution. The synthesis of R-(POCOP)Ni(Br) complexes occurred by reacting the corresponding ligand in presence of base and$\{NiBr_2(NC^iPr)\}_n$. This new nickel precursor is synthesized in isobutyronitrile with bromine and metallic nickel powder. It is stable under inert atmosphere and its solubility in polar solvents allowed the study of those complexes in homogenous solution. Mechanism of formation of complexes bearing pincer ligands ($PC_{sp3}P$) 1,3-(*i*-$Pr_2PCH_2CH_2)_2CH_2$, ($POC_{sp3}OP$) 1,3-(*i*-$Pr_2POCH_2)_2CH_2$, ($PC_{sp2}P$) 1,3-(*i*-$Pr_2PCH_2)_2C_6H_4$, R_n-($POC_{sp2}OP$) 1,3-(*i*-$Pr_2PO)_2C_6H_{4-n}$ via C-H nickelation has been investigated by a method of competition reactions. The nickelation step was determined to be electrophilic. New {R_n-2,6-($R'_2PO)_2C_6H_{4-n}$} ligands and corresponding nickel bromine complexes were characterized including linear correlation between ^{13}C NMR chemical shift of ipso carbon (δC_{ipso}) and oxidation potential E_{ox}. A new greener methodology for the one pot synthesis of (POCOP)Ni(Cl) from metallic nickel has been developed. Reacting at 75 °C at mixture of resorcinol, chlorodiisopropylphosphine and nickel power gives ($POC_{sp2}OP$)Ni(Cl) up to 93 %. Reactivity of this complex has been investigated for

fluorination and trifluoromethylation of benzyl halides. Synthesis of (POCOP)Ni(F) occurred starting from (POCOP)Ni(X) (X=Br, Cl) with excess of silver fluoride AgF. This complex catalyzes the fluorination of benzyl bromide and can be converted into (POCOP)Ni(CF_3) using Ruppert reagent Me_3SiCF_3. Reaction of (POCOP)Ni(CF_3) with benzyl bromide leads to its complete conversion into (POCOP)Ni(Br) and to the unexpected benzylation of the used aromatic solvent.

The second part concerns the synthesis of new unsymmetrical complexes bearing imidazolo-phosphine moiety (PIMCOP) 3-[2-(R_2P)-$C_3H_2N_2$]-(R_2PO)-C_6H_3, imidazoliophosphine (PIMIOCOP) 3-[2-(R_2P)-3-(CH_3)-$C_3H_2N_2$]-(R_2PO)-C_6H_3] and N-heterocyclique carbene (NHCCOP). (PIMCOP) ligands were synthesized by double deprotonation of 3-hydroxyphenyl-imidazole followed by addition of two equivalents of chlorodiphenylphosphine. Nickelation occured in a similar route as (POCOP)Ni. Methylation of the imidazole moiety of (PIMCOP)Ni(Br) using MeOTf leads the (PIMIOCOP)Ni(Br) complex. The latter can be converted into (NHCCOP)Ni(Br) after addition of tetraethylamonium chloride NEt_4Cl. Analogs P^iPr_2 of those complexes are synthesized replacing $ClPPh_2$ by ClP^iPr_2. Cationic species [(PIMCOP)Ni($NCCH_3$)][OTf], [(PIMIOCOP)Ni($NCCH_3$)][OTf]$_2$ et [(NHCCOP)Ni($NCCH_3$)][OTf] are obtained reacting their bromo homologue complexes with silver triflate in acetonitrile. Those species are used to catalyze amidine synthesis from benzonitrile with various aliphatic amines.

Finally orthonickellated complexes *trans*-Ni[(κ^2-*P*,*C*-P(OC_6H_4)-($^iPr_2$)($^iPr_2P(OC_6H_5)$)]Br, and dimeric specie {Ni(μ-Br){κ^2-*P*,*C*-$P^iPr_2(OC_6H_4)$}}$_2$ have been synthesized and characterized. Phosphinite ligand was synthesized reacting phenol

and $ClP^{i}Pr_2$ in presence of base. Nickellation occured heating in solution $\{NiBr_2(NC^{i}Pr)\}_n$ and base. An intermediate *trans*-$[NiBr_2\{P^{i}Pr_2(OC_6H_5)\}_2]$ of this reaction has been isolated. Ortho-functionalization of diisopropyl phosphinite can be achieved by reacting dimeric complex with electrophilic species.

Key-words: nickel (II), pincer complexes, POCOP pincer type complexes, PIMCOP pincer type complexes, PIMIOCOP pincer type complexes, NHCCOP pincer type complexes, C-H niceklation, fluorination, trifluoromethylation, cyclometalation, amidines synthesis, C-H functionalization.

Remerciements

Je tiens à remercier très sincèrement mon directeur de thèse Pr. **Davit Zargarian** qui a véritablement catalysé ma progression. Je tiens à lui exprimer toute ma reconnaissance pour son ouverture d'esprit, sa confiance, son soutien, sa disponibilité ainsi que pour tous les moments partagés à l'université et en congrès.

Merci aussi à mes collègues de laboratoire. Je garderai de bons souvenirs de nos instructives discussions. Je pense notamment aux étudiants post-doctorants Dr. **Denis Spasyuk**, Dr. **Laure Benhamou**, ou encore Dr. **Jingjun Hao**.

Ma formation de cristallographe est du en grande partie à la patience et à la pédagogie de Dr. **Michel Simard**. Il su maîtriser l'art de répéter et a réussi à me transmettre le goût de sa discipline. Pour tout cela je le remercie chaleureusement.

Je voudrais remercier bien entendu les personnes ayant collaborées aux travaux présentés dans cette thèse. Tout d'abord, Pr. **Remi Chauvin** et les membres de son équipe, Dr. **Yves Canac** et Dr. **Christine Lepetit** du LCC (Laboratoire de Chimie de Coordination) à Toulouse (France) où j'ai eu l'opportunité d'effectuer un stage. Le Pr. **Daniel Ess**, **Alban Petit** et **Mélinda Lambert** de Brigham Young University à Provo (États-Unis) pour leur travaux théoriques. **Fabien Lindeperg**, **Richard Declercq**, **Pauline Petiot** et **Félix Deschamps** que j'ai eu l'occasion d'encadrer durant leur stage. Je suis reconnaissant à Dr. **Annie Jutand** qui m'a appris beaucoup sur l'électrochimie lors de mon stage à l'ENS (École Normal Supérieur) à Paris (France).

Merci à **Éléna Nadezhina**, du laboratoire d'analyse élémentaires pour sa disponibilité et son sourire. Merci à **Antoine Hamel** et **Cédric Malveau** de l'équipe RMN.

Merci à Pr. **Frank Schaper** chez qui j'ai fait mes premiers pas en chimie organométallique à l'Université de Montréal. Merci à Pr. **Garry Hanan** et à Pr. **Christian Reber** ainsi qu'à leur groupes de recherche pour les discussions de nos réunions inorganiques.

Merci aux **membres du Jury** Pr. Frank Schaper (président-rapporteur), Pr. Garry Hanan (membre du jury) et Pr. Didier Bourissou (examinateur externe) qui ont accepté et pris le temps d'évaluer ce travail.

Enfin merci à mes sœurs, Cécile, Sophie, Aurélie, Corine et Crystelle ainsi qu'à mes parents. Malgré la distance ils ont toujours été présents à mes cotés.

Table des Matières

Liste des tableaux

Liste des Figures

Liste des Schémas

Liste des Abréviations

Bn	Groupement benzyle, CH_2Ph
br	Large (spectroscopie)
calcd	Calculé
d	Doublet (spectroscopie)
dd	Doublet de doublets (spectroscopie)
dh	Doublet d'heptuplet (spectroscopie)
DCM	Dichlorométhane
Equiv.	Équivalents
GC/MS	Chromatographie en phase gazeuse couplée à la spectroscopie de masse
HMQC	Corrélation Hétéronucléaire quantique simple (spectroscopie)
in situ	Latin, Sur place
i-Pr	Isopropyle
n-Bu	Groupement butyle primaire
vs	Latin, en face de
Mp	Point de fusion
Ph	Groupement Phényle, C_6H_5
$PC_{sp2}P$	1,3-bis(phosphinobenzene)
$PC_{sp3}P$	1,5-bis(phosphinopentane)

$POC_{sp2}OP$	1,3-bis(phosphinitobenzene)
$POC_{sp3}OP$	1,3-bis(phosphinitopropane)
PIMCOP	3-[2-(phosphanyl)-1H-imidazol-1-yl]phenyl phosphinite
R	Groupe générique
r.t.	Température ambiante
s	Singulet (spectroscopie)
t	Triplet (spectroscopie)
TON - TOF	Turn over number - Turn over frenquency
t-Bu	Groupement butyle tertiaire
THF	Tétrahydrofurane
δ	Déplacement chimique

Chapitre 1 : Introduction

1.1 Complexes pinces ECE : définition

Les complexes pinces comportent au moins un ligand mono-anionique tridentés. Les ligands forment souvent deux liaisons E→M datives (ou covalentes de coordination) entre un groupe "E" donneur d'électron (base de Lewis) et un métal "M" accepteur d'électron (acide de Lewis). Lorsque le troisième lien au centre, mono-anionique, est formé entre le métal et un carbone, on qualifiera de "ECE" ce type de complexe (figure 1.1). [1]

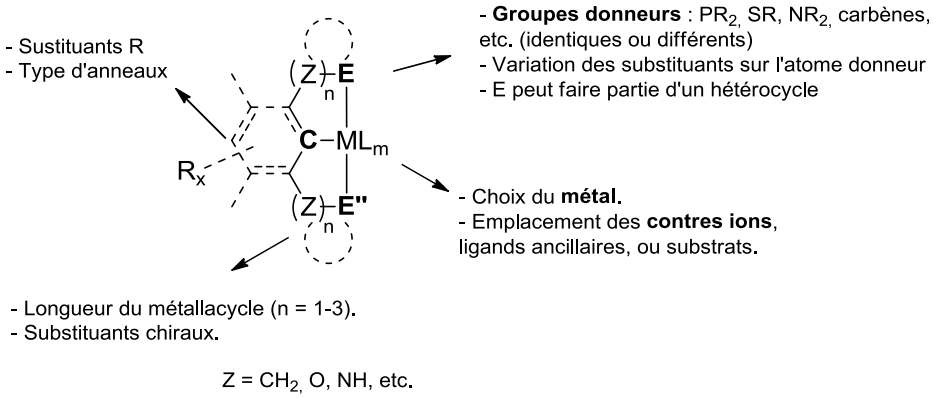

Figure 1.1 Modèle de complexes pince "ECE" et ses possibilités de design.

Il existe de nombreux complexes pinces de type ENE, [2] ESiE, [3] EPE, [4] EBE, [5] etc... . Néanmoins les travaux présentés se concentreront sur les complexes "ECE". La grande majorité des complexes pinces chélatent des métaux de transition et sont tridentés mer κ^3. Il existe aussi des complexes où l'atome central M = Al, [6] P, [7] Sn, [8]

Si, [9] et plusieurs composés peuvent être de géométrie variable κ^1, [10] κ^2, [11] (après protonation du ligand), ou encore fac κ^3. [12] Selon la définition classique le lien entre l'atome central et le métal doit être anionique pour être appelé pince. En effet, ce lien permet au complexe de gagner en stabilité, propriété caractéristique de ces composés. Dans le cas contraire ce type de complexe devrait être appelé "pincer like" mais sont parfois inclus dans la famille des complexes pinces comme par exemple les complexe CNC[13] ou PNP. [14] Des complexes liés au centre par un motif pyridine peuvent suite à une désaromatisation, former des liens N-M anioniques.[15] Une autre définition rejette pour des raisons historiques les complexes ne possédant pas de liaison C-M. [16] Les premiers complexes pinces étant en effet de type ECE.

Les possibilités de design des complexes sont extraordinaires. La majorité d'entre elles concernent le ligand. En les combinant à divers métaux, ligands ancillaires et contre-ions liés au métal, la littérature s'est enrichie d'un catalogue de complexes pinces considérable. Rien que pour les complexes ECE, selon la base de donnée cristallographique de Cambridge le nombre de structures cristallographiques pour les complexes PCP serait de 350, de 330 pour les NCN, 90 pour les SCS et 50 pour les OCO. Il est donc délicat d'établir une définition générale englobant toutes ces variétés. [17]

Les premiers complexes pinces ont été découvert par Shaw et al. en 1976.[18] Ils sont composés de métaux du groupe 9 (Rh, Ir) et 10 (Ni, Pd, Pt) et de ligands PCP {1,3-(*t*-$Bu_2PCH_2)_2$-C_6H_4}. Même si Shaw nomme ces complexes "pcp" dans l'article, la dénomination de "pincer" n'apparait qu'ultérieurement par Van Koten en 1989.[19] Le ligand est synthétisé à partir de 1,3-bis(bromométhyl)benzène et de di-t-

butylphosphine à reflux dans l'acétone pendant 45 min pour donner un sel de phosphonium. La déprotonation de ce sel avec de l'acétate de sodium mène au ligand avec des rendements quantitatifs (figure 1.2).

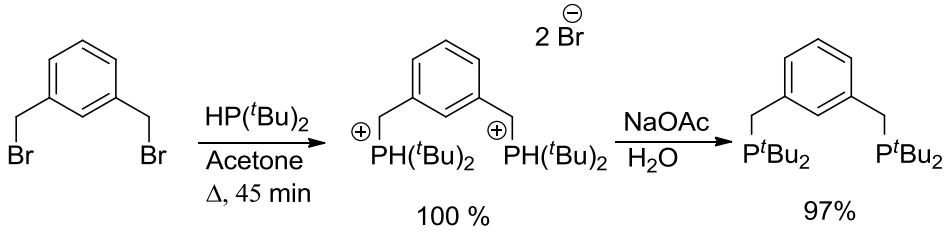

Figure 1.2 Synthèse du ligand PCP {1,3-(*t*-$Bu_2PCH_2)_2$-C_6H_4} reporté par Shaw.

Les complexes pinces plan carré de nickel, palladium et platine sont synthétisés dans les alcools à partir de précurseurs métalliques de valence 2+. Aucune base n'est ajoutée. À partir des complexes halogénés, des dérivés neutres hydrures, cyanures, alcynures sont synthétisés par transmétallation de sels de sodium et lithium, ainsi qu'un dérivé cationique carbonyle à partir de monoxyde de carbone et de tétraphényle borate de sodium ont été synthétisés (figure 1.3). On peut remarquer que près de 40 ans plus tard ces méthodes de synthèse de complexes pinces sont toujours utilisées.

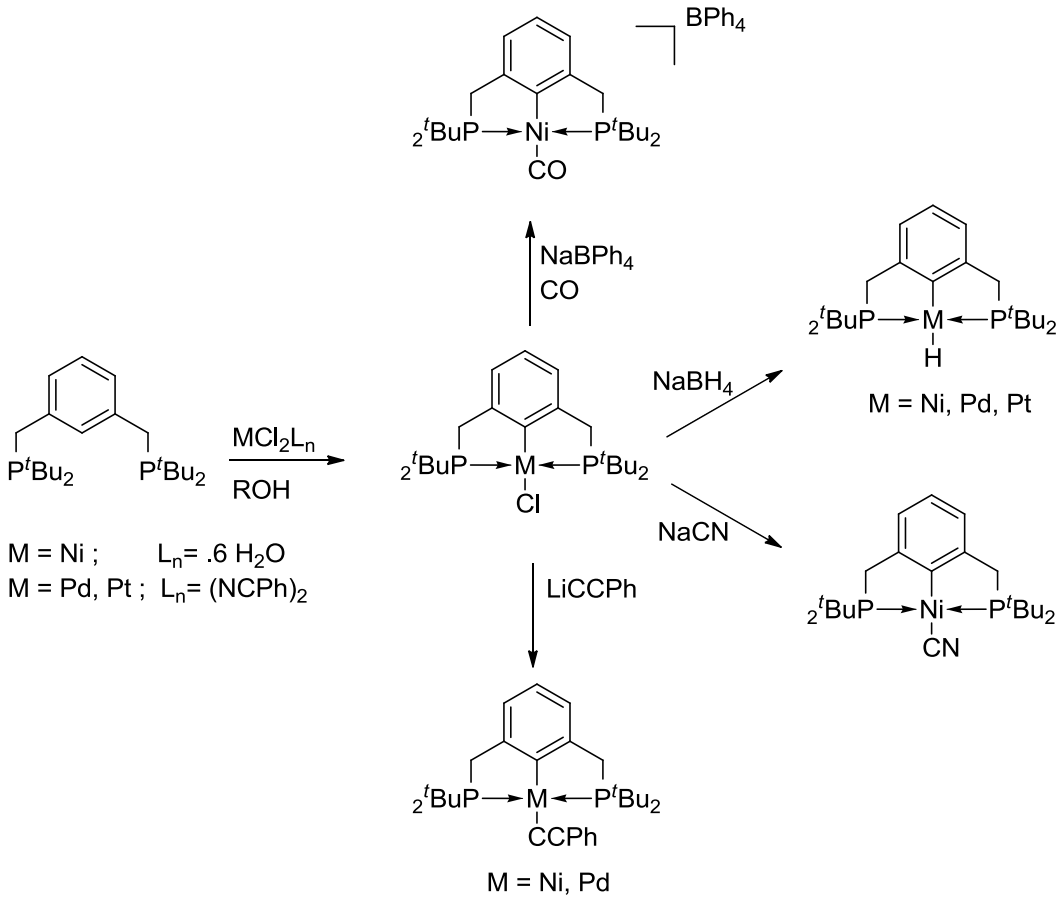

Figure 1.3 Premiers complexes pinces formés de métaux du groupe 10.

Des complexes de rhodium et d'iridium (III) sont aussi synthétisés à partir du ligand PCP (figure 1.4). À partir de précurseur de type $MCl_3.3H_2O$ des complexes de géométrie pyramide à base carré chlorure-hydrure sont obtenus. Il est étonnant de noter que ces complexes hydrures soient synthétisés dans un solvant protique en présence d'eau. Le monoxyde de carbone se coordonne ensuite pour donner un complexe octaédrique à 18 électrons.

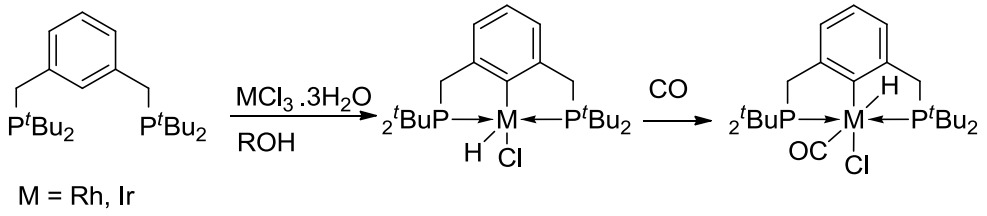

Figure 1.4 Premiers complexes pinces formés de métaux du groupe 9.

Ces complexes ont été caractérisés par RMN ^{1}H, ^{31}P, spectroscopie infrarouge et analyse élémentaire. Néanmoins aucune structure cristallographique n'est rapportée.

1.2 Méthodes de synthèses

Il existent différentes voies de synthèse des complexes pinces. En effet pour mener à la formation des deux métallacycles en forme de B, il faut passer par la formation d'une liaison anionique M-C. Cette étape de cyclométallation dépend du type de ligand, en particulier des atomes donneurs "E" qui le composent. Les méthodologies de synthèse peuvent être regroupées en diverses catégories développées ici.

1.2.1 Synthèses à partir de métaux de plus haute valence

Les premiers complexes pinces furent synthétisés à partir de précurseurs métalliques de haute valence. En effet, il a été vu précédemment que pour la synthèse

de complexes PCP, Shaw utilisait des précurseurs MX_2 pour le groupe 10 (M = Ni, Pd, Pt) et MX_3 pour le groupe 9 (M = Rh, Ir) (X = Cl).[18] En général, ce type de synthèse fonctionne très bien avec des ligands "ECE" mou (E = PR_2, SR_2) et des métaux d^8. Elle comprend une étape de cylométallation qui a lieu généralement via une activation de la liaison C_{sp2}-H ou C_{sp3}-H générant ainsi une molécule d'acide HX. Le métal ne change pas de degré d'oxydation lors de cette étape (Figure 1.5). Récemment, une étude concernant des complexes PCP pinces de palladium et platine, rapporte que plus le ligand PCP est basique (POCOP vs PCP), plus la métallation est facilitée, confirmant ainsi les constations préalablement établies au chapitre 2 de cette thèse. [20] Ces réactions sont directes, régiosélectives et donnent de bons rendements. De plus, les métaux de haute valence ont l'avantage d'être stables à l'air donc facilement manipulables.

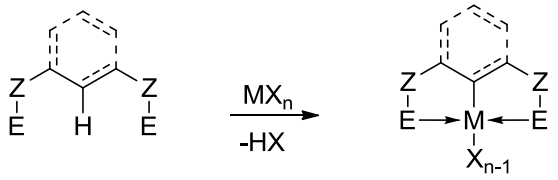

Figure 1.5 Formation d'un complexe pince avec des métaux de hautes valence via activation C-H.

Milstein et al. ont étudié la formation de complexes de type PCP par activation C_{sp2}-C_{sp3}, C_{sp3}-H et O-H avec NiI_2, C_{sp2}-O et C_{sp3}-O avec $Pd(OC(O)CF_3)_2$ et NiI_2 (figure 1.6).[21,22] Ces activations ont lieu à 130 °C dans l'éthanol sous pression avec le nickel, à température ambiante dans C_6D_6 pour l'activation C_{sp3}-O, et à 130 °C sous pression dans le toluène avec le palladium pour l'activation C_{sp2}-O. L'activation de liaison C_{sp3}-H à aussi été effectuée à partir de $(COD)PtCl_2$ ainsi qu'avec

$RuHCl(PPh_3)_3$, suivi l'activation de liaison C_{sp2}-C_{sp3} après l'ajout d'acide chlorhydrique pour le platine, ou d'hydrogène pour le ruthénium.[23,24] L'activation de la liaison C_{sp2}-C_{sp3} est directement observée en utilisant $OsHCl(PPh_3)_3$ à 90 °C. [25] Ces synthèses ont pour but l'étude du clivage de ces liens très stables.[26]

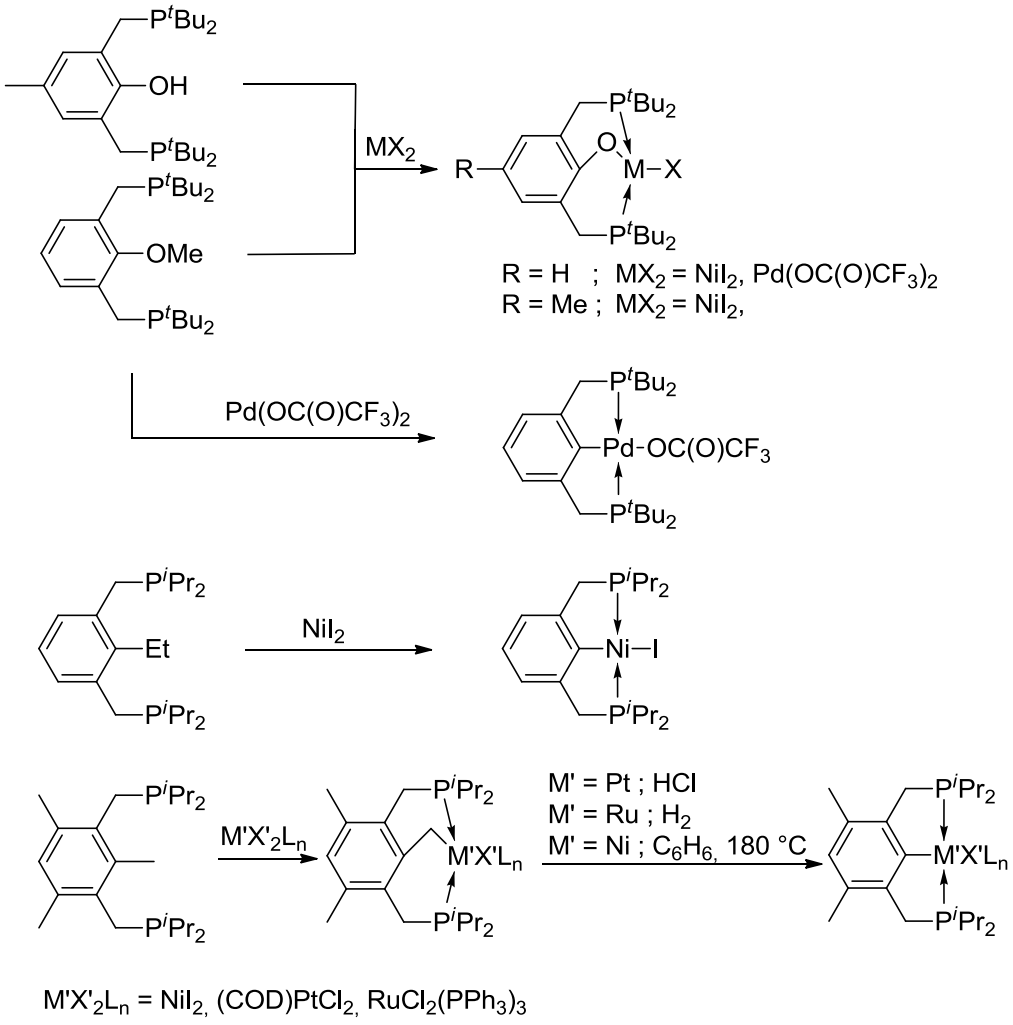

Figure 1.6 Formation de complexes pince PCP via activation des liens C_{sp2}-C_{sp3}, C_{sp3}-H, C_{sp3}-O, C_{sp2}-O et O-H

D'autres lien C-Z peuvent être activés avec une autre méthode. Comme par exemple si Z = $SiMe_3$, le lien C-Si est rompu à température ambiante avec $Pd(OAc)_2$ suivi par un traitement avec LiCl (figure 1.7). [27]

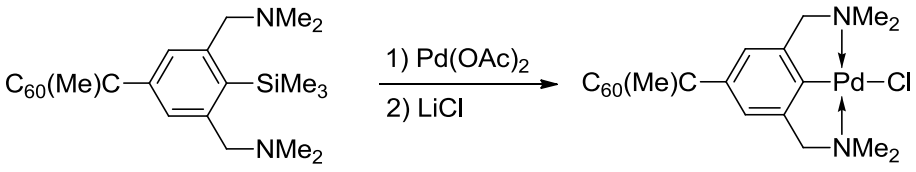

Figure 1.7 Formation d'un complexe pince NCN via activation C-Si.

Il faut noter que les ligands de type NCN ne peuvent généralement pas cyclométaller par simple activation C-H. Il existe néanmoins quelques exceptions. Un complexe NCN (N ∈ imine) de platine (II) a été synthétisé de cette façon avec K_2PtCl_4 comme précurseur métallique. [28] D'autre complexes NCN ont été formés avec $RhCl_3$, ou $RuCl_3$ en présence de métaux réducteur (Zn, Mg) (N ∈ oxazoline). [29] Ou encore un complexe de nickel (II) (N ∈ imidazolinyl) avec $NiCl_2$ à reflux dans le toluène pendant 48 h en présence de NEt_3. [30] Aucun de ces composés NCN n'est formé d'amines simples.

Les halogénures métalliques ne sont pas les seuls précurseurs utilisés. Par exemple le $(COD)PtMe_2$ est utilisé pour la synthèse d'un complexe (PCP)Pt(Me) [31] ou $Zr(NMe_2)_4$ pour la synthèse d'un complexe $(SPCPS)Zr((NMe_2)_2)$. [32]

1.2.2 Synthèse par addition oxydante

Lors de la formation de complexes pince par addition oxydante, le métal s'oxyde passant de $M^m \rightarrow M^{m+2}$ et donne lieu à la formation d'un métallacycle après le clivage d'une liaison C-X (X = Cl, Br, I, OTf, H, Me, ...) (figure 1.8).

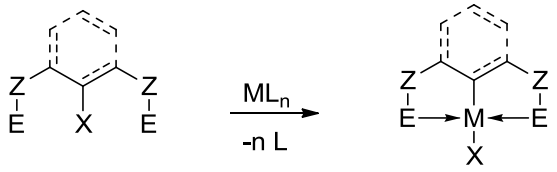

Figure 1.8 Formation d'un complexe pince via addition oxydante.

Cette voie de synthèse est moins pratique que la méthode utilisant des métaux de haute valence (*vide supra*) car elle nécessite la synthèse préalable d'un ligand qui possède un substituant X en position 2 ainsi que l'utilisation de précurseurs métalliques souvent chers et sensibles à l'air tels que $Ni(COD)_2$ ou $Pd(dba)_3$. C'est une voie de synthèse généralement utilisée pour les complexes n'effectuant pas de cyclométallation par activation C-H, comme par exemple les complexes NCN comprenant une amine (figure 1.9).[33]

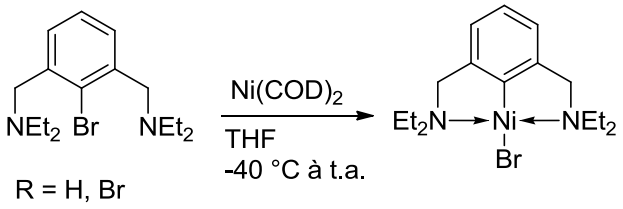

Figure 1.9 Formation d'un complexe NCN de nickel (II) via addition oxydante.

Cette méthode donne lieu à l'activation de liaisons en position 2 très stables avec du Rh(I) ou Ir(I). Par exemple, à partir de $1/2[(COD)_2RhCl]_2$ le complexe pince trivalent ^{tBu}(PCP)Rh(H)(Cl) est formé suite à l'activation d'une liaison C_{Sp2}-OMe suivie d'une elimination β-H, après 3h à 85 °C dans le benzène. [22] D'autres liens en position 2 peuvent être activés par ce précurseur métallique, comme le lien C_{sp2}-CF_3 à 180 °C pendant 9 h [34] ou C_{sp2}-C_{sp3} à 120 °C pendant 3 jours sous pression d'hydrogène. [35] Avec Rh (I) et Ir (I), les activations C_{sp2}-C_{sp3} et C_{sp2}-H ont lieu facilement à température ambiante et le produit d'activation C-H peut être converti en produit d'activation C-C (figure 1.10). [36]

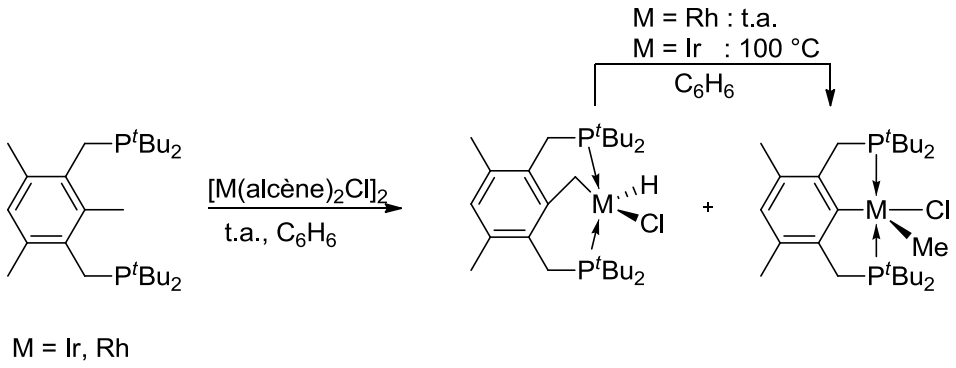

Figure 1.10 Formation de complexes pince PCP via activation C_{sp2}-C_{sp3} et C_{sp3}-H.

La cyclométallation par addition oxydante peut s'inscrire dans une stratégie de post dérivation des complexes pinces. Cette méthodologie est utilisée pour installer un motif chiral sur le ligand après formation du lien C-M comme avec les complexes NCN chiraux de palladium synthétisés par Uozumi et al (figure 1.11). [37]

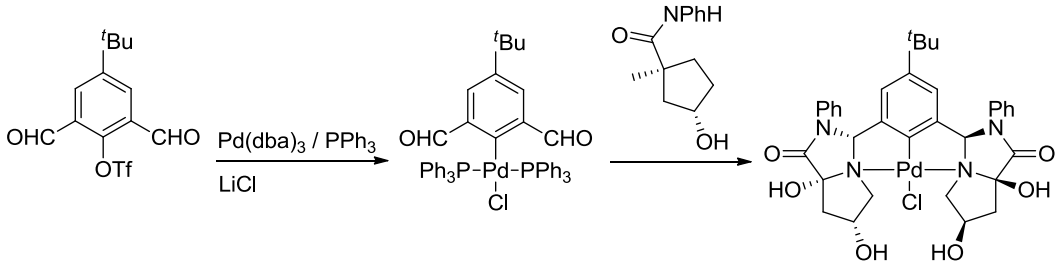

Figure 1.11 Formation de complexes pince NCN chiral par post dérivation.

1.2.3 Synthèse par transmétallation

La formation de complexes pinces par transmétallation se fait par échange du métal M de liaison C-M par une espèce métallique oxydée pour former une nouvelle liaison C-M' (figure 1.12). Elle permet l'utilisation de précurseur métallique de haute valence. La formation initiale de la liaison C-M est souvent obtenue par lithiation. Cette technique est utilisée pour former des complexes qui ne cyclométallerait, ni par activation C-H, ni par addition oxydante d'un lien C-X.

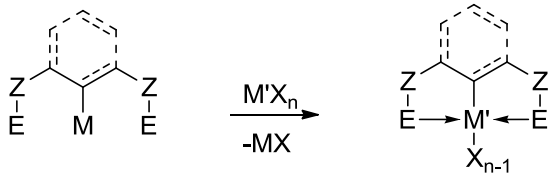

Figure 1.12 Formation d'un complexe pince via transmétallation.

Les complexes de type NCN peuvent aussi être synthétisé via transmétallation. La formation de complexe (NCN)Pd(Br) se fait à partir d'un lithien LiNCN formé par déprotonation du ligand par BuLi, suivi par l'addition d'un précurseur de $(COD)PdBr_2$. [38] C'est aussi de cette façon que sont synthétisés de

nombreux complexes pinces des groupes 13, 14 et 15. [39] Le lithien LiNCN peut se faire aussi par échange bromo-métal de la position 2 du ligand avec un équivalent de BuLi ou deux équivalents de lithiun métallique. [40] Pour que la lithiation du ligand soit sélective en position 2, l'ajout du BuLi doit se faire dans un solvant apolaire non coordonnant (Figure 1.13). [41]

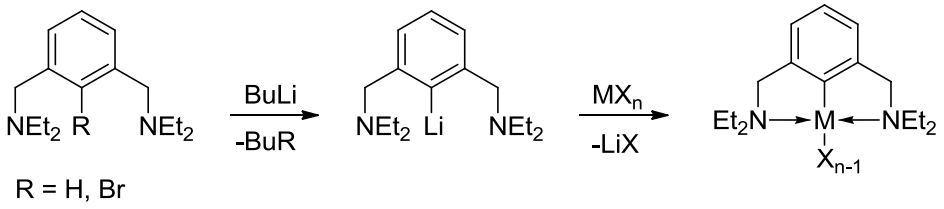

Figure 1.13 Formation d'un complexe pince NCN via transmétallation.

La transmétallation est utilisée pour la synthèse de complexes pinces NCN de zirconium et niobium. Une première transmétallation a lieu entre un lithien NCNLi et un complexe d'or (I) $[ClAuP(Ph)_2(C_6H_5)]_2$. Puis une seconde transmétallation a lieu entre le nouveau complexe (NCN)Au et un précurseur $Ti(IV)Cl_4$ ou $Nb(V)Cl_5$. Le composé d'or est retrouvé à la fin de la réaction (figure 1.14). [42] Une synthèse similaire utilisant $AuCl(PPh_3)$ comme précurseur d'or a aussi permis d'obtenir des complexes pinces NCN de Fe (III), Ni(II), Pd(II) et Pt (II). [43]

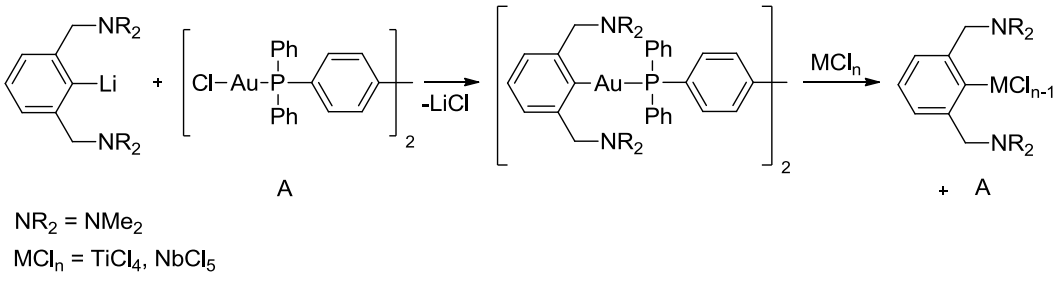

Figure 1.14 Formation de complexes pince NCN de titane et niobium via transmétallation.

1.2.4 Transcyclométallation

Lors de la formation d'un complexe pince par transcyclométallation (TCM), la liaisons C_{ipso}-H d'un ligand et C_{ipso}-M d'un complexe sont échangées donnant ainsi un nouveau complexe pince et le ligand du complexe de départ (figure 1.15).

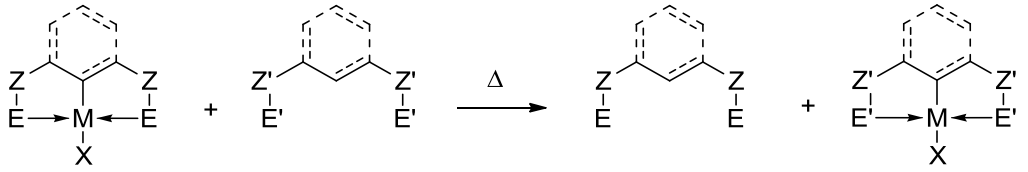

Figure 1.15 Formation d'un complexe pince via transcyclométallation.

Cette méthode est utilisée en dernier recours lorsque les autres méthodes de cyclométallation ne fonctionnent pas, comme pour la formation de dendrimères à base de complexes pinces de PCP de platine ou de ruthénium, à partir de complexe pince NCN (Figure 1.16). [44] La conversion est quantitative et sélective. Il existe plusieurs autres exemples de TCM avec Ru [45] ou Pt. [46]

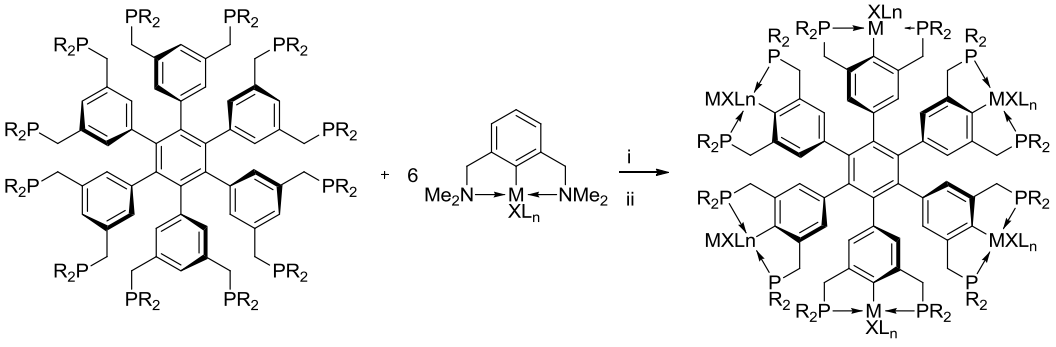

Figure 1.16 Formation de complexes Hexakis((PCP)Pt et (PCP)Ru) par TCM.

1.3 Réactivités des complexes pinces "ECE" de Nickel

Les premiers complexes pince de nickel ont été synthétisés en 1976 par Shaw et al. (*vide supra*). [18] Depuis le nombre de complexe de nickel a considérablement augmenté, en particulier lors de la dernière décennie (figure 1.17). [47]

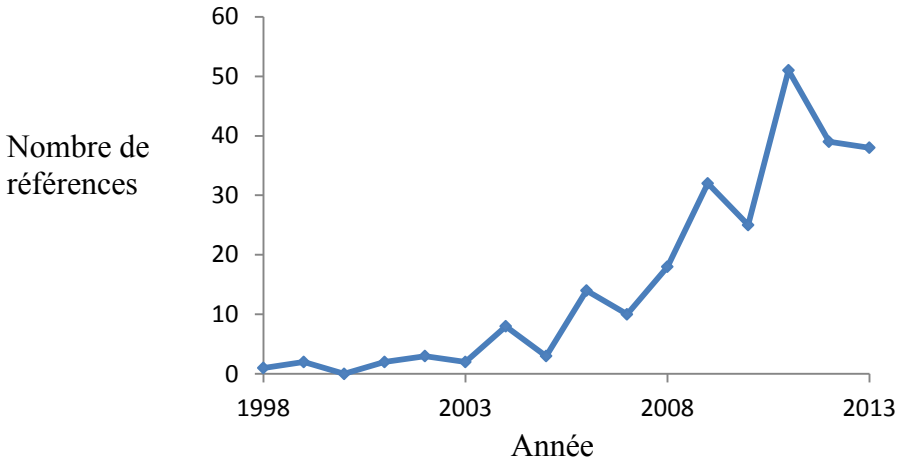

Figure 1.17 Nombres de références contenant le concept "nickel pincer complex" trouvées par le moteur de recherche "SciFinder®" par année.

Cette partie sera consacrée au sujet principal de cette thèse : les complexes "ECE" pinces de nickel et à leurs applications. La chimie de ces complexes sera présentée en fonction de leur apparition dans la littérature (figure 1.18). [48] Il est important de noter qu'il existe aussi d'autres familles de complexes pinces de nickel de type ENE, [49] ESiE, [50,3a] etc.

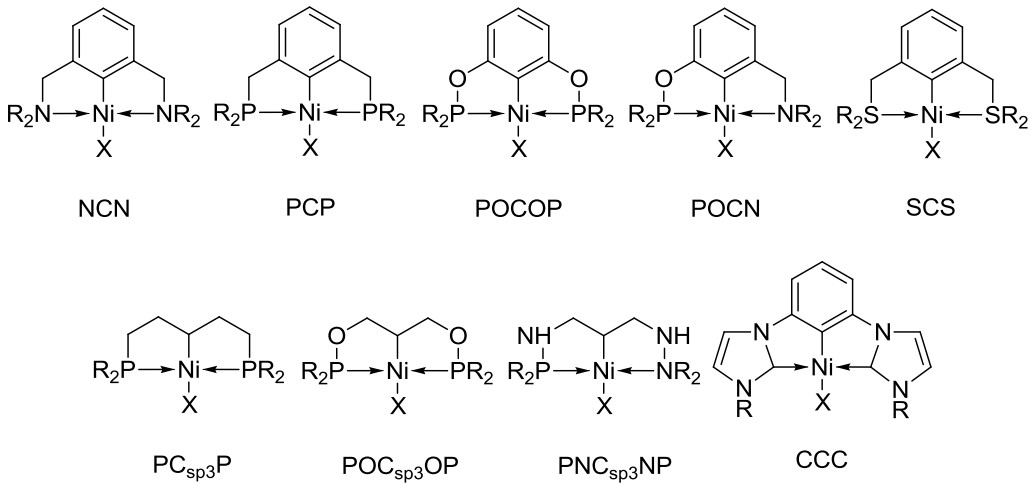

Figure 1.18 Différentes catégories de complexes pinces "ECE" de nickel.

Les complexes pinces sont principalement utilisés en catalyse. Dans ce domaine le faible coût du nickel est un avantage indéniable. En effet les métaux 3d sont très abondants par rapport aux métaux 4d et 5d. Mais comparativement leur activité catalytique est plus limitée, notamment pour les réactions de couplage. Une explication est la plus grande stabilité des liens C-M formés avec les métaux 4d et 5d. Certaines réactions sont néanmoins préférentiellement catalysées par le nickel plutôt qu'avec d'autres métaux comme l'addition de Kharasch ou la cyanométhylation des aldéhydes (*vide infra*).

Ces complexes présentent aussi des réactivités non catalytiques intéressantes. Les sections suivantes tenteront de présenter la chimie de complexes pinces "ECE" de nickel uniquement dont la réactivité a été étudiée. Il existent aussi des complexes PNC$_{sp3}$NP, [51] SCS, [52] ou CCC[53] de nickel dont la réactivité n'a pas encore été explorée.

1.3.1 Complexes (PCP)Ni

Les complexes PCP de nickel ont été les premiers complexes pinces qui furent découverts par Shaw et al. [18] Paradoxalement et contrairement aux complexes NCN, les complexes PCP de nickel n'ont été développés que récemment. La réactivité de ce type de complexes reste encore peu développée.

Hazari et al. ont reporté l'insertion du CO_2 dans des liaisons Ni-R (R = H, Me, η^1-allyle).[54] La réactivité dépend fortement de la nature de la liaison selon l'ordre suivant : H > η^1-allyle >>Me. En effet, à une pression de CO_2 d'un atmosphère, l'insertion se fait à température ambiante en quelques minutes pour le complexe hydrure, en six heures avec l'allyle et après un chauffage prolongé à 150 °C avec le méthyle. De plus l'utilisation de $^{13}CO_2$ avec les complexes résultant de l'insertion montre que la réaction est réversible uniquement avec l'hydrure. Une étude DFT montre que l'insertion s'effectuerait selon un mécanisme concerté à 4 centres entre Ni-H et C=O (de CO_2) alors que dans les autres cas le nickel ne serait pas impliqué. Les complexes (POCOP)Ni hydrures réussissent la réduction catalytique du CO_2 pour produire du méthanol (*vide infra*).

Les complexes hydrures ont fait l'objet d'étude par Peruzzini et al. en faisant réagir des espèces acides comme HBF_4, CF_3CH_2OH ou $CpW(CO)_3H$ avec ^{tBu}(PCP)Ni(H).[55a] La vitesse de la réaction dépend de l'acide utilisé et l'évolution de la production d'hydrogène est observée avec l'acide le plus fort HBF_4. De plus une espèce rare bimétallique $^{t\text{-}Bu}$(PCP)Ni-O≡C-$WCp(CO)_2$ a été isolée. La structure montre un lien

Ni-O-C-W presque linéaire. La réactivité des complexes $^{t\text{-}Bu}$ (PCP)Ni(X) a aussi été étudiée avec les acides de Lewis BX_3 (X = H, F). Les complexes (PCP)Ni(H) peuvent être synthétisés par transmétallation à partir de (PCP)Ni(Cl) et d'une source d'hydrure ($NaBH_4$, $LiEt_3BH$) [56] ou à partir du complexe $^{i\text{-}Pr}$(PCP)Ni(OMe) et de triéthoxysilane. [57] Le complexe borohydrure $^{t\text{Bu}}$(PCP)Ni(BH_4) cinétiquement stable (mais thermodynamiquement instable) est formé mais non isolé. Il relargue réversiblement le borane. Une réactivité similaire est observé quand X = F (Figure 1.19).[55b] Le chapitre 4 est consacré à la synthèse des complexes fluoré. Le cation [(PCP)Ni(OH_2)][BF_4] est obtenu comme produit secondaire. On peut aussi obtenir ce cation à partir de $AgBF_4$ et du complexe chloré et d'eau. Le composé cationique [(PCP)Ni($NCCH_3$)][BF_4] catalyse l'hydroamination de l'acrylonitrile.[58]

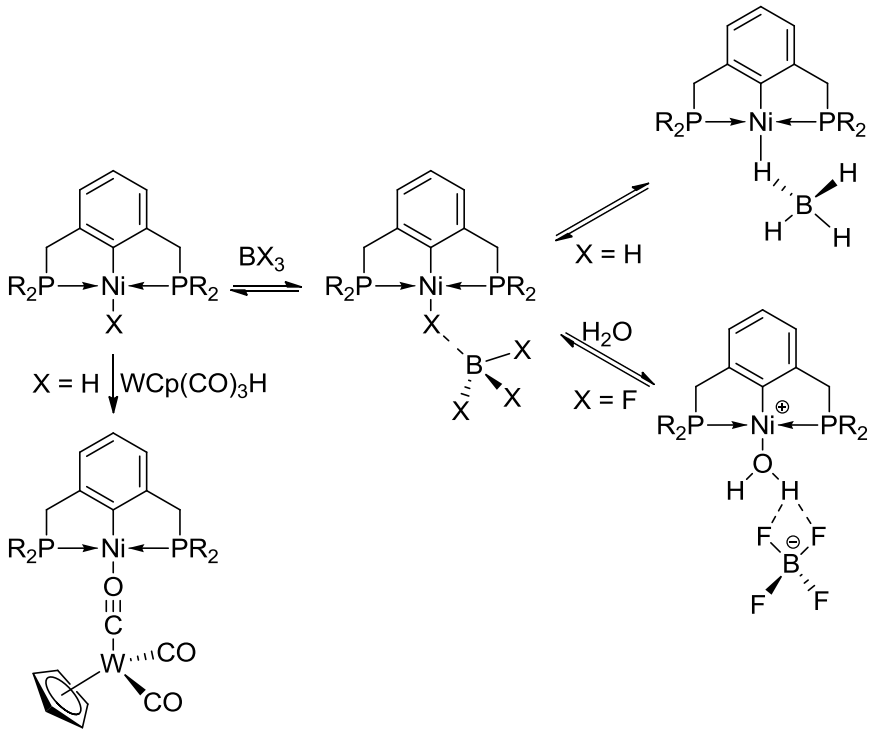

Figure 1.19 Interactions du complexe ($PC_{sp3}P^{t\text{-}Bu}$)-Ni-X avec $WCp(CO)_3H$ (X = H) et BX_3 (X= H, F).

Chapitre 1

La réduction électro-catalytique de proton et la production d'hydrogène avec des complexes (POCOP)Ni(Cl) et (PCP)Ni(Cl) ont été reporté récemment.[59] Une étude cinétique dans l'acétonitrile montre que le complexes PCP effectue la réduction de proton 4 fois plus rapidement qu'avec le POCOP. Le mécanisme impliquerait la formation initiale d'un complexe cationique $[(PCP)Ni(NCCH_3)][BF_4]$ et passerait pas la formation d'un complexe hydrure.[60]

Les complexes $PC_{sp3}P$ (1,5-bis(phosphinopentane)) de nickel ont été synthétisés récemment.[61] Ces complexes sont synthétisés à plus haute température que leurs homologues $PC_{sp2}P$, par activation C_{sp3}-H du ligand aliphatique. Les complexes $(PC_{sp3}P)Ni(X)$ (X= Cl, Br, I) sont stables à l'air et en solution. Grâce à une meilleure donation σ $C_{sp3}\rightarrow$Ni ils sont plus riches en électrons que les complexes $PC_{sp2}P$. Néanmoins le complexe alkyl $(PC_{sp3}P^{t\text{-}Bu})$-Ni-(*n*-Bu) se décompose par élimination β-H en complexe $(PC_{sp3}P^{t\text{-}Bu})$-Ni-H. Ce complexe hydrure n'a pas été isolé mais son analyse RMN ^{1}H montre un triplet (J_{PH} = 53Hz) très blindé (δH = -10 ppm). Ce composé ne peut pas faire l'insertion d'alcènes ou d'alcynes mais promeut l'oligomérisation du phénylsilane (Figure 1.20).

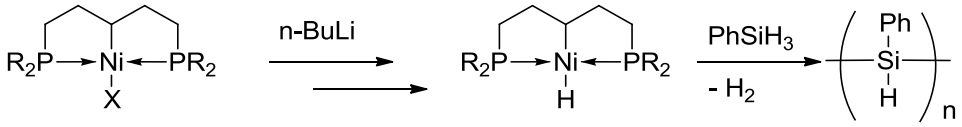

Figure 1.20 réactivité du complexe $(PC_{sp3}P^{t\text{-}Bu})$-Ni-H.

$PC_{sp3}P$-Ni-Me, formé à partir de MeMgCl, peut réagir avec PhX (X= Cl, Br, I) pour donner le produit de couplage correspondant Me-Ph.[62] Ce couplage de Corriu-Kumada peut être catalysé par 1% de (PCP)Ni(X) à reflux dans le THF avec des TON

allant jusqu'à 80. La formation minoritaire du produit d'homocouplage Ph-Ph est observée (figure 1.21). Des investigations supplémentaires montrent que le produit présent lors de la catalyse est le complexe $PC_{sp3}P$-Ni-Me et donc que le Ni(0) n'est pas impliqué. De plus la réactivité des complexes augmente selon la tendance suivante : $PC_{sp2}P$-Ni-Me < $^{t\text{-}Bu}PC_{sp3}P$-Ni-Me < $^{i\text{-}Pr}PC_{sp3}P$ -Ni-Me ce qui implique que la richesse électronique du métal et le facteur stérique sont importants. Finalement le complexe $PC_{sp3}P$-Ni-Ph ne réagit pas avec PhCl ce qui suggère que le produit Ph-Ph pourrait être formé via un mécanisme de transfert d'électron en dehors de la sphère de coordination.

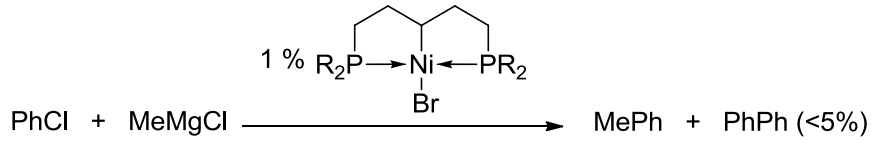

Figure 1.21 Complexe ($PC_{sp3}P^{t\text{-}Bu}$)-Ni-Br catalysant le couplage de Corriu-Kumada.

Le complexe de Ni(III) $PC_{sp3}P$-NiX_2 (X = Br, Cl) peut être synthétisé par oxydation du complexe divalent avec FeX_3. La chimie des complexes pinces de Ni(III) sera développée dans le chapitre suivant.

1.3.2 Complexes (NCN)Ni

Contrairement aux complexes PCP, les complexes NCN de nickel ont été étudiés depuis plus de trente ans par van Koten et al. Ces composés sont généralement synthétisés par transmétallation (*vide supra*). Une caractéristique des ligands pinces est leur capacité à stabiliser des métaux possédant un degré

d'oxydation inhabituel.[63] van Koten et al. ont synthétisé les premiers complexes pinces NCN de Ni(III) en utilisant des dihalogènes ou des dihalogénures de cuivre (II) comme oxydant. Ils sont stables à l'air et possèdent une géométrie pyramide à base carré déformée (Figure 1.22).[64] La liaison Ni-X en position apicale est significativement plus longue que celle en position basale (+ 0.01Å).[65] Une étude de résonnance paramagnétique électronique (RPE) et des calculs EHMO montrent que l'électron non apparié est situé dans une orbitale moléculaire antiliante hors du plan résultant d'une combinaison de l'orbitale d_z^2 du nickel et de l'orbitale p_z de l'halogénure en position apicale.

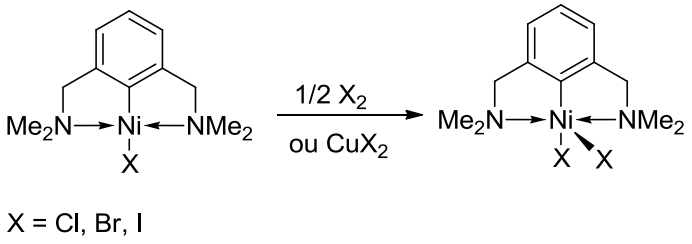

Figure 1.22 Synthèse de complexe pinces de Ni(III) (NCN)Ni(X)$_2$

La réaction de Kharasch est une réaction préférentiellement catalysée par les complexes NCN de nickel. En effet, ils ont une réactivité comparable aux meilleurs catalyseurs connus pour cette réaction comme $RuCl_2(PPh)_3$.[66] A température ambiante, l'addition de CCl_4 sur le méthacrylate de méthyle est complétée à 90% pour produire l'adduit 1 : 1 alors que le catalyseur de ruthénium n'est pas actif à moins de 40 °C. La nécessité du ligand NCN est démontrée car $NiCl_2(PR_3)_2$ n'est actif qu'à partir de 140 °C.[67]

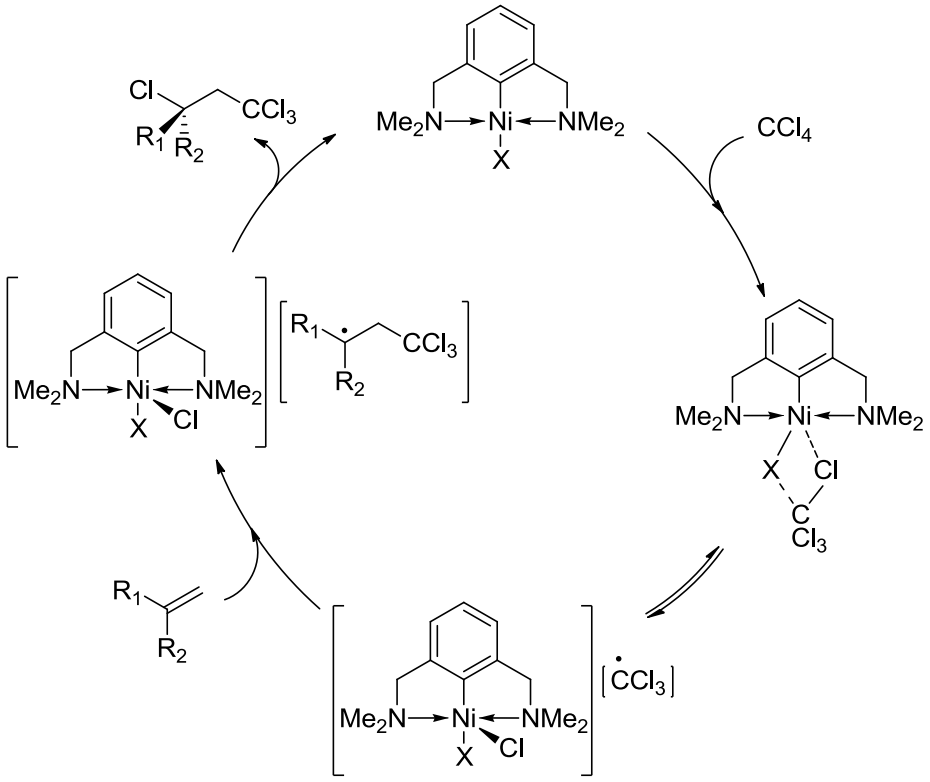

Figure 1.23 Mécanisme proposé pour la réaction De Kharasch catalysé par un complexe (NCN)Ni(Cl).

Les complexes de nickel (III) $(NCN)Ni(Cl)_2$ sont souvent retrouvés à la fin de la réaction d'addition de Kharasch catalysée par l'espèce divalente. Il sont néanmoins catalytiquement inactifs pour cette réaction. Le mécanisme proposé impliquerait une paire radicalaire persistante $[(NCN)Ni(Cl)_2][CCl_3]$ (figure 1.23).[68] Conformément au mécanisme, seul un faible excès énantiomérique (16%) est observé en utilisant un catalyseur chiral.[69]

Ces catalyseurs peuvent être greffés sur des dendrimères.[70] Ces macromolécules peuvent ainsi être recyclées à la fin de la catalyse et éviterait la contamination du produit par le catalyseur. L'activité catalytique par unité de site actif de ces dendrimères est néanmoins plus faible qu'avec le complexe libre. Cette

désactivation est causée par la formation de complexes trivalenst inactifs à la périphérie des dendrimères.[71]

D'autres types de complexe NCN ont été développés pour catalyser diverses réactions autre que le transfert radicalaire. Le complexe pince NCN contenant un ligand bisoxazoline (*phebox*) catalyse l'addition de Michael entre le cyanoacétate d'éthyle et la buténone. Le précatalyseur (NCN)Ni(OTf) est généré à partir du complexe bromo et de triflate d'argent mais n'a pas été caractérisé. Avec 5 % de catalyseur et 10 % de N,N-diisopropyléthylamine (base de Hünig), à 4 °C après 1h, un rendement de 55 % est obtenu (figure 1.24). Néanmoins ce catalyseur deviendrait inactif assez rapidement.[72]

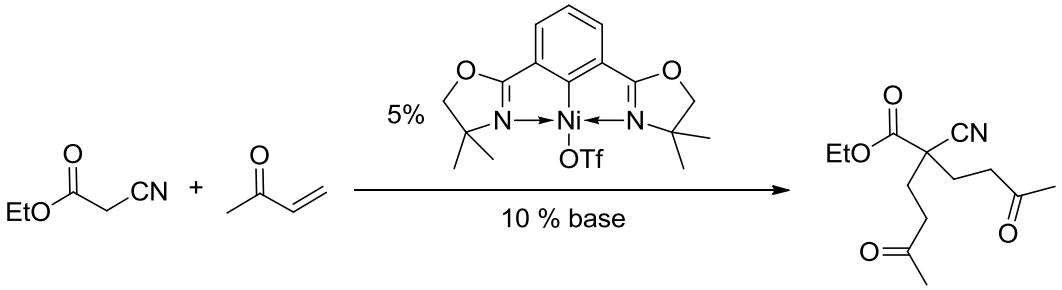

Figure 1.24 Addition de Michael catalysé par un complexe phebox de nickel.

A partir de ce même ligand, le complexe cationique $[(NCN)Ni(NCCH_3)][BF_4]$, aussi utilisé pour des réaction d'addition de Michael, peut catalyser la réaction de couplage de Heck (figure 1.25). Néanmoins, une longue période d'induction suggérerait que le cation n'est pas l'espèce active. Cette observation est cohérente avec la nécessité d'utiliser des complexes électroniquement

riches pour favoriser l'addition oxydante de PhI. De plus, à reflux de DMF, seul un TON = 5 est observé après 24h et TON = 16 après 48h. (figure 1.25).[73]

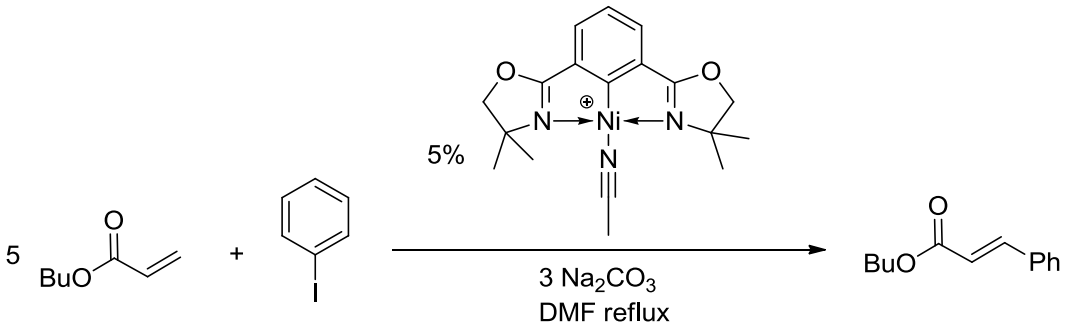

Figure 1.25 Couplage de Heck catalysé par un complexe phebox de nickel.

1.3.3 Complexes (POCOP)Ni

Le premier complexe pince de nickel de type POCOP a été développé par Morales-Morales et al. par activation C-H.[74] Il est utilisé pour la thiolation du iodobenzene en présence de zinc (schéma 1.26). Le zinc est utilisé pour réduire le Ni(II) en Ni(I). Les rendements sont quantitatifs et des produits d'homocouplage Ph-Ph sont obtenus selon le type de RSSR utilisé. Guan et al. utilise ce même complexe (1%) pour effectuer cette même réaction à partir de PhI et ArSH en présence de deux équivalent de KOH dans le DMF à 80 °C pendant 2 à 3h avec des rendements similaires.[75] Plusieurs produits de décomposition sont observés suite à la réaction de KOH avec la liaison P-O du complexe. De plus la réaction entre (POCOP)Ni(SAR) et PhI semble être difficile, ce qui suggère que ce n'est pas le complexe qui effectue la catalyse. Des rendements similaires sont obtenus en utilisant une combinaison de $Ni(COD)_2$ et $Ph_2P(O)H$.

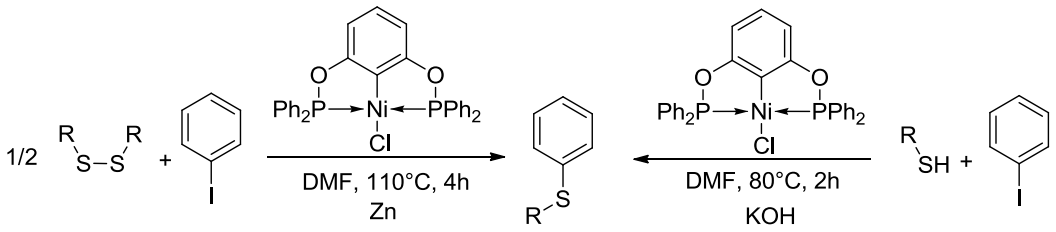

Figure 1.26 Thiolation du iodobenzene par un complexe ^{Ph}(POCOP)Ni(Cl) effectuée par Morales-Morales et al. (à gauche) et par Guan et al. (à droite).

Les composés cationiques POCOP sont utilisés pour les réaction d'addition de Michael. Les complexes [^{R}(POCOP)Ni(NCCH$_3$)][OTf] (R = ^{i}Pr, Ph) sont utilisés dans les réactions d'hydroamination et d'hydroalcoxylation d'oléfines activées (figure 1.27).[76] Dans les deux cas, les substituants phényles, plus électrophiles, favorisent ces réactions. Les mécanisme semble néanmoins être différent. Une attaque nucléophile de l'amine sur l'acrylonitrile coordonnée semble être le plus plausible. De meilleurs rendements sont obtenus avec des amines plus nucléophiles. Dans le cas de l'hydroalcoxylation, la nucléophilie des alcools défavorise la réactivité. Le mécanisme pourrait passer par l'attaque nucléophile d'un alcool activé par la formation d'une liaison hydrogène RO-H---O formée avec un complexe neutre généré in situ (POCOP)Ni(OR). L'acidité favoriserait la formation de ce type de liaisons.

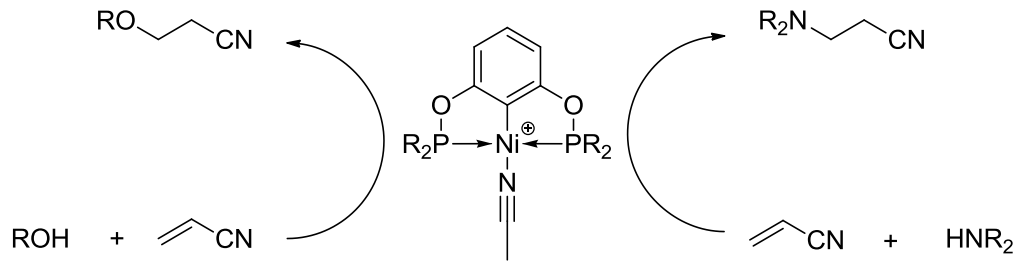

Figure 1.27 Hydroamination et alcoxylation de l'acrylonitrile par un complexe cationique [(POCOP)Ni(NCCH$_3$)][OTf].

Le complexe hydrure (POCOP)Ni(H) développé par Guan et al. a montré de bonnes capacités catalytiques.[77] Tout d'abord, ce complexe peut effectuer l'hydrosilylation des aldéhydes à partir de Ph_2SiH_2 ou de $PhSiH_3$. Après hydrolyse, les alcools correspondants sont obtenus (figure 1.28). Le mécanisme implique l'insertion C=O de l'aldéhyde dans la liaison Ni-H suivie du clivage du nouveau lien Ni-O par un silane. Les TON vont de 300 à 450.

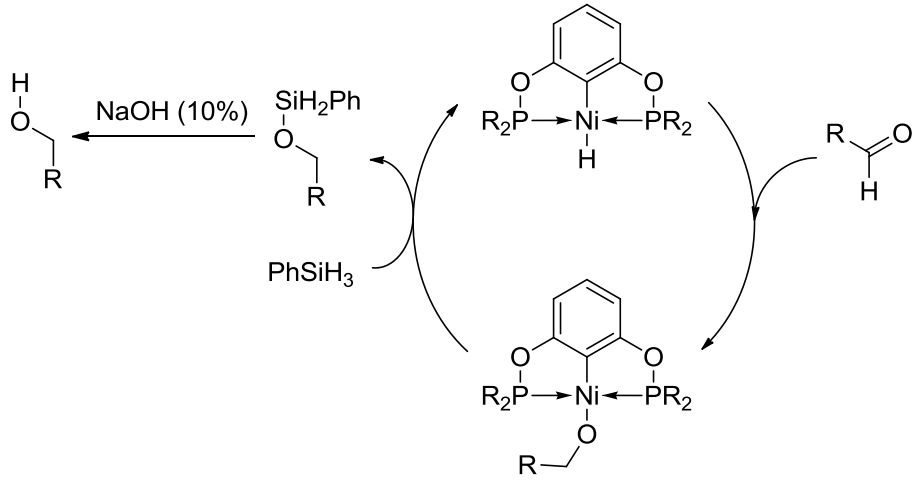

Figure 1.28 Hydrosilylation d'aldéhydes par un complexe (POCOP)Ni(H).

Le complexe hydrure peut aussi réduire catalytiquement le CO_2 avec le catécholborane comme source d'hydrure. Le CO_2 réagit réversiblement avec (POCOP)Ni(H) pour former le complexe formate (POCOP)Ni(OCO(H)). [78] Le cycle catalytique fait intervenir plusieurs intermédiaires et la formation / réduction de formaldéhyde est observée. Les produits obtenus sont MeOBCat et CatBOBCat. MeOBCat peut être ensuite hydrolysé pour donner du méthanol (schéma 1.29). [79]

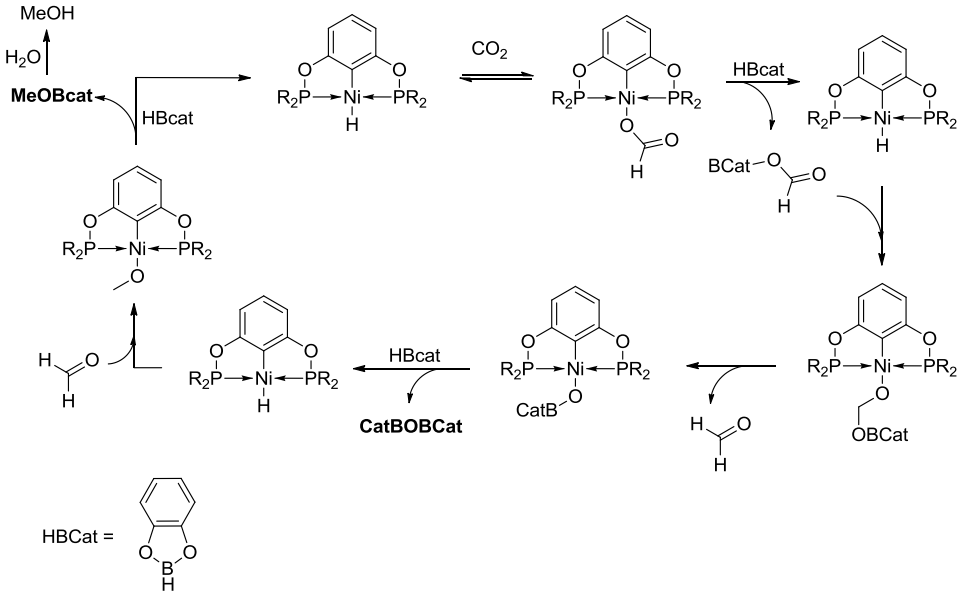

Figure 1.29 Réduction catalytique du CO_2 par le complexe (POCOP)Ni(H).

Récemment, Guan et al. ont reporté une cyanométhylation très efficace des aldéhydes avec l'acétonitrile comme source de cyanure de méthyle.[80] En partant du complexe (POCOP)Ni(CH_2CN) des TON = 82 000 avec TOF = 1139 h^{-1} sont obtenus avec p-$CF_3C_6H_4CHO$ à température ambiante. Cela en fait le complexe le plus réactif pour cette réaction. Les réactifs ne sont pas séchés et aucune base ni additif ne sont ajoutés (Figure 1.30). Le complexe (POCOP)Ni(CH_2CN) peut être obtenu par

transmétallation à partir du complexe (POCOP)Ni(Cl) et de $LiCH_2CN$ ou par déprotonation de l'acétonitrile coordonnée au complexe cationique $[(POCOP)Ni(NCCH_3)][OTf]$ par LiHMDS. Avec une tel activité, et comme indiqué à la fin de l'article, une version asymétrique de ce catalyseur est en cours de développement.

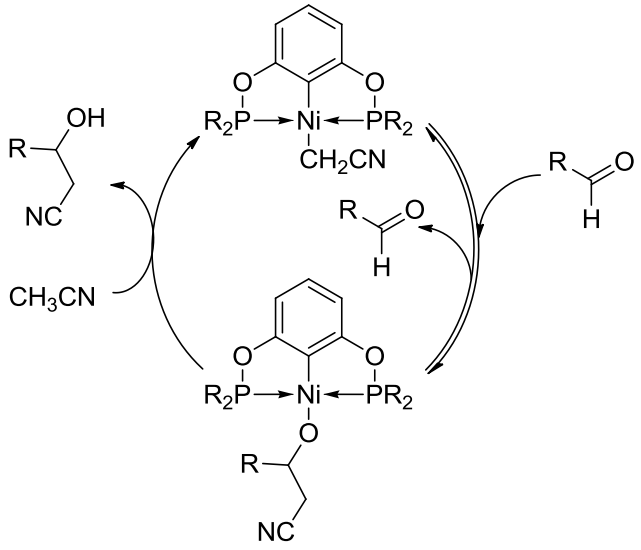

Figure 1.30 Cyanométhylation des aldéhydes par un complexe $(POCOP)Ni(CH_2CN)$.

Les complexes $POC_{sp3}OP$ de nickel on été reportés en 2007.[81] Comparativement aux complexes aromatiques, la chimie de ces composés aliphatiques reste peu développée. Comme leurs complexes homologues PCP, ils sont synthétisés via activation du lien C_{sp3}-H. L'activité catalytique du $POC_{sp3}OP$-Ni-Me lors du couplage de Kumada-Corriu est similaire. Les composés trivalents $POC_{sp3}OP$-Ni-X_2 ont été synthétisés. Ces composés POCOP de Ni(III) peuvent catalyser l'addition de Kharasch.[82] L'addition de CCl_4 sur divers alcènes (styrènes, 4-méthylstyrène, méthacrylate de méthyle, ...) se fait avec des TON compris entre 650

et 970. Les complexes NCN de nickel catalysent cette réaction à température ambiante à partir d'espèces divalentes (l'espèce trivalente inhibe la réaction). Il est donc envisageable que le complexe (POCOP)Ni$(X)_2$ se décompose initialement en (POCOP)Ni(X) pour effectuer ensuite la catalyse.

La stabilité des complexes $POC_{sp3}OP$-Ni-X varie fortement selon X. En effet, quand X = Cl, Br, I, les complexes sont très stables à l'air. Les complexes récemment synthétisés par transmétallation où X = $OSiMe_3$, OMes, NPh_2, CCMe ne sont stables que sous atmosphère inerte. Les tentatives de synthèses des dérivés Ni-O^{t}Bu ou Ni-$N(SiMe_3)_2$ donnent des produits de décomposition. De plus, lorsque $POC_{sp3}OP$-Ni-$OSiMe_3$ est traité avec AgF un des produit de décomposition isolé est une espèce zwitterionique trinucléaire rare [{(η^3-allyl)Ni}$_2$-{μ,κ^P, κ^O -(^{i}Pr$_2$PO)$_4$Ni}].[83] $POC_{sp3}OP$-Ni-CCPh se décompose graduellement en solution pour donner un composé de valence neutre (figure 1.31). Cette instabilité est liée à une plus grande réactivité en général des complexes aliphatiques versus leurs homologues aromatique.[84]

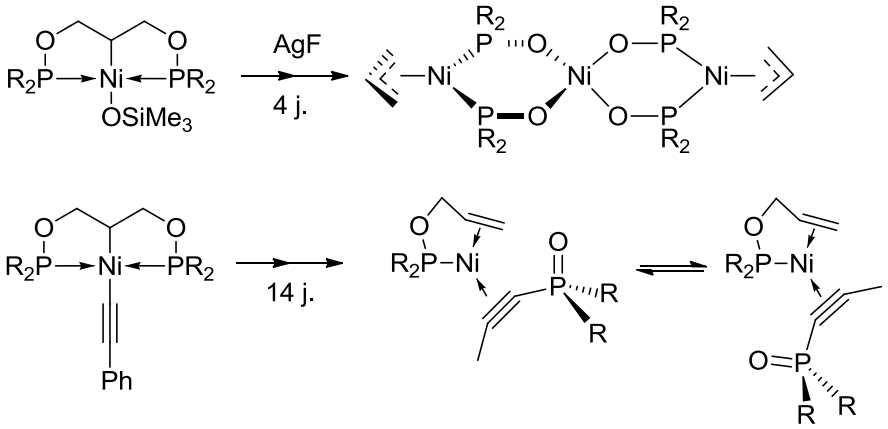

Figure 1.31 Décomposition graduelle de POC $_{sp3}$OP-Ni-CCPh, et de POC $_{sp3}$OP-Ni-OSiMe3 en présence de AgF.

1.3.4 Complexes (POCN)Ni et (PNCN)Ni

Le premiers complexes POCN de nickel (N = NMe_2, NEt_2, morpholinate ; P = P^iPr_2) ont été développés en 2009 via activation C-H à partir du précurseur $NiBr_2(NCCH_3)_x$.[85] Des complexes trivalents (POCN)Ni$(Br)_2$ sont synthétisés par oxydation à partir de dibrome. Ces composés présentent une bonne stabilité thermique à l'état solide ou en solution. Les complexes divalents et trivalents POCN (N = NMe_2, morpholinate) ont une faible activité catalytique lors de l'addition de Kharasch du CCl_4 sur le styrène (TON = 45, TOF = 2.5 h^{-1}) avec 2% de catalyseur à 80 °C pendant 18 h dans l'acétonitrile. La réaction est très influencée par la nature de l'amine puisqu'aucune activité n'est détectée lorsque N = NEt_2.

Lorsque le complexe est composé d'une amine secondaire, son traitement avec MeLi mène à la formation d'un dimère qui possède à l'état solide une forme de "papillon".[86] Il s'avère être un bon catalyseur pour l'hydroalcoxylation de

l'acrylonitrile avec des TON = 2000. Cette réaction est facilitée par les alcools acides non encombrés (*vide supra*). Ce dimère peut aussi donner l'espèce trivalente (POCN)Ni(Br)$_2$ (N= imine) suite à l'ajout de NBS (figure 1.32).[87]

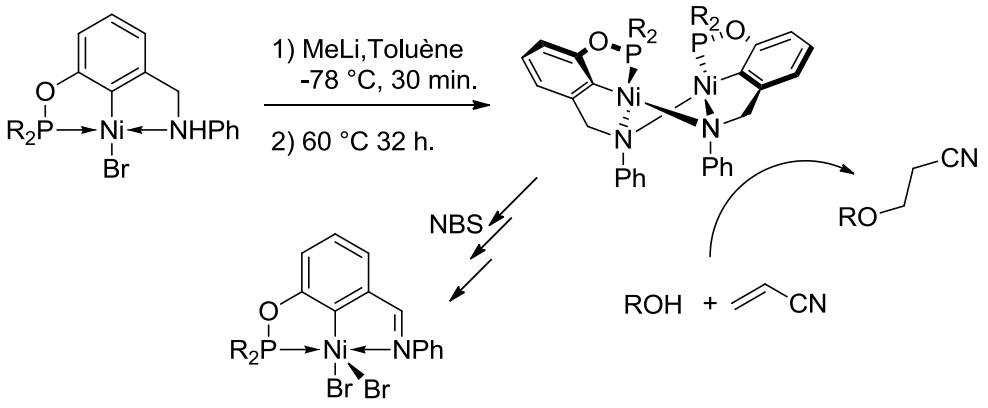

Figure 1.32 Synthèse et réactivité d'un complexe {(μ^N-POCN)Ni}$_2$.

Song, Gong et al. ont reporté le premier complexe POCN de nickel chiral (figure 1.33). La synthèse du complexe ce fait en 5 étapes en terminant par une phosphorylation / metallation "one pot".[88] Si les complexes de palladium catalysent le couplage asymétrique de Suzuki-Miyaura, les complexes de nickel sont inactifs. Le complexe PNCN analogue effectue l'hydrodiphénylphosphination de la chalcone. La réaction se fait 25 °C en présence de 10 % de KOAc et 5% de catalyseur pendant 12 h dans le dichlorométhane avec 1.5 eq. de chalcone, suivi par l'oxydation de la phosphine par H_2O_2. Un rendement de 45% est obtenu, mais aucune chiralité n'est induite. De meilleurs résultats sont obtenus avec les complexes analogues de palladium. [89] Le mécanisme proposé dans le cas du palladium ferait intervenir la formation initiale d'un complexe Pd-OAc suivi d'une transphosphination par $HPPh_2$ et la formation d'acide acétique. L'addition de la chalcone aurait ensuite lieu suivie d'une

étape de protonolyse par l'acide acétique libérant ainsi le produit final et reformant le complexe Pd-OAc.

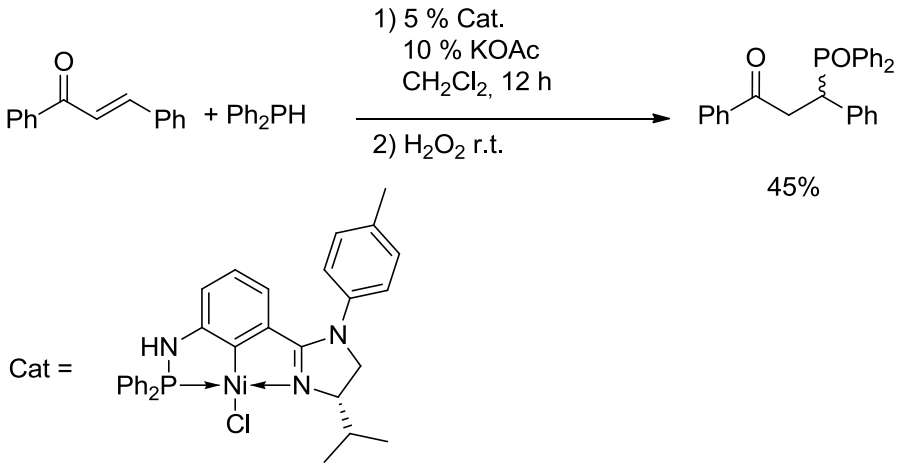

Figure 1.33 Hydro diphénylphosphination de la chalcone par un complexe PNCNP de nickel.

1.4 Objectifs de la thèse

Ma thèse a plusieurs objectifs regroupés autour de la synthèse de complexes cyclonickellés ayant un ligand de type phosphinite. Trois thèmes principaux ont été développés : les complexes pinces POCOP de nickel (II), les nouveaux complexes pinces PIMCOP et leur dérivés PIMIOCOP et NHCCOP et enfin les complexes orthonickellés de diisopropyl(phényl)phosphinite.

Les complexes $POC_{sp2}OP$ de nickel ont été développés depuis un peu moins d'un décennie. Ils font l'objet d'applications remarquables (*vide supra*). Ils sont facilement synthétisés à partir d'un précurseur dihalogénés de nickel (II) NiX_2 (X= Cl, Br, I). Le mécanisme de cette synthèse est développé au chapitre 2 (figure 1.34).

L'étude se porte particulièrement sur la facilité avec laquelle le lien C-H est activé. Les conclusions de ce projet permettront de faciliter le développement de système pouvant activer des liens C-H. Les nombreux dérivés synthétisés au cours de cette étude ont été caractérisés pour comprendre l'influence des substituants du squelette aromatique sur les propriétés spectroscopiques, électroniques et structurales des complexes. Finalement, une nouvelle méthode de synthèse "one pot" à partir de nickel métallique en poudre a été développée. Cette méthode plus "verte" permet d'éviter l'utilisation de dihalogènes lors de la synthèse du précurseur de nickel, et diminue le coût de la synthèse de ces composés. Le prix d'un complexe (POCOP)Ni(Cl) ainsi estimé à 6 $ / g (2.6 $ / mmol) reste néanmoins très dépendant du prix de ClP^iPr_2.[90] La synthèse et la réactivité des dérivés (POCOP)Ni(F) et (POCOP)Ni(CF_3) a été investiguée avec les bromure de benzyle.

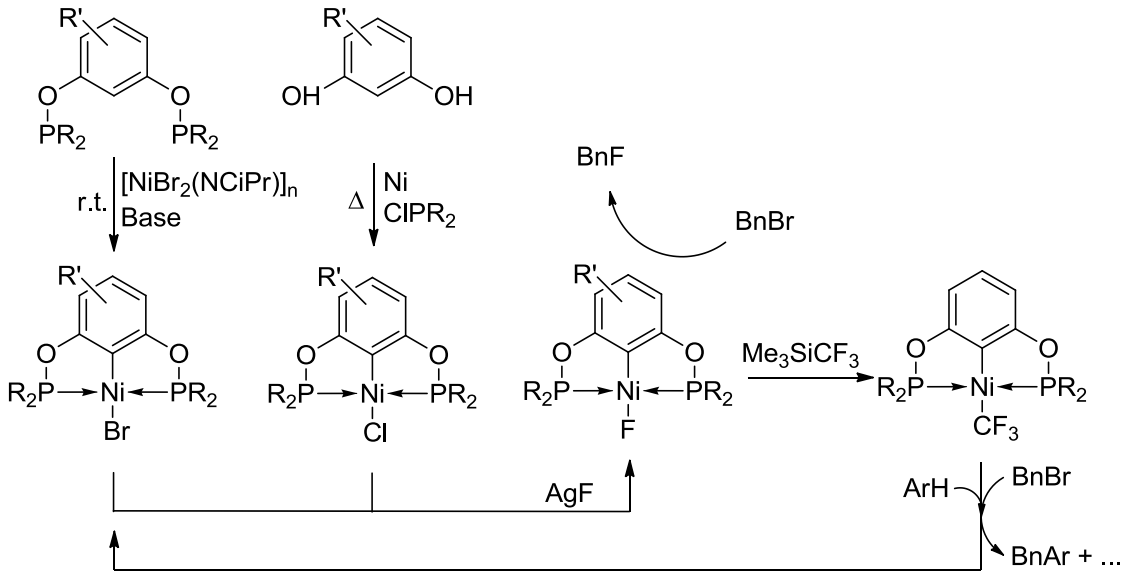

Figure 1.34 Chimie des composés (POCOP)Ni développée dans cette thèse.

La seconde partie concerne la synthèse de nouveaux ligands et complexes PIMCOP développés en collaboration avec l'équipe R. Chauvin du LCC (Laboratoire de Chimie de Coordination, Toulouse, France) (figure 1.35). La formation d'un complexe PIMIOCOP mène à un nouveau complexe de type NHCCOP comportant un carbène N-hétérocyclique rare pour les complexes pinces de nickel. Les dérivés cationiques sont synthétisés et utilisés pour la synthèse d'amidines à partir de benzonitrile.

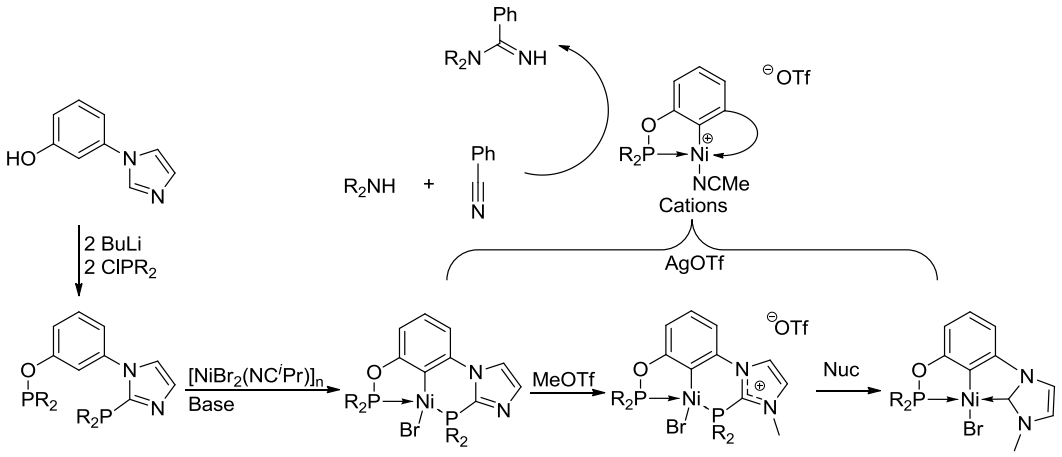

Figure 1.35 Chimie des composés PIMCOP, PIMIOCOP et NHCCOP de Ni(II) développée dans cette thèse.

Enfin de nouveaux complexes cyclonickellés ont été synthétisés à partir de diisopropyl(phényl)phosphinite et de bromure de nickel par activation C-H (figure 1.36). Des intermédiaires de réaction ont été identifiés. Leur réaction avec un électrophile mène à la fonctionnalisation en ortho de la phosphinite.

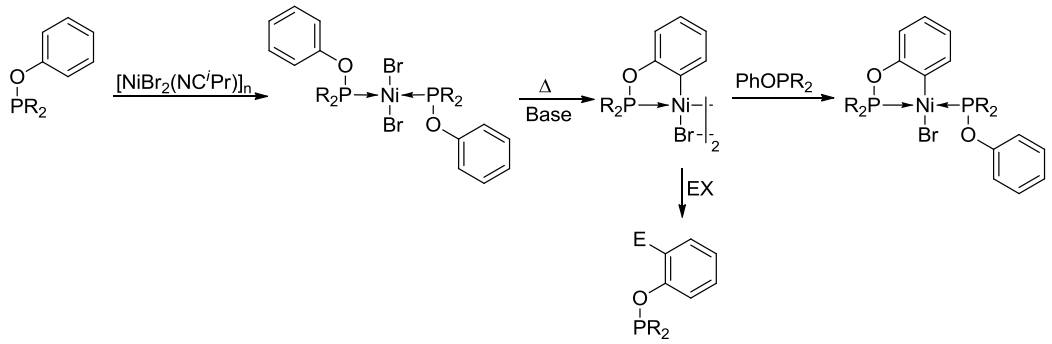

Figure 1.36 Chimie des composés cyclométallés de Ni(II) comportant un motif $PhOPR_2$ développée dans cette thèse.

1.5 Références

[1] *Organometallic Pincer Chemistry*; van Koten, G.; Milstein, D., Eds.; Springer Berlin, Heidelberg, **2013**; Vol. 40, pp. 1–20

[2] (a) G. T. Venkanna, S. Tammineni, H. D. Arman, Z. J. Tonzetich, *Organometallics* **2013**, *32*, 4656 (b) M. J. Ingleson, M. Pink, J. C. Huffman, H. Fan, K. G. Caulton, *Organometallics* **2006**, *25*, 1112.

[3] (a) S. Wu, X. Li, Z. Xiong, W. Xu, Y. Lu, H. Sun, *Organometallics* **2013**, *32*, 3227. (b) D. F. MacLean, R. McDonald, M. J. Ferguson, A. J. Caddell, L. Turculet, *Chem. Commun.* **2008**, 5146

[4] M. Mazzeo, M. Strianese, O. Kühl, J. C. Peters, *Dalton Transactions* **2011**, *40*, 9026.

[5] H. Ogawa, M. Yamashita, *Dalton Trans.* **2013**, *42*, 625.

[6] I. D'Auria, M. Lamberti, M. Mazzeo, S. Milione, C. Pellecchia, *J. Polym. Sci. A Polym. Chem.* **2014**, *52*, 49.

[7] D. E. Herbert, A. D. Miller, O. V. Ozerov, *Chem. Eur. J.* **2012**, *18*, 7696.

[8] R. Jambor, B. Kašná, K. N. Kirschner, M. Schürmann, K. Jurkschat, *Angew. Chem. Int. Ed.* **2008**, *47*, 1650.

[9] C.-H. Ottosson, D. Cremer, *Organometallics* **1996**, *15*, 5309.

[10] M. F. Davidson, D. M. Grove, G. van Koten, A. L. Spek, *J. Chem. Soc., Chem. Commun.* **1989**, 1562.

[11] M. Gandelman, A. Vigalok, L. J. W. Shimon, D. Milstein, *Organometallics* **1997**, *16*, 3981.

[12] (a) J.-P. Sutter, S. L. James, P. Steenwinkel, T. Karlen, D. M. Grove, N. Veldman, W. J. J. Smeets, A. L. Spek, G. van Koten, *Organometallics* **1996**, *15*, 941. (b) J. G. Donkervoort, J. T. B. H. Jastrzebski, B.-J. Deelman, H. Kooijman, N. Veldman, A. L. Spek, G. van Koten, *Organometallics* **1997**, *16*, 4174.

[13] (a) R. E. Andrew, A. B. Chaplin, *Dalton Trans.* **2014**, *43*, 1413. (b) Kuroda, J.; Inamoto, K.; Hiroya, K.; Doi, T. *Eur. J. Org. Chem.* **2009**, *2009*, 2251.

[14] (a) K. S. Sandhya, C. H. Suresh, *Organometallics* **2013**, *32*, 2926. (b) L. Schwartsburd, M. A. Iron, L. Konstantinovski, E. Ben-Ari, D. Milstein, *Organometallics* **2011**, *30*, 2721.

[15] Prechtl, M. H. G.; Wobser, K.; Theyssen, N.; Ben-David, Y.; Milstein, D.; Leitner, W. *Catal. Sci. Technol.* **2012**, *2*, 2039.

[16] J. C. Peters, S. B. Harkins, S. D. Brown, M. W. Day, *Inorg. Chem.* **2001**, *40*, 5083.

[17] Cambridge Crystallographic Data Base, www.ccdc.cam.ac.uk d'après *Organometallic Pincer Chemistry*; van Koten, G.; Milstein, D., Eds.; Springer Berlin, Heidelberg, **2013**; Vol. 40, pp. 1–20

[18] (a) C. J. Moulton, B. L. Shaw, *J. Chem. Soc., Dalton Trans.* **1976**, 1020. (b) Shaw synthétisera aussi les premiers complexes PCP aliphatiques : Empsall, H. D.; Hyde, E. M.; Markham, R.; McDonald, W. S.; Norton, M. C.; Shaw, B. L.; Weeks, B. *J. Chem. Soc., Chem. Commun.* **1977**, 589.

[19] Van Koten, G. *Pure Appl. Chem.* **1989**, *61*.

[20] Anderson, B. G.; Spencer, J. L. *Chem. Eur. J.* **2014**, *20*, 6421.

[21] Van der Boom, M. E.; Liou, S.-Y.; Shimon, L. J. W.; Ben-David, Y.; Milstein, D. *Inorganica Chimica Acta* **2004**, *357*, 4015.

[22] Van der Boom, M. E.; Liou, S.-Y.; Ben-David, Y.; Shimon, L. J. W.; Milstein, D. *J. Am. Chem. Soc.* **1998**, *120*, 6531.

[23] Van der Boom, M. E.; Kraatz, H.-B.; Ben-David, Y.; Milstein, D. *Chem. Commun.* **1996**, 2167.

[24] Van der Boom, M. E.; Kraatz, H.-B.; Hassner, L.; Ben-David, Y.; Milstein, D. *Organometallics* **1999**, *18*, 3873.

[25] Gauvin, R. M.; Rozenberg, H.; Shimon, L. J. W.; Milstein, D. *Organometallics* **2001**, *20*, 1719.

[26] Van der Boom, M. E.; Milstein, D. *Chemical Reviews* **2003**, *103*, 1759.

[27] Meijer, M. D.; Ronde, N.; Vogt, D.; van Klink, G. P. M.; van Koten, G. *Organometallics* **2001**, *20*, 3993–4000.

[28] Fossey, J. S.; Richards, C. J. *Organometallics* **2002**, *21*, 5259.

[29] Ito, J.; Nishiyama, H. *Synlett* **2012**, *23*, 509.

[30] Shao, D.-D.; Niu, J.-L.; Hao, X.-Q.; Gong, J.-F.; Song, M.-P. *Dalton Trans.* **2011**, *40*, 9012.

[31] Adams, J. J.; Lau, A.; Arulsamy, N.; Roddick, D. M. *Inorg. Chem.* **2007**, *46*, 11328.

[32] Oulié, P.; Nebra, N.; Saffon, N.; Maron, L.; Martin-Vaca, B.; Bourissou, D. *J. Am. Chem. Soc.* **2009**, *131*, 3493.

[33] Grove, D. M.; Van Koten, G.; Ubbels, H. J. C.; Zoet, R.; Spek, A. L. *Organometallics* **1984**, *3*, 1003.

[34] Van der Boom, M. E.; Ben-David, Y. *Chem. Commun.* **1998**, 917.

[35]Liou, S.-Y.; Gozin, M.; Milstein, D. *J. Chem. Soc., Chem. Commun.* **1995**, 1965.

[36] Rybtchinski, B.; Vigalok, A.; Ben-David, Y.; Milstein, D. *J. Am. Chem. Soc.* **1996**, *118*, 12406.

[37] Takenaka, K.; Minakawa, M.; Uozumi, Y. *J. Am. Chem. Soc.* **2005**, *127*, 12273.

[38] Van Koten, G.; Timmer, K.; Noltes, J. G.; Spek, A. L. *J. Chem. Soc., Chem. Commun.* **1978**, 250.

[39] Jambor R. and Dostál L. "The Chemistry of Pincer Complexes of 13–15 Main Group Elements" in Organometallic Pincer Chemistry, ed. G. van Koten and D. Milstein, Top. Organomet. Chem. (2013) 40: 175–202; Springer-Verlag Berlin Heidelberg 2013; DOI: 10.1007/978-3-642-31081-2_6.

[40] Van Koten, G.; Jastrzebski, J. T. B. H.; Noltes, J. G.; Spek, A. L.; Schoone, J. C. *J. Organomet. Chem.* **1978**, *148*, 233.

[41] (a) Gossage, R. A.; Jastrzebski, J. T. B. H.; van Koten, G. *Angew. Chem. Int. Ed.* **2005**, *44*, 1448. (b) Albrecht, M.; van Koten, G. *Angew. Chem. Int. Ed.* **2001**, *40*, 3750.

[42] Chuchuryukin, A. V.; Huang, R.; van Faassen, E. E.; van Klink, G. P. M.; Lutz, M.; Chadwick, J. C.; Spek, A. L.; van Koten, G. *Dalton Trans.* **2011**, *40*, 8887.

[43] Contel, M.; Stol, M.; Casado, M. A.; van Klink, G. P. M.; Ellis, D. D.; Spek, A. L.; van Koten, G. *Organometallics* **2002**, *21*, 4556.

[44] Dijkstra, H. P.; Albrecht, M.; Medici, S.; van Klink, G. P. M.; van Koten, G. *Adv. Synth. Catal.* **2002**, *344*, 1135.

[45] (a) Dani, P.; Karlen, T.; Gossage, R. A.; Smeets, W. J. J.; Spek, A. L.; van Koten, G. *J. Am. Chem. Soc.* **1997**, *119*, 11317. (b) Dani, P.; Albrecht, M.; van Klink, G. P. M.; van Koten, G. *Organometallics* **2000**, *19*, 4468.

[46] Albrecht, M.; Dani, P.; Lutz, M.; Spek, A. L.; van Koten, G. *J. Am. Chem. Soc.* **2000**, *122*, 11822.

[47] Selon le moteur de recherche de "SciFinder®" consulté sur le site web le 17 Mai 2014 à l'adresse suivante :
https://scifinder.cas.org/scifinder/view/scifinder/scifinderExplore.jsf

[48] Zargarian, D.; Castonguay, A.; Spasyuk, D. M. in “ECE-Type Pincer Complexes of Nicekl” in Organometallic Pincer Chemistry, ed. G. van Koten and D. Milstein, Top. Organomet. Chem. (2013) 40: 131–174; Springer-Verlag Berlin Heidelberg 2013; DOI: 10.1007/978-3-642-31081-2_5.

[49] (a) Adhikari, D.; Huffman, J. C.; Mindiola, D. J. *Chem. Commun.* **2007**, 4489. (b) Vechorkin, O.; Barmaz, D.; Proust, V.; Hu, X. *J. Am. Chem. Soc.* **2009**, *131*, 12078. (c) Csok, Z.; Vechorkin, O.; Harkins, S. B.; Scopelliti, R.; Hu, X. *J. Am. Chem. Soc.* **2008**, *130*, 8156. (d) Breitenfeld, J.; Ruiz, J.; Wodrich, M. D.; Hu, X. *J. Am. Chem. Soc.* **2013**, *135*, 12004. (e) Ozerov, O. V.; Guo, C.; Fan, L.; Foxman, B. M. *Organometallics* **2004**, *23*, 5573. (f) Ingleson, M. J.; Fullmer, B. C.; Buschhorn, D. T.; Fan, H.; Pink, M.; Huffman, J. C.; Caulton, K. G. *Inorg. Chem.* **2008**, *47*, 407.

[50] Mitton, S. J.; McDonald, R.; Turculet, L. *Angew. Chem. Int. Ed.* **2009**, *48*, 8568

[51] Gwynne, E. A.; Stephan, D. W. *Organometallics* **2011**, *30*, 4128.

[52] Kruithof, C. A.; Dijkstra, H. P.; Lutz, M.; Spek, A. L.; Gebbink, R. J. M. K.; van Koten, G. *Organometallics* **2008**, *27*, 4928.

[53] (a) A. Liu, X. Zhang, and W. Chen, *Organometallics*, 2009, **28**, 4868. (b) T. K. Hollis and X. Zhang, Patent Application PCT , WO2011/050003 A2

[54] Schmeier, T. J.; Hazari, N.; Incarvito, C. D.; Raskatov, J. A. *Chem. Commun.* **2011**, *47*, 1824.

[55] (a) Levina, V. A.; Rossin, A.; Belkova, N. V.; Chierotti, M. R.; Epstein, L. M.; Filippov, O. A.; Gobetto, R.; Gonsalvi, L.; Lledós, A.; Shubina, E. S.; Zanobini, F.; Peruzzini, M. *Angew. Chem. Int. Ed.* **2011**, *50*, 1367. (b) Rossin, A.; Peruzzini, M.; Zanobini, F. *Dalton Trans.* **2011**, *40*, 4447.

[56] Boro, B. J.; Duesler, E. N.; Goldberg, K. I.; Kemp, R. A. *Inorg. Chem.* **2009**, *48*, 5081.

[57] Martínez-Prieto, L. M.; Melero, C.; del Río, D.; Palma, P.; Cámpora, J.; Álvarez, E. *Organometallics* **2012**, *31*, 1425.

[58] Castonguay, A.; Spasyuk, D. M.; Madern, N.; Beauchamp, A. L.; Zargarian, D. *Organometallics* **2009**, *28*, 2134.

[59] Luca, O. R.; Blakemore, J. D.; Konezny, S. J.; Praetorius, J. M.; Schmeier, T. J.; Hunsinger, G. B.; Batista, V. S.; Brudvig, G. W.; Hazari, N.; Crabtree, R. H. *Inorg. Chem.* **2012**, *51*, 8704.

[60] Luca, O. R.; Blakemore, J. D.; Konezny, S. J.; Praetorius, J. M.; Schmeier, T. J.; Hunsinger, G. B.; Batista, V. S.; Brudvig, G. W.; Hazari, N.; Crabtree, R. H. *Inorg. Chem.* **2012**, *51*, 8704.

[61] Castonguay, A.; Sui-Seng, C.; Zargarian, D.; Beauchamp, A. L. *Organometallics* **2006**, *25*, 602.

[62] Castonguay, A.; Beauchamp, A. L.; Zargarian, D. *Organometallics* **2008**, *27*, 5723.

[63] Pour un complexe NCN de Rh(II) (non métallé) voir : (a) Gerisch, M.; Krumper, J. R.; Bergman, R. G.; Tilley, T. D. *Organometallics* **2003**, *22*, 47. Pour un complexe pince NCN macrocycle de Cu(III) voir : (b) Xifra, R.; Ribas, X.; Llobet, A.; Poater, A.; Duran, M.; Solà, M.; Stack, T. D. P.; Benet-Buchholz, J.; Donnadieu, B.; Mahía, J.; Parella, T. *Chem. Eur. J.* **2005**, *11*, 5146. Pour un complexe NCN de Ru(III) voir : (c) Steenwinkel, P.; Grove, D. M.; Veldman, N.; Spek, A. L.; van Koten, G. *Organometallics* **1998**, *17*, 5647.

[64] Grove, D. M.; Van Koten, G.; Zoet, R.; Murrall, N. W.; Welch, A. J. *J. Am. Chem. Soc.* **1983**, *105*, 1379.

[65] Grove, D. M.; Van Koten, G.; Mul, P.; Zoet, R.; Van der Linden, J. G. M.; Legters, J.; Schmitz, J. E. J.; Murrall, N. W.; Welch, A. J. *Inorg. Chem.* **1988**, *27*, 2466.

[66] Sasson, Y.; Rempel, G. L. *Synthesis* **1975**, *1975*, 448.

[67] Singleton, J. T. *Tetrahedron* **2003**, *59*, 1837.

[68] (a) Grove, D. M.; Van Koten, G.; Verschuuren, A. H. M. *J. Mol. Catal.* **1988**, *45*, 169. (b) Grove, D. M.; Verschuuren, A. H. M.; van Koten, G.; van Beek, J. A. M. *J. Organomet. Chem.* **1989**, *372*, C1–C6. (c) Van de Kuil, L. A.; Grove, D. M.; Gossage, R. A.; Zwikker, J. W.; Jenneskens, L. W.; Drenth, W.; van Koten, G. *Organometallics* **1997**, *16*, 4985.

[69] Van de Kuil, L. A.; Veldhuizen, Y. S. J.; Grove, D. M.; Zwikker, J. W.; Jenneskens, L. W.; Drenth, W.; Smeets, W. J. J.; Spek, A. L.; van Koten, G. *Recl. Trav. Chim. Pays-Bas* **1994**, *113*, 267.

[70] (a) Knapen, J. W. J.; van der Made, A. W.; de Wilde, J. C.; van Leeuwen, P. W. N. M.; Wijkens, P.; Grove, D. M.; van Koten, G. *Nature* **1994**, *372*, 659. (b) Gossage, R. A.; Jastrzebski, J. T. B. H.; van Ameijde, J.; Mulders, S. J. E.; Brouwer, A. J.; Liskamp, R. M. J.; van Koten, G. *Tet. Lett.* **1999**, *40*, 1413.

[71] Kleij, A. W.; Gossage, R. A.; Klein Gebbink, R. J. M.; Brinkmann, N.; Reijerse, E. J.; Kragl, U.; Lutz, M.; Spek, A. L.; van Koten, G. *J. Am. Chem. Soc.* **2000**, *122*, 12112.

[72] Fossey, J. S.; Richards, C. J. *J. Organomet. Chem.* **2004**, *689*, 3056.

[73] Mitsudo, K.; Imura, T.; Yamaguchi, T.; Tanaka, H. *Tet. Lett.* **2008**, *49*, 7287.

[74] Gómez-Benítez, V.; Baldovino-Pantaleón, O.; Herrera-Álvarez, C.; Toscano, R. A.; Morales-Morales, D. *Tet. Lett.* **2006**, *47*, 5059.

[75] Zhang, J.; Medley, C. M.; Krause, J. A.; Guan, H. *Organometallics* **2010**, *29*, 6393.

[76] (a) Lefèvre, X.; Durieux, G.; Lesturgez, S.; Zargarian, D. *J. Mol. Catal. A Chem.* **2011**, *335*, 1 (b) Salah, A. B.; Offenstein, C.; Zargarian, D. *Organometallics* **2011**, *30*, 5352.

[77] Chakraborty, S.; Krause, J. A.; Guan, H. *Organometallics* **2009**, *28*, 582.

[78] Chakraborty, S.; Patel, Y. J.; Krause, J. A.; Guan, H. *Polyhedron* **2012**, *32*, 30.

[79] (a) Chakraborty, S.; Zhang, J.; Krause, J. A.; Guan, H. *J. Am. Chem. Soc.***2010**, *132*, 8872. (b) Huang, F.; Zhang, C.; Jiang, J.; Wang, Z.-X.; Guan, H. *Inorg. Chem.* **2011**, *50*, 3816.

[80] Chakraborty, S.; Patel, Y. J.; Krause, J. A.; Guan, H. *Angew. Chem. Int. Ed.* **2013**, *52*, 7523.

[81] Pandarus, V.; Zargarian, D. *Chem. Commun.* **2007**, 978.

[82] Pandarus, V.; Zargarian, D. *Organometallics* **2007**, *26*, 4321.

[83] Hao, J.; Mougang-Soumé, B.; Vabre, B.; Zargarian, D. *Angew. Chem. Int. Ed.* **2014**, *53*, 3218.

[84] Hao, J..; Vabre, B.; Zargarian, D *résultats non publiés*

[85] Spasyuk, D. M.; Zargarian, D.; van der Est, A. *Organometallics* **2009**, *28*, 6531.

[86] Spasyuk, D. M.; Zargarian, D. *Inorg. Chem.* **2010**, *49*, 6203.

[87] Spasyuk, D. M.; Gorelsky, S. I.; van der Est, A.; Zargarian, D. *Inorg. Chem.* **2011**, *50*, 2661.

[88] Zhang, B.-S.; Wang, W.; Shao, D.-D.; Hao, X.-Q.; Gong, J.-F.; Song, M.-P. *Organometallics* **2010**, *29*, 2579.

[89] Yang, M.-J.; Liu, Y.-J.; Gong, J.-F.; Song, M.-P. *Organometallics* **2011**, *30*, 3793.

[90] Calculé selon les prix des réactifs du catalogue Sigma-Aldrich®

Chapitre 2 : On The Nickellation of PCP- and POCOP-Type Pincer Ligands: Kinetics and Mechanism

Article 1

Boris Vabre,[†] Melinda L. Lambert,[‡] Alban Petit,[‡] Daniel H. Ess,[‡] and Davit Zargarian[†]

[†]Département de chimie, Université de Montréal, Montréal (Québec), Canada H3C 3J7

[‡]Department of Chemistry and Biochemistry, Brigham Young University, Provo, Utah, United States of America, 84602

Organometallics **2012**, *31*, 6041–6053

Chapitre 2

2.1 Abstract

This report describes the results of a combined experimental and computational investigation on the kinetics and mechanism of the C-H metallation step involved in the formation of PCP- and POCOP-type complexes of nickel. The kinetics of C-H nickellation reaction was probed through competition studies involving two ligands reacting with a sub-stoicheometric quantity of $\{(i\text{-}PrCN)NiBr_2\}_n$. These experiments have confirmed that metallation is more facile for: aromatic ligands 1,3-(i-$Pr_2PE)_2C_6H_4$ vs. their aliphatic counterparts 1,3-(i-$Pr_2PECH_2)_2CH_2$ (sp^2 C-H > sp^3 C-H; E= O or CH_2); ligands bearing phosphine moieties vs. those with phosphinite moieties (PCP>POCOP); ligands bearing *P*-substituents i-Pr_2P vs. t-Bu_2P and Ph_2P; and $POC_{sp2}OP$ ligands 1,3-(i-$Pr_2PO)_2C_6R_nH_{4-n}$ bearing electron-donating vs. electron-withdrawing substituents (*p*-OMe~*m*-OMe>*p*-Me>*m*-CO_2Me>*p*-CO_2Me>*m,m*-Cl_2). Among the latter, there is a six-fold difference in C-H metallation rate between ligands bearing *p*-OMe and *p*-COOMe, whereas the most readily metallating ligand, 1,3-(i-$Pr_2PCH_2)_2C_6H_4$, is metallated ca. 270 times more readily relative to the least reactive ligand, 1,3-(i-$Pr_2POCH_2)_2CH_2$. DFT studies indicate that PCP- or POCOP-type pincer ligands react with $NiBr_2$ to generate non-metallated intermediates that form the corresponding pincer complexes via a two-step mechanism involving an ionic dissociation of the bromide to give a tight ion-pair intermediate, followed by bromide-assisted deprotonation of the C-H moiety. The type of structure adopted by the non-metallated intermediates (mono- or dinuclear; tetrahedral, *cis*- or *trans*-square planar) and the energy barriers for the

metallation transition states depend on the steric properties of the PR_2 moiety. The presence of a base that can neutralize the HBr generated in the metallation step is crucial for rendering the metallation process exergonic. One rationale for the more facile metallation of PCP ligands compared to their POCOP counterparts is the greater donor character of phosphine moieties, which allows a more effective stabilization of the metallation transition state wherein the strongly donor halide ligand is displaced by the much weaker donor C-H moiety. The aromatic ligands metallate more readily than their aliphatic analogues for multiple reasons, including the higher ground state energy of the non-metallated intermediates formed with aromatic ligands, the stronger C_{sp2}-Ni bond forming via the metallation, and the more stabilized anionic charge on the C atom being metallated.

2.2 Introduction

Recent advances in metal-promoted activation of "inert" C-H bonds have facilitated the development of efficient activation-functionalization protocols in organic synthesis.[1,2] Historically, bulk of the experimental efforts dedicated to promoting transition metal-mediated C-H activation reactions has involved complexes of 4d and 5d transition metals. Their stronger M-H and M-C bonds have contributed to our perception of these metals as being much more adept at promoting C-H activation reactions relative to their lighter counterparts. Nevertheless, many reports of C-H activation/metallation by 3d metals have appeared over the past decades, and such reactions are appearing more frequently as a result of increasing

attention being paid to the use of first-row metals in organic synthesis.[3] Indeed, Kleiman and Dubeck reported an early instance of chelate-assisted C-H nickellation nearly 50 years ago,[4] while pincer-type complexes of nickel were among the first such complexes reported. Thus, Shaw showed that heating $[Ni(H_2O)_6]Cl_2$ and 1,3-(*t*-$Bu_2PCH_2)_2$-C_6H_4 in EtOH at 80 °C for 5 min gave the corresponding PCP-type complex **A** shown in figure 2.1.[5]

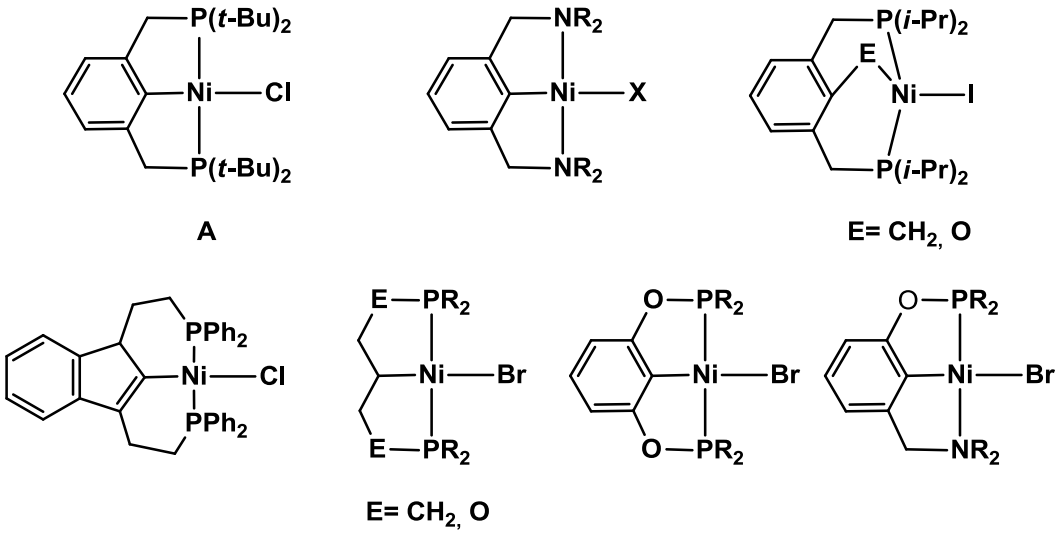

Figure 2.1 Various nickel pincer complexes.

Shaw's early reports have inspired many other groups to use a C-H nickellation strategy for preparing a variety of nickel complexes featuring pincer ligands based on both aromatic and aliphatic skeletons (Scheme 2.1);[6] there is also increasing reliance on direct C-H metallation reactions for preparation of pincer complexes of other 3d metals.[7,8] While formation of a pincer complex is an overall intermolecular metallation process, the C-H metallation step involved in this process is considered to be intramolecular in nature, because it is thought to occur in the intermediate generated following the initial binding of the ligand moieties (double chelate-assisted

activation). In some instances, intermediates en route to a pincer complex featuring a C-H moiety "poised" for metallation have been detected or isolated.[9]

A broad survey of the literature on pincer complexes of nickel reveals that they can be prepared via C-H nickellation in the case of bis(phosphine) (PCP),[6,10] bis(phosphinite) (POCOP),[11,12] and amino(phosphinite) (POCN)[13] ligands, whereas virtually all reported cases of complexes featuring bis(amino) moieties (NCN) are prepared via alternative synthetic routes,[14,15] C-H nickellation being generally inaccessible for this family of ligands.[16] Indeed, the success of C-H nickellation step depends not only on the nature of ligand donor moieties, but also on the hybridization of the C atom being nickellated (sp^2 vs. sp^3), the type of nickel precursor used, and the reaction conditions (temperature, solvent, etc.). The importance of the "linker" moiety is evident from the observation that aromatic ligands of the type 1,3-Q_2-C_6H_4 (Q_2= $(R_2PCH_2)_2$, $(R_2PO)_2$, and R_2PO/R_2NCH_2) nickellate much more readily and in most cases without detectable intermediates,[17] whereas the analogous ligands based on aliphatic backbones generate mixtures of nickellated and non-nickellated products, some of which are illustrated in Scheme 1.[10a,b,18,19]

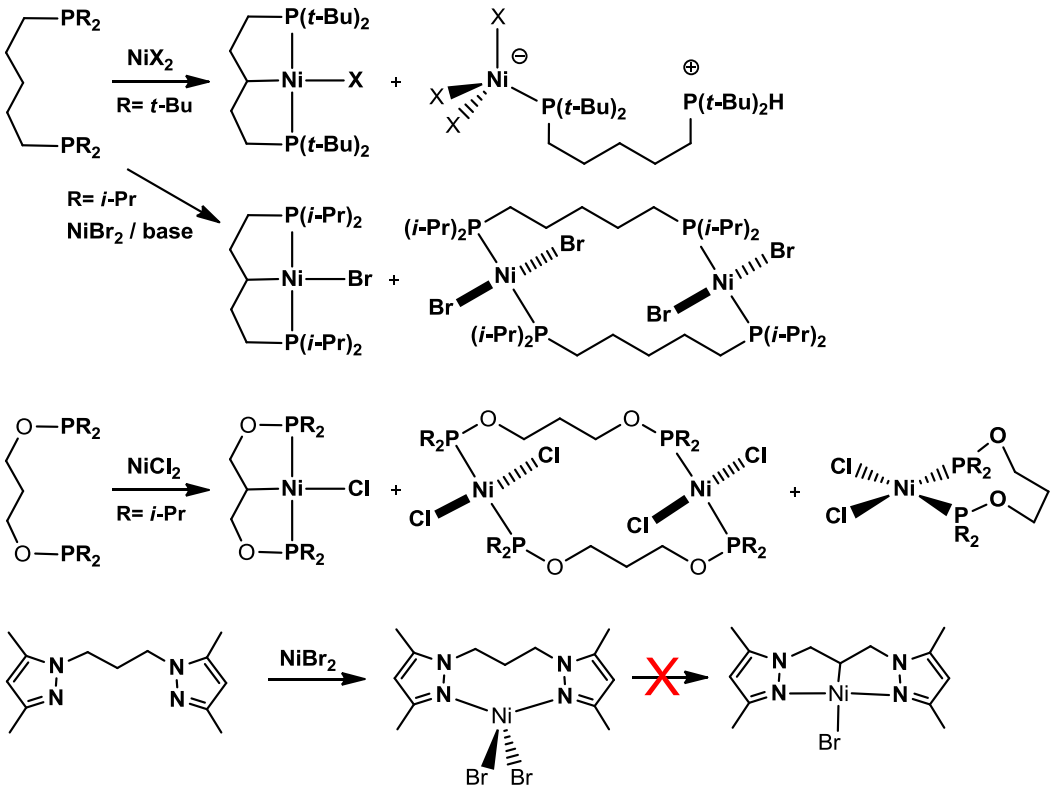

Scheme 2.1 Intermediates of aliphatic nickel pincer complexes.

In an effort to understand the different aptitudes of pincer ligands for C-H nickellation, we have undertaken a combined experimental and computational study to probe the rates and mechanisms of these reactions. The experimental work has sought to quantify the relative nickellation rates for PCP- and POCOP-type pincer ligands as a function of donor moiety (i.e., *P*-substituents), hybridization of the central carbon atom (sp^2 vs. sp^3), and ring substituents R′ in 1,3-$(R_2PO)_2C_6H_nR'_{4-n}$. The computational studies, on the other hand, have focused on identifying the reaction pathways and structures of intermediates and/or transition states, with a view to identifying the factors governing C-H nickellation reactions and shedding light on their mechanisms.[20] The overall objective is to determine whether the C-H

nickellation reactions involved in the synthesis of PCP- and POCOP-type pincer nickel complexes are best viewed as proceeding by oxidative addition/reductive elimination steps, being electrophilic or nucleophilic in nature, or otherwise belonging to other reaction schemes under consideration by the community of researchers.[21]

2.3 Results and Discussion

Experimental Studies.

The ligands required for the kinetic studies are shown in figure 2.2. Ligands **1-4** were selected to quantify how nickellation rates are influenced by the type of donor moiety (PCP vs. POCOP) and linker skeleton (aromatic vs. aliphatic), while **1a-1j** were selected to evaluate the impact of ring-substituents on the nickellation of this family of ligands. The experimental work began by synthesizing the PCP and POCOP using modified versions of previously reported procedures.[22] In general, the POCOP ligands can be prepared by reacting the requisite diol pre-ligands with $ClPR_2$ in the presence of base.[23] This methodology is much more straight forward and often gives better yields compared to the synthesis of PCP ligands, which are obtained from the reaction of suitable dihalides with $[R_2P]^-$ or R_2PH/base.[24,25]

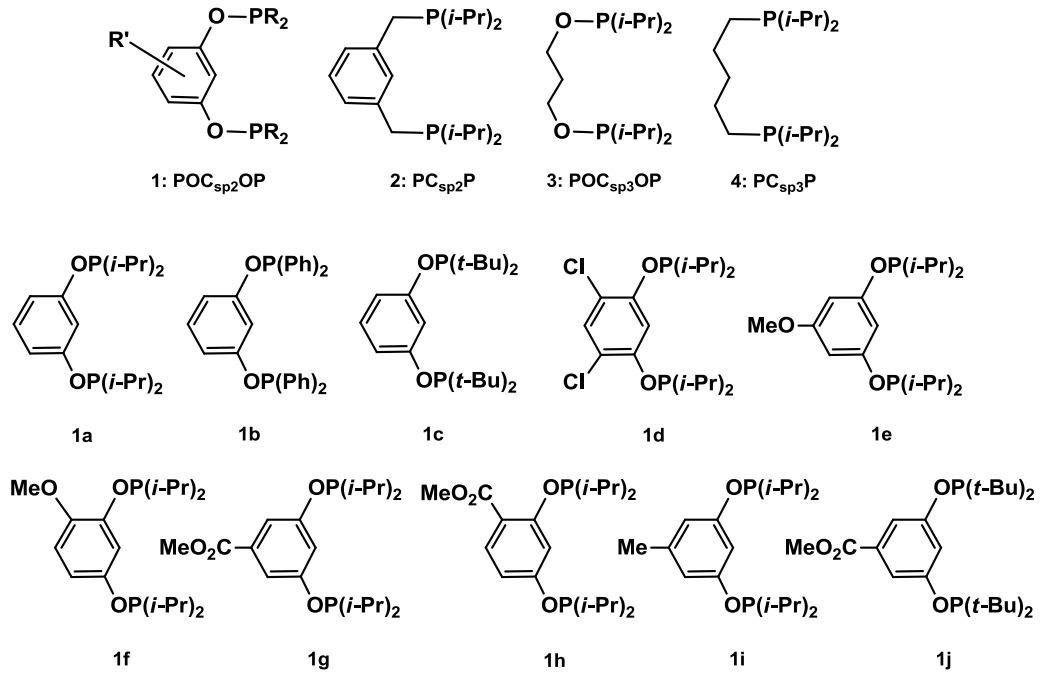

Figure 2.2 Pincer ligands used for this study.

Previous reports have indicated that the choice of Ni precursor and presence of a suitable base are important factors for success in the synthesis of PCP- and POCOP-type pincer complexes.[10,11b,c,13a,18] In our experience, the best precursors for C-H nickellation of pincer ligands are $(MeCN)_nNiBr_2$[26] and $\{(i\text{-PrCN})NiBr_2\}_n$,[27] the latter being more suitable for conducting kinetic studies owing to its well-defined molar mass.[28] The importance of base for the nickellation of PCP ligands has been demonstrated by the low yields of (PCP)NiBr (<50%) and recovery of the protonated (unmetallated) ligand as a precipitate.[10a] Similarly, the complexes (POCN)NiBr can be prepared in 80-90% yields when NEt_3 is added to the reaction mixture, whereas much lower yields are obtained (~35%) in the absence of added base.[13a,b] On the other hand, Morales-Morales's group has reported that refluxing POC^HOP^{Ph} and $NiCl_2$ in toluene in the absence of any added base gives $(POCOP^{Ph})NiCl$ with 80% yield.[11a]

To further probe the importance of base for nickellation of POCOP ligands, we used ^{31}P NMR to monitor the reaction of ligand **1a** with $\{(i\text{-PrCN})NiBr_2\}_n$ in the absence of an added base. The signal for **1a** (148.1 ppm) disappeared over time and we observed a singlet resonance at 188.6 ppm due to the pincer complex (POCOP)NiBr, **1a'**, in addition to a new peak at 134.7 ppm. Addition of NEt_3 to the reaction mixture led to the formation of a white precipitate and caused the suppression of the latter peak and the reappearance of the original signal for ligand **1a**. An independent test established that reaction of **1a** with excess HX generates the diprotic species shown in Scheme 2.2 (no hydrolysis back to resorcinol); we conclude, therefore, that the HX generated during the formation of our pincer complexes must be quenched to prevent protonation of unreacted ligands. Thus, the competition nickellation reactions were conducted in the presence of NEt_3 to ensure that these reactions are driven to completion.

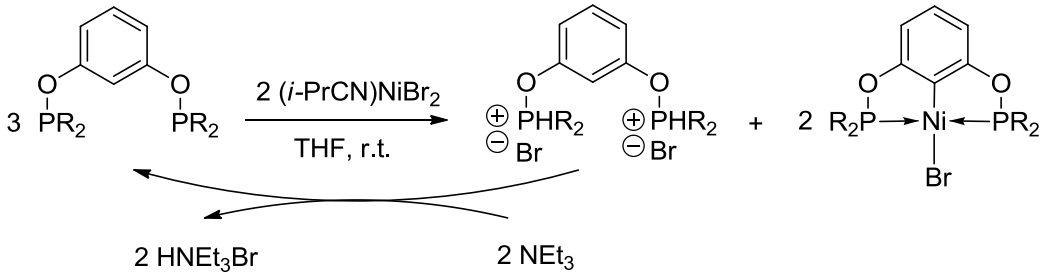

Scheme 2.2 Role of the base on metalation.

Kinetic Studies.

Initial tests showed that UV-vis spectroscopy could not be used for monitoring the metallation reactions due to significant overlap in the absorption energies of some ligands and their respective complexes; in contrast, the $^{31}P\{^{1}H\}$ NMR chemical shifts of various ligands and complexes were free of overlap for the most part, making this the most suitable method for kinetic studies. Preliminary measurements showed that, under the pseudo-first order conditions, nickelation of the aromatic ligands **1** and **2** is too rapid for monitoring by NMR: most reactions were essentially finished in the time of mixing. Employing low reaction temperatures or very dilute sample slowed down these reactions somewhat (2-5 min), but not sufficiently to allow convenient rate measurements.[29] As a result, we have opted to measure *relative* rates of nickelation via competition experiments, as described below.

Relative nickellation rates. The competition experiments were conducted as follows. Mixtures of 1.0-1.1 equiv of each of the two ligands under study were prepared and analyzed by ^{31}P NMR to register the initial molar ratio. THF was used as solvent for mixtures of aromatic ligands **1** and **2**, whereas toluene was used in the case of aliphatic ligands **3** and **4**. Each mixture was then added to a homogenous solution containing $\{(i\text{-PrCN})NiBr_2\}_n$ and NEt_3 stirring at room temperature; the initial Ni : L : L' : NEt_3 molar ratio was approximately 0.75 : 1.0 : 1.0 : 2.0 (eq. 1). Stirring the resulting mixture at room temperature for a few min was sufficient to

nickellate the aromatic ligands **1** and **2**, as signaled by the nearly instantaneous color change from blue to brown and then yellow, followed by the gradual precipitation of a white solid ($HNEt_3Br$). It is worth noting that these mixtures remain homogeneous throughout the reaction, except for the precipitation of the ammonium salt at the end. Nickellation of the aliphatic ligands **3** and **4** followed a different path: stirring the mixture at room temperature caused a color change from blue to deep purple, which changed to yellow only after the reaction mixture was heated to ca. 70-90 °C for 2-3 days. The ^{31}P NMR spectra of these mixtures have established that the yellow color corresponds to the target pincer complexes, whereas the sparingly soluble deep purple species is an NMR silent nonmetallated species described previously.[10a,b,18]

Integration of the ^{31}P signals due to the pincer complexes present in the final reaction mixtures allowed us to establish the relative nickellation aptitudes of the ligands studied. That the nickellation rates can be considered invariable under the conditions of these kinetic studies was confirmed by the observation that no reaction occurs after stirring for 24 h mixtures of complex **1e'** and the free ligand **1a** (1 day at 55°C) or complex **3'** and ligand **4** (70 °C).[30] Most experiments were carried out in triplicate and showed fairly reproducible results, the relative rates varying by ca. 10% on average. The results of these competition experiments are presented in Table 1 and discussed below.

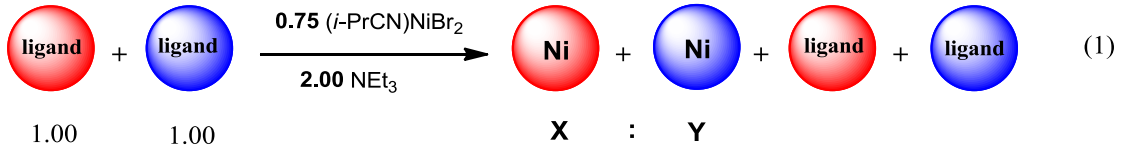

(1)

Table 2.1 Relative nickellation rates for various POCOP and PCP ligands*

Entry	Nickelation Ratio, X : Y	Entry	Nickelation Ratio, X : Y
1	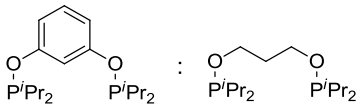 100 : 2	9	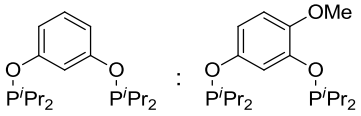 100 : 200
2	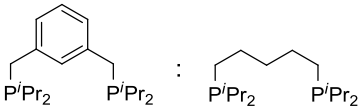 100 : 2	10	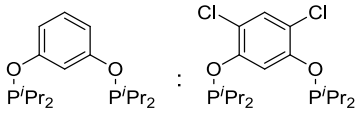 100 : 31
3	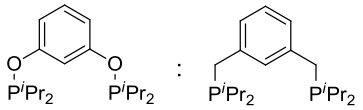 100 : 547	11	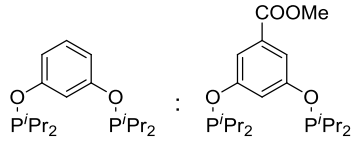 100 : 36
4	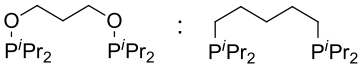 100 : 577	12‡	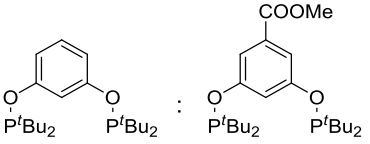 100 : 7
5	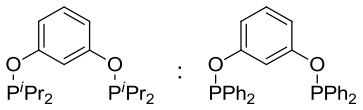 100 : 0	13	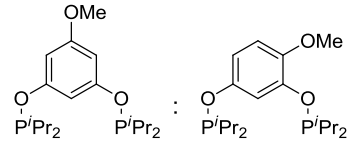 100 : 105
6	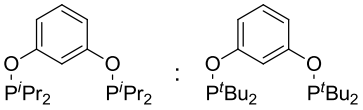 100 : 0	14	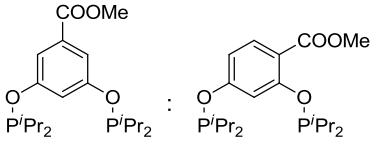 100 : 238
7†	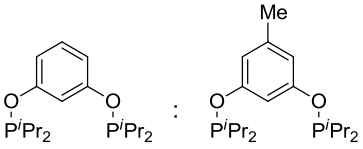 100 : 132	15	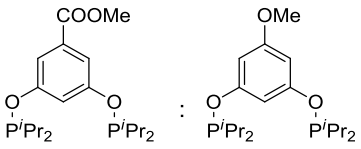 100 : 617

8	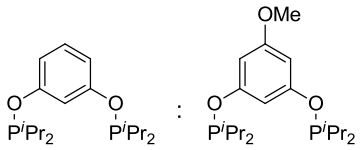 100 : 203	

* For details of the procedure used for conducting these competition studies see the main text or the Experimental section.

† The relative rates of nickellation for these ligands could not be determined directly, because the ^{31}P NMR signals of their complexes overlapped. We integrated, instead, the signals for free ligands remaining after the nickellation and used their ratio for deducing the relative rates of nickelation.

‡ In this case, addition of $\{(i\text{-PrCN})NiBr_2\}_n$ caused the reaction mixture to turn green initially and the nickellation was fairly slow: the mixture was analyzed one hour later after the anticipated white precipitate ($HNEt_3Br$) and yellow color appeared.

The first two entries of Table 1 show the results of competition experiments that served to quantify our previous observations that nickellation is much more facile for the aromatic ligands. Monitoring these experiments by ^{31}P NMR also revealed important insights about how the nickellation proceeds. For instance, holding the reaction mixture containing **1a**/**3**/$\{(i\text{-PrCN})NiBr_2\}_n$/$NEt_3$ at room temperature over several hours led to none of the anticipated nickellated product, **1a'**: the ^{31}P NMR spectra of this mixture showed only the signals for **1a** (major) and **3** (trace), but none for **1a'**, which was unexpected because nickellation of **1a** to **1a'** normally occurs in less than 2 min at room temperature in the absence of **3**. Based on our previous

observation that **3** reacts with $Br_2Ni(NCMe)_n$ to give a non-metallated, NMR-silent species that does not undergo metallation at ambient temperature,[31] we infer that at room temperature the nickel precursor is ligated by the aliphatic ligand **3** and remains trapped in the form of a non-metallated (and NMR-silent) species. Heating the mixture for several hours at 70 °C in the presence of **3** led to the appearance of the pincer complex **1a'** and free ligand **3**, presumably because heating releases the nickel precursor and allows it to react with **1a**. These observations can be rationalized by invoking a reaction scheme under Curtin-Hammett control: the non-metallated intermediates interconvert rapidly via a binding equilibrium that favors ligation of Ni(II) by **3**, and the subsequent nickellation steps are slower and irreversible (Scheme 2.3).

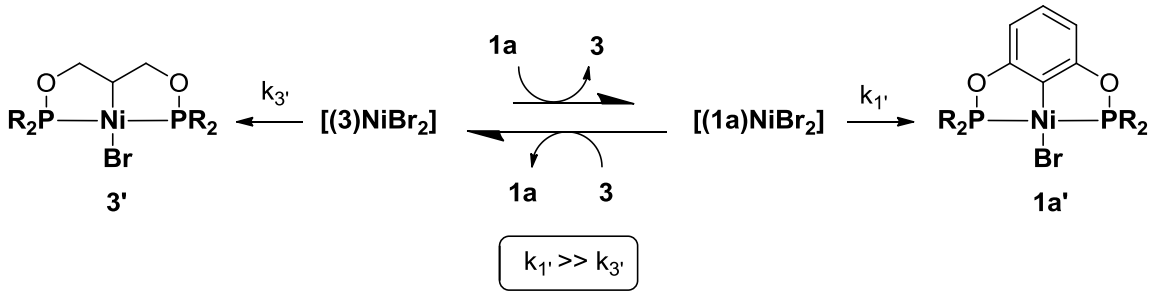

Scheme 2.3 Mechanism of competition reactions.

Next, we probed the question of which donor moiety, phosphine or phopsphinite, would be more adept at facilitating the nickellation of pincer ligands. The results shown in entries 3 and 4 establish that nickellation is more than five times faster for the PCP ligands **2** and **4** vs. their POCOP analogues **1** and **3**. These

observations, combined with the fact that NCN-type ligands 1,3-$(CH_2NR_2)_2$-C_6H_4 do not undergo nickellation,[14,15,16,18] demonstrate the importance of the donor moiety character (PCP>POCOP>>NCN). *P*-substituents were also found to have a major influence on the nickellation rates of $POC_{sp2}OP$ ligands (entries 5 and 6: *i*-Pr_2P >> *t*-Bu_2P, Ph_2P); previous studies have also shown that nickellation proceeds more readily with the PCP ligand **4** compared to its *t*-Bu_2P analogue.[10a,b]

The impact of ring-substituents on the nickellation rates was studied next. Among the variously substituted $POC_{sp2}OP$ ligands, those bearing the electron-donating substituents Me and OMe accelerated the nickellation rates relative to the unsubstituted ligand **1a** (entries 7-9), while ligands bearing electron-withdrawing substituents showed significantly slower nickellation rates (entries 10-12; see SI for a plot of the Hammett parameters). It appears, therefore, that nickellation of these aromatic POCOP ligands is akin to an electrophilic aromatic substitution,[32] whereas the opposite has been observed for direct palladation of aromatic C-H bonds. For instance, the groups of Maseras and Echavaren have demonstrated a Pd-catalyzed C-H activation/cyclization reaction that proceeds preferentially on aromatic rings bearing electron withdrawing groups,[33] and Fagnou's group has reported extensively on the much more facile palladation of electron-poor aromatic rings.[34]

In the case of MeO-substituted ligands, the substitution pattern (*meta* vs. *para*) seems to have little or no effect on metallation (entry 13), which is very different than in the case of MeO_2C-substituted ligands: a *p*-COOMe group appears to be more effective in hindering the nickellation than a *m*-COOMe group (entry 4).[35] Finally, comparison of the results shown in entry 15 vs. entries 3 and 4 demonstrates

that judicious choice of ring substituents can induce as significant an impact on the nickellation rate as induced by the character of the donor moiety. figure 2.3 shows the relative rates of metallation for all the pincer ligands studied here, normalized to the $POC_{sp3}OP$ ligand **3**.

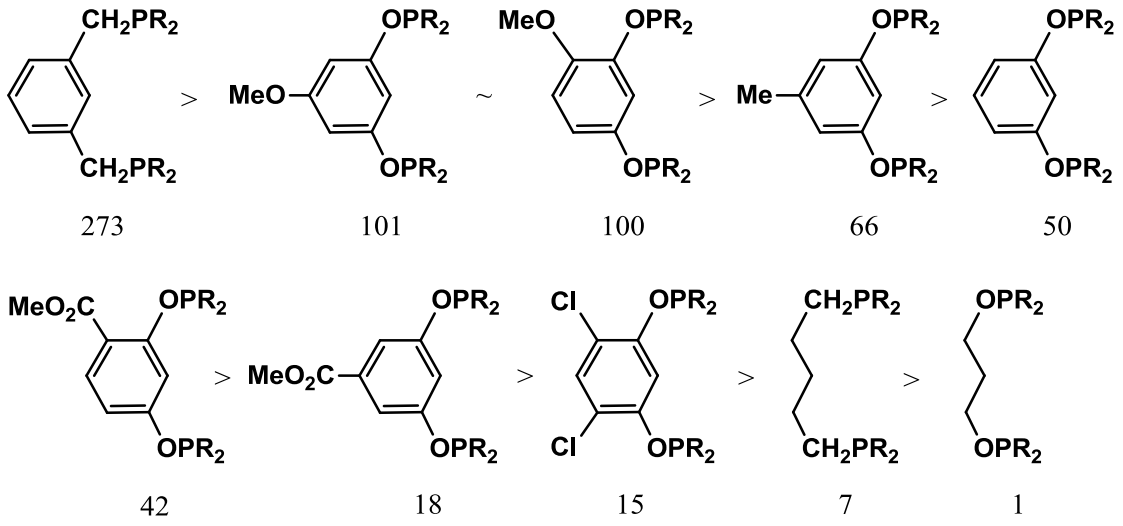

Figure 2.3 Relative nickelation rates for PCP and POCOP ligands.

Density functional investigation.

Nickellation of the PCP and POCOP pincer ligands has been investigated by quantum mechanical calculations to shed light on reaction mechanisms and interpret the observed relative rates of nickellation. Our efforts have focused on identifying possible ground-state structures for the nonmetallated $(LH)NiBr_2$ complexes and the corresponding pincer species LNiBr (L= PCP- and POCOP-type pincer ligands), in addition to any plausible intermediates and transition states involved in the metallation pathway. All stationary point structures presented were verified as minima or saddle points with full calculation of the Hessian using Gaussian 09[36] with

the M06[37] density functional method using an ultrafine integration grid. Choice of M06, which is a hybrid meta functional that was designed for broad applicability including transition metals,[38] was predicated on several recent computational benchmark and experimental comparative studies showing that M06 is the most accurate functional currently available for organometallic systems.[39] In addition, the M06 functional is known to accurately reproduce Ni-P type bond energies whereas many other common density functionals fail.[40] Nevertheless, comparison is also made throughout the present study to results obtained from computations based on B3LYP, BP86, and MPWPW91 functionals.

All optimizations were carried out in implicit THF solvent using the CPCM model combined with UAKS radii. The basis set employed consisted of LANL2TZ(f) with the polarizing f exponent set to 3.130 for Ni, LANL2DZdp for Br, and 6-311G(2d,p) for all other atoms. Unless otherwise noted, all reported energy values are free energies in THF at 298 K. Singlet-triplet spin-crossing (SC) points, also called minimum energy crossing points (MECP), were located using the algorithm developed by Harvey et al. in conjunction with Gaussian 09.[41] The 3D ball and stick structures were rendered using CYLview.[42]

Ground State Ligand Coordination in ($PC_{sp3}^{H}P$)$NiBr_2$. To begin, we have explored tetrahedral as well as *cis*- and *trans*-square planar coordination geometries for the mononuclear nonmetallated species ($PC_{sp3}^{H}P$)$NiBr_2$ **1** (Figure 2.4). As expected, structures featuring square planar geometries (**^{1}trans-1**, **^{1}trans-1-twist**, and **^{1}cis-1)** are singlet species while the tetrahedral species **^{3}tetra-1** is a triplet. Interestingly, **^{3}tetra-1** was found to be the lowest energy structure at the M06 level of

theory, being 4.7, 4.4, and 3.7 kcal/mol lower than **^{1}cis-1**, **^{1}trans-1**, and **^{1}trans-1-twist**, respectively; this difference in stability was found to be even greater (by ca. 10 kcal/mol) when B3LYP functional was used. The observed order of stabilities, which is contrary to the usual preference for square planar structures in $(PR_3)_2NiX_2$, arises mostly from the minimization of CH_2-CH_2 eclipsing interactions in the highly twisted configuration adopted in **^{3}tetra-1** by the $PC_{sp3}{}^HP$ ligand backbone. Among the square planar structures, the eclipsing interactions seem to be highest in **^{1}cis-1**, followed by **^{1}trans-1** and **^{1}trans-1-twist**. Another important factor is the smaller-than-ideal P-Ni-P angles in **^{1}trans-1** (157°) and **^{1}trans-1-twist** (148°) structures compared to the nearly-ideal P-Ni-P angle of ca. 106° in **^{3}tetra-1**. The closest C-H….Ni distance (at 2.367Å in **^{1}trans-1**) does not induce any C-H bond elongation, implying that none of these non-metallated structures involves η^2 C-H agostic interactions.

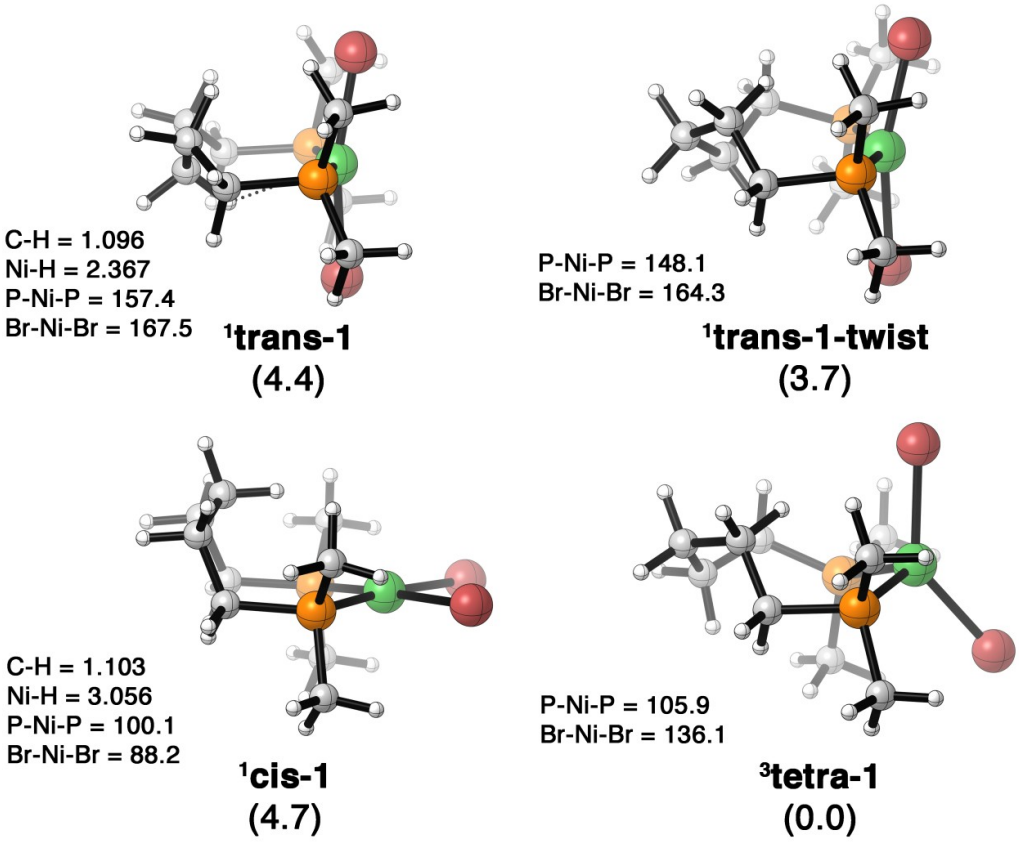

Figure 2.4 Lowest energy square planar and tetrahedral ground-state complexes for the nonmetallated ($PC_{sp3}{}^{H}P$)$NiBr_2$. Free energies relative to **^{3}tetra-1** (kcal/mol).

The structures depicted in Figure 2.5 are for 1:1 $PC_{sp3}{}^{H}P$: $NiBr_2$ species. Exploring the energetics of 2:2 species has led us to the structure *trans,trans*-($PC_{sp3}{}^{H}P)_2Ni_2Br_4$ (**^{1}trans,trans-1**) shown in Figure 2.[43] The conversion of two equivalents of **^{3}tetra-1** into **^{1}trans,trans-1** is exergonic by 7.5 kcal/mol at the M06 level of theory (eq. 2), because this dinuclear structure can adopt a nearly optimal square planar geometry with P-Ni-P angles of ca. 176º. In contrast, B3LYP predicted that conversion of **^{3}tetra-1** to **^{1}trans,trans-1** should be endergonic by 1.3 kcal/mol. However, this endergonic estimate is likely the result of B3LYP overestimating the high-spin state. When *i*-Pr_2P groups were modeled instead of Me_2P, **^{3}tetra-1** was

found to be more stable than **^{1}trans,trans-1** even by M06 (ΔG= 2.1 kcal/mol), indicating that the steric bulk plays a significant role in whether dimeric or monomeric nickel species are favored. It is worth noting that if **^{1}trans,trans-1** is formed, either as a kinetic product or in equilibrium, it must convert to a mononuclear species prior to metallation. In other words, factors leading to stabilization of dimeric structures will likely hinder the metallation step.[44]

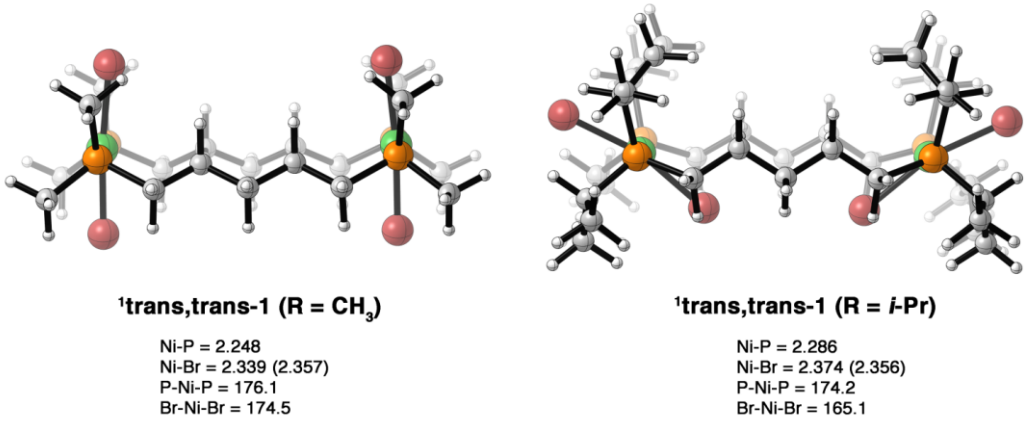

Figure 2.5 Possible non-metallated *trans*-dinuclear species.

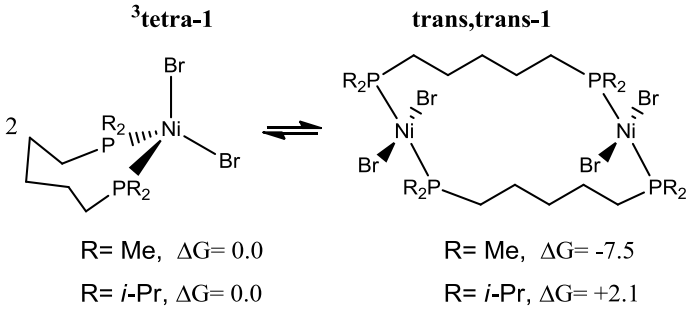

(eq. 2)

Mechanism of (PC$_{sp3}$^{H}P)NiBr$_2$ metallation. The first mechanism we explored for the metallation of (PC$_{sp3}$^{H}P)NiBr$_2$ involves oxidative addition of the central C-H bond of the coordinated ligand onto the Ni^{II} metal center to give an octahedral, tetravalent hydrido-pincer intermediate (Scheme 2.4 a). Oxidative addition is typically a closed-shell process and is unlikely to proceed from the triplet

species **[3]tetra-1**. Accordingly, the lowest energy oxidative addition transition-state structure located for the bromo precursor (X= Br) is the closed-shell singlet **[1]trans-OXadd**, which leads to the hydrido-pincer intermediate **[1]trans-INT** (Figure 2.6). The free energy barrier for this process is 20.7 relative to **[3]tetra-1** and the hydrido-pincer intermediate is endergonic by 19.7 kcal/mol relative to **[3]tetra-1**. It is also worth noting that **[1]trans-INT** faces a reductive elimination barrier of only 1.4 kcal/mol; such shallow M-H intermediates have also been detected in other oxidative addition reactions analyzed by DFT.[45]

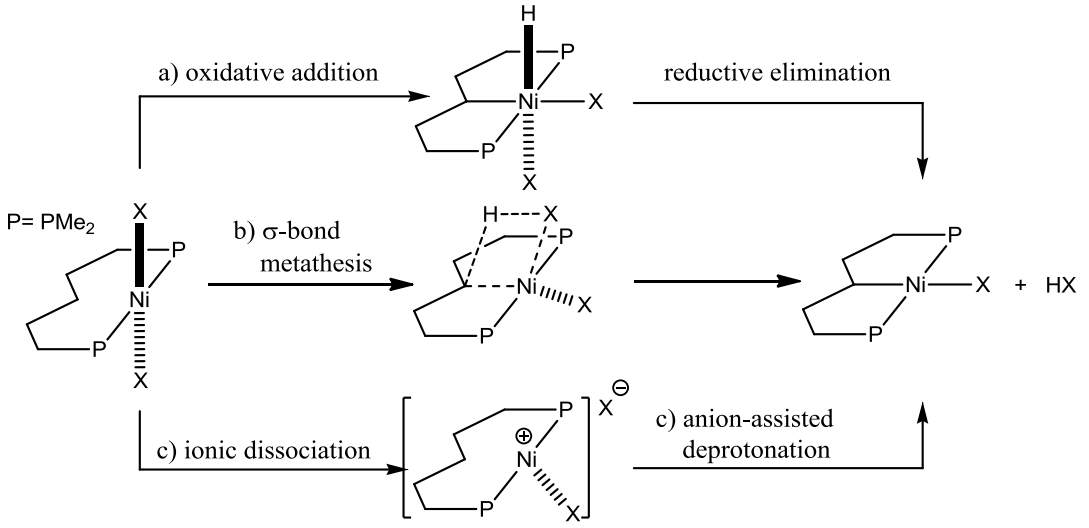

Scheme 2.4 Different pathways possible.

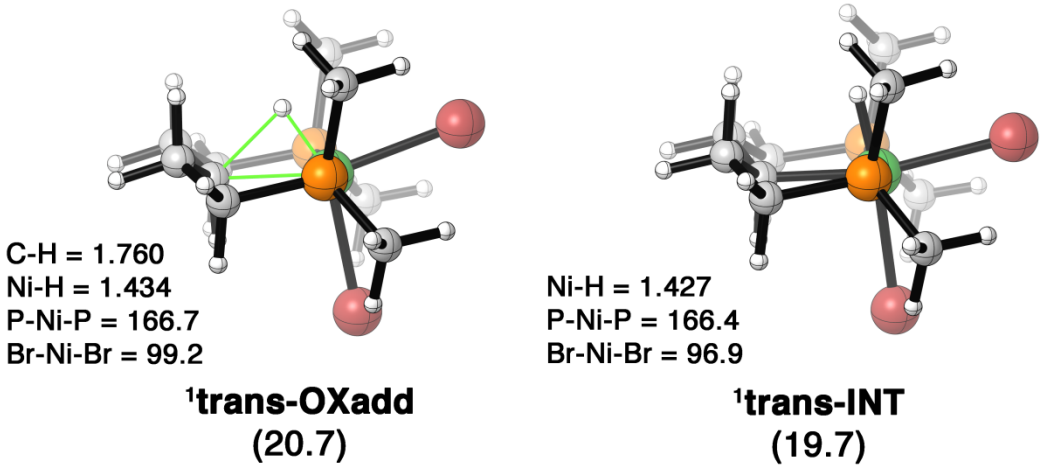

Figure 2.6 Oxidative addition transition structure and nickel hydride intermediate for sp^3 PCP metallation. Free energies are expressed in kcal/mol relative to **^{3}tetra-1**.

The reaction pathway leading to **^{1}trans-OXadd** goes through the singlet species **^{1}trans-2** (Figure 2.7), which resembles **^{1}trans-1** except for the proximity of the nickel center to the methylene group that eventually undergoes metallation. At 1.958 Å, the C-H---Ni distance in **^{1}trans-2** is typical of an agostic type interaction, but the relatively non-perturbed C-H bond (1.108 Å) and the higher energy of **^{1}trans-2** relative to **^{3}tetra-1** (by 9.9 kcal/mol) indicate that the C-H bond does not participate in an agostic interaction. This is a reasonable conclusion, because there is no low-lying and geometrically accessible vacant orbital on the nickel center. Unexpectedly, **^{1}trans-2** was found to be a spin-contaminated species ($<S^2>= 0.17$), and its re-optimization as a triplet gave a nearly equal energetic structure **^{3}trans-2** (10.0 kcal/mol, Figure 2.7). The possible pathways leading to **^{1}trans-2** and **^{3}trans-2** are shown in Scheme 2.5.

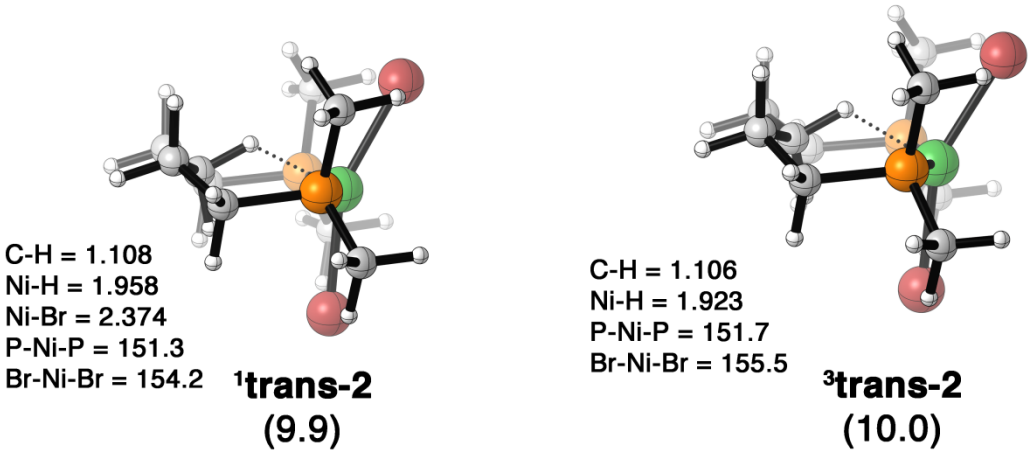

Figure 2.7 Singlet and triplet intermediates prior to sp^3 PCP ligand metallation. Free energies are expressed in kcal/mol relative to **^{3}tetra-1**.

The next mechanism we explored was σ-bond metathesis that would directly generate the metallated product ($PC_{sp3}P$)NiBr and HBr (Scheme 2.4 b). All attempts to locate a transition state for the bromo precursor traversing this pathway converged on structure **^{1}trans-TS** (Figure 2.8), for which the free energy was found to be lower than **^{1}trans-OXadd** by 3.3 kcal/mol (M06) or 10.6 kcal/mol (B3LYP). The most significant feature of **^{1}trans-TS** is the completely dissociated character of the bromide ion during the deprotonation of the C-H bond. This aspect differentiates the C-H nickellation scheme operating in the present system from analogous mechanistic schemes in which the base remains coordinated to the metal center throughout the metallation process (*cf.* Concerted Metallation Deprotonation[46] and Ambiphilic Metal−Ligand Activation[21b,47]).

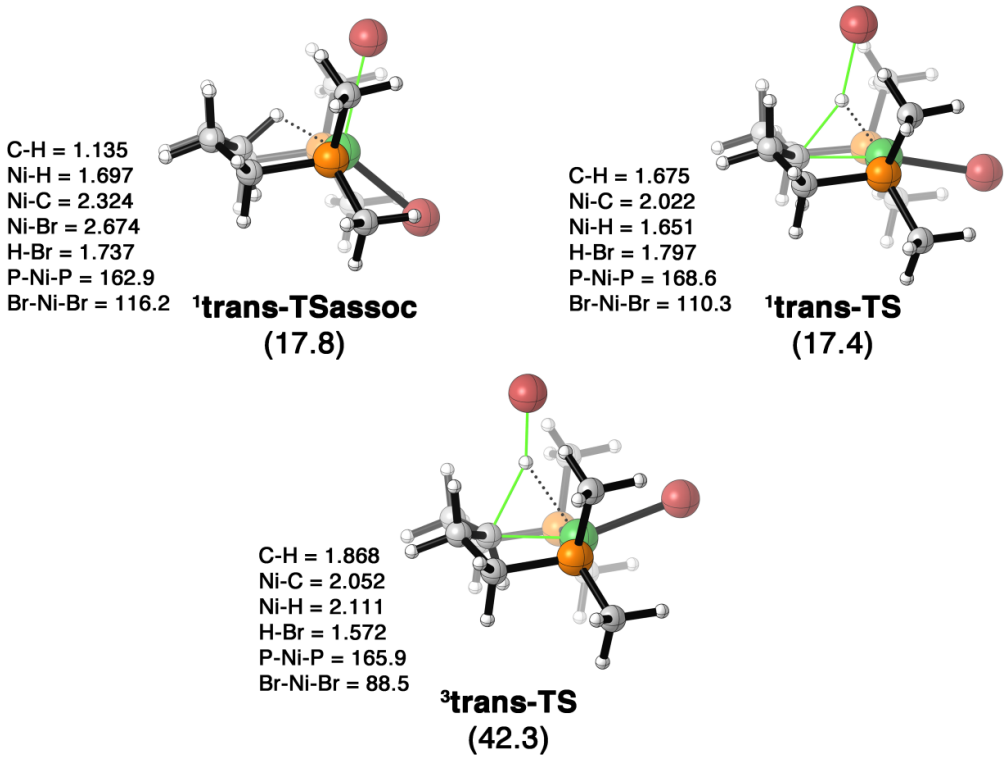

Figure 2.8 Singlet and triplet transition structures for sp^3 PCP ligand metallation. Free energies relative to ^{3}**tetra-1** (kcal/mol).

Modeling the transition structure with *i*-Pr_2P moieties leads to a greater predicted activation free energy for the two-step ionic pathway (17.4 vs. 21.2 kcal/mol), which is not surprising given the congested transition states found for such concerted pathways. It should be noted, however, that oxidative addition remains the higher energy pathway (29.4 vs. 21.2 kcal/mol) even with *i*-Pr_2P moieties. The closed shell structure ^{1}**trans-TS** does not have a lower energy unrestricted energy solution; a similar transition structure was also identified on the triplet energy surface, but this triplet structure (^{3}**trans-TS**, Figure 2.8) is 24.9 kcal/mol higher in free energy than the singlet transition structure.

The imaginary vibrational frequency in **^{1}trans-TS** suggests that this structure connects an ion-pair intermediate to the metallated product and liberated HBr. However, calculation of the forward and reverse intrinsic reaction coordinates (IRC) only showed product formation while optimization of a slightly perturbed **^{1}trans-TS** structure gave **^{1}trans-2**. Since the IRC calculations were not definitive, we explored the homolytic and heterolytic Ni-Br bond dissociation energies (BDE). The unreasonably large BDE value for homolytic cleavage of the Ni-Br bond (53.0 kcal/mol relative to **^{1}trans-2**) indicates that all scenarios requiring such a step can be discounted. Heterolytic cleavage of the Ni-Br bond (24.7 kcal/mol relative to **^{1}trans-2**) is significantly lower than homolytic cleavage but higher than **^{1}trans-TS**, suggesting that the bromide anion likely undergoes an incomplete dissociation prior to **^{1}trans-TS** to form a tight ion-pair intermediate between **^{1}trans-2** and **^{1}trans-TS**. To explore this possibility, we carried out Ni-Br bond scans on **^{1}trans-2** from 2.40 Å to 4.00 Å, which revealed that a closed-shell minimum energy structure **ion-pair** (Scheme 2.5) exists at a Ni-Br bond length of 3.90 Å.

The tight **ion-pair** intermediate is generated from an associative type transition structure where the incoming C-H bond begins to form an agostic interaction with concomitant displacement of the bromide ion via **^{1}trans-TSassoc** (Figure 2.8). In this transition structure, the C-H bond is lengthened to 1.135 Å from 1.108 Å in **^{1}trans-2**, and the Ni-Br bond increases by 0.3 Å to an elongated bond length of 2.674 Å. IRC calculations for **^{1}trans-TSassoc** indeed confirm the connection between **^{1}trans-2** and **ion-pair**. The activation free energy of **^{1}trans-TSassoc** is 0.4 kcal/mol higher than the activation free energy of **^{1}trans-TS**.

Scheme 2.5 outlines a computed free energy surface for metallation of ($PC_{sp3}^{H}P$)$NiBr_2$ starting with **^{3}tetra-1**. The structural transformation of this species from a tetrahedral to a square planar geometry prior to C-H bond cleavage can proceed via two possible triplet-singlet spin crossing points. The first crossing can occur as **^{3}tetra-1** converts into **^{1}trans-1-twist** (**SC-1**, Scheme 2.5). Alternatively, it is also possible that the structures **^{1}trans-1-twist** and **^{1}trans-1** are bypassed and **^{3}tetra-1** is directly converted into **^{1}trans-2** via **SC-2**. In this mechanism the spin crossing likely occurs near the geometry of **trans-2** since the singlet and triplet energies are degenerate at this geometry. Indeed, the located minimum energy crossing point **SC-2** and its geometry and energy are nearly identical to **^{1}trans-2** and **^{3}trans-2** (see ESI for structure).

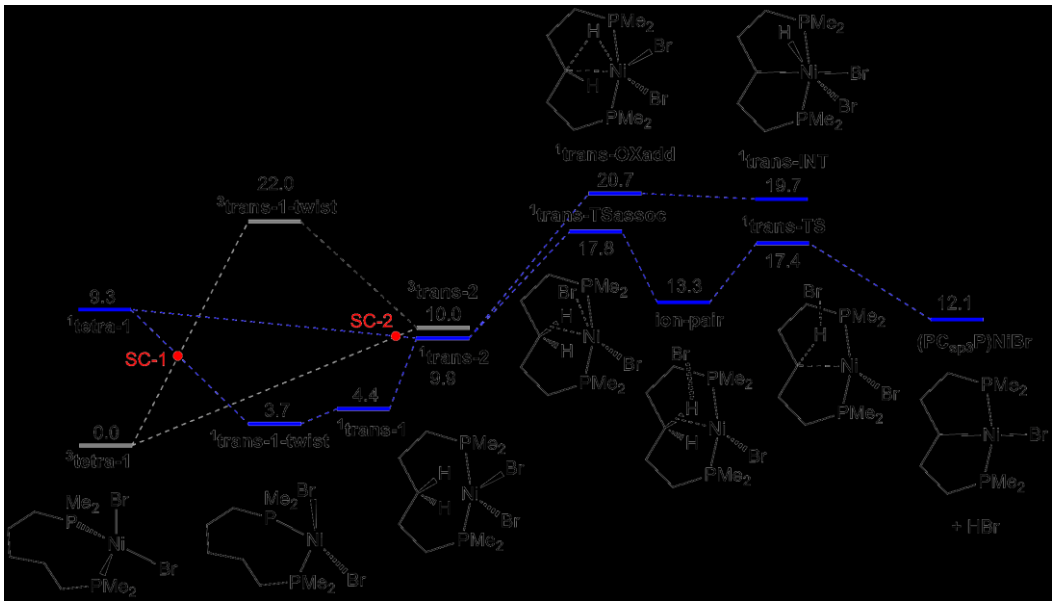

Scheme 2.5 Proposed free energy surface for conversion of (PCsp3HP)NiBr2 to the pincer species (PCsp3P)NiBr. Grey lines indicate triplet surface. Blue lines indicate singlet surface. SC = singlet-triplet energy surface crossings. All energies are expressed in kcal/mol.

The **^{1}trans-2** structure is then a branching point for the oxidative addition and the stepwise ion-pair pathways. As discussed above, the lower-energy pathway goes through a tight ion pair intermediate (**ion-pair**) that forms via an associative type transition state featuring a rupturing Ni-Br bond. The C-H bond is then cleaved via **^{1}trans-TS** to liberate HBr and generate the pincer species. Interestingly, the overall free energy of the nickellation reaction to give ($PC_{sp3}P$)NiBr and HBr is endergonic by 12.1 kcal/mol relative to **^{3}tetra-1**; moreover, this free energy decreases by only 0.5 kcal/mol when *i*-Pr_2P groups are modeled. All other density functionals tested also indicate that this metallation reaction is endergonic: B3LYP predicts a slightly higher reaction free energy while BP86 and MPWPW91 functionals predict the reaction free energy to be endergonic by only 2-3 kcal/mol. These results indicate that the added base likely plays an important thermodynamic role in quenching the one equivalent of HBr generated in the metallation reaction. In THF, the acid-base reaction equilibrium between NEt_3 and HBr to give $Et_3NH^+Br^-$ is computed to be -15.6 kcal/mol, which would render the overall process exergonic. Alternatively, it is feasible that excess phosphine ligand plays a role as the base required to quench the generated HBr.

Comparing Metallation of ($PC_{sp3}^{H}P$)$NiBr_2$ and **($PC_{sp2}^{H}P$)$NiBr_2$**. Investigating the nickellation of arene-based pincer ligands revealed a similar mechanism for C-H activation compared to the reaction of their saturated hydrocarbon analogues, the major difference being the barrier heights for C-H bond cleavage. The lower barrier for metallation of these aromatic ligands is in part due to the fact that $PC_{sp2}^{H}P$ also coordinates less favorably with $NiBr_2$ to give either a tetrahedral triplet complex or a trans singlet complex, both of which are less stable

than the corresponding non-metallated intermediates in the metallation of $PC_{sp3}{}^{H}P$. The greater ground state energy of ($\kappa^{P,P'}$-$PC_{sp2}{}^{H}P$)$NiBr_2$ might explain the lower barrier for the metallation of these aromatic ligands. Despite the more favorable Ni-C(sp^2) bond present in the final product, M06 predicts the overall reaction free energy to be endergonic by 10.5 kcal/mol with Me_2P and 5.4 kcal/mol with *i*-Pr_2P moieties. This implies that here, too, the base plays a crucial role in rendering the C-H metallation thermodynamically favorable. Figure 2.9 shows the monomeric tetrahedral triplet ($\kappa^{P,P'}$-$PC_{sp2}{}^{H}P$)$NiBr_2$ complex **^{3}tetra-3** and the singlet C-H bond cleavage transition structure **^{1}trans-TS3**. The M06 activation free energy for **^{1}trans-TS3** is 13.9 kcal/mol, 3.5 kcal/mol lower than the above-discussed **^{1}trans-TS**. As before, this reaction pathway is favored over oxidative addition that has a free energy barrier of 24.3 kcal/mol. The lower barrier for sp^2 vs. sp^3 C-H bond metallation likely results from forming a shorter and stronger Ni-C bond (1.946 Å) and a more stabilized anionic sp^2-C as the reaction proceeds through the ionic pathway. These transition effects combine with the above-mentioned favorable ground state effects to facilitate the metallation of sp^2 C-H bonds.

We note that despite significant effort, we were unable to locate either an associative transition-state structure or a tight ion-pair intermediate on the potential energy surface. Nevertheless, by analogy to the free energy surface shown in Scheme 2.5 for metallation of $PC_{sp3}{}^{H}P$, we assume that the free energy for an associative-like transition structure for $PC_{sp2}{}^{H}P$ would be very similar to **^{1}trans-TS3** since the bromide is dislodged from the nickel center.

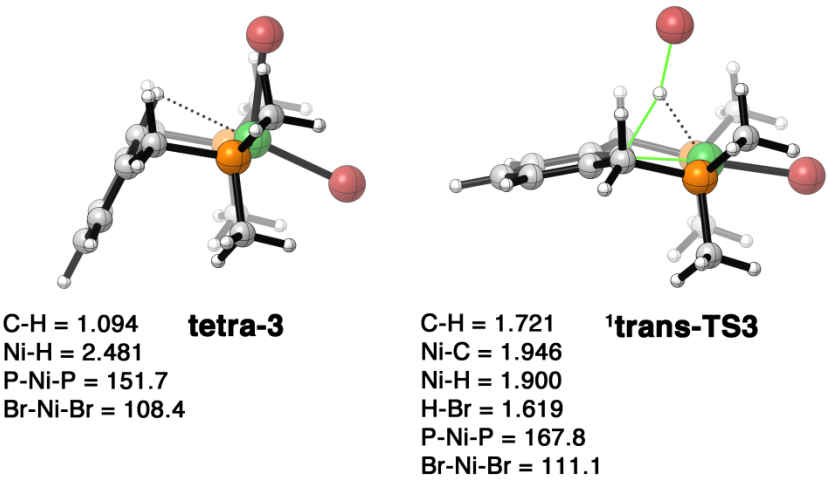

Figure 2.9 Tetrahedral intermediate and transition structure for ($PC_{sp2}{}^{H}P$)$NiBr_2$ nickellation.

Comparing nickellation of PCP and POCOP ligands. The competition experiments discussed earlier have revealed that PCP type ligands are metallated more readily than their POCOP counterparts. To explore the kinetic and thermodynamic roots of this phenomenon, we have computed the ionic reaction pathway for the sp^3 POCOP ligand in order to allow a comparison to the nickellation of $PC_{sp3}{}^{H}P$. The geometrics of the triplet tetrahedral ground state for ($\kappa^{P,P'}$-$POC_{sp3}{}^{H}OP$)$NiBr_2$ (**^{3}tetra-4**, Figure 2.10) are nearly identical to its PCP analogue **^{3}tetra-1**. In THF solvent, coordination to tetrahedral nickel is 3.3 kcal/mol more favorable in **^{3}tetra-4** relative to **^{3}tetra-1** (eq. 3), whereas the opposite order of stabilities is observed for the trans species (eq. 4).

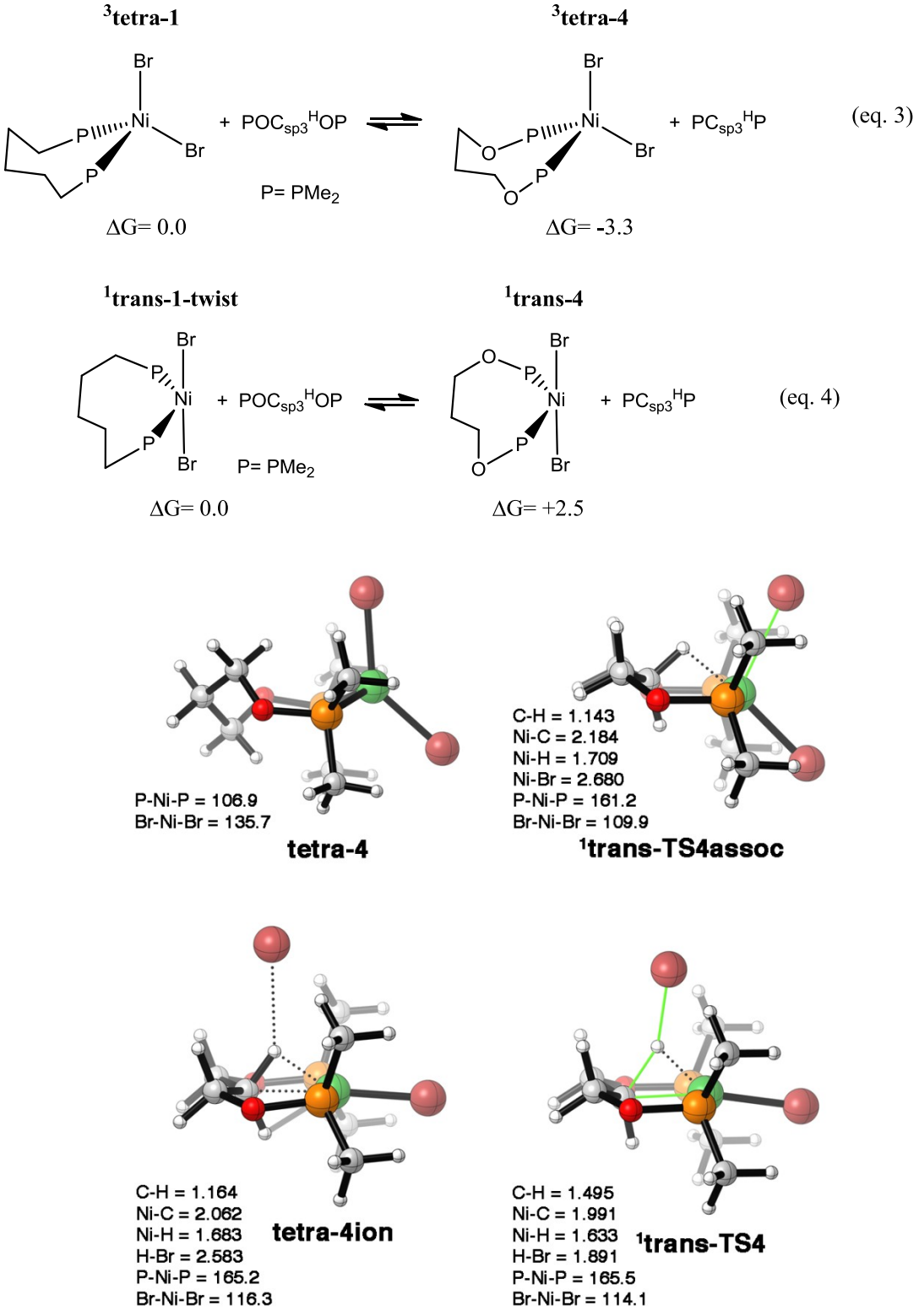

Figure 2.10 Triplet tetrahedral ground state and closed-shell ionic transition structures and intermediate for nickellation of POCsp3HOP.

As before, the ionic pathway mechanism begins with an associative transition structure, **^{1}trans-TS4assoc**, that induces an agostic C-H bond interaction with the nickel metal center and results in cleavage of the Ni-Br bond to give the tight ion pair structure **^{1}trans-4ion**. The free energy barrier for **^{1}trans-TS4assoc** relative to **^{3}tetra-4** is 27.4 kcal/mol and the ion pair intermediate free energy is 23.5 kcal/mol. This activation free energy is ~10 kcal/mol higher than the free energy barrier for the associative transition structure for nickellation of $PC_{sp3}{}^{H}P$. This substantially higher barrier can be understood in terms of the significantly weaker donor character of phosphinite-type donor moieties relative to phosphines, which would not allow an effective stabilization of a transition state involving substitution of the bromide ligand by a weakly donating C-H bond.

The C-H bond cleavage transition structure, **^{1}trans-TS4**, shows marked differences compared to **^{1}trans-TS**. The breaking C-H bond distance is shorter by 0.22Å and the forming Ni-C bond is also shorter by 0.03Å, while the forming H-Br bond is 0.09Å longer. This comparison indicates that the C-H bond cleavage transition structure for $POC_{sp3}{}^{H}OP$ is "earlier" along the reaction coordinate than the corresponding $PC_{sp3}{}^{H}P$ transition structure. The activation free energy for **^{1}trans-TS4** is 28.3 kcal/mol, 0.9 kcal/mol higher than **^{1}trans-TS4assoc**. The barrier for C-H cleavage relative to the **^{1}trans-4ion** intermediate is 4.8 kcal/mol, which is similar to the 3.4 kcal/mol barrier for the analogous step in the nickellation of $PC_{sp3}{}^{H}P$; this confirms that the most energetically important step is the Ni-Br bond rupture. As before, formation of the pincer species ($\kappa^{P,C,P'}$-$POC_{sp3}O$)PNiBr is endergonic with a

reaction free energy of 14.2 and 7.8 kcal/mol for Me_2P and *i*-Pr_2P moieties, respectively. Finally, we have also found that the pincer complex featuring the $PC_{sp3}P$ ligand is slightly more stable (by 1.1 kcal/mol) compared to its $POC_{sp3}OP$ analogue.

2.4 Conclusion

The combined experimental and computational investigations described above have shed some light on the relative rates and mechanisms of the direct nickellation of the PCP- and POCOP-type pincer ligands studied. We have confirmed and quantified the more facile nickellation of PCP vs. POCOP ligands and aromatic vs. aliphatic backbones. The more facile metallation of the aromatic C-H bonds is related to their more effective coordination to the electrophilic Ni center and better stabilization of the developing Ni-C bond, as well as to the absence of dinuclear species in the ground states of the aromatic ligands. The preference for PCP vs. POCOP nickellation likely results from the better chelation of the phosphine moieties; the importance of chelation is also reflected in the preference for P(*i*-Pr)$_2$ vs. P(*t*-Bu)$_2$ and PPh_2 moieties.

The experimental finding that electron releasing substituents favor the nickellation of aromatic POCOP ligands is consistent with a mechanism resembling electrophilic aromatic substitution, which is in stark contrast to what has been observed for direct C-H palladation reactions of aromatic substrates.[33,34] Our DFT studies indicate that a classical oxidative addition mechanism based on a three-

centered transition state is accessible but more energetic than a two-step, constant-oxidation-state pathway characterized by a complete rupture of the H-acceptor bromide ligand. The crucial stabilization of the electron-depleted metal center in such a pathway explains the importance of Ni-C(H) interactions and hence the preference for electron-rich aromatic ligands. These features, namely the preference for activation of more electron-rich C-H bonds and the complete dissociation of the internal H-acceptor (Br^-), distinguish the direct metallation process in our Ni-promoted systems from the much more extensively investigated Pd-based systems wherein electron-deficient C-H bonds are metallated preferentially and the H-transfer involves Pd-bound acceptors (halides, acetate, carbonate, etc.).

Future studies will be directed at examining the C-H metallation of other pincer ligands (PCN, POCN, NCN, etc.). If these investigations confirm the main findings of the current study, it should be possible to develop successful strategies for facilitating C-H nickellation reactions by using more electron-rich aromatic substrates and Ni precursors featuring more easily ionized Ni-X bonds.

2.5 Experimental Section

General Procedures. Unless otherwise indicated, all manipulations were carried out under nitrogen using standard Schlenk procedures and a Drybox. Solvents were dried by passage over molecular sieves contained in MBRAUN systems. Triethylamine is dried by distillation over CaH_2. The reagents Isobutyronitrile, Nickel powder, Bromine, ClP(*i*-Pr)$_2$, ClP(*t*-Bu)$_2$, ClP(Ph)$_2$, 5-Methyl-1,3-benzenediol, 4,6-Dichloro-1,3-benzenediol, Methyl 2,4-dihydroxybenzoate, Methyl 3,5-dihydroxybenzoate, and NaH were purchased from Aldrich and used without further purification. 5-Methoxyresorcinol is purchased from Chemsavers. 4-Methoxyresorcinol has been synthesized following a published procedure.[48] The synthesis and characterization of the ligands and their Ni complexes used in the present study have been described in previously published reports.[22] The Ni-Cl analogue of **1c'** and the *t*-Bu$_2$P analogues of ligands **1e** and **1i** have been reported previously.[11d]

Most NMR spectra were recorded at 400 (^{1}H) and 161.9 MHz (^{31}P) using a Bruker AV400rg spectrometer, or at 400 (^{1}H) and 100.56 MHz (^{13}C{^{1}H}) using a Bruker ARX400 spectrometer. The ^{31}P{^{1}H} NMR spectrum of complex **1h'** was recorded at 202.5 MHz using a Bruker AV500 spectrometer. Chemical shift values are reported in ppm (δ) and referenced internally to the residual solvent signals (^{1}H and ^{13}C: 7.26 and 77.16 ppm for $CDCl_3$; 7.16 and 128.06 ppm for C_6D_6) or externally (^{31}P, H_3PO_4 in D_2O, δ= 0). Coupling constants are reported in Hz. UV/vis spectra were measured on a Varian Cary 500i.

General procedure for competition reactions

Ligands 1a-j. A THF solution (650 μL) containing approximately equimolar quantities of ligands **6** (0.175 mmol, 60mg) and **1** (0.175 mmol, 65 mg) was analyzed by ^{31}P NMR to confirm the molar ratio of the ligands, and then added to a homogenous THF solution (650 μL) containing $\{(i\text{-PrCN})NiBr_2\}_n$ (0.132 mmol, 38mg) and NEt_3 (49 μL, 0.35 mmol). The initial blue color of the reaction mixture changed instantly, turning to brown first and then yellow, and a white precipitate formed over time. The mixture was stirred for 5 min at room temperature and samples were withdrawn over regular intervals for analysis by ^{31}P NMR. Reaction progress was determined on the basis of the relative intensities of the ^{31}P signals for the ligands and the in-situ formed complexes. To confirm the irreversible nature of the nickellation process, the samples were also analyzed after 24 h.

Ligands 3 and 4. Applying the above procedure to the aliphatic ligands (but in Toluene instead of THF) results in formation of a homogenous, dark brown solution, which was heated over three days at 100 °C before analysis by ^{31}P NMR.

2.6 Acknowledgments.

The authors are grateful to: Brigham Young University for financial support to D. H. E., access to the Fulton Supercomputing Center, and student fellowships to M. L. L.; NSERC of Canada for a Discovery Grant to D.Z.; Université de Montréal and Centre in Green Chemistry and Catalysis for graduate fellowships to B.V.; the Center for Catalytic Hydrocarbon Functionalization, an Energy Frontier Research Center funded by the the U.S. Department of Energy, Office of Science, Office of

Basic Energy Sciences (Award Number DE-SC0001298, DHE); the American Chemical Society Petroleum Research Fund (D. H. E.). We have also benefited from valuable discussion with Dr. Laure Benhamou and Dr. Denis Spasyuk.

2.7 Supporting information

Substituent	relative rate	ln(kX/kH)	σ value
p-Ome	101	0,703	-0,268
m-Ome	100	0,693	0,115
p-COOMe	18	-1,022	0,31
m-COOMe	42	-0,174	0,39
p-Me	66	0,278	-0,17
H	50	0,000	0

Table 2.2 Relative nickellation rates, ln(kX/kH), and σ values of various substituents on the POCOP ligands

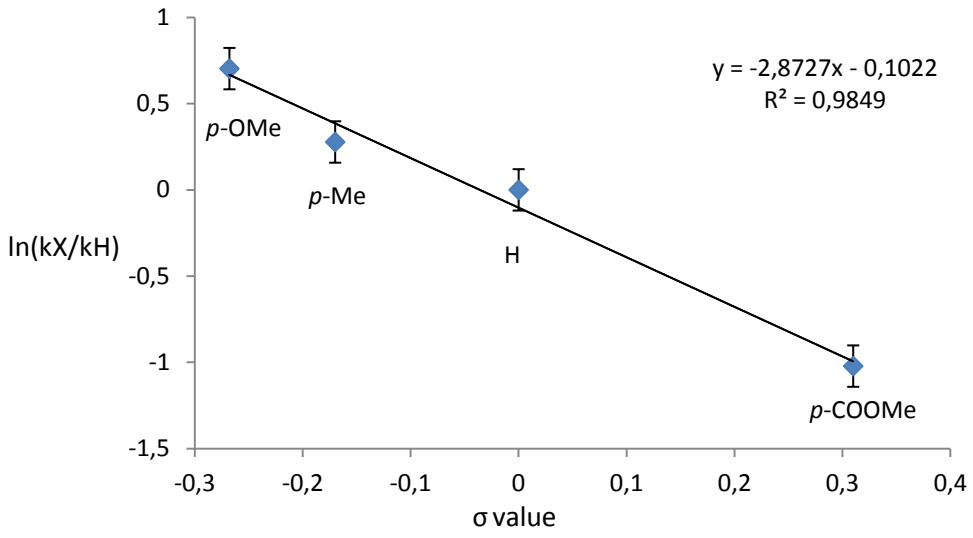

Figure 2.12 Hammett correlation for nickellation of various *para*-substituted POCOP ligands

2.8 References

[1] (a) Shilov, A. E.; Shul'pin, G. B. *Chem. Rev.* **1997**, *97*, 2879. (b) Crabtree, R. H. *J. Chem. Soc.*, *Dalton Trans.* **2001**, 2437. (c) Labinger, J. A.; Bercaw. J. E. *Nature* **2002**, *417*, 507. (d) Crabtree, R. H. *J. Organomet. Chem.* **2004**, *689*, 4083. (e) *Activation and Functionalization of C-H Bonds*, ed. A. S. Goldman and K. I. Goldberg, ACS Symposium Series 885, Washington DC, 2004.

[2] (a) Kakiuchi, F.; S. Murai *Acc. Chem. Res.* **2002**, *35*, 826. (b) Ritleng, V.; Sirlin, C.; Pfeffer, M. *Chem. Rev.* **2002**, *102*, 1731. (c) Dick, A. R.; Sanford, M. *Tetrahedron* **2006**, *62*, 2439. (d) Alberico, D.; Scott, M. E.; Lautens, M. *Chem. Rev.* **2007**, *107*, 174. (e) Lewis, J. C.; Bergman, R. G.; Ellman, J. A. *Acc. Chem. Res.* **2008**, *41*, 1013. (f) Stuart, D. R.; Fagnou, K. *Science* **2007**, *316*, 1172.

[3] (a) Bolig, A. D.; Brookhart, M. *J. Am. Chem. Soc.* **2007**, *129*, 14544. (b) Bullock, R. M. "Catalysis Without Precious Metals", Wiley-VCH: Weinheim, 2010. (c) Kulkarni, A. A.; Daugulis, O. *Synthesis* **2009**, 4087. (d) Chakraborty, S.; Guan, H. *Dalton Trans.* **2010**, *39*, 7427.

[4] Kleiman, J. P.; Dubeck, M. *J. Am. Chem. Soc.* **1963**, *85*, 1544.

[5] Moulton, C. J.; Shaw, B. L. *J. C. S. Dalton* **1976**, 1020.

[6] (a) Rimml, H.; Venanzi, L. M. *J. Organomet. Chem.* **1983**, *259*, C6-C7. (b) Rimml, H.; Venanzi, L. M. *J. Organomet. Chem.* **1984**, *260*, C52-C54. (c) Kennedy, A. R.; Cross, R. J.; Muir, K. W. *Inorg. Chim. Acta* **1995**, *231*, 195. (d) Huck, W. T. S.; Snellink-Ruël, B.; van Veggel, F. C. J. M.; Reinhoudt, D. N. *Organometallics* **1997**, *16*, 4287. (e) Kozhanov, K. A.; Bubnov, M. P.; Cherkasov, V. K.; Fukin, G. K.; Abakumov, G. A. *Chem. Commun.* **2003**, 2610. (f) van der Boom, M. E.; Liou, S. Y.; Shimon, L. J. W.; Ben-David, Y.; Milstein, D. *Inorg. Chim. Acta* **2004**, *357*, 4015. (g) Groux, L. F.; Bélanger-Gariépy, F.; Zargarian, D. *Can. J. Chem.* **2005**, *83*, 634. (h) Castonguay, A.; Charbonneau, F.; Beauchamp, A. L.; D. Zargarian, *Acta Cryst*. **2005**, *E61*, m2240. (i) Sui-Seng, C.; Castonguay, A.; Chen, A. Y.; Gareau, D.; Groux, L. F.; Zargarian, D. *Topics in Catalysis* **2006**, *37*, 81. (j) Castonguay, A.; Beauchamp, A. L.; Zargarian D., *Acta Cryst*. **2007**, *E63*, m196. (k) Boro, B. J.; Duesler, E. N.; Goldberg, K. I.; Kemp, R. A. *Inorg. Chem.* **2009**, *48*, 5081. (l) Boro, B. J.; Dickie, D. A.; Goldberg, K. I.; Kemp, R. A. *Acta Cryst. E* **2008**, *E64*, m1304. (m) Boro, B. J.; Dickie, D. A.; Duesler, E. N.; Goldberg, K. I.; Kemp, R. A. *Acta Cryst. E* **2008**, *E64*, m1402. (n) Schmeier, T. J.; Hazari, N.; Incarvitoa, C. D.; Raskatovb, J. A. *Chem. Commun.* **2011**, *47*, 1824.

[7] For pincer complexes of Fe see: (a) Creaser, C. S.; Kaska, W. C. *Inorg. Chim. Acta* **1978**, *30*, L325–L326. (b) de Koster, A.; Kanters, J. A.; Spek, A. L.; van der Zeijden, A. A. H.; van Koten, G.; Vrieze, K. *Acta Cryst.* **1985**, *C41*, 893. (c) Fryzuk, M. D.; Leznoff, D. B.; Ma, E. S. F.; Rettig, S. J.; Young, Jr., V. G. *Organometallics* **1998**, *17*, 2313. (d) Ingleson, M. J.; Fullmer, B. C.; Buschhorn, D. T.; Fan, H.; Pink, M.; Huffman, J. C.; Caulton, K. G. *Inorg. Chem.* **2008**, *47*, 407. (e) Adhikari, D.; Basuli, F.; Fan, H.; Huffman, J. C.; Pink, M.; Mindiola, D. J. *Inorg. Chem.* **2008**, *47*, 4439. (f) Xu, G.; Sun, H.; Li, X. *Organometallics* **2009**, *28*, 6090. (g) Hosokawa, S.; Ito, J.; Nishiyama, H. *Organometallics* **2010**, *29*, 5773. (h) Bhattacharya, P.; Krause, J. A.; Guan, H. *Organometallics* **2011**, *30*, 4720.

[8] (PCP)Co complexes can be prepared via direct C-H metallation (see ref. 7f), but preparation of the analogous POCOP complexes via direct C-H metallation has proven difficult (see Xavier Lefèvre, M. Sc. thesis, Université de Montréal, 2010). A recent report has described the preparation of (POCOP)Co complexes via salt metathesis using lithiated ligands: Hebden, T. J.; St. John, A. J.; Gusev, D. G.; Kaminsky, W.; Goldberg, K. I.; Heinekey, D. M. *Angew. Chem. Int. Ed.* **2011,** *50*, 1873.

[9] (a) Gusev, D. G.; Madott, M.; Dolgushin, F. M.; Lyssenko, K. A.; Antipin, M. Yu. *Organometallics* **2000,** *19,* 1734. (b) Dani, P.; Toorneman, M. A. M.; van Klink, G. P. M.; van Koten, G. *Organometallics* **2000**, *19*, 5287. (c) Agapie, T.; Bercaw, J. E. *Organometallics* **2007,** *26,* 2957.

[10] (a) Castonguay, A.; Sui-Seng, C.; Zargarian, D.; Beauchamp, A. L. *Organometallics* **2006**, *25*, 602. (b) Castonguay, A.; Beauchamp, A. L.; Zargarian, D.

Organometallics **2008**, *27*, 5723. (c) Castonguay, A.; Spasyuk, D. M.; Madern, N.; Beauchamp, A. L.; Zargarian, D. *Organometallics* **2009**, *28*, 2134. (d) Castonguay, A.; Beauchamp, A. L.; Zargarian, D. *Inorg. Chem.* 2009, **48**, 3177.

[11] (a) Valente, G. B.; Oscar, B. P.; Cesar, H- A.; Toscano, R. A.; Morales-Morales, D. *Tet. Lett.* **2006**, *47*, 5059. (b) Pandarus, V.; Zargarian, D. *Chem. Commun*. **2007**, 978. (c) Pandarus, V.; Zargarian, D. *Organometallics* **2007**, *26*, 4321. (d) Chakraborty, S.; Krause, J. A.; Guan, H. *Organometallics* **2009**, *28*, 582. (e) Zhang, J.; Medley; Krause, J. A.; Guan, H. *Organometallics* **2010**, *29*, 6393. (f) Chakraborty, S.; Zhang, J.; Krause, J. A.; Guan, H. *J. Am. Chem. Soc.* **2010***, 132,* 8872. (g) Lefèvre, X.; Spasyuk, D. M.; Zargarian, D. *J. Organomet. Chem*. **2011**, 864. (h) Lefèvre, X.; Durieux, G.; Lesturgez, S.; Zargarian, D. *J. Mol. Catal. A*. **2011**, *335*, 1. (i) Salah, A. B.; Zargarian, D. *Dalton Trans.* **2011**, *40*, 8977. (j) Salah, A.; Offenstein, C.; Zargarian, D. *Organometallics* **2011**, *30*, 5352. (k) Huang, F.; Zhang, C.; Jiang, J.; Wang, Z.-X.; Guan, H. *Inorg. Chem.* **2011**, *50*, 3816. (l) Chakraborty, S.; Patel, Y. J.; Krause, J. A.; Guan, H. *Polyhedron* **2012**, *32*, 30. (m) Xu, G.; Li, X.; Sun, H. *J. Organomet. Chem*. **2011**, *696*, 3011.

[12] A recent report (Gwynne, E. A.; Stephan, D. W. *Organometallics* **2011**, *30*, 4128–4135) has shown that the closely related PNCNP-type complexes of nickel can be prepared in the presence of a strong Lewis acid such as $B(C_6F_5)_3$. This strong Lewis acid appears to be required for converting a species formed initially via nickellation at the N-H moiety of the ligand; in contrast, palladation of the central C-H moiety of this PNCNP ligand proceeds readily and in the absence of Lewis acids.

[13] (a) Spasyuk, D. M.; van der Est, A.; Zargarian, D. *Organometallics* **2009**, *28*, 6531; (b) Spasyuk, D. M.; Zargarian, D. *Inorg. Chem.* **2010**, *49*, 6203. (c) Spasyuk, D. M.; Gorelsky, S. I.; van der Est, A.; Zargarian, D. *Inorg. Chem*. **2011**, *50*, 2661. (d) Zhang, B.-S.; Wang, W.; Shao, D.-D.; Hao, X.-Q.; Gong, J.-F.; Song, M.-P. *Organometallics* **2010**, *29*, 2579. (e) Niu, J.-L.; Chen, Q.-T.; Hao, X.-Q.; Zhao, Q.-X.; Gong, J.-F.; Song, M.-P. *Organometallics* **2010**, *29*, 2148. (f) Yang, M.-J.; Liu, Y.-J.; Gong, J.-F.; Song, M.-P. *Organometallics* **2011**, *30*, 3793.

[14] Most NCN-Ni complexes of nickel have been prepared via strategies based on lithiation/nickellation (using Ni(II) precursors) or oxidative addition of C-halide moieties (using Ni(0) precursors). For representative examples see: (a) Grove, D. M.; van Koten, G.; Ubbels, H. J. C.; Zoet, R. *Organometallics* **1984**, *3*, 1003. (b) Stol, M.; Snelders, D. J. M.; Godbole, M. D.; Havenith, R. W. A.; Haddleton, D.; Clarkson, G.; Lutz, M.; Spek, A. L.; van Klink, G.; P. M.; van Koten, G. *Organometallics* **2007**, *26*, 3985. (c) Bugarin, A.; Connell, B. T. *Organometallics* **2008**, *27*, 4357. (d) Lee, D. H.; Sungwon, J. H.; Park, S. *Bull. Korean Chem. Soc.* **2008**, *29*, 187. (e) Hurtado, J.; Ibanez, A.; Rojas, R.; Valderrama, M.; Fröhlich, R. *J. Braz. Chem. Soc.* **2011**, *22*, 1750. (f) For a review on this subject see: Gossage, R. A.; van de Kuil, L. A.; van Koten, G. *Acc. Chem. Res.* **1998**, 31, 423.

[15] Van Koten's group has reported an alternative synthetic path to (NCN)Ni complexes using gold as transmetallation agent: Contel, M.; Stol, M.; Casado, M. A.; van Klink, G. P. M.; Ellis, D. D.; Spek, A. L.; van Koten, G. *Organometallics* **2002**, *21*, 4556.

[16] To our knowledge, there is only one reported example of a (NCN)Ni complex prepared by direct C-H nickellation: Shao, D.-D.; Niu, J.-L.; Hao, X.-Q.; Gong, J.-F.; Song, M.-P. *Dalton Trans.* **2011**, *40*, 9012.

[17] For rare examples of Ni complexes featuring non-metallated aromatic pincer ligands see: (a) Smith, R. C.; Protasiewicz, J. D. *Organometallics* **2004**, *23*, 4215. (b) Johnson, M. T.; Wendt, O. F. *Inorg. Chim. Acta* **2011**, *367*, 222. For an example of *cis* Pd complex featuring a chelating, non-metallated aliphatic bis(phosphine) ligand see: (c) Sjövall, S.; Johansson, M. H.; Andersson, C. *Eur. J. Inorg. Chem.* **2001**, 2907.

[18] Pandarus, V.; Castonguay, A.; Zargarian, D. *Dalton Trans.* **2008**, 4756.

[19] Di- or trinuclear macrocyclic complexes featuring non-metallated pincer complexes have also been reported for Rh, Pd, Pt, and Au : (a) Pryde, A. J.; Shaw, B. L.; Weeks, B. *J. Chem.Soc., Chem. Commun.* **1973**, 947. (b) Al-Salem, N. A.; Empsall, H. D.; Markham, R.; Shaw, B. L.; Weeks, B. *J. Chem. Soc., Dalton Trans.* **1979**, 1972. (c) Al-Salem, N. A.; McDonald, W. S.; Markham, R.; Norton, M. C.; Shaw, B. L. *J. Chem. Soc., Dalton Trans.* **1980**, 59. (d) Crocker, C.; Errington, R. J.; Markham, R.; Moulton, C. J.; Odell, K. J.; Shaw, B. L. *J. Am. Chem. Soc.* **1980**, *102*, 4373. (e) Hill, W. E.; Minahan, D. M. A.; Taylor, J. G.; McAuliffe, C. A. *J. Am. Chem. Soc.* **1982**, *104*, 6001. (f) Al-Baker, S.; Hill, W. E.; McAuliffe, C. A. *J. Chem. Soc. Dalton Trans.* **1985**, 2655 (g) van der Boom, M. E.; Gozin,M.; Ben-David, Y.; Shimon, L. J. W.; Frolow, F.; Kraatz, H.-B.; Milstein, D. *Inorg. Chem.* **1996,** *35,* 7068. (h) Dilworth, J. R.; Zheng, Y.; Griffiths, D. V. *J. Chem. Soc*., *Dalton Trans*. **1999**, 1877.

[20] For representative reviews on the contribution of computational methods to delineating the mechanisms of C-H activation reactions see: (a) Dedieu, A. *Chem. Rev.* **2000**, *100*, 543. (b) Frenking, G.; Fröhlich, N. *Chem. Rev.* **2000**, *100*, 717. (c) Niu, S.; Hall. M. B. *Chem. Rev.* **2000**, *100*, 353. (d) Ke, Z.; Cundari, T. R. *Organometallics* **2010**, *29*, 821.

[21] For recent reviews on C-H bond activation mechanisms see: (a) Balcells, D.; Clot, E.; Eisenstein, O. *Chem. Rev.* **2010**, *110*, 749. (b) Boutadla, Y.; Davies, D. L.; Macgregor, S. A.; Poblador-Bahamonde, A. I. *Dalton Trans.* **2009**, 5820. (c) Perutz, R. N.; Sabo-Etienne, S. *Angew. Chem. Int. Ed.* **2007**, *46*, 2578. (d) Niu, S. and Hall, M. B. *Chem. Rev.* **2000**, *100*, 353. (e) Torrent, M., Solà, M. and Frenking, G. *Chem. Rev.* **2000**, *100*, 439, (f) Dedieu, A. *Chem. Rev.* **2000**, *100*, 543.

[22] The synthesis and characterization of these ligands and their (pincer)NiX complexes have been reported previously, as follows: **1a** and **3** (ref.11b,c); **1b** (ref. 11a,i,j,k); **1c** (ref. 11d,e); **1d** (ref. 10c); **1e**-**1j** (ref. 27); **2** (ref. 6l, 10c); **4** (ref. 10b). The nickel pincer complexes (POCOP$^{t\text{-Bu}}$)NiX (X= Cl, H, SAr, etc.) have been reported by Guan's group: refs. 11d-f,k.

[23] (a) Bedford, R. B.; Draper, S. M.; Scully, P. N.; Welch, S. L. *New J. Chem*. **2000** *24*, 745. (b) Morales-Morales, D.; Grause, C.; Kasaoka, K.; Redon, R.; Cramer, R. E.; Jensen, C. M. *Inorg. Chim. Acta* **2000**, *300*‑*302*, 958.

[24] (a) The synthesis of 1,5-(*i*-$Pr_2P)_2$-$(CH_2)_5$ has been reported in Geier, S.; Goddard, R.; Holle, S; Jolly, P. W.; Krüger, C.; Lutz, F. *Organometallics* **1997**, *16*, 1612. (b) An optimized protocol for the synthesis of the *t*-Bu analogue of this ligand has been published by Gusev: Gusev, D. G.; Lough, A. J. *Organometallics* **2002**, *21*, 5091. (c)

We reported subsequently a more detailed and higher-yielding protocol for the preparation of 1,5-(*i*-$Pr_2P)_2$-$(CH_2)_5$: See ref. 10b.

[25] (a) For a report on the synthesis of 1,3-(*i*-$Pr_2PCH_2)_2$-C_6H_4 see : Rybtchinski, B.; Ben-David, Y.; Milstein, D. *Organometallics* **1997**, *16*, 3786. (b) More recently, we have reported a more detailed and optimized protocol (see ref. 10a).

[26] (a) For the original report on the preparation of this precursor see: Hathaway, B. J.; Holah, D. G. *J. Chem. Soc.* **1964**, 2400. (b) For examples of its use in the preparation of pincer complexes of nickel see refs. 10c, 11b,c,h-j, and 13a,b.

[27] Vabre, B.; Zargarian, D. Unpublished results.

[28] The molar mass of $(MeCN)_nNiBr_2$ is somewhat uncertain because of the poorly defined acetonitrile content that varies considerably as a function of the sample's age and the specific protocol used for the recrystallization and drying steps. This uncertainty in the molar mass is not a major concern when conducting preparative experiments wherein the precursor is often used in excess, but this issue is crucial for the kinetic measurements reported in this study.

[29] It should be noted that nickellation of the aliphatic ligands **3** and **4** proceeds sufficiently slowly to allow direct rate measurements, but using large excess of Ni and NEt_3, as required under the pseudo-first order conditions, often led to variable amounts of unidentified side-products and gave irreproducible rates. In contrast, nickellation reactions using small excess of NEt_3 and Ni do not generate side-products.

[30] One of the reviewers of our manuscript urged us to explore the possibility that in some instances the initially formed pincer complexes might react with unreacted

ligands to generate new pincer complexes; this type of "trans-cyclometallation" reactions have been observed earlier between (NCN)PtCl complexes and $PC^{H}P$ ligands to generate (PCP)PtCl and $NC^{H}N$ ligands. (See: Albrecht, M.; Dani, P.; Lutz, M.; Spek, A.L.; van Koten, G. J. Am. Chem. Soc. 2000, 122, 11822.) We can confirm here that trans-cyclometallation reactions do indeed occur in some cases under forcing (thermodynamic) conditions. Thus, heating a mixture of pre-formed complex **2'** and three equiv of ligand **1a'** in toluene at 100 °C for 18 h showed the formation of ligand **2** and complex **1a'** (final ratio of **2':1a** ~ 3:2 by ^{31}P NMR). It should be emphasized, however, that the nickellation ratios reported here are invariable over 24 h under the conditions of the kinetic experiments, i.e., equimolar quantities of ligands reacting with a slight deficiency of $\{(i\text{-PrCN})NiBr_2\}_n$ at r.t. (for aromatic ligands) or 70 °C (for aliphatic ligands).

[31] We have proposed that this non-metallated intermediate is the dinuclear species $\{trans\text{-}(\mu\text{-}\mathbf{3})NiBr_2\}_2$ featuring a 16-membered metallacycle. (ref.18) Such complexes have also been isolated during the attempted nickellation of the $PC_{sp3}P$ ligand $\{i\text{-}Pr_2P(CH_2)_2\}_2CH_2$ and fully characterized. (ref. 10b)

[32] Plotting σ_p vs. ln(relative rates) gave the Hammett reaction constant of -2.87, which indicates a positive charge developing on the *p*-C atom during nickellation. (See SI.)

[33] (a) Garcia-Cuadrado, D.; Braga, A. A. C.; Maseras, F.; Echavaren, A. M. *J. Am. Chem. Soc.* **2006**, *128*, 1066. (b) Garcia-Cuadrado, D.; de Mendoza, P.; Braga, A. A. C.; Maseras, F.; Echavaren, A. M. *J. Am. Chem. Soc.* **2007**, *129*, 6880. (c) Pascual,

S.; de Mendoza, P.; Braga, A. A. C.; Maseras, F.; Echavaren, A. M. *Tetrahedron* **2008**, *64*, 6021.

[34] (a) Lafrance, M.; Rowley, C. N.; Woo, T. K.; Fagnou, K. *J. Am. Chem. Soc.* **2006**, *128*, 8754. (b) Campeau, L. C.; Fagnou, K. *Chem. Comm.* **2006**, 1253.

[35] A reviewer of our manuscript has suggested that substituents located at the *meta*-position with respect to the central C-H bond would be expected to favor nickellation by sterically restricting the conformational freedom of the donor moiety in its proximity and hence increasing its rate of coordination to the Ni center. This explanation is consistent with the relative nickellation rates we have observed for ligands **1g** and **1h**, and hence should be taken into consideration when discussing the impact of *meta*-substituents on the nickellation of aromatic POCOP ligands.

[36]. Gaussian 09, Revision A.02, M. J. Frisch, et al. Gaussian, Inc., Wallingford CT, 2009.

[37]. Zhao, Y.; Truhlar, D. G. *Theor. Chem. Acc.* **2008**, *120*, 215.

[38]. Zhao, Y.; Truhlar, D. G. *Acc. Chem. Res.* **2008**, *41*, 157.

[39]. (a) Sieffert, N.; Bühl, M. *Inorg. Chem.* **2009**, *48*, 4622. (b) Minenkov, Y.; Occhipinti, G.; Jensen, V. R. *J. Phys. Chem. A* **2009**, *113*, 11833. (c) Stewart, I. C.; Benitez, D.; O'leary, D. J.; Tkatchouk, E.; Day, M. W.; Goddard, W. A. III; Grubbs, R. H. *J. Am. Chem. Soc.* **2009**, *131*, 1931. (d) Benitez, D.; Tkatchouk, E.; Goddard, W. A. III *Organometallics* **2009**, *28*, 2643. (e) Fedorov, A.; Couzijn, E. P. A.; Nagornova, N. S.; Boyarkin, O. V.; Rizzo, T. R.; Chen, P. *J. Am. Chem. Soc.* **2010**, *132*, 13789. (f) Takatani, T.; Sears, J. S.; Sherrill, C. D. *J. Phys. Chem. A* **2010**, *114*,

11714. (g) Pratt, L. M.; Voit, S.; Okeke, F. N. *J. Phys. Chem. A* **2011**, *115*, 2281. (h) Kulkarni, A. D.; Truhlar, D. G. *J. Chem. Theory Comput.* **2011**, *7*, 2325.

[40]. Minenkov, Y.; Occhipinti, G.; Jensen, V. R. *J. Phys. Chem. A* **2009**, *113*, 11833.

[41]. (a) Harvey, J. N.; Aschi, M.; Schwarz, H.; Koch, W. *Theor. Chem. Acc*. **1998**, *99*, 95. (b) Harvey, J. N.; Aschi, M. *Phys. Chem. Chem. Phys.* **1999**, *1*, 5555.

[42]. CYLview, 1.0b; Legault, C. Y., Université de Sherbrooke, 2009 (http://www.cylview.org)

[43] We note that only dinuclear coordination has been explored here. It is plausible that an oligomeric species similar to **trans,trans-1** might be formed upon complexation of the $PC_{sp3}{}^{H}P$ ligand with $NiBr_2$.

[44] We have obtained a calculated ΔG value of 34.7 Kcal/mol for a single C-H nickellation from the dinuclear intermediate, confirming that nickellation pathways going through a prior dissociation of the dinuclear intermediates into mononuclear species is significantly more favorable. This preference for nickellation from the mononuclear species can be ascribed to the significant contortion of the PCP ligand and the formation of a highly distorted geometry around the Ni center required for bringing the C-H bond into the coordination sphere of the Ni center in the dinuclear species.

[45] See, for instance, the proposed mechanism for C-H activation reactions of (tris(pyrazolyl)borate)Ru(PH_3)CH_3 : Lam, W. H.; Jia, G. C.; Lin, Z. Y.; Lau, C. P.; Eisenstein, O. *Chem.- Eur. J.* **2003**, *9*, 2775.

[46]. Gorelsky, S. I.; Lapointe, D.; Fagnou, K. *J. Am. Chem. Soc.* **2008**, *130*, 10848.

[47]. Ess, D. H.; Bischof, S. M.; Oxgaard, J.; Periana, R. P.; Goddard, W. A. III *Organometallics* **2008**, *27*, 6440.

[48] Foti, M. C.; Daquino, C.; Mackie, I. D.; DiLabio, G. A.; Ingold, K. U. *J. Org. Chem.* **2008**, *73*, 9270.

Full citation of ref. 36:

G09 full reference

Gaussian 09, Revision A.02, Frisch, M. J.; Trucks, G. W.; Schlegel, H. B.; Scuseria, G. E.; Robb, M. A.; Cheeseman, J. R.; Scalmani, G.; Barone, V.; Mennucci, B.; Petersson, G. A.; Nakatsuji, H.; Caricato, M.; Li, X.; Hratchian, H. P.; Izmaylov, A. F.; Bloino, J.; Zheng, G.; Sonnenberg, J. L.; Hada, M.; Ehara, M.; Toyota, K.; Fukuda, R.; Hasegawa, J.; Ishida, M.; Nakajima, T.; Honda, Y.; Kitao, O.; Nakai, H.; Vreven, T.; Montgomery, Jr., J. A.; Peralta, J. E.; Ogliaro, F.; Bearpark, M.; Heyd, J. J.; Brothers, E.; Kudin, K. N.; Staroverov, V. N.; Kobayashi, R.; Normand, J.; Raghavachari, K.; Rendell, A.; Burant, J. C.; Iyengar, S. S.; Tomasi, J.; Cossi, M.; Rega, N.; Millam, N. J.; Klene, M.; Knox, J. E.; Cross, J. B.; Bakken, V.; Adamo, C.; Jaramillo, J.; Gomperts, R.; Stratmann, R. E.; Yazyev, O.; Austin, A. J.; Cammi, R.; Pomelli, C.; Ochterski, J. W.; Martin, R. L.; Morokuma, K.; Zakrzewski, V. G.; Voth, G. A.; Salvador, P.; Dannenberg, J. J.; Dapprich, S.; Daniels, A. D.; Farkas, Ö.; Foresman, J. B.; Ortiz,

J. V.; Cioslowski, J.; Fox, D. J. Gaussian, Inc., Wallingford CT, 2009.

Chapitre 3 : Impact of Backbone Substituents on POCOP-Ni Pincer complexes: A Structural, Spectroscopic and Electrochemical Study

Article 2

Boris Vabre, Denis M. Spasyuk and Davit Zargarian

Département de chimie, Université de Montréal, Montréal (Québec), Canada H3C 3J7

Organometallics **2012**, *31*, 8561–8570.

Chapitre 3

3.1 Abstract

When treated at room temperature and in the presence of NEt_3 with $\{(i\text{-PrCN})NiBr_2\}_n$, the pincer-type ligands R-POC^{H}OP$^{R'}$ undergo direct C-H nickellation to give the pincer complexes (R-POCOP$^{R'}$)NiBr in 45-92% yields (R-POCOP = $\kappa^P,\kappa^C,\kappa^P$-$\{R_n$-2,6-$(R'_2PO)_2C_6H_{3-n}\}$; R_n = 4-OMe, 4-Me, 4-CO_2Me, 3-OMe, 3-CO_2Me, 3,5-*t*-Bu_2 ; R' = *i*-Pr, *t*-Bu). These complexes have been characterized by multinuclear NMR and UV-vis spectroscopy as well as single crystal X-ray diffraction studies to delineate the impact of R and R' on Ni-ligand interactions. The solid state structural data have revealed slightly shorter Ni-Br bonds in the complexes bearing a 4-CO_2Me substituent, shorter Ni-P bonds in the complex bearing *t*-Bu substituents at the 3- and 5-positions, and longer Ni-P bonds in complexes featuring OP(*t*-Bu)$_2$ donor moieties. The UV-vis spectra indicate that a 4-CO_2Me substituent causes a red-shift in the frequency of the MLCT bands (330-365 nm), whereas the ligand field transitions appearing in the 380-420 nm region are influenced primarily by the *P*-substituents. Cyclic voltammetry measurements have shown that the oxidation potentials of the title complexes are affected by P- and ring-substituents, oxidation being somewhat easier with t-Bu_2PO (vs. i-Pr_2PO), OMe and Me (vs. CO_2Me), and t-Bu (vs. Cl). Moreover, oxidation potentials are affected more by the aromatic substituents at the 4-position vs. those at the 3- and 5-positions.

Chapitre 3

3.2 Introduction

Pincer complexes of nickel based on the 1,3-bis(phosphinomethyl)- and 1,3-bis(aminomethyl)phenyl ligands were among the first pincer complexes reported by the groups of Shaw[1] and van Koten,[2] respectively. The organonickel chemistry of these so-called PCP- and NCN-type pincer ligands has received increasing scrutiny over the past three decades and led to the development of interesting applications based on both divalent and trivalent systems.[3] The past decade has also witnessed exciting discoveries emerging from the chemistry of nickel pincer complexes based on related new ligands such as $PC_{sp3}P$,[4] POCOP[5] and $POC_{sp3}OP$,[5b,c] POCN,[6] PNP,[7] NNN,[8] etc. (Figure 3.1). These developments have underlined the possibility of fine-tuning the reactivities of nickel pincer complexes through modifications in donor moieties and ligand backbone.

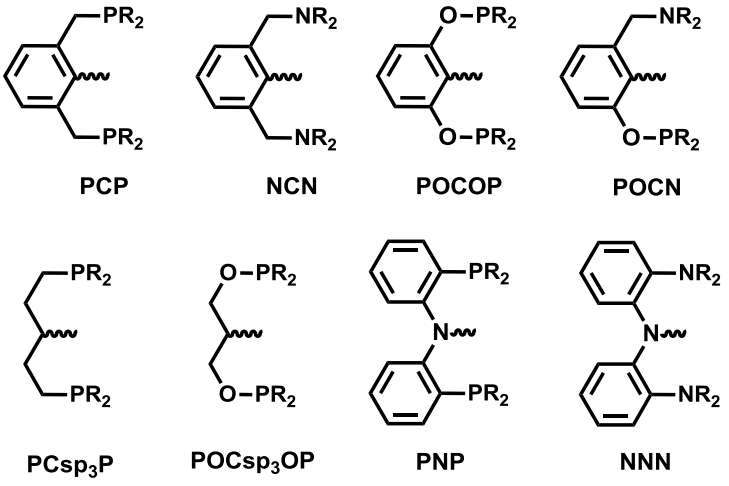

Figure 3.1 Various pincer ligands.

In this context, the groups of Guan, Goldberg, Peruzzini, and Hazeri have reported on the reactivities of (POCOP)Ni(H)[9] and (PCP)Ni(H)[10] as a function of *P*-substituents, while our group has reported on the structures and reactiviteis of charge-neutral and cationic PCP- and POCOP-type complexes of nickel as a function of different *P*-substituents and pincer backbones (aromatic vs. aliphatic).[11] The impact of ring-substituents on the structures and reactivities of aromatic PCP- and POCOP-Ni complexes has not been examined in a systematic manner, but this issue is beginning to attract interest. For instance, Morales-Morales' group has reported very recently the synthesis of POCOP-type systems based on 4-*n*-dodecylresorcinol[12] and 1,3-dihydroxynaphthalene,[13] and examined the effectiveness of the latter complex in Suzuki coupling, whereas Huang's group has studied the homocoupling of benzyl halides by (R-POCOP$^{R'}$)NiX (X= Cl, Br, I) to ascertain the influence of ring- and *P*-substituents R and R′ on this reaction.[14] Our group has also shown that in the cationic complexes $[(POCOP)Ni(NCMe)]^+$ the *P*-substituents have greater influence on structures and reactivities relative to chloride substituents at the 3- and 5-positions (with respect to the metallated carbon).[11a] In contrast to these sporadic and limited studies for POCOP-Ni systems, the impact of ring- and *P*-substituents on the properties of POCOP-Ir complexes has been investigated in much more detail.[15] Similar studies have been reported on NCN-Ni and NCN-Pt complexes.[16]

As a continuation of our investigations on the chemistry of POCOP-Ni complexes, we have set out to examine how the Ni center is influenced by ring-substituents, in particular those at the more sensitive 4-position (*para* with respect to the metallated carbon). The present report describes the synthesis and characterization

of the complexes (R-POCOP$^{R'}$)NiBr where R and R' represent, respectively, the substituents on the resorcinol ring and the phosphinite moiety (figure 3.2). The impact of R and R' on solid state structures, electronic transitions, and electrochemical properties of these compounds will be discussed.

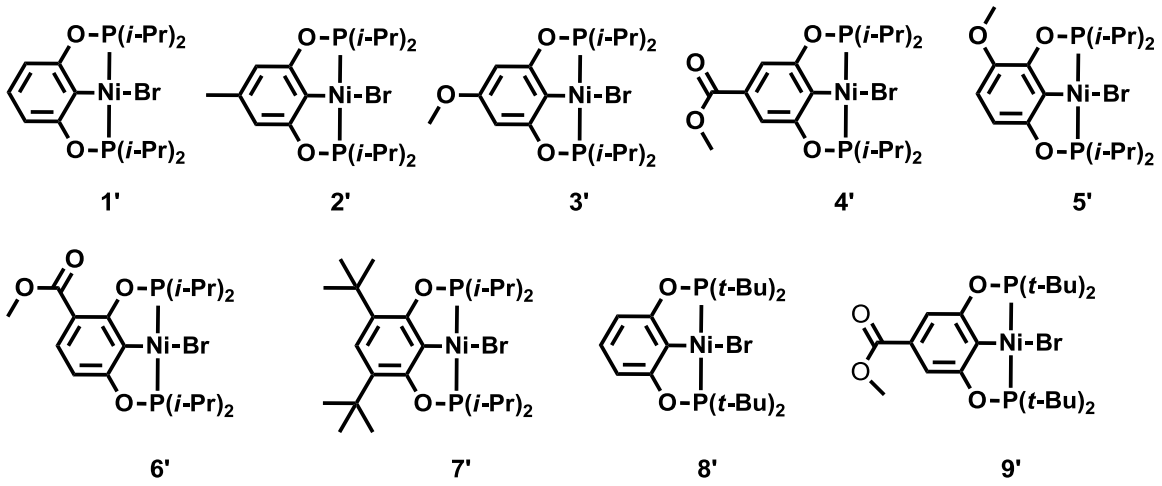

Figure 3.2 Nickel pincer complexes presented in this study.

3.3 Results and discussion

The synthesis of *m*-phenylene-based POC^{H}OP ligands used in this study involved treating the doubly deprotonated resorcinol or its substituted derivatives R_n-POC^{H}OP with ClPR'$_2$ (Scheme 1)[17] and vacuum distillation of the oily products where possible; this methodology furnished six new ligands in 60-94% yields (Table 3.1). The new ligands were characterized by combustion analysis and NMR spectroscopy; the previously reported ligand POC^{H}OP$^{t\text{-}Bu}$ was also subjected to single crystal X-ray diffraction analysis (vide infra). All the ligands were then treated with a small excess of $\{(i\text{-PrCN})NiBr_2\}_n$ in the presence of NEt_3 at ambient temperature to give the corresponding pincer complexes via a direct nickellation step (Scheme 3.1).[18]

This straight forward methodology has allowed the preparation of eight new complexes in 45-92% yields (Table 3.1). It is interesting to note that the lowest yield is obtained from the ligand bearing bulky *t*-Bu substituents at the 3- and 5-positions on the ring (45% for complex **7'**), whereas in the case of *t*-Bu_2P-based derivatives placing a COOMe substituent at the *para* position appears to favor the yield (52% for complex **8'** vs. 72 for complex **9'**).[19] The new complexes have been characterized by combustion analysis, NMR and UV-Vis spectroscopy, and single crystal diffraction studies (vide infra).

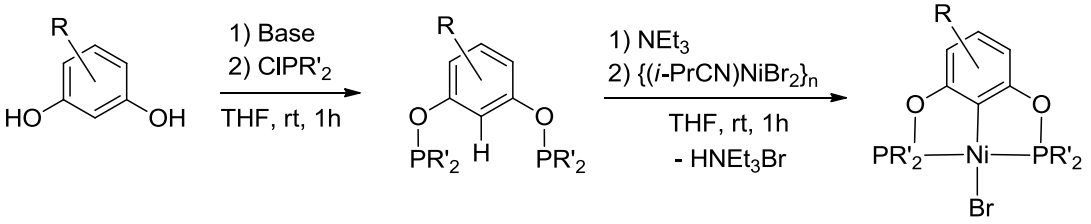

Scheme 3.1 Ligands and complexes synthesis.

Table 3.1 POCOP ligands and complexes synthesized

R'	R	Ligands			Complexes		
		no.	Yield (%)	$^{31}P\ \delta^{\dagger}$	no.	Yield (%)	$^{31}P\ \delta^{b}$
i-Pr	---	**1** [a]	-	149.0	**1'** [a]	-	188.2
	4-Me	**2**	85	148.9	**2'**	76	189.1
	4-OMe	**3**	70	147.5	**3'**	74	190.6
	4-CO_2Me	**4**	89	151.9	**4'**	92	190.6
	3-OMe	**5**	60	151.7, 157.2	**5'**	90	187.5 (d), 192.2 (d) [c]
	3-CO_2Me	**6**	94	151.2, 151.6	**6'**	86	190.4 (d), 192.1 (d) [d]

	3,5-*t*-Bu_2	**7** [a]	**-**	139.5	**7'**	45	185.2
t-	H	**8** [a]	-	153.1	**8'**	57	191.0
Bu	4-CO_2Me	**9**	63	155.8	**9'**	72	191.8

a) Previously reported ligands/complexes. b) Unless otherwise indicated, all signals are singlet resonances. c) AB signal, J_{PP} ~ 318 Hz. d) AB signal, J_{PP} ~ 323 Hz.

NMR analyses.

Assignments of NMR spectra for the new ligands and complexes were facilitated by comparison to the corresponding data obtained previously for fully characterized analogues.[5] Interestingly, the NMR data is only slightly affected by the ring-substituents R as reflected in the fairly narrow ranges of ^{31}P δ values observed for all ligands (ca. 147-156 ppm) and complexes (ca. 188-192 ppm). In this regard, ^{31}P δ values of the ligand signals are more strongly affected as a result of nickellation, which causes a deshielding by ca. 40 ppm on average; the nearly linear relationship between ligand/complex ^{31}P chemical shift values is apparent from a plot of ^{31}P δ values provided as supporting information. In contrast, the impact of nickellation on the $^{13}C\{^1H\}$ δ values appears to be more complex: the aromatic carbon nucleus directly bonded to the Ni center experiences a downfield shift of ca. 17-24 ppm, whereas upfield shifts were noted for the remaining aromatic carbon nuclei (ca. 1-6 ppm) as well as most aromatic protons (ca. 0.2-0.4 ppm).

The ^{31}P NMR spectra of the non-symmetrical ligands **5** and **6** and their complexes **5'** and **6'** were particularly instructive. The two inequivalent phosphinite moieties of these ligands showed two singlets appearing at fairly different chemical shifts in **5** (151.7 and 157.2 ppm), but very close to each other in **6** (151.1 and 151.6 ppm). The spectrum for complex **5'** displayed a "normal" AB pattern consisting of two doublets at 187.5 and 192.2 ppm ($^2J_{P\text{-}P}$= 318 Hz; $\Delta\nu/J_{P\text{-}P}$~ 2.5), whereas the spectrum for **6'** appeared to consist of two closely spaced singlets (192.06 and 192.13 ppm) instead of the expected AB doublets. The $^{31}P\{^1H\}$ NMR spectrum of a more concentrated sample recorded on a higher field instrument (ca. 202.5 MHz) showed a four-peak AB-type signal displaying very weak outer peaks (~1:20:20:1, Fig. 3.3), which is presumably caused by the very similar chemical shifts of the two P nuclei and their large coupling constant ($\Delta\nu/J_{P\text{-}P}$~ 0.96).[20] A similar 'roof effect' has already been observed in an asymmetric PCP platinum pincer complex.[21]

Crystallographic analyses.

X-Ray diffraction studies have been conducted on single crystals of complexes **3'-7'** as well as ligand **8**. Reliable structural data could not be obtained for compounds **5'** and **6'** due to the inferior quality of the single crystals obtained for these complexes, but the overall quality of the data was very good for all other products including complex **8'** which displayed disordered t-Bu substituents.[22] The ORTEP diagrams are shown in Figure 3.3 (**8**) and Figure 3.4 (**3'-4'**, **7'** and **8'**), and the main structural parameters are listed in Table 3.2; details of the diffraction studies are listed in Table 3.9 and Table 3.10 (Supporting Information).

The *t*-Bu_2PO moieties in ligand **8** adopt positions that minimize steric interactions, with one moiety being in the plane of the aromatic ring while the other phosphorus is out of plane by 0.798 Å. Comparison of the P-O distances in **8** and **8'** reveals a significant shrinkage (by 0.024 Å) upon complexation to nickel; this might arise from the P→Ni donation in the complexes that would enhance the dipolar character of the P-O bond. This is the first solid state structure of a POCOP-type ligand.

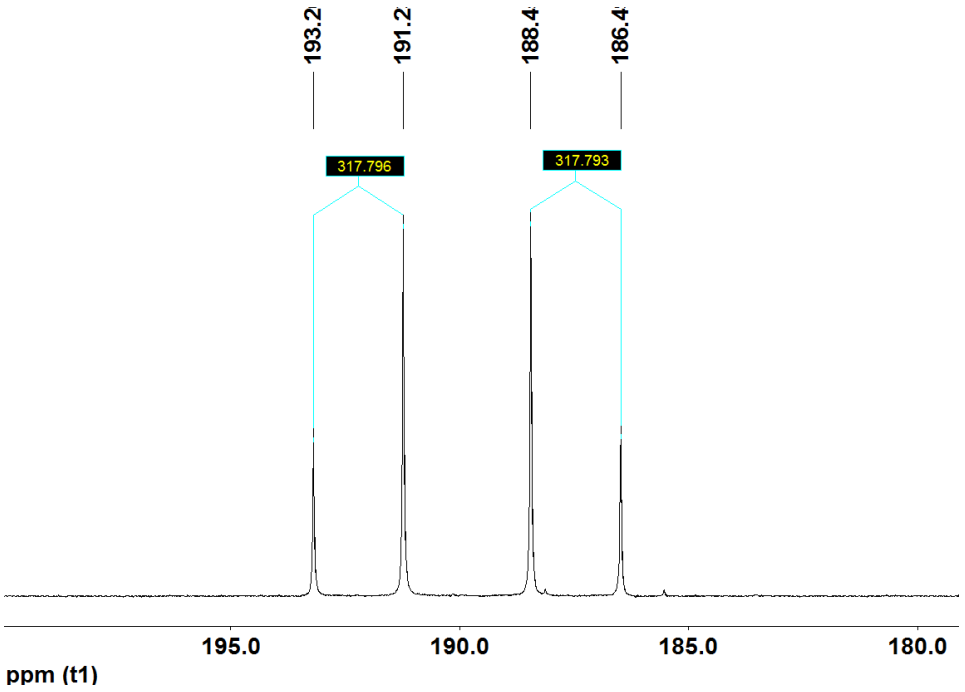

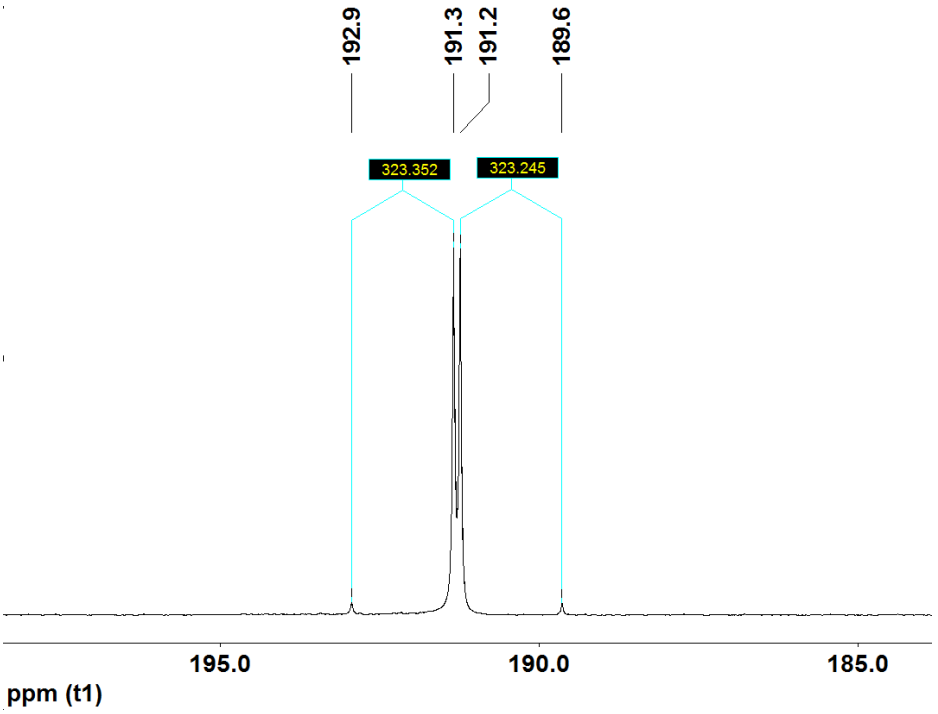

Figure 3.3 31P{1H} NMR spectra of complexes 5' (above) and 6' (below).

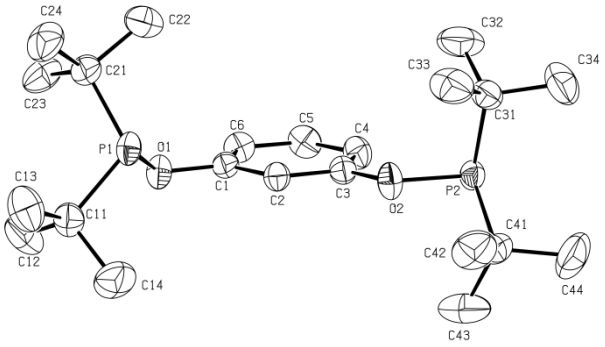

Figure 3.4 ORTEP diagrams for ligand **8**. Thermal ellipsoids are shown at the 50% probability level. Hydrogen atoms are omitted for clarity.

Table 3.2 Selected bond distances (Å) and angles (°) for ligand **7** and complexes **1'**-**4'**, **7'**, **8'**, and **9'** (molecule 1)

Compound	Ni-C	Ni-Br	Ni-P_1	Ni-P_2	P_1-Ni-P_2	P_1-O_1
1' *	1.885 (3)	2.323 (1)	2.153 (1)	2.142 (1)	164.92 (4)	1.663 (2)
2'	1.885 (3)	2.330 (1)	2.158 (1)	---	164.21 (3)	1.655 (2)
3'	1.877 (2)	2.319 (1)	2.155 (1)	2.152 (1)	164.65 (2)	1.663 (2)
4'	1.872 (2)	2.312 (1)	2.157 (1)	2.159 (1)	165.26 (2)	1.656 (2)
7'	1.892 (4)	2.320 (1)	2.139 (1)	2.143 (1)	165.06 (5)	1.650 (3)
8'	1.887 (2)	2.338 (2)	2.193 (1)	2.189 (1)	164.13 (3)	1.654 (2)
8	---	---	---	---	---	1.678 (1)
9'	1.877 (2)	2.321 (1)	2.189 (1)	2.194 (1)	164.58 (3)	1.652 (2)

* The data for **1'** is taken from ref. 5b

The nickel center in all complexes adopts a distorted square-planar geometry due, primarily, to the small bite angle of the POCOP ligands (P-Ni-P~ 164-165°). The Ni-C distances are fairly similar in all cases (~1.87-1.89 Å) as are Ni-Br distances (~ 2.31-2.34 Å), but the latter appear to be shortest in complexes bearing a 4-CO_2Me substituent. This point is best illustrated by comparing the Ni-Br distances in unsubstituted complexes **1'** (2.323(1) Å) and **8'** (2.338(2) Å) vs. their 4-CO_2Me counterparts **4'** (2.312(1) Å) and **9'** (2.321(1) Å). The shorter Ni-Br distances in the complexes bearing electron-withdrawing substituents can be attributed to the weaker trans influence of the electron-depleted aryl rings.[23]

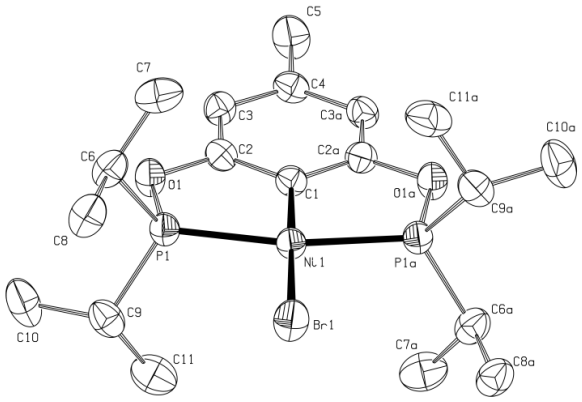
C5
C7
C4
C3
C3a
C11a
C10a
C6
C2
C2a
O1
C1
O1a
C9a
C8
P1
Ni1
P1a
C6a
C9
C10
Br1
C7a
C11
C8a

2'

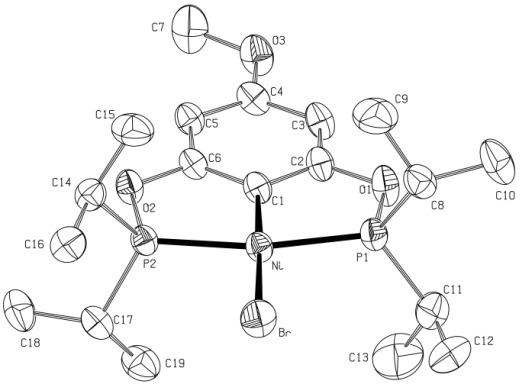
C7
O3
C4
C15
C5
C3
C9
C6
C2
C14
O1
C8
C10
O2
C1
C16
P2
Ni
P1
C11
C17
Br
C18
C19
C13
C12

3'

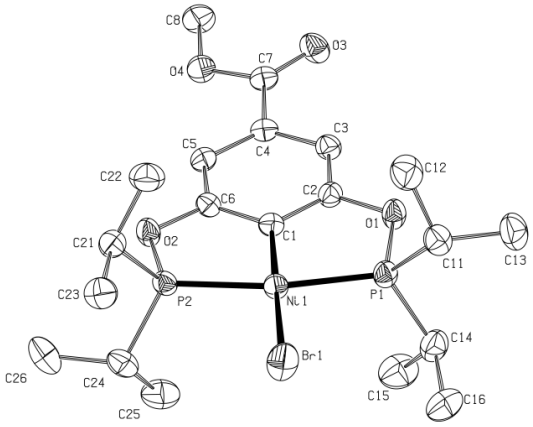
C8
O4
C7
O3
C5
C4
C3
C22
C6
C2
C12
O1
C21
O2
C1
C11
C13
C23
P2
Ni1
P1
Br1
C14
C26
C24
C15
C16
C25

4'

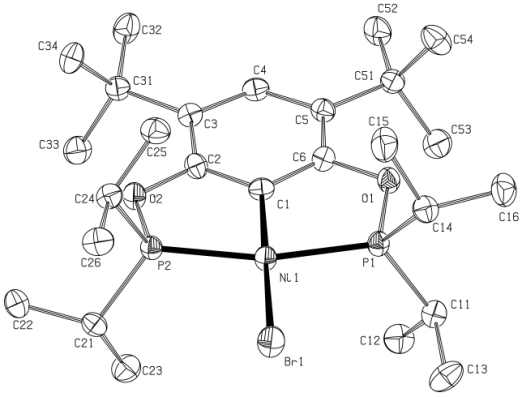
C52
C32
C54
C34
C31
C4
C51
C3
C5
C15
C33
C53
C25
C2
C6
C24
O2
C1
O1
C16
C14
C26
P2
Ni1
P1
C22
C11
C21
C12
C23
Br1
C13

7'

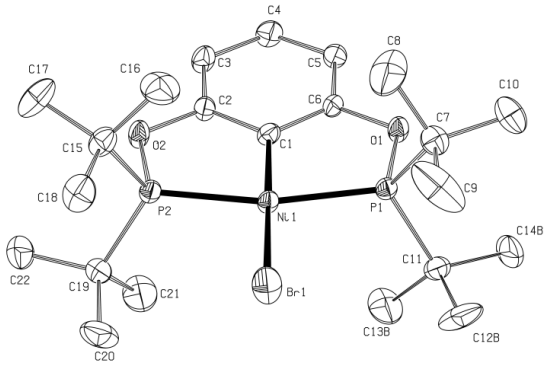
C4
C3
C5
C8
C17
C16
C2
C6
C10
C7
C15
O2
C1
O1
C9
C18
P2
Ni1
P1
C14B
C22
C19
C21
Br1
C11
C13B
C12B
C20

8'

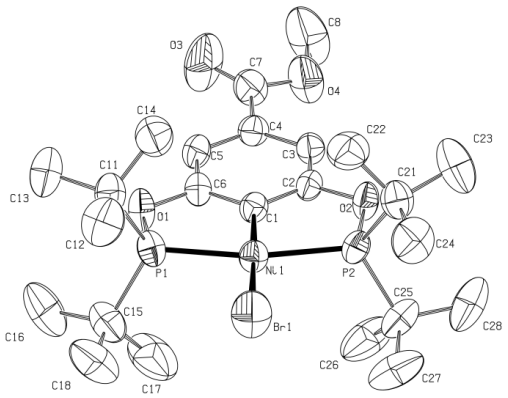
C8
O3
C7
O4
C14
C4
C22
C23
C11
C5
C3
C21
C13
C6
C2
O2
C1
O1
C24
C12
P1
Ni1
P2
C25
C15
Br1
C28
C16
C26
C18
C17
C27

9'

Figure 3.5 ORTEP diagrams for complexes **2'-4'** and **7'-9'**. Thermal ellipsoids are shown at the 50% probability level. Hydrogen atoms are omitted for clarity.

The Ni-P distances were found to be fairly insensitive to the ring-substituents R, but important variations were noted as a function of *P*-substituents R' (~ 2.19 Å with *t*-Bu and ~2.14-2.16 Å with *i*-Pr). It is interesting to note that the shortest Ni-P bond distances in the *i*-Pr_2PO series are found in **7'**, implying that the presence of bulky t-Bu substituents on the 3- and 5-positions of the aromatic ring reinforces the Ni-P interactions.

Absorption spectroscopy.

UV-Vis spectra were recorded for ca. 10^{-4} M CH_2Cl_2 solutions of the ligands (pale yellow) and complexes (yellow). The ligand spectra displayed multiple intense bands in the UV region below 250 nm, in addition to one or two bands of moderate intensity centered at higher wavelengths. The energies of the latter bands appear to be much more sensitive to the ring-substituents R than the *P*-substituents R'. For instance, the ligands bearing electron-releasing substituents or none absorb at 272-276 nm regardless of R' (e.g., ligands **3**, **2**, and **8**), whereas those bearing the electron-withdrawing substituent 4-CO_2Me absorb at 306 nm (ligand **4**) or 308 nm (ligand **9**). We conclude that these bands involve $\pi \rightarrow \pi^*$ transitions, and the difference between the frequencies observed for ligands **4** and **9**, on the one hand, and all other ligands (ca. 4,000 cm^{-1}) can be rationalized by considering that such transitions should be

lower in energy when the build-up of charge in the excited state can be stabilized more effectively. In other words, ligands bearing the most effective electron-accepting ring- substituent should exhibit lower energy $\pi \rightarrow \pi^*$ transitions; a similar phenomenon is at work for the MLCT transitions in the complexes (vide infra).

Similarly to the ligands, the complexes displayed multiple high-intensity bands in the UV region, in addition to a few less intense bands in the regions 330-365 nm and 380-420 nm (Fig. 3.6 and Table 3.3). Since the latter bands are absent in the ligand spectra, they can be assigned to electronic transitions involving the metal ions. Moreover, since the lowest energy bands are fairly insensitive to ring-substituents R and more sensitive to P-substituents R', they can be attributed to d-d transitions involving the ligand fields. This is anticipated for metal-centered transitions and most evident when we compare the energies of these bands for complexes **4'** and **9'** (ca. 26,000 vs. 24,000 cm^{-1}). On the other hand, the more intense transitions in the region 330-365 nm that show greater sensitivity to the ring-substituents R are considered to be spin-allowed charge transfer bands (MLCT).[24]

The frequencies of MLCT transitions range from ca. 30,000 cm^{-1} in the spectra of complexes bearing either electron-releasing substituents (**2'**, **3'**, **5'**, and **7'**) or none (**1'** and **8'**) to ca. 28,000 cm^{-1} observed in the spectra of complexes **4'** and **9'** bearing 4-CO_2Me substituents. Evidently, the largest electronic impact on MLCT transition frequencies (ca. 2000 cm^{-1}) is caused by 4-CO_2Me, and this observation can be rationalized as was discussed above for the $\pi \rightarrow \pi^*$ transitions of the unmetallated ligands. It is also worth noting that in some cases the energy of the MLCT band is more sensitive to the position of the ring-substituent R as opposed to its electronic

character. Thus, the MLCT band of complex **6'** appears ca. 1600 cm^{-1} higher than that of **4'**, implying that the CO_2Me substituent exerts greater electronic influence at the 4- vs. 3-position. As will be discussed below, the cyclic voltammetry measurements corroborate the greater impact of the 4-CO_2Me substituent on oxidation potentials of the complexes. The electron-releasing substituents Me, *t*-Bu, and OMe also influence the oxidation potentials of the complexes (vide infra), but they show little or no impact on the energies of the MLCT bands regardless of the substitution position. Thus, complexes **3'** and **5'** bearing a OMe substituent at the 3- or 4-position show MLCT bands at virtually identical energies.

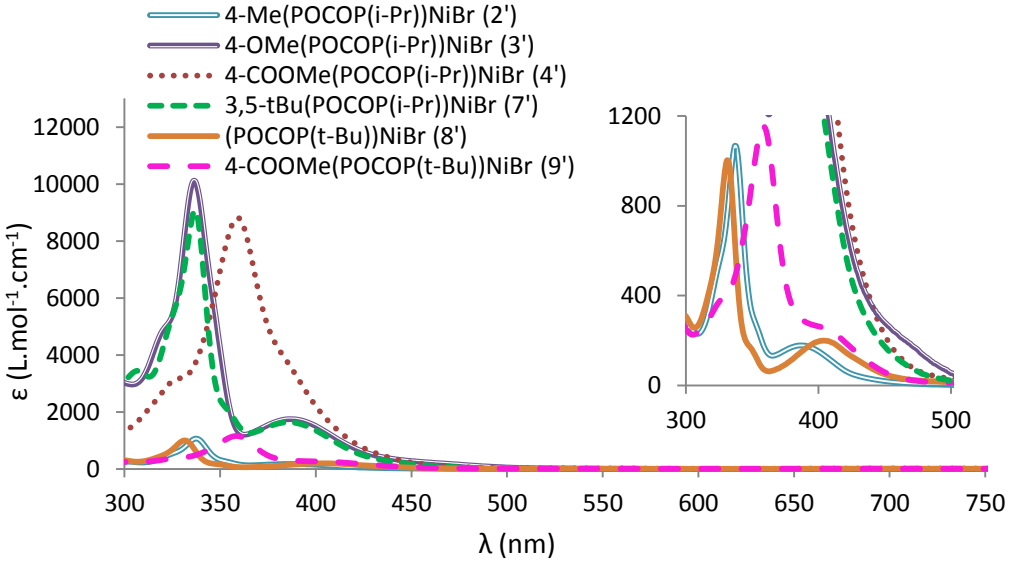

Figure 3.6 UV-Vis spectra (CH_2Cl_2. r.t.) for complexes **3'-4'** and **8'-7'**.

Table 3.3 Absorption spectral data for complexes **1'-9'** (CH_2Cl_2. r.t.).

R'	R	no.	λ_{max} (nm) (ε , $M^{-1}.cm^{-1}$)	
i-Pr	H	**1'**	337(9400)	389(1970)
	4-Me	**2'**	338(1060)	396(160)
	4-OMe	**3'**	336(10100)	387(1750)
	4-CO_2Me	**4'**	362(8550)	384(3860)
	3-OMe	**5'**	337(900)	389(150)
	3-CO_2Me	**6'**	341(810)	397(150)
	3,5-*t*-Bu_2	**7'**	337(9060)	388(1630)
t-Bu	---	**8'**	334(910)	407(190)
	4-CO_2Me	**9'**	360(1040)	413(220)

Cyclic voltammetry measurements.

Figure 3.7 shows the cyclic voltammograms of (R-POCOP$^{R'}$)NiBr, and Table 3.4 lists the potentials (vs ferrocene) in each case. Previous studies have established that PCP-,[4] POCOP-,[5b,c,d] and POCN-Ni[6a,b,c] complexes undergo one-electron oxidation of the nickel center that can be irreversible or reversible, depending on the

specific complex and the conditions under which the measurements are made. The CV curves obtained for the complexes under discussion here show that the oxidation process is reversible for **2'** and **7-9'**, quasi-reversible for **3'** and **5'**, and irreversible for **6'**.

Comparison of the potentials for complexes **3'-7'** relative to complex **1'** (Table 3.4) provides valuable insights into the impact of ring- and *P*-substituents on one-electron oxidation in this family of complexes. Thus, the oxidation process is much easier for complexes containing electron-releasing substituents Me, OMe, and *t*-Bu (complexes **3'**, **2'**, **5'** and **7'**). The greatest influence is exerted by the 4-OMe substituent, which lowers the oxidation potential by nearly 200 mV, whereas the 3-OMe has less influence.[25] By comparison, *P*-substituents appear to have less influence over the oxidation potential of these complexes, as seen from the nearly equal potentials of **1'** and **8'**. However, it is worth noting that the Ph_2PO analogue of these complexes shows a somewhat higher oxidation potential,[5d] as anticipated on account of the weaker donor aptitude of the Ph substituents. Finally, oxidation is more difficult for complexes containing electron-withdrawing ring-substituents (**4'**, **6'** and **9'**), the greatest influence (ca. 130 mV) being exerted by 4-CO_2Me. Thus, the electrochemical oxidation potential of (R-POCOP)NiBr can be modulated over a range of 300 mV (**3'** vs. **4'**) by judicious choice of the ring- substituents R.

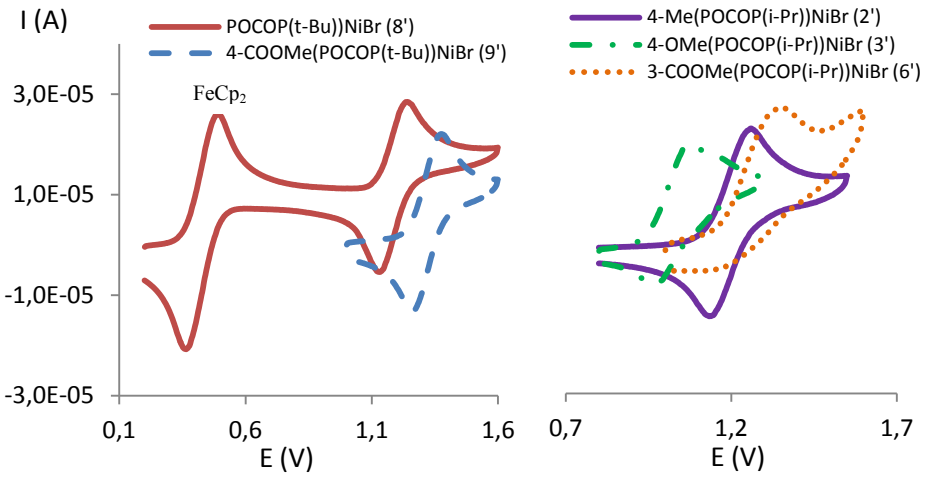

Figure 3.7 Cyclic voltammograms of **3'**, **2'**, **6'**, an equimolar mixture of **8'** and ferrocene, and **9'**. The measurements were carried out at 298 K on CH_2Cl_2 solutions containing the sample complexes (1 mM) and $[Bu_4N][PF_6]$ as electrolyte (0.1 M). A scan rate of 100 $mV.s^{-1}$ was used, and the potentials were referenced to the Ag/Ag^+ redox couple.

Table 3.4 Redox and oxidation potentials of (R-POCOPR')NiBr vs $FeCp_2/FeCp_2^+$

R'	R	$E_{1/2}$ (mV)	E_{ox} (mV)
***i*-Pr**	**H (1')**	---	810
	4-Me (2')	735	800
	4-OMe (3')	565	620
	4-CO_2Me (4')	---	940
	3-OMe (5')	715	761
	3-CO_2Me (6')	---	900
	3,5-*t*-Bu_2 (7')	687	750
	3,5-Cl_2	---	840[b]
***t*-Bu**	**H (8')**	750	800
	4-CO_2Me (9')	860	920

a) See captions of Figures 3.7, or the Experimental section, for the measurements details. b) Reported in ref. 11a.

The question arises as to how closely oxidation potentials reflect the level of electron density at the Ni center in the complexes under discussion. In the absence of reactivity data, it is tempting to seek other correlations that might shed light on this question. As discussed above, the energies of metal-centered electronic transitions are influenced by *P*-substituents, but they appear fairly insensitive to ring-substituents. We sought to establish whether or not there is any correlation between oxidation potentials obtained from CV measurements, on the one hand, and the ^{13}C (δ C1) and ^{31}P chemical shifts on the other. Figure 3.8 shows plots of the ^{13}C and ^{31}P chemical shifts of various complexes against the corresponding oxidation potentials. These plots reveal a moderate degree of correlation between E_{ox} and δ C1 but a much more tenuous correlation with ^{31}P chemical shifts.

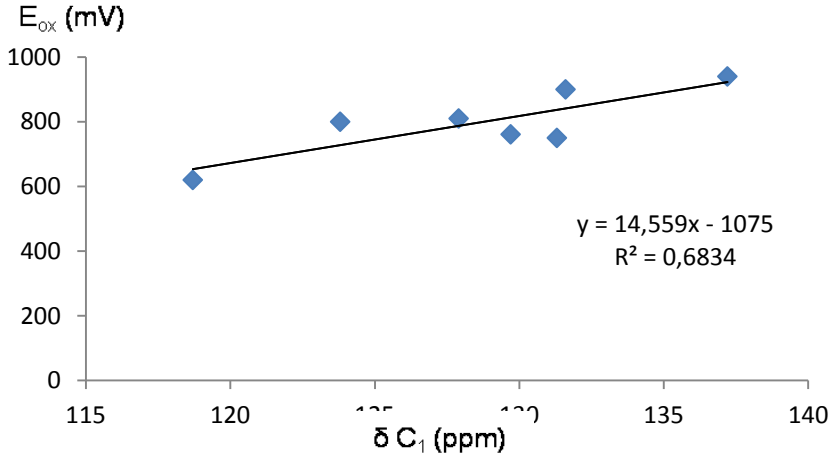

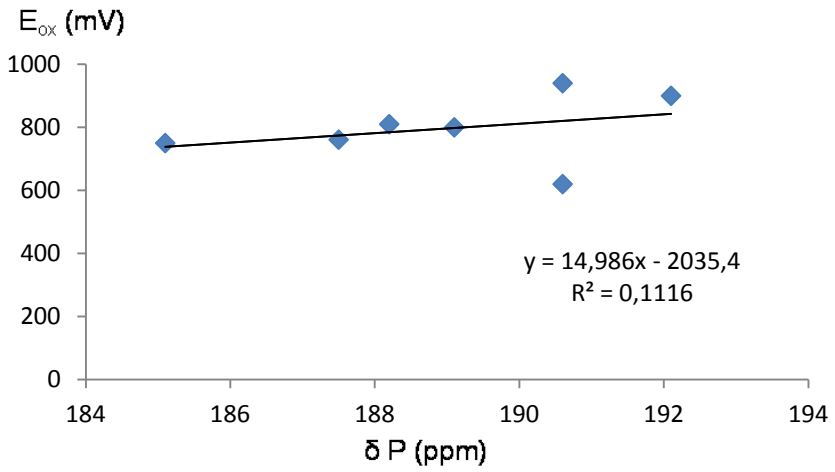

Figure 3.8 Plots of oxidation potentials vs. NMR chemical shifts for the C_1 (above) and P (below) nuclei.

3.4 Conclusion

A previous study helped establish that substituents placed on the aromatic ring of resorcinol-based POCOP-type ligands can influence the nickellation step leading to the formation of pincer complexes.[18] The present study is the first systematic attempt to measure the influence of ring-substituents on the electronics of the Ni center as manifested in its spectral, structural, and redox properties. Our findings point to a strong correlation between redox potential of a given complex (R-POCOP)NiBr and the electronic nature of the ring-substituent R placed at the *para* position with respect to the nickellated carbon. An observable impact was also observed in the electronic spectra of the complexes bearing electron-withdrawing substituents COOMe at the 3- or 4-positions. On the other hand, the electronic properties of ring-substituents appear to have little or no impact on solid state structures, but the steric bulk of the *t*-Bu substituents at the 3- and 5-positions appears to reinforce Ni-P interactions. The insights gleaned from the present study will help us design future investigations aimed at probing the impact of ring- substituents on the reactivities of this family of complexes.

3.5 Experimental

General Procedures. Unless otherwise indicated, all manipulations were carried out under nitrogen atmosphere using standard Schlenk and glove box techniques. Solvents were dried by passage over activated alumina contained in MBRAUN systems. Triethylamine is dried by distillation over CaH_2. The reagents isobutyronitrile, nickel powder, bromine, $ClP(i\text{-}Pr)_2$, $ClP(t\text{-}Bu)_2$, $ClP(Ph)_2$, 5-Methyl-

1,3-benzenediol, 4,6-Dichloro-1,3-benzenediol, Methyl 2,4-dihydroxybenzoate, Methyl 3,5-dihydroxybenzoate, and NaH were purchased from Sigma-Aldrich and used without further purification. 5-Methoxyresorcinol is purchased from Chemsavers. 4-Methoxyresorcinol has been synthesized following a published procedure.[26]

Most NMR spectra were recorded at 400 (^{1}H) and 161.9 MHz (^{31}P) using a Bruker AV400rg spectrometer, or at 400 (^{1}H) and 100.56 MHz (^{13}C{^{1}H}) using a Bruker ARX400 spectrometer. The ^{31}P{^{1}H} NMR spectrum of complex **6'** was recorded at 202.5 MHz using a Bruker AV500 spectrometer. Chemical shift values are reported in ppm (δ) and referenced internally to the residual solvent signals (^{1}H and ^{13}C: 7.26 and 77.16 ppm for $CDCl_3$; 7.16 and 128.06 ppm for C_6D_6) or externally (^{31}P, H_3PO_4 in D_2O, δ= 0). Coupling constants are reported in Hz. UV/vis spectra were measured on a Varian Cary 500i. The IR spectra were recorded on Bruker Alpha-P FTIR (4000-400 cm^{-1}). The elemental analyses were performed by the Laboratoire d'Analyse Élémentaire, Département de chimie, Université de Montréal.

{(*i*-PrCN)NiBr$_2$}$_n$. To a suspension of nickel powder (1 g, 17.04 mmol) in isobutyronitrile (50 mL) at 0 °C bromine was added drop-wise (1.00 mL, 19.05 mmol), which caused a color change to green after a few minutes. Stirring the reaction mixture overnight at room temperature, followed by filtration, washing of the solid residue with Et_2O (2 × 25 mL), and drying under vacuum gave the desired product as a beige powder (4.58 g, 98%). This compound must be protected from ambient atmosphere, because it appears to be hygroscopic: the beige powder turns

green after overnight exposure to air, and becomes a green liquid after days. This compound has been identified based on its IR spectrum and elemental analysis. Multiple attempts to grow crystals of this compound have failed to produce single crystals. IR (cm^{-1}): 2974m, 2914m, 2864w, 2288vs, 1452vs, 1387w, 1367w, 1314w, 1278w, 1168w, 1103vs, 936w, 915w, 774w, 571w, 556s. Anal. Calcd for $C_4H_7Br_2NNi$ (287.61) : N, 4.87 ; C, 16.70 ; H, 2.45. Found: N, 4.85; C, 17.00; H, 2.42. UV-Vis (^{i}PrCN, 1.66 × 10^{-3} M) [λ_{max}, nm (ε, $L.mol^{-1}$ $.cm^{-1}$)]: 648 (103), 381(609), 313(1429), 284 (2001), 247 (1182), 223 (1885). $T_{decomposition}$ = 155 °C.

General procedure for synthesis of ligands. We have followed previously published procedures for the synthesis of ligands **1**[5b] and **7**.[27] Ligand **9** was prepared using the same method as reported for **8**,[15c] whereas the remaining ligands were prepared using slightly modified versions of these procedures, as described below.

1,3-(*i*-$Pr_2PO)_2$-5-OMe-C_6H_3, 3. Drop-wise addition of Cl*P*(*i*-Pr)$_2$ (2.56 mL, 16.13 mmol) to a solution of 5-methoxyresorcinol (1.13g, 8.06 mmol) and NEt_3 (2.47mL, 17.7 mmol) in THF (50 mL) led to the formation of a white precipitate. The reaction mixture was stirred at room temperature for 1 h, followed by removal of the volatiles and extraction of the solid residues with hexane (3 x 25 mL) to give the crude product as pale yellow oil (0.93 g, 70%). This material, which was shown by NMR spectroscopy to be greater than 98% pure, was used for the synthesis of the target complexes without further purification. ^{1}H NMR (400 MHz, C_6D_6): δ 0.97 (dd, J_{HP} = 19.6, J_{HH} = 7.2, 12H, CH(CH_3)$_2$), 1.13 (dd, J_{HP} = 10.4, J_{HH} = 7.0, 12H, CH(CH_3)$_2$), 1.74 (dh, J_{HP} = 2.5, J_{HH} = 7.0, 4H, PC*H*(CH$_3$)$_2$) 3.30 (s, 3H, OCH_3), 6.70 (m, 2H, *Ar*), 7.13 (m, 1H, *Ar*). ^{31}P{^{1}H} NMR (162 MHz, C_6D_6): δ 147.5 (s). ^{13}C{^{1}H} NMR (101

MHz, C_6D_6) : δ 17.15 (d, J_{CP} = 8.6, 4C, CH_3), 17.9 (d, J_{CP} = 20.6, 4C, CH_3), 28.6 (d, J_{CP} = 18.5, 4C, P*C*H(CH3)2), 54.9 (s, 1C, OCH_3), 98.8 (d, J_{PC}=11.0, 2C, 4,6-C_{Ar}), 101.9 (t, J_{PC} =12.0, 1C, 2-C_{Ar}), 161.7 (d, J_{PC}=9.4, 2C, C_{Ar}OP), 162.0 (s, 1C, C_{Ar}OMe). Anal. Calcd. for $C_{19}H_{34}O_2P_2$ (372,42): C, 61.28 ; H, 9.20. Found: C, 60.73; H, 9.30.

1,3-(*i*-Pr$_2$PO)-5-Me-C$_6$H$_3$, 2. This ligand (a colorless oil) was prepared in 85% yield (2.45 g) using the same procedure described for the synthesis of **3**. ^{1}H NMR (300 MHz, $CDCl_3$): δ 1.09 (d, J_{HH} = 7.2, CH(CH_3)$_2$, 6H), 1.13 (d, J_{HH} = 7.2, CH(CH_3)$_2$, 6H), 1.17 (d, J_{HH} = 7.0, CH(CH_3)$_2$, 6H), 1.19 (d, J_{HH} = 7.0, CH(CH_3)$_2$, 6H), 1.92 (dh, J_{HP} = 2.2, J_{HH} = 7.1, 4H, PC*H*(CH$_3$)$_2$) 2.28 (s,CH_3, 3H), 6.58 (m, *Ar*, 2H), 6.72 (m, *Ar*, 1H). ^{31}P{^{1}H} NMR (162 MHz, CDCl3): δ 148.9 (s). ^{13}C{^{1}H} NMR (101 MHz, $CDCl_3$) : δ 17.10 (d, J_{CP} = 8.5, 4C, CH_3), 17.8 (d, J_{CP} = 20.2, 4C, CH_3), 21.6 (s, 1C, CH_3), 28.35 (d, J_{CP} = 17.5, 4C, P*C*H(CH3)2), 106.3 (t, J_{PC} = 10.36, 1C, 2-C_{Ar}), 112.7 (d, J_{PC}=10.7, 2C, 4,6-C_{Ar}H), 139.85 (s, 1C, C_{Ar}Me), 160.1 (d, J_{PC}=8.7, 2C, C_{Ar}OP), Anal. Calcd. for $C_{19}H_{34}O_2P_2$ (356.42): C, 64.03; H, 9.62. Found: C, 63.83; H, 10.06.

1,3-(*i*-Pr$_2$PO)$_2$-5-COOMe-C$_6$H$_3$, 4. This ligand (a yellow oil) was prepared in 89% yield (4.23 g) using the same procedure described for the synthesis of 3. ^{1}H NMR (400 MHz, $CDCl_3$): δ 1.09 (dd, J_{HP} = 16, J_{HH} = 7.2, 12H, CH(CH_3)$_2$), 1.16 (dd, J_{HP} = 10.8, J_{HH} = 7.0, 12H, CH(CH_3)$_2$), 1.91 (dh, J_{HP}= 2.4, J_{HH} = 7.1, 4H, PC*H*(CH$_3$)$_2$), 3.88 (s, 3H, OCH_3), 7.08 (m, J_{HP}= 2.0, 1H, *Ar*), 7.38 (m, 2H, *Ar*). ^{31}P {1H} NMR (162 MHz, $CDCl_3$): δ 151.9 (s). ^{13}C{^{1}H} NMR (101 MHz, $CDCl_3$) : δ 17. 0 (d, J_{CP}= 8.4, 4C, CH_3), 17.7 (d, J_{CP}= 20.1, 4C, CH_3), 28.3 (d, J_{CP}= 17.8, 4C, P*C*H(CH3)$_2$), 52.1 (s, 1C, OCH_3), 113.0 (d, J_{PC}=10.8, 2C, 4,6-C_{Ar}), 113.4 (t, J_{PC}=11.0, 1C, 2-C_{Ar}),

131.7 (s, 1C, C_{Ar}CO), 160.2 (d, J_{PC}=9.1, 2C, C_{Ar}OP), 166.5 (s, 1C, C=O) Anal. Calcd. for $C_{20}H_{34}O_4P_2$ (400,43): C, 59.99; H, 8.56. Found: C, 59.45; H, 8.66.

1,3-(*i*-Pr$_2$PO)$_2$-4-OMe-C$_6$H$_3$, 5. The standard procedure described for the synthesis of 3 gave a yellow oil after vacuum distillation (1.5 g, 60%). ^{1}H NMR (400 MHz, $CDCl_3$): δ 1.07 (dd, J_{HP} = 6.8, J_{HH} = 7.0, 6H, CH(CH_3)$_2$), 1.11 (dd, J_{HP} = 7.2, J_{HH} = 7.0, 6H, CH(CH_3)$_2$), 1.16 (dd, J_{HP} = 11.2, J_{HH} = 7.1, 6H, CH(CH_3)$_2$), 1.21 (dd, J_{HP} = 10.8, J_{HH} = 7.1, 6H, CH(CH_3)$_2$), 1.88 (dh, J_{HH} = 7.1, J_{HP} = 2.2, 2H, 3-OPCH(CH$_3$)$_2$), 1.94 (dh, J_{HH} = 7.1, J_{HP} = 1.8, 2H, 1-OPCH(CH$_3$)$_2$), 3.77 (s,OCH_3, 3H), 6.64 (dm(AB) J_{HH} = 9.4, 1H, 6-H$_{Ar}$), 6.72 (d(AB), J_{HH} = 8.8, 1H, 5-H$_{Ar}$), 6.98 (m, 1H, 2-H$_{Ar}$,). ^{31}P{1H} NMR (162 MHz, $CDCl_3$): δ 151.7 (s), 157.2 (s). ^{13}C{^{1}H} NMR (101 MHz, $CDCl_3$) : δ 17.08 (d, J_{CP} = 8.6, 2C, CH$_3$), 17.17 (d, J_{CP} = 9.0, 2C, CH$_3$), 17.73 (d, J_{CP} = 8.4, 2C, CH$_3$), 17.93 (d, J_{CP} = 8.4, 2C, CH$_3$), 28.3 (d, J_{CP} = 17.9, 2C, PCH(CH$_3$)$_2$), 28.5 (d, J_{CP} = 18.5, 2C, PCH(CH$_3$)$_2$), 56.7 (s, 1C, OCH$_3$), 111.1 (dd, $J_{CP'}$ = 9.1, $J_{CP''}$ = 8.8, 1C, 2-C_{Ar}), 111.2 (d, J_{PC} =10.7, 1C, 6-C_{Ar}), 113.3 (s, IC, 5-C_{Ar}), 145.6 (s, 1C, C_{Ar}OMe), 149.0 (d, J_{PC} =8.25, 1C, 1-C_{Ar}OP or 3-C_{Ar}OP), 153.4 (d, J_{PC} =9.1, 1C, 3-C_{Ar}OP or 1-C_{Ar}OP). Anal. Calcd. for $C_{19}H_{34}O_2P_2$ (372,42): C, 61.28 ; H, 9.20. Found: C, 60.97; H, 9.72

1,3-(*i*-Pr$_2$PO)$_2$,4-(COOMe)-C$_6$H$_3$, 6. This ligand (a yellow oil) was prepared in 94% yield (4.5 g) using the same procedure described for the synthesis of 3. ^{1}H NMR (400 MHz, $CDCl_3$): δ 1.03 (dd, J_{HP} = 16, J_{HH} = 7.2, 6H, CH(CH_3)$_2$), 1.10 (dd, J_{HP} = 15.6, J_{HH} = 7.2, 6H, CH(CH_3)$_2$), 1.17 (dd, J_{HP} = 10.8, J_{HH} = 7.0, 6H, CH(CH_3)$_2$), 1.31 (dd, J_{HP} = 10.8, J_{HH} = 7.0, 6H, CH(CH_3)$_2$), 1.81 (dh, J_{HH}= 7.1, J_{HP}= 2.8, 2H, 1-OPCH(CH$_3$)$_2$), 1.96 (dh, J_{HH}= 7.0, J_{HP}= 3.5, 2H, 3-OPCH(CH$_3$)$_2$), 3.65 (s, 3H,

O*CH*$_3$), 6.92 (dm, J_{HH}= 8.7, 1H, 6-H$_{Ar}$), 7.87 (m, 1H, 2-H$_{Ar}$), 8.05 (d, J_{HH} = 8.7, 1H, 5-H$_{Ar}$). ^{31}P{1H} NMR (162 MHz, $CDCl_3$): δ 151.1 (s), 151.6 (s). ^{13}C{^{1}H} NMR (75 MHz, $CDCl_3$) : δ 16.88 (d, J_{CP} = 8.5, 2C, *C*H$_3$), 16.92 (d, J_{CP} = 8.5, 2C, *C*H$_3$), 17.41 (d, J_{CP} = 9.3, 2C, *C*H$_3$), 17.7 (d, J_{CP} = 10.1, 2C, *C*H$_3$), 28.14 (d, J_{CP} = 17.8, 2C, P*C*H(CH$_3$)$_2$), 28.2 (d, J_{CP} = 18.1, 2C, P*C*H(CH$_3$)$_2$), 51.36 (s, 1C, O*C*H$_3$), 108.3 (dd, $J_{CP'}$ = 12.7, $J_{CP''}$ = 11.8, 1C, 2-C_{Ar}), 110.9 (d, J_{PC} =10.9, 1C, 6-C_{Ar}), 114.4 (s, *I*C, 5-C_{Ar}), 132.9 (s, 1C, C_{Ar}COOMe), 160.7 (d, J_{PC} =9.2, 1C, 1-C_{Ar}OP or 3-C_{Ar}OP), 163.5 (d, J_{PC} =8.5, 1C, 3-C_{Ar}OP or 1-C_{Ar}OP), 166.2 (s, 1C, C=O). Anal. Calcd. for $C_{20}H_{34}O_4P_2$ (400,43): C, 59.99; H, 8.56. Found: C, 60.06; H, 8.61.

1,3-(*t*-Bu$_2$PO)-5-COOMe-C$_6$H$_3$, 9. This ligand was obtained as a colorless oil in 63% yield (1.7 g) using the same method as reported for ligand **8**.[15c] ^{1}H NMR (400 MHz, C_6D_6): δ 1.17 (d, J_{HP} = 11.7, C(C*H*$_3$)$_3$, 36H), 3.56 (s,O*CH*$_3$, 3H), 7.72 (m, *Ar*, 1H), 7.97 (m, *Ar*, 2H). ^{31}P NMR {1H} (162 MHz, C_6D_6): δ 155.8 (s). ^{13}C{^{1}H} NMR (101 MHz, $CDCl_3$) : δ 27.5 (d, J_{CP} = 15.6, 12C, *C*H$_3$), 35.8 (d, J_{CP} = 26.7, 4C, *C*CH$_3$), 51.8 (s, 1C, OMe), 113.1 (t, J_{PC}=11.9, 1C, 2-C_{Ar}), 113.2 (d, J_{PC} =10.8, 2C, 4,6-C_{Ar}), 133.0 (s, 1C, C_{Ar}CO), 161.4 (d, J_{PC}=10.1, 2C, C_{Ar}OP), 166.3 (s, 1C, C=O) Anal. Calcd. for $C_{24}H_{42}O_4P_2$ (456.54): C, 63.14; H, 9.27. Found: C, 63.75; H, 9.87.

Synthesis of the complexes. Previously published reports have described the synthesis and characterization of complex **1'** [5b] and the chloro analogue of complex **8'**.[22] Slightly modified versions of these procedures were used to prepare all other complexes, as described below.

{2,6-(*i*-Pr$_2$PO)$_2$-4-OMe-C$_6$H$_2$}NiBr, 3'. To the solution of ligand **3** (1.05 g, 2.81 mmol) and NEt_3 (469 µL, 3.37 mmol) in THF (30 mL) was added $\{(i\text{-PrCN})NiBr_2\}_n$ (807 mg, 2.81 mmol) and the mixture was stirred at room temperature for one hour during which it turned brown initially and then yellow, and a white precipitate appeared. Filtration of the final mixture and evaporation of the filtrate followed by extraction of the residual solids with hexane (3 × 25mL) gave a solution that yielded yellow crystals by slow evaporation. Washing the crystals with a small quantity of cold hexane gave the desired product (0.81 g, 74 %). ^{1}H NMR (400 MHz, C_6D_6): δ 1.18 (dt^v, J_{HH} = 4.3, 12H, CH(CH_3)$_2$), 1.40 (dt^v, J_{HH} = 6.1, 12H, CH(CH_3)$_2$), 2.26 (m, 4H, PCH(CH$_3$)$_2$), 3.25 (s, 3H,OCH_3), 6.33 (s, 2H, *Ar*). ^{31}P{^{1}H} NMR (162 MHz, C_6D_6): δ 190.63 (s). ^{13}C{^{1}H} NMR (101 MHz, $CDCl_3$) : δ 16.79 (s, 4C, *C*H$_3$), 17.89 (s, 4C, *C*H$_3$), 28.29 (vt, J_{CP} = 11.2, 4C, P*C*H(CH3)$_2$), 55.5 (s, 1C, O*C*H$_3$), 92.9 (vt, J_{PC} =6.1, 2C, *C*H$_{Ar}$), 118.7 (t, J_{PC}=21.4, 1C, Ni-C_{Ar}), 162.65 (s, 1C, C_{Ar}OMe), 169.5 (vt, J_{PC}=10.4, 2C, C_{Ar}OP). UV-Vis (CH_2Cl_2, 1.19 × 10^{-4} M) [λ_{max}, nm (ε, L.mol^{-1} .cm^{-1})]: 389(1748), 338(9895), 320(4876). Anal. Calcd. for $C_{19}H_{33}O_3P_2NiBr$ (510.01): C, 44.75; H, 6.52. Found: C, 44.82; H, 6.46.

{2,6-(*i*-Pr$_2$PO)$_2$-4-Me-C$_6$H$_2$}NiBr, **2'**. The standard procedure described above for **3'** gave the desired product as a yellow solid (1.05 g, 76 %). ^{1}H NMR (300 MHz, $CDCl_3$): δ 1.33 (dt^v, J_{HH} = 7.0, J_{HP} = 6.7, CH(CH_3)$_2$, 12H), 1.43 (dt^v, J_{HH} = 8.3, J_{HP} = 8.0, (CH(CH_3)$_2$)$_2$, 12H), 2.20 (s,CH_3, 3H), 2.45 (m, J_{HH} = 6.8, 4H, PCH(CH$_3$)$_2$), 6.28 (s, *Ar*, 2H). ^{31}P{^{1}H} NMR (162 MHz, CDCl3): δ 189.11 (s). ^{13}C{^{1}H} NMR (101 MHz, $CDCl_3$) : δ 16.82 (s, 4C, *C*H$_3$), 17.88 (s, 4C, *C*H$_3$), 21.6 (s, 1C, *C*H$_3$), 28.07 (vt, J_{CP} = 11.3, 4C, P*C*H(CH3)$_2$), 106.1 (vt, J_{PC} =6.0, 2C, 3,5-C_{Ar}), 123.7 (t, J_{PC}=21.5,

1C, Ni-C_{Ar}), 139.65 (s, 1C, C_{Ar}Me) 168.6 (vt, J_{PC}=10.0, 2C, C_{Ar}OP). UV-Vis (CH_2Cl_2, 13.56 × 10^{-4} M) [λ_{max}, nm (ε, L.mol^{-1} .cm^{-1})]: 396(164), 355(237), 338(1063), 324(517). Anal. Calcd. for $C_{19}H_{33}O_2P_2NiBr$ (494.01): C, 46.19; H, 6.73. Found: C, 46.17; H, 6.66.

{2,6-(*i*-Pr$_2$PO)$_2$,4-(COOMe)C$_6$H$_2$}NiBr, **4'**. The standard procedure described above for 3' gave the desired product as yellow solid (0.87 g, 92 %). ^{1}H NMR (400 MHz, $CDCl_3$): δ 1.20 (dt^v, J_{HH}= 7.26 J_{HP}= 7.1, 12H, CH(CH_3)$_2$), 1.43 (dt^v, J_{HH}= 8.64 J_{HP}= 8.02, 12H, CH(CH_3)$_2$), 2.30 (m, 4H, PCH(CH$_3$)$_2$), 3.54 (s, 3H,OCH_3), 7.66 (s, 2H, *Ar*). ^{31}P{^{1}H} NMR (162 MHz, C_6D_6): δ 190.56 (s). ^{13}C{^{1}H} NMR (101 MHz, C_6D_6) : δ 16.68 (s, 4C, CH$_3$), 17.75 (s, 4C, CH$_3$), 28.34 (vt, J_{CP} = 11.24, 4C, PCH(CH3)$_2$), 51.7 (s, 1C, OCH$_3$), 106.8 (vt, 2C, CH$_{Ar}$), 131.9 (s, 1C, C_{Ar}COOMe), 137.19 (t, J_{PC}=20.8, 1C, Ni-C_{Ar}), 166.6 (s, 1C, C=O), 169.0 (vt, J_{PC}=10.0, 2C, C_{Ar}OP). UV-Vis (CH_2Cl_2, 2.68 × 10^{-4} M) [λ_{max}, nm (ε, L.mol^{-1} .cm^{-1})]: 384(3863), 362(8552), 326(3118). Anal. Calcd. for $C_{20}H_{33}O_4P_2NiBr$ (538.02): C, 44.65; H, 6.18. Found: C, 44.66; H, 6.49.

{2,6-(*i*-Pr$_2$PO)$_2$-3-OMe-C$_6$H$_2$}NiBr, 5'. The standard procedure described above for 3' gave the desired product as a yellow solid (0.86 g, 90 %). ^{1}H NMR (400 MHz, $CDCl_3$): δ 1.33-1.45 (m, 24H, CH(CH_3)$_2$), 2.45 (m, 2H, 3-OPCH(CH$_3$)$_2$), 2.51 (m, 2H, 1-OPCH(CH$_3$)$_2$), 3.77 (s, 3H, OCH_3), 6.35 (d (AB) J_{HH} = 7.25, 1H, 4-H$_{Ar}$), 6.61 (d (AB), J_{HH} = 7.18, 1H, 5-H$_{Ar}$). ^{31}P{^{1}H} NMR (162 MHz, $CDCl_3$): δ 187.5 (d, (AB) J_{PP} = 317.8, 1P), 192.2 (d, (AB) J_{PP} = 317.8, 1P). ^{13}C{^{1}H} NMR (101 MHz, $CDCl_3$) : δ 16.79 (s, 2C, CH$_3$), 16.93 (s, 2C, CH$_3$), 17.86 (s, 2C, CH$_3$), 17.90 (s, 2C, CH$_3$), 28.16 (vt, J_{CP}= 19.1, 2C, PCH(CH3)$_2$), 28.19 (vt, J_{CP}= 18.9, 2C, PCH(CH3)$_2$), 57.2

(s, 1C, O*C*H$_3$), 103.9 (d, J_{PC}=12.6, 1C, 5-C_{Ar}), 113.2 (s, 1C, 4-C_{Ar}), 129.7 (vt, J_{PC}=20.4, 1C, Ni-C_{Ar}), 140.6 (d, J_{PC}=13.9, 1C, MeOC_{Ar}), 156.9 (m, 1C, 2-C_{Ar}OP), 162.6 (dd, 1C, 6-C_{Ar}OP). UV-Vis (CH_2Cl_2, 6.47 × 10^{-4} M) [λ_{max}, nm (ε, L.mol^{-1} .cm^{-1})]: 394(153), 358(170), 339(852). Anal. Calcd. for $C_{19}H_{33}O_3P_2NiBr$ (510.01): C, 44.75; H, 6.52. Found: C, 45.11; H, 6.59.

{2,6-(*i*-Pr$_2$PO)$_2$-3-COOMe-C$_6$H$_2$}NiBr, 6'. The standard procedure described above for 3' gave the desired product as a yellow solid (0.81 g, 86 %). ^{1}H NMR (300 MHz, C_6D_6): δ 1.11 (dt^v, J_{HH}= 7.63, 7.03, 6H, CH(CH_3)$_2$), 1.21 (dt^v, J_{HH}= 7.8, J_{HP}= 6.8, 6H, CH(CH_3)$_2$), 1.33 (dt^v, J_{HH}= 7.4, J_{HP}= 7.4, 6H, CH(CH_3)$_2$), 1.36 (dt^v, J_{HH}= 7.5, J_{HP}= 7.5, 6H, CH(CH_3)$_2$), 2.20 (dh, J_{HH}= 5.3, J_{HP}= 1.6, 2H, 6-OPC*H*(CH$_3$)$_2$), 2.29 (dh, J_{HH}= 5.1, J_{HP}= 1.7, 2H, 2-OPC*H*(CH$_3$)$_2$), 3.53 (s, 3H, OCH_3), 6.52 (d J_{HH}= 8.5, 1H, 5-H$_{Ar}$), 7.88 (d, J_{HH}= 8.4, 1H, 4-C$_{Ar}$*H*). ^{31}P{1H} NMR (202 MHz, C_6D_6): δ 190.4 (d, (AB) J_{PP} = 323, 1P), 192.1 (d, (AB) J_{PP} = 323, 1P). ^{13}C{^{1}H} NMR (75 MHz, C_6D_6) : δ 16.66 (s, 2C, *C*H$_3$), 16.81 (s, 2C, *C*H$_3$), 17.73 (t, J_{CP}= 2.4, 2C, *C*H$_3$), 17.83 (t, J_{CP}= 2.4, 2C, *C*H$_3$), 28.27 (vt, J_{CP}= 12.4, 2C, P*C*H(CH3)$_2$), 28.41 (vt, J_{CP}= 13.4, 2C, P*C*H(CH3)$_2$), 51.27 (s, 1C, O*C*H$_3$), 106.1 (dd, $J_{P'C}$=5.3, $J_{P''C}$=5.1, 1C, 5-C_{Ar}), 110.62 (dd, $J_{P'C}$=5.3, $J_{P''C}$=5.5, 1C, C_{Ar}C=O), 131.33 (vt, J_{PC}=20.1, 1C, Ni-C_{Ar}), 132.77 (s, 1C, 4-C_{Ar}), 165.37 (s, 1C, C=O), 168.71 (t, J_{CP}= 10.5, 1C, 6-C_{Ar}OP), 172.0 (t, J_{CP}= 10.2, 1C, 2-C_{Ar}OP). UV-Vis (CH_2Cl_2, 6.88 × 10^{-4} M) [λ_{max}, nm (ε, L.mol^{-1} .cm^{-1})]: 397(157), 360(201), 343(776). Anal. Calcd. for $C_{20}H_{33}O_4P_2NiBr$ (538.02): C, 44.65; H, 6.18. Found: C, 44.56; H, 6.15.

{2,6-(*i*-Pr$_2$PO)$_2$-3,5-*t*-Bu$_2$-C$_6$H}NiBr, 7'. The standard procedure described above for **3'** gave the desired product as a yellow solid (577 mg, 45 %). ^{1}H NMR (400

MHz, C_6D_6): δ 1.33 (s, 18H, C(CH_3)$_3$), 1.36 (dt^v, J_{H-H}= 10.8, $^vJ_{H-P}$= 7.3, 12H, CH_3), 1.44 (dt^v, J_{H-H}= 8.3, $^vJ_{H-P}$= 7.6, 12H, CH_3), 2.48 (m, 4H, PCH(CH$_3$)$_2$), 6.92 (s, 1H, H$_{Ar}$). ^{31}P{^{1}H} NMR (162 MHz, C_6D_6): δ 185.15 (s). ^{13}C{^{1}H} NMR (101 MHz, $CDCl_3$) : δ 17.08 (s, 4C, CH$_3$), 18.01 (t^v, J_{CP} = 2.48, 4C, CH$_3$), 28.18 (t^v, J_{CP} = 11.8, 4C, PCH(CH3)$_2$), 30.06 (s, 6C, C(CH$_3$)$_3$), 34.41 (s, 2C, C(CH_3)$_3$), 123.89 (s, 1C, CH$_{Ar}$), 126.52 (t^v, J_{CP} = 5.17, 2C, C_{Ar}(^{t}Bu)), 131.28 (t, J_{PC}=19.8, 1C, Ni-C_{Ar}), 164.15 (t^v, J_{PC}=9.55, 2C, C_{Ar}OP). UV-Vis (CH_2Cl_2, 3.68 × 10^{-4} M) [λ_{max}, nm (ε, L.mol^{-1} .cm^{-1})]: 389(1622), 355(1987), 338(8923), 325(5378), 307 (3445) Anal. Calcd. for $C_{26}H_{47}O_2P_2NiBr$ (592,20): C, 52.73; H, 8.00. Found: C, 53.06; H, 8.08.

{2,6-(*t*-Bu$_2$PO)$_2$-C$_6$H$_3$}NiBr, **8'**. The standard procedure described above for 3' gave the desired product as a yellow solid (0.4 g, 57 %). ^{1}H NMR (400 MHz, C_6D_6): δ 1.46 (vt, J_{HP}= 6.6, 36H, CH_3), 6.6 (d, J_{HH}= 7.8, 2H, H$_{Ar}$), 6.88 (t, J_{HH}= 7.6, 1H, H$_{Ar}$). ^{31}P{^{1}H} NMR (162 MHz, C_6D_6): δ 191.00 (s). ^{13}C{^{1}H} NMR (101 MHz, $CDCl_3$) : δ 27.39 (s, 12C, CH$_3$), 38.75 (vt, J_{CP}= 7.1, 4C, PC), 103.84 (vt, J_{CP}= 5.6, 2C, 3,5-C_{Ar}), 126.14 (t, J_{CP}= 20.0, 1C, Ni-C_{Ar}), 127.37 (s, 1C, 4-C_{Ar}) 168.38 (vt, J_{PC}=9.4, 1C, C_{Ar}OP). UV-Vis (CH_2Cl_2, 4.51 × 10^{-4} M) [λ_{max}, nm (ε, L.mol^{-1} .cm^{-1})]: 407(198), 352(138), 334(916). Anal. Calcd. for $C_{20}H_{33}O_4P_2NiBr$ (536.09): C, 49.29; H, 7.33. Found: C, 49.28; H, 7.39.

{2,6-(*t*-Bu$_2$PO)$_2$-4-COOMe-C$_6$H$_2$}NiBr, 9'. The standard procedure described above for **3'** gave the desired product as a yellow solid (0.94 g, 72 %). ^{1}H NMR (400 MHz, C_6D_6): δ 1.41 (vt, J_{HP} = 6.1, CH_3, 36H), 3.50 (s, 3H, OCH_3), 7.45 (s, 2H, H$_{Ar}$). ^{31}P{^{1}H} NMR (162 MHz, C_6D_6): δ 191.81 (s). ^{13}C{^{1}H} (101 MHz, $CDCl_3$) : δ 28.27 (s, 12C, CH$_3$), 39.94 (vt, J_{CP} = 6.9, 4C, PC(CH3)$_3$), 52.06 (s, 1C, OCH$_3$), 105.86 (vt, J_{CP} = 5.3, 2C, 3,5-C_{Ar}), 130.48 (s, 1C, C_{Ar}COOMe), 135.91 (t, J_{PC}=19.0, 1C, Ni-

C_{Ar}), 167.04 (s, 1C, C=O), 169.0 (vt, J_{PC}= 8.9, 2C, C_{Ar}OP). UV-Vis (CH_2Cl_2, 10.6 × 10^{-4} M) [λ_{max}, nm (ε, $L.mol^{-1}.cm^{-1}$)]: 413(228), 360(1043), 326(378). Anal. Calcd. for $C_{20}H_{33}O_4P_2NiBr$ (594.12): C, 48.52; H, 6.96. Found: C, 48.64; H, 7.16.

Cyclic Voltammetry Experiments. Cyclic voltammetry measurements were performed using a SP50 BioLogic Science Instrument potentiostat. A typical three-electrode system consisting of a graphite working electrode, a Pt auxiliary electrode, and a Ag/AgCl reference electrode was employed. The experiments were carried out at room temperature on analyte solutions prepared in dry CH_2Cl_2 containing [*n*-Bu_4N][PF_6] as electrolyte (0.1 M). The samples were bubbled with nitrogen before each experiment. Under the experimental conditions of our studies, the redox potential ($E_{1/2}$) for the Cp_2Fe^+/Cp_2Fe couple was +0.43 V.

Crystal Structure Determinations. The crystallographic data for compounds **2'**, **4'** and **8'** were collected on a Bruker. Microstar generator (micro source) equipped with a Helios optics, a Kappa Nonius goniometer, and a Platinum135 detector. The crystallographic data for complexes **3'**, **8**, and **9'** were collected on a Nonius FR591 generator (rotating anode) equipped with a Montel 200, a D8 goniometer, and a Bruker Smart 6000 area detector. The crystallographic data for complexes **7'** were collected on a a Bruker APEX II equipped with a Incoatec I\muS Microsource and a Quazar MX monochromator.Cell refinement and data reduction were done using SAINT[28]. An empirical absorption correction, based on the multiple measurements of equivalent reflections, was applied using the program SADABS[29]. The space group was confirmed by XPREP routine[30] in the program SHELXTL[31]. The structures were solved by direct methods and refined by fullmatrix least-squares and difference

Fourier techniques with SHELX-97[32]. All non-hydrogen atoms were refined with anisotropic displacement parameters. Hydrogen atoms were set in calculated positions and refined as riding atoms with a common thermal parameter.

3.6 Acknowledgments.

The authors are grateful to: NSERC of Canada for a Discovery Grant to D.Z.; Université de Montréal and Centre in Green Chemistry and Catalysis for graduate fellowships to B.V. ; Dr. Laure Benhamou for valuable discussions, Mr. Olivier Marcadet for technical assistance with some of the experiments, and Dr. Michel Simard and Ms. Francine Bélanger-Gariépy for their valuable assistance with crystallography.

3.7 Supporting information

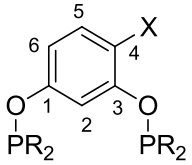

Table 3.5 Tabulated 1H NMR data for ligands

^{1}H δ ($H_{aromatiques}$)	2-H	4,6-H	5-H
5-OMePOC$_{sp2}$OP(iPr)	7.13 (m, 1H)	6.7 (m, 2H)	
5-COOMePOC$_{sp2}$OP(iPr)	7.08 (m, 1H)	7.38(m, 2H)	
4-OMePOC$_{sp2}$OP(iPr)	6.98 (m, 1H)	6.72 (dm, 1H)	6.72 (d, 1H)
4-COOMePOC$_{sp2}$OP(iPr)	7.87 (m, 1H)	6.92 (dm, 1H)	8.05 (d, 1H)
5-COOMePOC$_{sp2}$OP(tBu)	7.72 (m, 1H)	7.97 (m, 2H)	
5-MePOC$_{sp2}$OP(iPr)	6.72 (m, 1H)	6.58 (m, 2H)	

Table 3.6 Tabulated 13C{1H} NMR data for ligands

^{13}C δ ($C_{aromatiques}$)	2-C	3-C	4-C	5-C	6-C	1-C	O*Me* / C_{Ar} *Me*	C=O
5-OMePOC$_{sp2}$OP(iPr)	101.95 (t)	161.7 (d)	98.9 (d)	162.0 (s)			54.9 (s)	
5-COOMePOC$_{sp2}$OP(iPr)	113.5 (t)	160.2 (d)	113.0 (d)	131.8 (s)			52.1 (s)	166.5 (s)
4-OMePOC$_{sp2}$OP(iPr)	111.1 (dd)	153.4 (d) OR 149.0 (d)	145.6 (s)	113.5 (s)	111.2 (d)	149.0 (d) OR 153.4 (d)	55.7 (s)	
4-COOMePOC$_{sp2}$OP(iPr)	108.3 (dd)	160.5 (d) OR 163.4 (d)	139.9 (s)	114.4 (s)	110.9 (d)	163.4 (d) OR 160.5 (d)	51.3 (s)	166.2 (s)
5-COOMePOC$_{sp2}$OP(tBu)	113.1 (t)	161.4 (d)	113.2 (d)	133.0 (s)			52.7 (s)	166.3 (s)
5-MePOC$_{sp2}$OP(iPr)	106.4 (t)	160.0 (d)	112.7 (d)	139.8 (s)			21.6 (s)	

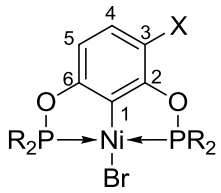

Table 3.7 Tabulated 1H NMR data for complexes.

^{1}H δ ($H_{aromatiques}$)	4-H	3,5-H
4-OMePOC$_{sp2}$OP(iPr)		6.33 (s, 2H)
4-COOMePOC$_{sp2}$OP(iPr)		7.66 (s, 2H)
3-OMePOC$_{sp2}$OP(iPr)	6.36 (d, 1H)	6.60 (d, 1H)
3-COOMePOC$_{sp2}$OP(iPr)	7.88 (d, 1H)	6.52 (d, 1H)
3,5-(^{t}Bu)POC$_{sp2}$OP(iPr)	6.92 (s, 1H)	
4-COOMePOC$_{sp2}$OP(tBu)		7.45 (s, 2H)
4-MePOC$_{sp2}$OP(iPr)		6.28 (s, 2H)
POC$_{sp2}$OP(tBu)	6.88 (t, 1H)	6.57 (d, 2H)

Table 3.8 Tabulated 13C{1H} NMR data for complexes.

^{13}C δ ($C_{aromatiques}$)	1-C	2-C	3-C	4-C	5-C	6-C	O*Me* / C_{Ar}*Me*	C=O
4-OMePOC$_{sp2}$OP(iPr)	118.7 (t)	169.4 (vt)	92.9 (vt)	162.6 (s)			55.1 (s)	
4-COOMePOC$_{sp2}$OP(iPr)	137.2 (t)	169.0 (vt)	106.8 (vt)	131.9 (s)			51.7 (s)	166.6 (s)
3-OMePOC$_{sp2}$OP(iPr)	129.7 (vt)	156.9 (m)	140.6 (d)	113.2 (s)	103.9 (d)	162.6 (dd)	57.2 (s)	
3-COOMePOC$_{sp2}$OP(iPr)	131.6 (vt)	172.3 (vt)	110.9 (dd)	133.1 (s)	106.4 (dd)	169.0 (vt)	51.6 (s)	165.7 (s)
3,5-(^{t}Bu)POC$_{sp2}$OP(iPr)	131.3 (t)	164.1 (vt)	126.5 (vt)	123.9 (s)				
4-COOMePOC$_{sp2}$OP(tBu)	135.9 (t)	169.0 (vt)	105.9 (vt)	130.5 (s)			52.1 (s)	167.0 (s)
4-MePOC$_{sp2}$OP(iPr)	123.8 (t)	168.6 (vt)	106.2 (vt)	139.7 (s)			21.7(s)	
POC$_{sp2}$OP(tBu)	126.1 (t)	168.4 (vt)	103.8 (vt)	127.7 (s)				

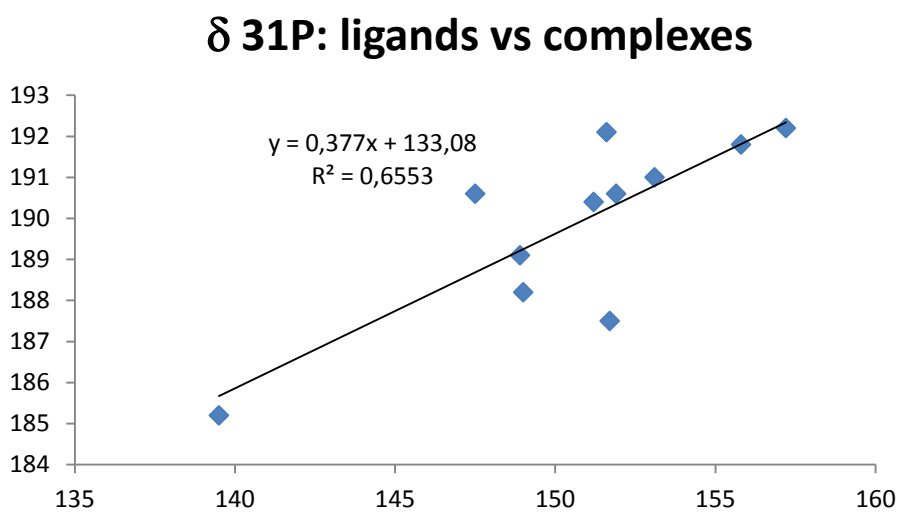

Figure 3.9 Correlation between ligand and complex ^{31}P chemical shifts

Table 3.9 Crystal Data Collection and Refinement Parameters for ligand 8 and compounds **2'-4'**.

Compound	**8**	**2'**	**3'**	**4'**
chemical formula	$C_{22}H_{40}O_2P_2$	$C_{19}H_{33}BrNiO_2P_2$	$C_{19}H_{33}BrNiO_3P_2$	$C_{20}H_{33}BrNiO_4P_2$
Fw	398.48	494.01	510.01	537.99
T (K)	200 (2)	150(2)	200(2)	150(2)
wavelength (Å)	1.54178	1.54178	1.54178	1.54178
space group	P2(1)/n	C2/c	C2/c	P2(1)/c
a (Å)	8.6696(2)	9.1135(4)	19.1645(3)	15.9555(8)
b (Å)	24.0144(5)	18.9783(8)	18.2062(3)	13.2237(6)
c (Å)	12.1011(3)	13.2056(5)	15.0872(3)	11.2503(5)
α (deg)	90.00	90.00	90	90.00
β (deg)	98.6780(10)	93.568(2)	116.845(1)	91.393(2)
γ (deg)	90.00	90.00	90.00	90.00
Z	4	4	8	4
V (Å^3)	2490.55(10)	2279.60(16)	4696.81(14)	2373.0(2)
ρcalcd (g cm^{-3})	1.063	1.439	1.443	1.506
μ (mm-1)	1.666	4.678	4.592	4.610
θ range (deg)	3.68 − 72.44	6.72 − 69.78	3.55 − 72.48	2.77 − 69.90
R_1[a] [I > 2ó(I)]	0.0374	0.0299	0.0356	0.0318
wR_2[b] [I > 2ó(I)]	0.1068	0.0828	0.0958	0.0844
R_1 [all data]	0.0414	0.0301	0.0363	0.0319
wR_2 [all data]	0.1102	0.0830	0.0967	0.0845
GOF	1.074	1.098	1.043	1.100

[a] R1=Σ(||Fo|-|Fc||)/Σ|Fo| [b] wR2={Σ[w(Fo2–Fc2)2]/Σ[w(Fo2)2]}½

Table 3.10 Crystal Data Collection and Refinement Parameters for Compounds **7'-9'**

Compound	**7'**	**8'**	**9'**
chemical formula	$C_{26}H_{47}BrNiO_2P_2$	$C_{22}H_{39}BrNiO_2P_2$	$C_{24}H_{41}BrNiO_4P_2$
Fw	592.20	1043.96	594.13
T (K)	100 (2)	150(2)	296(2)
wavelength (Å)	1.54178	0.71073	1.54178
space group	P2(1)/n	Pī	P2(1)/c
a (Å)	10.4807(4)	8.348(5)	10.6200(5)
b (Å)	13.9807(6)	11.922(8)	26.9129(14)
c (Å)	20.4439(8)	13.399(9)	20.7434(10)
α (deg)	90.00	99.967(10)	90.00
β (deg)	100.7470(18)	96.001(10)	90.656(2)
γ (deg)	90.00	104.747(10)	90.00
Z	4	2	8
V (Å^3)	2943.0(2)	1254.6(14)	5928.4(5)
ρcalcd (g cm^{-3})	1.337	2.764	1.331
μ (mm-1)	3.710	5.013	3.741
θ range (deg)	3.85 − 71.12	1.56 − 27.51	2.69 − 73.00
R_1[a] [I > 2ó(I)]	0.0525	0.0334	0.0458
wR_2[b] [I > 2ó(I)]	0.1452	0.0799	0.1258
R_1 [all data]	0.0545	0.0442	0.0484
wR_2 [all data]	0.1463	0.0850	0.1283
GOF	1.298	1.024	1.038

[a] R1=Σ(||Fo|-|Fc||)/Σ|Fo| [b] wR2={Σ[w(Fo2–Fc2)2]/Σ[w(Fo2)2]}½

Table 3.11 Absorption spectral data for ligands and complexes

R'	R	no.	λ_{max} (nm) (ε , $M^{-1}.cm^{-1}$)				
			R-POC^{H}OP$^{R'}$	(R-POCOP$^{R'}$)NiBr			
i-Pr	4-CO_2Me	**4/4'**	306(3248)	326(3118)	362(8552)	---	384(3863)
	3-CO_2Me	**6/6'**		---	341(817)	360(201)	397(157)
	H	**1/1'**		327(5652)	337(9409)	368(1656)	389(1975)
	4-Me	**2/2'**	276(1435)	324(517)	338(1063)	355(237)	396(164)
	3-OMe	**5/5'**		---	337(900)	353(197)	389(158)
	3,5-*t*-Bu_2	**7/7'**		325(5378)	337(9060)	354(2070)	388(1631)
	4-OMe	**3/3'**	272(861)	321(4970)	336(10109)	---	387(1753)
t-Bu	4-CO_2Me	**9/9'**	308(3109)	326(378)	360(1043)	---	413(228)
	H	**8/8'**	276(2194)	319 (455)	334(916)	352(138)	407(198)

3.8 References

[1] Moulton, C. J.; Shaw, B. L. *J. C. S. Dalton* **1976**, 1020.

[2] (a) Grove, D. M.; van Koten, G.; Zoet, R. *J. Am. Chem. Soc.* **1983**, *105*, 1379. (b) Grove, D. M.; van Koten, G.; Ubbels, H. J. C.; Zoet, R. *Organometallics* **1984**, *3*, 1003.

[3] (a) van Koten, G. *Pure App. Chem.* **1989**, *61*, 1681. (b) Albrecht, M.; van Koten, G. *Angew. Chem. Int. Ed.* **2001**, *40*, 3750. (c) Gossage, R. A.; van de Kuil, L. A.; van Koten, G. *Acc. Chem. Res.* **1998**, 31, 423. (d) Zargarian, D.; Castonguay, A.; Spasyuk, D. M. "ECE-Type Pincer Complexes of Nickel", *Topics in Organometallic Chemistry* **2013***, 40*, 2013, 131-173.

[4] (a) Castonguay, A.; Sui-Seng, C.; Zargarian, D.; Beauchamp, A. L. *Organometallics* **2006**, *25*, 602. (b) Castonguay, A.; Beauchamp, A. L.; Zargarian, D. *Organometallics* **2008**, *27*, 5723.

[5] (a) Gómez-Benítez, V.; Baldovino-Pantaleón, O.; Herrera-Álvarez, C.; Toscano, R. A.; Morales-Morales, D. *Tet. Lett.* **2006**, *47*, 5059. (b) Pandarus, V.; Zargarian, D. *Chem*. *Commun*. *2007*, 978. (c) Pandarus, V.; Zargarian, D. *Organometallics*, **2007**, *26*, 4321. (d) Salah, A. B.; Zargarian, D. *Dalton Trans.* **2011**, *40*, 8977 (d) Salah, A. B.; Offenstein, C.; Zargarian, D. *Organometallics* **2011**, *30*, 5352. (e) Lefèvre, X.; Durieux, G.; Lesturgez, S.; Zargarian, D. *J. Mol. Catal. A : Chem.* **2011**, *335*, 1. (f) Xu, G.; Li, X.; Sun, H. *J. Organomet. Chem.* **2011**, *696*, 3011.

[6] (a) Spasyuk, D. M.; van der Est, A.; Zargarian, D. *Organometallics* **2009**, *28*, 6531; (b) Spasyuk, D. M.; Zargarian, D. *Inorg. Chem.* **2010**, *49*, 6203. (c) Zhang, B.-S.;

Wang, W.; Shao, D.-D.; Hao, X.-Q.; Gong, J.-F.; Song, M.-P. *Organometallics* **2010**, *29*, 2579. (d) Niu, J.-L.; Chen, Q.-T.; Hao, X.-Q.; Zhao, Q.-X.; Gong, J.-F.; Song, M.-P. *Organometallics* **2010**, *29*, 2148. (e) Spasyuk, D. M.; Gorelsky, S. I.; van der Est, A.; Zargarian, D. *Inorg. Chem*. **2011**, *50*, 2661. (f) Yang, M.-J.; Liu, Y.-J.; Gong, J.-F.; Song, M.-P. *Organometallics* **2011**, *30*, 3793. (g) Sanford, J.; Dent, C.; Masuda, J. D.; Xia, A. *Polyhedron* **2011**, *30*,1091.

[7] (a) Fan, L.; Foxman, B. M.; Ozerov, O. V. *Organometallics* **2004**, *23*, 326. (b) Ozerov, O. V.; Guo, C.; Fan, L.; Foxman, B. M. *Organometallics* **2004**, *23*, 5573. (c) Liang, L.-C.; Chien, P.-S.; Huang, Y.-L. *J. Am. Chem. Soc.* **2006**, *128*, 15562. (d)) Liang, L.-C.; Chien, P.-S.; Lin, J.-M.; Huang, M.-H.; Huang, Y.-L.; Liao, J.-H. *Organometallics* **2006**, *25*, 1399. (e) Adhikari, D.; Huffman, J. C.; Mindiola, D. J. *Chem. Commun.* **2007**, 4089. (e) Adhikari, D.; Mossin, S.; Basuli, F.; Huffman, J. C.; Szilagyi, R. K.; Meyer, K.; Mindiola, D. J. *J. Am. Chem. Soc.* **2008**, *130*, 3676. (f) Adhikari, D.; Pink, M.; Mindiola, D. J. *Organometallics* **2009**, *28*, 2072.

[8] (a) Vechorkin, O.; Proust, V.; Hu, X. *J. Am. Chem. Soc.* **2009**, *131*, 9756. (b) Madhira, V. N.; Ren, P.; Vechorkin, O.; Hu, X.; Vicic; D. A. *Dalton Trans.* **2012**, *41*, 7195. (c) Breitenfeld, J.; Scopelliti, R.; (c) Hu, X. *Organometallics* **2012**, *31*, 2128.

[9] (a) Chakraborty, S.; Krause, J. A.; Guan, H. *Organometallics* **2009,** *28*, 582. (b) Chakraborty, S.; Patel, Y. J.; Krause, J. A.; Guan, H. *Polyhedron* **2012**, *32*, 30. (c) Zhang, J.; Medley, C. M.; Krause, J. A.; Guan, H. *Organometallics* **2010,** *29*, 6393. (d) Chakraborty, S.; Zhang, J.; Krause, J. A.; Guan, H. *J. Am. Chem. Soc.* 2010, 132, 8873. (e) Huang, F.; Zhang, C.; Jiang, J.; Wang, Z.-X.; Guan, H. *Inorg. Chem.* **2011**, *50*, 3816.

[10] (a) Boro, B. J.; Duesler, E. N.; Goldberg, K. I.; Kemp, R. A. *Inor. Chem.* **2009**, *48*, 5081. (b) Schmeier, T. J.; Hazari, N.; Incarvitoa, C. D.; Raskatovb, J. A. *Chem. Commun.* **2011**, *47*, 1824. (c) Rossin, A.; Peruzzini, M.; Zanobini, F. ***Dalton Trans*.** **2011**,***40*, 4447.**

[11] (a) Castonguay, A.; Spasyuk, D. M.; Madern, N.; Beauchamp, A. L.; Zargarian, D. *Organometallics* **2009**, *28*, 2134. (b) Castonguay, A.; Beauchamp, A. L.; Zargarian, D. *Inorg. Chem.* **2009**, *48*, 3177.

[12] Solano-Prado, M. A.; Estudiante-Negrete, F.; Morales-Morales, D. *Polyhedron* **2010**, *29*, 592.

[13] Estudiante-Negrete, F.; Hernàndez-Ortega, S.; Morales-Morales, D. *Inorg. Chim. Acta* **2012**, *387*, 58.

[14] Chen, T.; Yang, L.; Li, L.; Huang, K.-W. *Tetrahedron* **2012**, *68*, 6152.

[15] (a) Zhu, K.; Achord, P. D.; Zhang, X.; Krogh-Jespersen, K.; Goldman, A. S. *J. Am. Chem. Soc.* **2004**, *126*, 13044. (b) Göttker-Schnetmann, I.; White, P. S.; Brookhart, M. *Organometallics* **2004**, *23*, 1766. (c) Göttker-Schnetmann I.; White P. S.; Brookhart, M. *J. Am. Chem. Soc.*, **2004**, *126*, 1804. (d) Huang, Z.; Brookhart, M.; Goldman, A. S.; Kundu, S.; Ray, A.; Scott, S. L.; Vicente, B. C. *Adv. Syn. Catal.* **2009**, *351*, 188. (e) Polukeev, A. V.; Kuklin, S. A.; Petrovskii, P. V.; Peregudov, A. S.; Dolgushin, F. M.; Ezernitskaya, M. G.; Koridze, A. A. *Russ. Chem. Bull, Int. Ed.,*. **2010**, *59*, 745.

[16] (a) van de Kui1, L. A.; Luitjes, H.; Grove, D. M. Zwikker, J. W.; van der Linden, J. G. M.; Roelofsen, A. M.; Jenneskens, L. W.; Drenth, W.; van Koten, G. *Organometallics* **1994**,*13*, 468-477. (b) Slagt, M. Q.; RodrÌguez, G.; Grutters, M. M.

P.; Gebbink, R. J. M. K.; Klopper, W.; Jenneskens, L. W.; Lutz, M.; Spek, A. L.; van Koten, G. *Chem. Eur. J.* **2004**, *10*, 1331- 1344.

[17] For the original reports on preparation of POC^{H}OP-type ligands see: (a) Bedford, R. B.; Draper, S. M.; Scully, P. N.; Welch, S. L. *New J. Chem*. **2000** *24*, 745. (b) Morales-Morales, D.; Grause, C.; Kasaoka, K.; Redon, R.; Cramer, R. E.; Jensen, C. M. *Inorg. Chim. Acta* **2000**, *300*‑*302*, 958.

[18] A recent study has shown that nickellation of the central C-H moiety in these POCOP ligands proceeds by an electrophilic mechanism: Vabre, B.; Lambert, M. L.; Petit, A.; Ess, D. H.; Zargarian, D. Organometallics **2012**, 31, 6041.

[19] In the case of low yielding reactions, NMR spectra of the final reaction mixtures did not show any unreacted ligands. We have no definitive explanation at this point for the observed low yields other than the possibility that the chelated intermediates formed in these cases decompose into intractable dimeric or polymeric species instead of proceeding to nickellation. For a discussion of related reactions leading to non-metallated species see: Pandarus, V.; Castonguay, A.; Zargarian, D. *J. Chem. Soc., Dalton Trans.* **2008**, 4756-4761.

[20] Canet D.; Boudel J.C; Canet Soula E., La RMN : Concepts, méthodes et applications, 2e edition Dunod, Paris, 2002.

[21] Schwartsburd, L.; Poverenov, E.; Shimon, L. J. W.; Milstein, D. *Organometallics* **2007**, *26*, 2931.

[22] The synthesis and solid state structure of the chloro analogue of complex **8'** has been reported previously: ref. 9a.

[23] The following alternative interpretations have been suggested by reviewers of our manuscript to explain the shorter Ni-Br distances observed in complexes **4'** and **9'**: the electron-withdrawing substituent CO_2Me present in these complexes tends to create a more polarized Ni-C_{ispo} interaction in the direction of C_{ipso}, thus enhancing both the Coulombic interaction between Ni^+ and Br^- and/or the extent of Br→Ni π-donation.

[24] (a) Jude, H.; Bauer, J.A.K.; Connick, W. B. *Inorg. Chem.* **2002**, *41*, 2275. (b) Jude, H.; Bauer, J.A.K.; Connick, W. B. *Inorg. Chem.* **2004**, *43*, 725. (c) Jude, H.; Bauer, J.A.K.; Connick, W. B. *Inorg. Chem.* **2005**, *44*, 1211.

[25] The fairly significant impact of *para*-substituents on the observed redox rules out the possibility of the observed redox events occurring on the PR_2 moieties.

[26] Foti, M. C.; Daquino, C.; Mackie, I. D.; DiLabio, G. A.; Ingold, K. U. *J. Org. Chem.* **2008**, *73*, 9270.

[27] Bedford, R. B.; Betham, M.; Blake, M. E.; Coles, S. J.; Draper, S. M.; Hursthouse, M. B.; Scully, P. N. *Inorg. Chim. Acta* **2006**, *359*, 1870.

[28] *SAINT*, *Release 6.06; Integration Software for Single Crystal Data*; Bruker AXS Inc.: Madison, WI, 1999

[29] Sheldrick, G. M. *SADABS, Bruker Area Detector Absorption Corrections;* Bruker AXS Inc., Madison, WI, 1999

[30] *XPREP, Release 5.10; X-ray Data Preparation and Reciprocal Space Exploration Program*; Bruker AXS Inc.: Madison, WI, 1997.

[31] *SHELXTL, Release 5.10; The Complete Software Package for Single Crystal Structure Determination*; Bruker AXS Inc.: Madison, WI, 1997.

[32] (a) Sheldrick, G. M. *SHELXS97, Program for the Solution of Crystal Structures*; Univ. of Gottingen: Germany, 1997. (b) Sheldrick, G. M. *SHELXL97, Program for the Refinement of Crystal Structures*; University of Gottingen: Germany, 1997.

Chapitre 4

Chapitre 4 : Direct, One-Pot Synthesis of POCOP-Type Pincer Complexes from Metallic Nickel

Article 3

*Boris Vabre, Fabien Lindeperg and Davit Zargarian**

Département de chimie, Université de Montréal, Montréal (Québec), Canada H3C 3J7

Green Chemistry **2013**, *15*, 3188-3194.

Chapitre 4

4.1 Abstract

A one-pot procedure has been developed for the direct and atom-economical preparation of the pincer-type complexes (R'-POCOP^{R})NiCl (R'-POCOP^{R}= $\kappa^{P},\kappa^{C},\kappa^{P}$-(2,6-($R_2PO)_2$-R'$_n$-$C_6H_{3-n}$); R= *i*-Pr, Ph; R'$_n$ = H, 4-OMe, 4-COOMe, 3,5-(*t*-Bu)$_2$). This convenient synthetic protocol involves heating a 1 : 2 : 1-2 mixture of resorcinol (or its substituted derivatives), R_2PCl, and nickel powder in toluene (at 100 ºC) or acetonitrile (at 75 °C) for 18 h. The target nickel compounds can be obtained from this procedure in up to 93% yield. Using metallic palladium in this protocol instead of nickel gives the corresponding palladium complexes in low yields only (ca. 10%).

4.2 Introduction

Transition metal compounds play a central role in promoting efficient catalytic transformations that are at the heart of global efforts to develop sustainable chemical manufacturing processes. The overall viability of a process based on catalysis depends on a number of considerations, including the catalytic efficacy of the system in terms of turn-over numbers and rates, as well as more general processing issues such as product isolation, waste disposal, etc. In cases where the catalysts (or, more accurately, pre-catalysts) are elaborate organometallic complexes as opposed to simple metal salts, another important determinant of process viability is the overall cost and ease of preparation of the pre-catalyst. A viable pre-catalyst should be based on abundant metals and inexpensive ligands, and its preparation should not involve an elaborate, multi-step protocol. Ideally, pre-catalysts should be

accessible via a simple, single-step protocol requiring commercially available starting materials.[1]

One emerging class of organometallic complexes proven to be effective pre-catalysts for diverse reactions are pincer complexes of nickel and palladium based on *m*-bis(phosphinite)phenyl ligands (POCOP, figure 4.1). These complexes promote Heck and Suzuki coupling,[2] allylic additions,[3] Michael additions,[4] hydrosilylation of aldehydes,[5] reduction of CO_2,[6] and C-S coupling reactions.[7] The increasing popularity of POCOP complexes in comparison to their PCP counterparts (figure 4.1) is partly due to the significant stability of POCOP-based systems toward aerobic and thermal decomposition, as well as the greater ease and simplicity of their preparation relative to PCP-type ligands.[8]

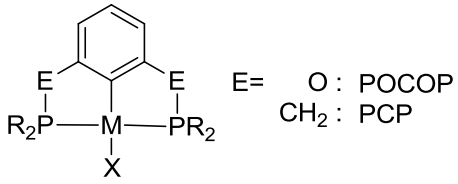

Figure 4.1 Complexes POCOP et PCP

A typical synthesis for resorcinol-based POCOP-type complexes of Ni or Pd involves begins with preparation of the ligand R'-POC(H)OP^R by the reaction of resorcinol or its substituted derivatives with chlorophosphines. The resulting ligand is then reacted with a suitable metal precursor MX_n to generate the desired complexes (R'-POCOP^R)MX_{n-1} (Scheme 4.1).[9,10] This standard two-step synthetic protocol normally requires three equivalents of base to remove the three equivalents of acid generated during ligand synthesis (two equivalents of HCl) and the metallation step

(one equivalent of HX).[11] Indeed, the success of such syntheses depends in many cases on the efficient neutralization/removal of the acid generated in-situ in order to avoid protonating the nucleophilic donor moieties.[12] The salt formed during the neutralization process must then be removed by filtration.

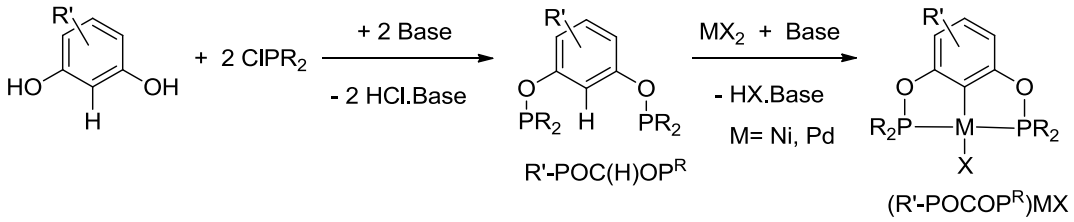

Scheme 4.1 Synthesis of POCOP complexes

A number of attempts have been made to introduce new, simplified protocols for the synthesis of POCOP-type Pd and Ni complexes. For instance, Uozumi's group reported in 2006 that ($POCOP^R$)PdI can be prepared via an intermediate complex obtained from the oxidative addition of 2-iodoresorcinol to $Pd(PPh_3)_4$; the subsequent reaction of this intermediate with $ClPR_2$ and NEt_3 furnishes the desired product in good yield (Scheme 4.1).[13] The main advantages of this approach are the mild reaction conditions, short reaction times, and high yields; its main drawback is the requirement of a more elaborate, activated derivative of resorcinol as well as an expensive (and air-sensitive) Pd(0) precursor. Moreover, the non-productive generation of four equivalents of PPh_3 renders this protocol atom-inefficient.

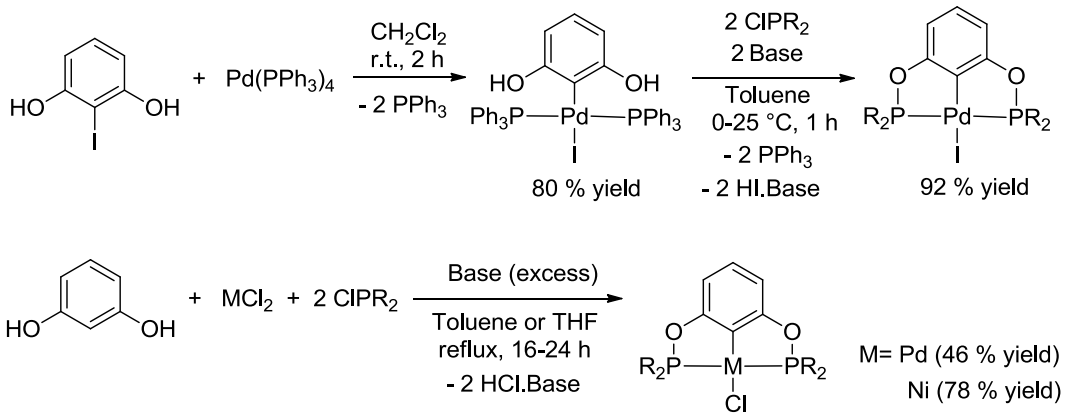

Scheme 4.2 Synthesis of POCOP palladium complexes by post derivatization, and one pot synthesis of POCOP complexes with MX_2 metallic precursor.

Shortly after Uozumi's report, Song's group reported a new synthetic route that involved heating $PdCl_2$, resorcinol, $ClPR_2$, and excess NEt_3 together in a one-pot fashion (Scheme 4.2).[14] Compared to Uozumi's protocol described above, this new approach is simpler (one step only) and works with inexpensive Pd(II) sources, but it requires refluxing in toluene for 24 h and gives low yields (<50%). A similar one-pot protocol was reported recently by Guan's group for the synthesis of ($POCOP^{cPe}$)NiCl (cPe= cyclopentyl) from $NiCl_2$, resorcinol, $ClPR_2$, and excess dimethylaminopyridine (DMAP); this protocol requires milder reaction conditions (refluxing THF over 16 h) and gives the desired product in 78% yield (Scheme 4.2).[15]

During the course of our investigations on the reactivities of (POCOP)NiX, we set out to develop a more streamlined route to this family of complexes. Described herein is a new synthetic route to (R'_n-$POCOP^R$)NiCl (R= *i*-Pr: R'_n = H, 4-OMe, 4-COOMe, 3,5-(*t*-Bu)$_2$; R= Ph: R'_n = H) based on the one-pot reaction of nickel powder, $ClPR_2$, and resorcinol or a substituted derivative. This base-free protocol is simpler to implement, because it sidesteps the need for prior preparation of ligands

and eliminates the additional step required for removal of the in-situ generated salts. Indeed, the HCl generated in-situ during the formation of the POCOP ligand is used to generate the nickel halide precursors, making this new methodology an effective and atom-economic alternative for the preparation of the target complexes.

4.3 Results and discussion

Our initial attempts at improving the synthesis of resorcinol-based (POCOP)NiX focused on developing effective Ni precursors L_nNiX_2 that would facilitate nickellation of POC(H)OP ligands under mild reaction conditions. Extensive tests demonstrated that the precursors $(R"CN)_nNiBr_2$ (R"= Me (n= 1-4), *i*-Pr (n= 1)) can nickellate these ligands in the presence of NEt_3 at room temperature over an hour or less, giving the corresponding pincer complexes in 80-95% yields with most substrates (scheme 4.3).[16] In terms of yields and reaction conditions, this protocol is superior to the classical approaches that used as-purchased NiX_2 as precursors (X= Cl, Br, I, NO_3, and OAc); nevertheless, this otherwise practical protocol is not atom-economical, because it still requires added base to remove in-situ generated HX. Another drawback of this protocol is the requirement of a pre-formed Ni precursor, which introduces a third step to the synthetic route. More importantly, the synthesis of $(R"CN)_nNiBr_2$ involves the reaction of metallic Ni(0) with bromine, a highly corrosive reagent which requires stringent safety precautions. These shortcomings prompted us to seek a more practical synthesis for (POCOP)NiX.

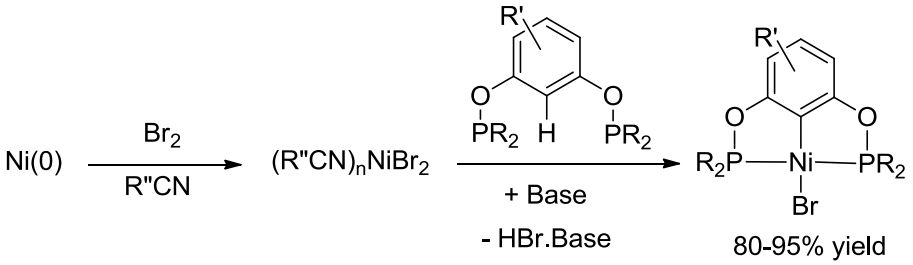

Scheme 4.3 Synthesis of POCOP complexes and $NiBr_2(NCR)_n$ nickel precursor.

We reasoned that a practical synthesis should be a one-pot methodology, require safe-to-handle reagents and inexpensive sources of metal, and avoid using an added base for neutralizing the in-situ generated acid. It occurred to us that these requirements could be accomplished if resorcinol and $ClPR_2$ were allowed to react in the presence of nickel powder, because the HCl generated during the formation of the POC(H)OP would convert Ni(0) into $NiCl_2$ that should, in turn, serve as a competent precursor for the nickellation step. Initial tests indicated that this idea is viable, thus allowing us to elaborate a practical and atom-economical methodology for the preparation of (POCOP)NiCl, as described below.

The initial protocol for the preparation of the known complex (POCOP$^{i\text{-}Pr}$)NiCl, **1**,[10a] involved heating a 1:1:2 mixture of nickel powder, resorcinol and *i*-Pr_2PCl in toluene at 75 °C (eq. 1; [*i*-Pr_2PCl]~ 1.16 M). The initially heterogeneous mixture turned yellow over the course of several hours and gas bubbles evolved (presumably H_2). Evaporation of the final reaction mixture, extraction of the solid residues with hexane, and removal of hexane from the resulting solution gave analytically pure crystals of **1** in 31% yield (Table 4.1, entry 1).

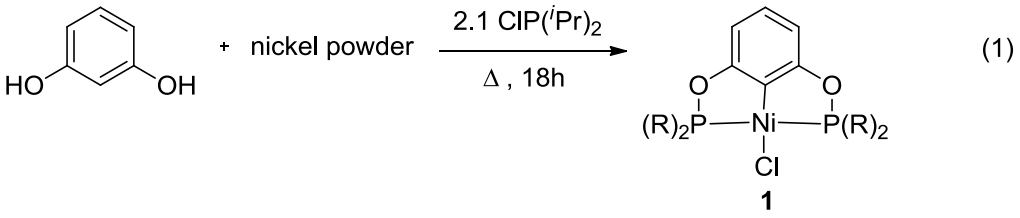

1 (1)

Table 4.2 Optimization of conditions for preparation of complex 1

Entry	Solvent	Ni : Resorcinol	Temp. (°C)	Yield (%)
1	Toluene	1.0 : 1	75	31
2			100	69
3	Acetonitrile	1.0 : 1	25	<5
4			75	72
5			50*	84
6	Toluene	1.5 : 1	100	91
7	Acetonitrile	1.5 : 1	75	88
8		2.0 : 1		93
9	Ethyl acetate	2.0 : 1	75	75

* For Entry 5, the reaction was allowed to run for 72h, in all other cases, the reactions were conducted over 18h.

While the initial results were very encouraging, we carried out optimization studies to improve the final yield of **1** to 90% or better in order to make this new protocol competitive with the protocols described above. The impact of temperature and reaction time was studied first: heating to 100 °C gave a much higher yield (Table 4.1, entry 2), but extending the reaction time further failed to improve the yield beyond 70%. Next, we tested the impact of using acetonitrile as solvent since it can dissolve resorcinol and the in-situ generated $NiCl_2$ more effectively than toluene.

Stirring the mixture of nickel powder, resorcinol and ClP(*i*-Pr)$_2$ in acetonitrile at ambient temperature led to a pale yellow reaction mixture in which most of nickel powder remained insoluble. Analysis of the final solution by ^{31}P NMR showed that it consisted mostly of the protonated ligand (137 ppm) and an unidentified species (94 ppm), in addition to minor amounts of complex **1** (product ratio by integration ~ 13:13:1). We reckoned that the HCl generated from the reaction of resorcinol with ClP(*i*-Pr)$_2$ protonates the newly formed pincer ligand in preference over reacting with nickel powder to generate the required $NiCl_2$. Two approaches were adopted for favoring the reaction of in-situ generated HCl with Ni(0). First, we tested the impact of temperature: heating the reaction mixture to 75 °C over 18 h increased the yield of complex **1** to 72% (entry 4); interestingly, heating to only 50 °C but over longer periods (3 days) gave a higher yield (entry 5). Another effective approach involved using an excess of nickel powder: conducting the syntheses with 50% excess of Ni powder led to a substantial improvement in the yield of **1**, both in toluene (91%, entry 6) and in acetonitrile (88 %, entry 7). The highest yield was obtained when the synthesis was conducted in acetonitrile at 75 °C with 2 equiv of Ni powder (entry 8). The latter reaction can also be carried out in the "greener" solvent ethyl acetate instead of acetonitrile, but a lower yield is obtained in this case (entry 9, 75%).

The above results prompted us to test the new protocols for the preparation of analogous derivatives. We began by applying the toluene-based protocol for the preparation of derivatives of **1** bearing various functional groups on the central aromatic ring. Thus, replacing resorcinol in equation 1 by 1,3-(OH)$_2$-4-OMe-C$_6$H$_2$, 1,3-(OH)$_2$-4-CO$_2$Me-C$_6$H$_2$, and 1,3-(OH)$_2$-4,6-(*t*-Bu)$_2$-C$_6$H$_2$ and working up the reaction mixtures as described above furnished the anticipated products (R_n-

POCOP)NiCl **2-4** in 62-75% yield (Table 4.2, entries 1, 3, and 5).[17] Curiously, conducting these syntheses in acetonitrile and using an excess of Ni powder did not afford significant beneficial advantages except for synthesis of complex **2** (entry 1 vs. 3 and 4), but even for this complex the use of excess nickel powder in toluene gave a somewhat better yield. Better yields were also obtained from toluene reactions for the preparation of complex **3** (e.g., entry 6 vs. 8), whereas the toluene and acetonitrile reactions gave virtually identical yields for complex **4** (entry 9 vs. 10).

Table 4.2 Syntheses of (R'-POCOP^{R})NiCl

Entry	Complex	Solvent	Ni : resorcinol	Yield (%)
1	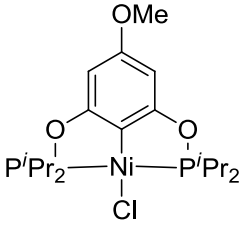 **2**	toluene	1 : 1	62
2			2 : 1	86
3		acetonitrile	1.5 : 1	75
4			2 : 1	81
5	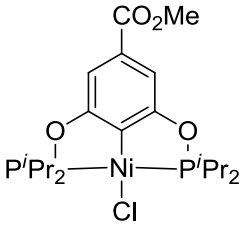 **3**	toluene	1 : 1	75
6			2 : 1	85
7		acetonitrile	1.5 : 1	58
8			2 : 1	72
9	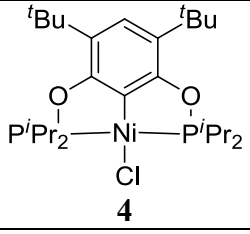 **4**	toluene	1 : 1	69
10		acetonitrile	1.5 : 1	68
11	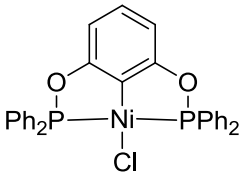 **5***	acetonitrile	1 : 1	35
12			1.5 : 1	37
13			2 : 1	28

Depending on the reaction solvent, mixtures of Ni powder, resorcinol, and 2 equivalents of $ClPR_2$ were heated to 75 °C (acetonitrile) or 100 °C (toluene) over 18h. * Complex **5** has been reported previously; see references 7 and [10]d.

The lowest yields were obtained for the synthesis of (POCOP^{Ph})NiCl, **5**: the reaction with $ClPPh_2$ in toluene did not give the anticipated product at all, whereas conducting this synthesis in acetonitrile gave a better yield of **5** (entry 11). Unfortunately and contrary to what was observed in the case of *i*-Pr_2PCl complexes, using an excess of Ni powder did not improve the yield of (POCOP^{Ph})NiCl appreciably (entries 12 and 13). It appears, therefore, that the new protocols described here are well-suited for the preparation of (R-POCOP$^{i\text{-}Pr}$)NiCl but for the synthesis of their Ph_2P analogue **5** the conventional synthetic protocols using $NiCl_2$ (82 %)[7] or $(MeCN)_nNiBr_2$ (88 %)[10d] are more efficient.

The new methodology has also proven ineffective for the synthesis of analogous pincer complexes of other metals. For instance, using palladium powder instead of nickel in equation 1 led to the formation of (POCOP)PdCl in low yields only (estimated yield based on integration of ^{31}P NMR signal at 188.3 ppm was about 10%). Indeed, most of the palladium powder did not react even after prolonged reaction times. We believe that this lack of reactivity is related to the more difficult oxidation of Pd(0) by HCl: E^o_{ox} (Ni) - E^o_{ox} (Pd) = +1.24 V .[18] The much more favorable oxidation potential of cobalt relative to palladium prompted us to apply our methodology for the preparation of (POCOP)CoCl. The analogous reaction of metallic cobalt with resorcinol and $ClP(i\text{-}Pr)_2$ produced a blue solution (presumably a

chloride salt) and we detected the anticipated ^{31}P NMR peaks corresponding to the free POCOP ligand and its protonated form in a ~12:88 ratio; unfortunately, however, none of the anticipated products (POCOP)CoCl was isolated. In this case, we believe that the problem is the difficult C-H metallation step, not the oxidation of Co(0).[19]

Proposed operating mechanism for the new protocol. Scheme 4.4 outlines the individual steps believed to be involved in the one-pot synthetic protocol described above. As pointed out earlier, reaction of $ClPR_2$ with resorcinol or its derivatives should generate the corresponding POC(H)OP ligand and its diprotonated form, POC(H)OP.2HCl; the detection of both of these species by ^{31}P NMR in many cases supports this assertion. The HCl generated in the first step then oxidizes the metallic nickel to generate $NiCl_2$ and hydrogen gas. [20] The crucial role of HCl in the oxidation of metallic Ni was confirmed when an experiment in the presence of NEt_3 failed to generate any of the desired (POCOP)NiCl complex. Moreover, absorption of the in-situ generated HCl by basic moieties in the ligand is believed to be the reason why this protocol is unsuccessful with amine- or imine-bearing pre-ligands (e.g., [3-((Morpholino)methyl)phenol] and 3-imino-phenol).[21]

Another crucial parameter for the oxidation of metallic nickel is heating. Reactions carried out at room temperature gave protonated ligands, but little or no metallation was observed; this implies that the initial reaction between the chlorophosphine and resorcinol does proceed at r.t., but the in-situ generated HCl is trapped by the phosphinite moieties, thus preventing the oxidation of Ni(0). Heating the reaction mixture serves presumably to displace the ligand protonation equilibrium to liberate HCl and facilitate the irreversible oxidation of metallic nickel. The beneficial effect

of using a coordinating solvent such as acetonitrile in the synthesis of **5** can be ascribed to the fact that the more soluble species $(MeCN)_nNiX_n$ are much more effective for metallation of difficult ligands such as POC(H)OP^{Ph}.

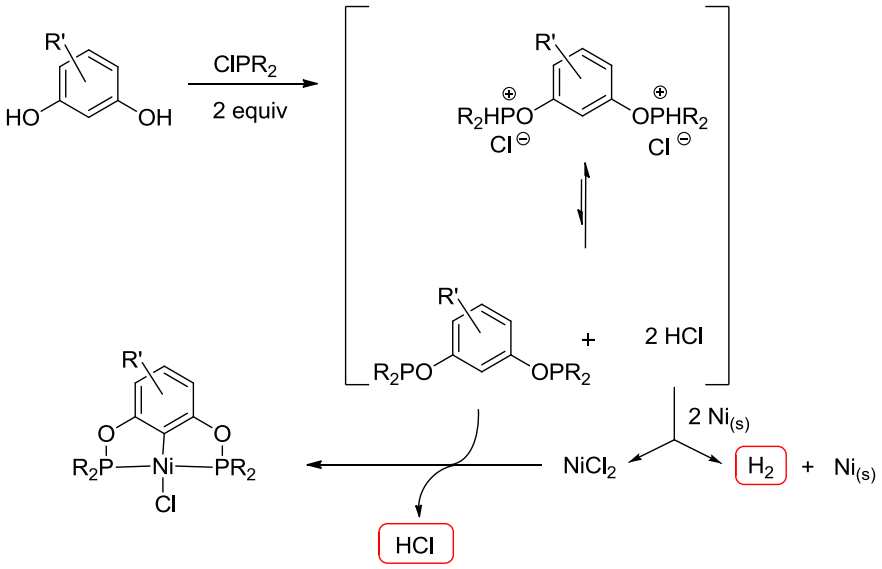

Scheme 4.4 Proposed operating mechanism for the new protocol

Characterization of complexes 2-4. As stated above, complexes **1** and **5** have been reported previously, but **2-4** are new products[17] that were characterized by NMR spectroscopy, elemental analysis, and X-ray diffraction analysis. Thus, complexes **2-4** displayed one singlet $^{31}P\{^{1}H\}$ NMR resonance each in the chemical shift range of ca. 180-190 ppm, which is characteristic for this family of complexes. The ^{1}H NMR spectra of these complexes displayed the characteristic signals for their *i*-Pr moieties as well as the anticipated singlet resonances for the ring substituents, as follows: 3.23 ppm for OCH_3 in **2**, 3.44 ppm for CO_2CH_3 in **3**, and 1.32 ppm for the two $C(CH_3)_3$ groups in **4**.

The solid state structures of **2-4** were also determined by X-ray diffraction studies. The ORTEP diagrams are shown in Figure 4.2 and a selection of structural parameters are tabulated in Table 4.3. The nickel center in all complexes adopts a square-planar geometry which is distorted because of the small bite angle of the POCOP ligands (P-Ni-P~ 165°). The Ni-Cl distances are fairly similar in all cases (2.185-2.192 Å) as are the Ni-C distances (1.875-1.893 Å). The Ni-P distances were found to be fairly insensitive to the OMe and CO_2Me ring-substituents R, but important variations were noted with bulky t-Bu substituents on the 3- and 5-positions (~ 2.14 Å with *t*-Bu and ~2. 16 without substituent). This difference is attributed to steric effects.[16]

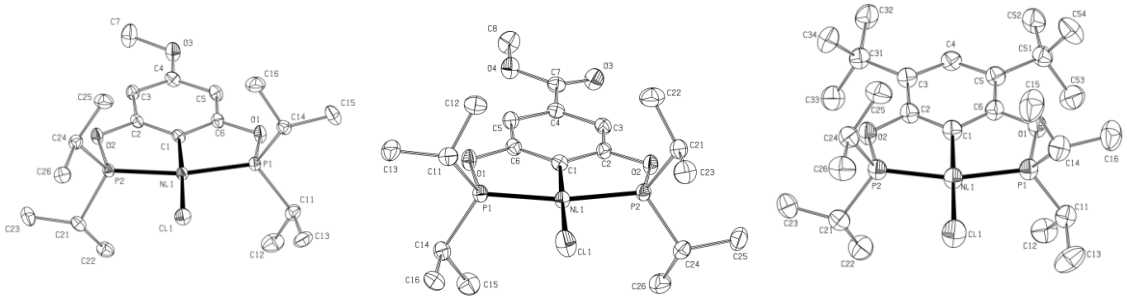

Figure 4.2 ORTEP diagrams for **2**, **3** and **4** Thermal ellipsoids are shown at the 50% probability level. Hydrogens are omitted for clarity. Selected bond distances (Å) and angles (°).

Table 4.3. Selected bond distances (Å) and angles (°) for complexes **2, 3** and **4** (molecule 1).

Compound	Ni-C	Ni-Cl	Ni-P_1	Ni-P_2
1*	1.879 (2)	2.194 (1)	2.158 (1)	2.160 (1)
2	1.877 (1)	2.188 (1)	2.150 (1)	2.157 (1)
3	1.875 (1)	2.185 (1)	2.161 (1)	2.158 (1)
4	1.893 (2)	2.192 (1)	2.142 (1)	2.146 (1)

* Reported in reference 10a.

Chapitre 4

4.4 Conclusions

This study has led to the elaboration of a new method for the efficient synthesis of (R-POCOP$^{i\text{-}Pr}$)NiCl. The hallmark of this method is the use of in-situ formed ligand and nickel precursor. The POC(H)OP ligand is generated in the first step from the reaction of resorcinol and i-Pr_2PCl, and the HCl generated in this step oxidizes elemental nickel to the divalent form required for the nickellation step. The latter reaction also obviates the need for external base, which would otherwise be necessary to prevent protonation of the ligand. Eliminating the need for external base avoids generation of solid waste in the form of HCl.Base to be removed at the end of the reaction, thus simplifying product isolation and rendering the synthesis atom-economical (atomic efficiency of 90%). The new synthetic method protocol can also be considered a "green" alternative to classical approaches for the synthesis of (POCOP)NiCl, because it condenses three synthetic steps into a one-pot protocol, uses an economical source of nickel and avoids using corrosive starting material such as Br_2, eliminates the need for isolation and handling of an air-sensitive ligand, and produces fairly benign side-products (H_2 and excess $NiCl_2$). Indeed, the environmental (E) factor of this protocol is 0.09.[22] Of the three solvents that work fairly well for our synthetic method, toluene and ethyl acetate satisfy green chemistry requirements better than acetonitrile, but newly developed methods for the production of the latter promise to close this gap.[23] Future efforts will be directed at modifications that will allow an expansion of the synthetic scope of this methodology to complexes of other metal-ligand combinations.

4.5 Experimental Section

General Procedures. Unless otherwise indicated, all manipulations were carried out using standard Schlenk and glove box techniques under a dry nitrogen atmosphere using solvents which were dried to water contents of less than 10 ppm (determined using a Mettler-Toledo C20 coulometric Karl Fischer titrator) by passing through activated aluminum oxide columns (MBraun SPS). The starting materials were purchased from Aldrich (nickel powder: ~3 micron, 99.7% metals basis; resorcinol, 1,3-$(OH)_2$-4,6-(t-Bu)$_2$-C_6H_2, 1,3-$(OH)_2$-5-CO_2Me-C_6H_3, i-Pr_2PCl, and Ph_2PCl) and Chemsavers (5-methoxyresorcinol), and used without further purification.

The NMR spectra were recorded on the following spectrometers: Bruker AV400rg (^{1}H at 400 MHz and ^{31}P at 161.9 MHz) and Bruker ARX400 (^{1}H at 400 MHz and $^{13}C\{^1H\}$ at 100.56 MHz). Chemical shift values are reported in ppm (δ) and referenced internally to the residual solvent signals (^{1}H and ^{13}C: 7.26 and 77.16 ppm for $CDCl_3$; 7.16 and 128.06 ppm for C_6D_6) or externally (^{31}P, H_3PO_4 in D_2O, δ= 0). Coupling constants are reported in Hz. UV/vis spectra were measured on a Varian Cary 500i. The elemental analyses were performed by the Laboratoire d'Analyse Élémentaire, Département de chimie, Université de Montréal.

Syntheses of (R'-POCOP$^{i\text{-}Pr}$)NiCl. The one-pot synthetic protocol described below for the preparation of **1** (R'= H) was also used with minor variations to prepare complexes **2**-**4**.

{2,6-(i-Pr_2PO)$_2$$C_6H_3$}NiCl, **1**. To a Schlenk flask containing resorcinol (416 mg, 3.78 mmol) and nickel powder (333 mg, 5.67 mmol) in acetonitrile (5 mL) was added

$ClP(i\text{-}Pr)_2$ (1.2 mL, 7.57 mmol) at room temperature and the mixture was then stirred under a static atmosphere of nitrogen and heated to 75 °C. After a few minutes, the reaction turned light yellow and gas bubbles evolved slowly; after 18h, the reaction mixture consisted of a black solid residue in a yellow-orange solution. Evaporation of the volatiles followed by extraction of the solid residues with hexane (ca. 70 mL), filtration and slow evaporation of the filtrate at ambient temperature produced yellow crystals, which were washed with small amounts of cold hexane (1.45 g, 88%). (N.B.: Using toluene for the extraction step is advantageous as the complexes are more soluble in it and hence less solvent is required; on the other hand, toluene is harder to evaporate and precipitation of the complex from toluene solutions is less facile in comparison to hexane solutions.) Characterization data for **1** have been reported previously.[10a]

{2,6-(i-Pr$_2$PO)$_2$-4-(OMe)C$_6$H$_2$}NiCl, 2. Yield: 1.31 g of a yellow solid (75%). ^{1}H NMR (400 MHz, C_6D_6): δ 1.19 (dt^v, J_{HH} = 7.2, 12H, CH(CH_3)$_2$), 1.41 (dt^v, J_{HH} = 7.8, 12H, CH(CH_3)$_2$), 2.20 (m, 4H, PCH(CH$_3$)$_2$), 3.23 (s, 3H, OCH_3), 6.33 (s, 2H, *Ar*). ^{31}P{^{1}H} NMR (162 MHz, C_6D_6): δ 186.66 (s). ^{13}C{^{1}H} NMR (101 MHz, $CDCl_3$) : δ 16.75 (s, 4C, *C*H$_3$), 17.56 (t^v, 4C, *C*H$_3$), 28.04 (t^v, J_{CP} = 10.8, 4C, P*C*H(CH$_3$)$_2$), 54.98 (s, 1C, O*C*H$_3$), 92.99 (t^v, J_{PC} =6.5, 2C, *C*H$_{Ar}$), 115.91 (t, J_{PC}=22.6, 1C, Ni-C_{Ar}), 162.58 (s, 1C, C_{Ar}OMe), 169.63 (t^v, J_{PC}=10.6, 2C, C_{Ar}OP). Anal. Calcd. for $C_{19}H_{33}O_3P_2NiCl$ (464.814): C, 49.02; H, 7.14. Found: C, 49.44; H, 7.49.

{2,6-(i-Pr$_2$PO)$_2$,4-(COOMe)C$_6$H$_2$}NiCl 3. Yield: 1.09 g of a yellow-orange solid (58 %). ^{1}H NMR (400 MHz, C_6D_6): δ 1.12 (dt^v, J_{HH}= 7.21 J_{HP}= 7.05, 12H, CH(CH_3)$_2$), 1.33 (dt^v, J_{HH}= 8.59 J_{HP}= 8.02, 12H, CH(CH_3)$_2$), 2.14 (m, 4H, PCH(CH$_3$)$_2$), 3.44 (s,

3H, OCH_3), 7.51 (s, 2H, *Ar*). RMN $^{31}P\{^1H\}$ (162 MHz, C_6D_6): δ 186.63 (s). RMN $^{13}C\{^1H\}$ (101 MHz, C_6D_6) : δ 16.51 (s, 4C, CH_3), 17.29 (t^v, 4C, CH_3), 27.96 (t^v, J_{CP} = 10.90, 4C, P$CH(CH3)_2$), 51.46 (s, 1C, OCH_3), 106.73 (t^v, 2C, CH_{Ar}), 131.77 (s, 1C, $C_{Ar}CO_2Me$), 134.74 (t, J_{PC}=20.8, 1C, Ni-C_{Ar}), 166.48 (s, 1C, C=O), 169.11 (t^v, J_{PC}=10.0, 2C, C_{Ar}OP), Anal. Calcd. for $C_{20}H_{33}O_4P_2NiCl$ (493.57): C, 48.67; H, 6.74. Found: C, 48.69; H, 6.79.

{2,6-(*i*-Pr$_2$PO)$_2$,3,5-(*t*-Bu)C$_6$H}NiCl, **4**. Yield: 1.41 g of a yellow solid (68 %). ^1H NMR (400 MHz, C_6D_6): δ 1.32 (s, 18H, C(CH_3)$_3$), 1.37 (dt^v, J_{H-H}= 7.0, $^vJ_{H-P}$= 6.8, 12H, CH_3), 1.44 (dt^v, J_{H-H}= 8.3, $^vJ_{H-P}$= 7.9, 12H, CH_3), 2.44 (m, 4H, PC$H(CH_3)_2$), 6.91 (s, 1H, H_{Ar}). $^{31}P\{^1H\}$ NMR (162 MHz, C_6D_6): δ 182.75 (s). $^{13}C\{^1H\}$ NMR (101 MHz, $CDCl_3$) : δ 17.01 (s, 4C, CH_3), 17.69 (s, 4C, CH_3), 27.87 (t^v, J_{CP} = 10.2, 4C, P$CH(CH3)_2$), 30.03 (s, 6C, C(CH_3)$_3$), 34.32 (s, 2C, C(CH_3)$_3$), 123.79 (s, 1C, CH_{Ar}), 126.45 (s, 2C, C_{Ar}(^{t}Bu)), 128.49 (t, J_{PC}=18.7, 1C, Ni-C_{Ar}), 164.3 (t^v, J_{PC}=10.7, 2C, C_{Ar}OP). Anal. Calcd. for $C_{26}H_{47}O_2P_2NiCl$ (547,74): C, 57.01; H, 8.65. Found: C, 57.04; H, 8.72

{2,6-(Ph$_2$PO)$_2$,C$_6$H$_3$}NiCl, **5.** To a Schlenk flask containing resorcinol (833 mg, 7.56 mmol) and nickel powder (444 mg, 7.56 mmol) in acetonitrile (4 mL) was added $ClPPh_2$ (2.7 mL, 15.13 mmol) at room temperature and the mixture stirred under a static atmosphere of nitrogen and heated to 75 °C. After a few minutes, the reaction turned light yellow and gas bubbles evolved slowly; after 18h, the reaction mixture consisted of a black solid residue in a yellow-orange solution. Evaporation of the volatiles followed by flash chromatography of the solid residues on silica gel with chloroform gave a yellow solid (1.51g, 35 %). Characterization data for **5** have been reported previously.[7]

Crystal Structure Determinations. The crystallographic data for compounds **2** were collected on a Nonius FR591 generator (rotating anode) equipped with a Montel 200, a D8 goniometer, and a Bruker Smart 6000 area detector. Cell refinement and data reduction were done using SAINT[24]. An empirical absorption correction, based on the multiple measurements of equivalent reflections, was applied using the program SADABS[25]. The space group was confirmed by XPREP routine[26] in the program SHELXTL[27]. The structures were solved by direct methods and refined by fullmatrix least-squares and difference Fourier techniques with SHELX-97[28]. All non-hydrogen atoms were refined with anisotropic displacement parameters. Hydrogen atoms were set in calculated positions and refined as riding atoms with a common thermal parameter.

4.6 Acknowledgments.

The authors are grateful to: NSERC of Canada for a Discovery Grant to D.Z.; Université de Montréal and Centre in Green Chemistry and Catalysis for graduate fellowships to B.V. ; Dr. Michel Simard and Ms. Francine Bélanger-Gariépy for their valuable assistance with crystallography.

4.7 Supporting Information

Table 4.4 : Crystal Data Collection and Refinement Parameters for Compound **2, 3** and **4**

Compound	**2**	**3**	**4**
chemical formula	$C_{19}H_{33}ClNiO_3P_2$	$C_{20}H_{33}ClNiO_4P_2$	$C_{26}H_{47}ClNiO_2P_2$
Fw	465.55	493.56	547.74
T (K)	100	150	200
wavelength (Å)	1.54178	1.54178	1.54178
space group	C2/c	P2(1)/c	P2(1)/n
a (Å)	18.8143(2)	15.9080 (12)	10.4275(4)
b (Å)	18.2714(2)	13.0746 (10)	14.0330(5)
c (Å)	14.9031(2)	11.1340 (8)	20.5730(7)
α (deg)	90	90	90.00
β (deg)	117.8053(4)	91.464	101.1800(10)
γ (deg)	90	90	90.00
Z	8	4	4
V (Å^3)	4531.62(9)	2315.0 (3)	2953.30(18)
ρcalcd (g cm^{-3})	1.365	1.416	1.232
μ (mm-1)	3.778	3.766	2.944
θ range (deg)	3.59 - 71.18	2.78 - 69.76	3.84 - 72.53
R_1[a] [I > 2ó(I)]	0.0253	0.0304	0.0448
wR_2[b] [I > 2ó(I)]	0.0951	0.0844	0.1176
R_1 [all data]	0.0265	0.0305	0.0464
wR_2 [all data]	0.0984	0.0845	0.1192
GOF	0.918	1.004	1.074

[a] $R_1=\Sigma(||F_o|-|F_c||)/\Sigma|F_o|$ [b] $wR_2=\{\Sigma[w(F_o^2-Fc^2)^2]/\Sigma[w(F_o^2)^2]\}^{½}$

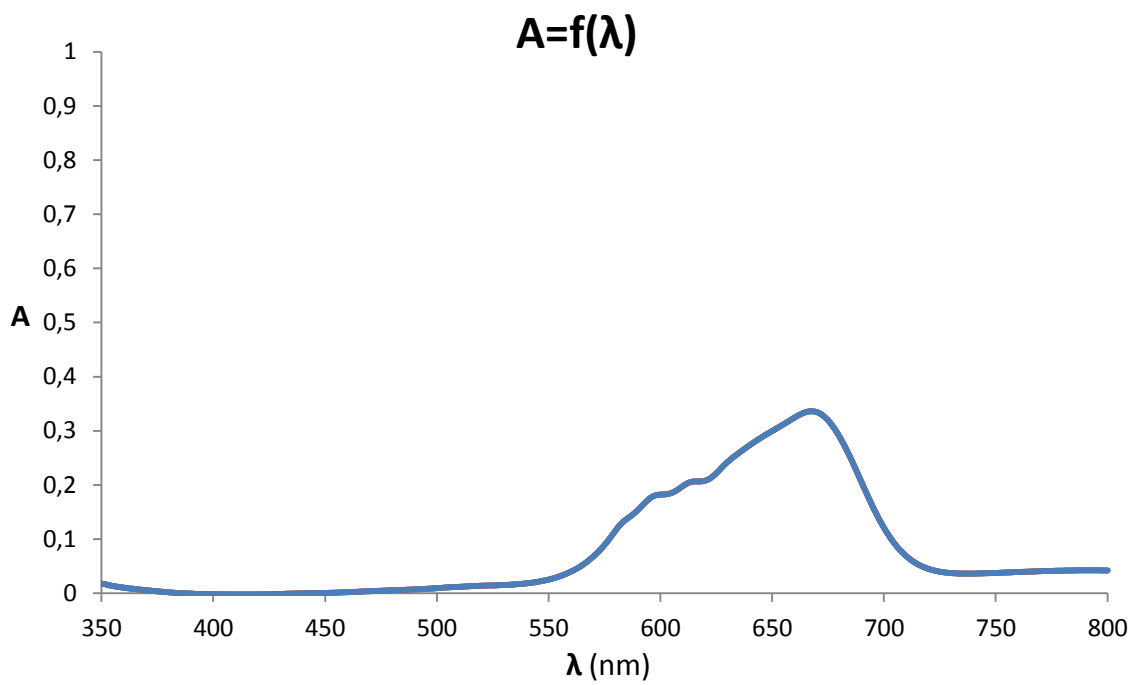

Figure 4.3 : UV-vis spectra (CH_2Cl_2, r.t.) of a sample of Co (0) one pot reaction.

4.8 Reference

[1] (a) Mohapatra, S.; Kumar, R. K.; Maji, T. K. *Chem. Phys. Lett.* **2011**, *508*, 76–79. (b) Hewer, T. L. R.; Soeira, L. S.; Brito, G. E. S.; Freire, R. S. *J. Mater. Chem.* **2013**, *1*, 6169.

[2] (a) Morales-Morales, D.; Grause, C.; Kasaoka, K.; Redón, R.; Cramer, R. E.; Jensen, C. M. *Inorg. Chim. Acta* **2000**, *300*, 958. (b) Bedford, R. B.; Draper, S. M.; Scully, P. N.; Welch, S. L. *New J. Chem.* **2000**, *24*, 745. (c) Miyazaki, F.; Yamaguchi, K.; Shibasaki, M. *Tet. Lett.* **1999**, *40*, 7379. (d) Naghipour, A.; Sabounchei, S. J.; Morales-Morales, D.; Canseco-González, D.; Jensen, C. M. *Polyhedron* **2007**, *26*, 1445.

[3] (a) Wallner, O. A.; Olsson, V. J.; Eriksson, L.; Szabò, K. J. *Inorg. Chim. Acta* **2006**, *359*, 1767. (b) Wang, Z.; Eberhard, M. R.; Jensen, C. M.; Matsukawa, S.; Yamamoto, Y. *J. Organomet. Chem.* **2003**, *681*, 189. (c) Wallner, O. A.; Szabò, K. J. *Org. Lett.* **2004**, *359*, 1829.

[4] (a) Pandarus, V.; Zargarian, D. *Organometallics*, **2007**, *26*, 4321. (b) Castonguay, A.; Spasyuk, D. M.; Madern, N.; Beauchamp, A. L.; Zargarian, D. *Organometallics*, **2009**, *28*, 196. (c) Spasyuk, D. M.; Zargarian, D. *Inorg. Chem.*, **2010**, 49, 6203–6213. (d) Lefèvre, X.; Durieux, G.; Lesturgez, S.; Zargarian, D. *J. Mol. Catal. A.*, **2010**, 335, 1–7. (e) Salah, A.; Offenstein, C.; Zargarian, D. **2011**, *Organometallics 30*, 5352.

[5] Chakraborty S., Krause J. A., Guan H., *Organometallics* **2009**, *28*, 582.

[6] Chakraborty, S.; Zhang, J.; Krause, J. A.; Guan. H. *J. Am. Chem. Soc.* **2010**, *132*, 8872.

[7] Gómez-Benítez, V.; Baldovino-Pantaleón, O.; Herrera-Álvarez, C.; Toscano, R. A.; Morales-Morales, D. *Tet. Lett.* **2006**, *47*, 5059.

[8] Zargarian, D.; Castonguay, A.; Spasyuk, D. M. in "ECE-Type Pincer Complexes of Nicekl" in Organometallic Pincer Chemistry, ed. G. van Koten and D. Milstein, Top. Organomet. Chem. (2013) 40: 131–174; Springer-Verlag Berlin Heidelberg 2013.

[9] For the original reports on preparation of POCHOP-type ligands and their Pd complexes see references 2a and 2b.

[10] For representative reports on preparation of POCOP-Ni complexes see refs. 5-7 and the following reports: (a) Pandarus, V.; Zargarian, D. *Chem. Commun.* **2007**, 978. (b) Chakraborty, S.; Krause, J. A.; Guan, H. *Organometallics* **2009**, *28*, 582. (c) Zhang, J.; Medley, C. M.; Krause, J. A.; Guan, H. *Organometallics* **2010**, *29*, 6393. (d) Salah, A. B.; Zargarian, D. *Dalton Trans.* **2011**, *40*, 8977.

[11] It should be mentioned that in some instances the metallation step is carried out in the absence of an added base; e.g., see ref. 7. In these protocols, the in-situ generated HX is presumably driven off thermally.

[12] We have noted, for example, that conducting the synthesis of PCP- and POCN-type Ni complexes in the absence of base leads to significantly reduced yields as a result of the protonation of the ligand donor moieties by the in-situ generated HX. In some cases, the non-metallated species bearing the protonated ligand were isolated and fully characterized. See: (a) Castonguay, A.; Sui-Seng, C.; Zargarian, D.; Beauchamp, A. L. *Organometallics* **2006**, *25*, 602. (b) Spasyuk, D. M.; Zargarian, D.; van der Est, A. *Organometallics* **2009**, *28*, 6531.

[13] Kimura, T.; Uozumi, Y. *Organometallics* **2006**, *25*, 4883.

[14] Gong, J.-F.; Zhang, Y.-H.; Song, M.-P.; Xu, C. *Organometallics* **2007**, *26*, 6487.

[15] Chakraborty, S.; Patel, Y. J.; Krause, J. A.; Guan, H. *Polyhedron* **2012**, *32*, 30.

[16] Vabre, B.; Spasyuk, D. M.; Zargarian, D. *Organometallics* **2012**, *31*, 8561.

[17] The bromo derivatives of complexes 2-4 (LNi-Br) have been reported previously. See ref 16.

[18] Handbook of Chemistry and Physics, 89th Edition, CRC Press 2008. Tests have confirmed that metallic nickel is oxidized instantaneously in conc. HCl (aq.), whereas metallic palladium is much less reactive.

[19] Previous studies in our group have shown that the synthesis of (POCOP)CoX from POC(H)OP and CoX_2 is quite sluggish, giving 5-10% yields only: Xavier Lefèvre, M. Sc. Dissertation, Université de Montréal, 2010.

[20] It should be added that $NiCl_2$ can react further with HCl to form other species such as $H_2[NiCl_4]$: Klygin, A.E.; Glebov, V. A.; Lekae,V.; A. Kolyada, N. S.; Smirnova, I. D.; Nikol'skaya, N. A.; Zavrazhovam, D. M. *Russ. J. Inorg. Chem.* **1971**, *16*, 840.

[21] For the preparation of these POCN-type species see ref. 4c.

[22] Sheldon, R. A. *Pure and Applied Chemistry* **2000**, *72*, 1233.

[23] Mentzel, E. C.; Mielby, U. V. J.; Riisager, A.; Fehrmann, R. *Green Chemistry* **2013**, *15*, 928.

[24] SAINT, Release 6.06; Integration Software for Single Crystal Data; Bruker AXS Inc.: Madison, WI, 1999

[25] Sheldrick, G. M. SADABS, Bruker Area Detector Absorption Corrections; Bruker AXS Inc., Madison, WI, 1999

[26] XPREP, Release 5.10; X-ray Data Preparation and Reciprocal Space Exploration Program; Bruker AXS Inc.: Madison, WI, 1997.

[27] SHELXTL, Release 5.10; The Complete Software Package for Single Crystal Structure Determination; Bruker AXS Inc.: Madison, WI, 1997.

[28] (a) Sheldrick, G. M. SHELXS97, Program for the Solution of Crystal Structures; Univ. of Gottingen: Germany, 1997. (b) Sheldrick, G. M. SHELXL97, Program for the Refinement of Crystal Structures; University of Gottingen: Germany, 1997

Chapitre 5

Chapitre 5 : Fluoro and Trifluoromethyl Derivatives of POCOP-Type Pincer Complexes of Nickel : Preparation and Reactivities in S_N2 Fluorination and Direct Benzylation of Unactivated Arenes

Article 4

Boris Vabre, Pauline Petiot, Richard Declercq and Davit Zargarian*

Department of Chemistry, Université de Montréal, Montréal, Québec, Canada

Organometallics **2014**, *33,* 5173-5184.

Chapitre 5

5.1 Abstract

This report describes the synthesis, characterization, and reactivities of the pincer-type complexes $\kappa^{P},\kappa^{C},\kappa^{P'}$-(R-POCOP)NiX (R-POCOP= 2,6-(*i*-$Pr_2PO)_2$,4-R-C_6H_3; R= H: X= F (**2**), CF_3 (**3a**); R= OMe: X= CF_3 (**3b**)). These complexes were prepared by treating their Ni-Br analogue with excess AgF at r.t. or excess AgF and Me_3SiCF_3 (**3a** and **3b**) at 45 °C. The Ni-F derivative **2** was shown to be an intermediate for the formation of the Ni-CF_3 derivatives **3**. All new complexes were fully characterized by multinuclear NMR spectroscopy, cyclic voltammetry, and X-ray diffraction analysis. Variable temperature NMR analysis of **2** helped elucidate the interaction of the fluoride ligand with in-situ generated hydrofluoric acid. Complex **2** or its bromo precursor catalyzed fluorination of benzyl halides at 90 °C in the presence of excess AgF, whereas the Ni-CF_3 complexes **3** failed to promote trifluoromethylation of benzyl bromide, leading instead to a direct benzylation of the aromatic reaction solvent (benzene, toluene, xylene, or bromobenzene). Possible mechanisms for this benzylation reaction have been probed and discussed.

5.2 Introduction

Fluoroorganic compounds containing one or more CR_mF_n moieties possess unique and desirable properties that have led to applications in diverse fields ranging from agrochemicals[1] and pharmaceuticals[2] (including tracers for positron emission tomography)[3] to industrial materials such as fluoropolymers,[4] refrigerants, etc.[5] The practical utility of fluoroorganics has served as a potent driving force for the development of multiple synthetic methodologies for the introduction of F atoms in activated/functionalized organics or unactivated hydrocarbons. Among these methodologies are non-transition-metal-based organic/inorganic compounds that serve as stoichiometric synthons for nucleophilic "F^-" (e.g., DAST,[6] DFI,[7] Deoxofluor,[8a] Ishikawa's and Yarovenko's reagents,[8b] and Riter's reagent)[8c] or electrophilic "F^+" (e.g., Selectfluor, NFSI, and *N*-fluoropyridinium triflate),[2b,9] "CF_2",[10] or "CF_3" (Ruppert-Prakash reagent,[2b,11] trifluoroacetamides[12]). In addition, many transition-metal-based methodologies have been developed for catalytic fluorination,[13,14,15,16,17] difluoromethylation,[18] or trifluoromethylation.[19]

In the context of metal-catalyzed fluorination and trifluoromethylation, methodologies based on Cu appear to be the most versatile, but Pd complexes have been used most frequently to probe mechanistic issues. For instance, model studies on reductive elimination of Ar-F have been conducted for a series of $L_2Pd(Ar)F$ complexes,[13b] and reactivity studies have been reported for pincer-type fluoride derivatives such as (PNP)PdF,[20] (NCN)PdF,[21] and (PCP)PdF,[22] as well as "pincer-like" complexes such as (CNC)PdF.[23] Similarly, Pd-CF_3 complexes have been used

as models for the C-C bond formation step in catalytic trifluoromethylation of organic halides.[24] These studies have furnished valuable mechanistic data about the Pd-catalyzed trifluoromethylation reaction, culminating in the development by Buchwald's group of an efficient process for conversion of Ar-Cl to Ar-CF_3 using $(Et)_3SiCF_3$/KF as source of 'CF_3'.[24h]

Fluorination reactivities have also been investigated with Ni,[25] but in comparison to Cu and Pd there have been fewer studies focused on well-characterized Ni complexes. For instance, Ni(II) precursors have been used as chiral Lewis acids in various fluorinations,[26] and many reports have appeared on reactivities of non-pincer type Ni-F and Ni-Ar^F complexes,[27] including a recent study on the formation of ^{18}F-Ar from reaction of a divalent Ni-Ar species with a hypervalent iodine oxidant.[28] Similarly, there have been a few reports on Ni-CF_3 derivatives,[29] but no Ni-catalyzed methodology has been developed for trifluoromethylations. Finally, there are even fewer pincer-type analogues of these complexes. Thus, the first fluoride derivative of a pincer complex of nickel, ($PCP^{t\text{-}Bu}$)NiF, was reported in 2011 by Peruzzini's group,[30] and Cámpora's group reported the analogous $PCP^{i\text{-}Pr}$ complex in 2012;[22] the latter complex was shown to promote the catalytic fluorination of dodecyliodide in the presence of AgF. As for pincer-type M-CF_3 complexes, a recent search of the literature has resulted in only two complexes for M= Ni,[31] and none for M= Pd or Pt.

This paucity of data on (pincer)NiF and (pincer)NiCF_3 species is somewhat surprising given the practical importance of fluorination methodologies and the documented reactivities of pincer-Ni complexes in diverse catalytic transformations, including: cyanomethylation,[32] hydrosilylation,[33] and CO_2 reduction;[34] Kumada,[35]

Suzuki-Miyaura,[36] and Mizoroki-Heck coupling;[37] Zn-mediated homocoupling;[38] electrocatalytic hydrogen production;[39] ethylene polymerization,[40] Michael-type hydroamination,[41] hydroalkoxylation,[41bc,42] and C-C bond formation;[37,43] Kharasch addition;[41a,44] The intense interest in pincer complexes of nickel is also due to their ease of synthesis, enhanced thermal stabilities and diverse reactivities compared to analogous complexes based on non-chelating ligands, and the relative abundance of nickel.[45] The above considerations and our interest in the reactivities of pincer-type nickel complexes prompted us to prepare fluoro and trifluoromethyl derivatives of these complexes and explore their reactivities. The present report describes the synthesis and full characterization of complexes (POCOP)NiF and (R-POCOP)Ni(CF_3) (R= H, OMe), including multinuclear NMR spectra, electrochemical measurements, solid state structures, and a study of their reactivities.

5.3 Résults and discussion

Initial attempts to prepare our target (pincer)NiF complexes based on the resorcinol-based POC(H)OP ligand showed that direct C-H nickelation[46] does not proceed with simple nickel fluoride salts. This observation is in stark contrast to the facile nickelation of these ligands with the heavier halide analogues NiX_2 or L_nNiX_2 (Scheme 5.1, Route A; L= none, THF, CH_3CN, *i*-PrCN),[41a,44a,34,36,47] and even metallic nickel can serve as precursor for the chloro derivatives (POCOP)NiCl via a convenient one-pot procedure (Scheme 5.1, Route B).[48] The unsuccessful C-H

activation observed with NiF_2 was attributed to the limited solubility of this precursor or the weak basicity of fluoride anions, and we sought alternative synthetic routes.

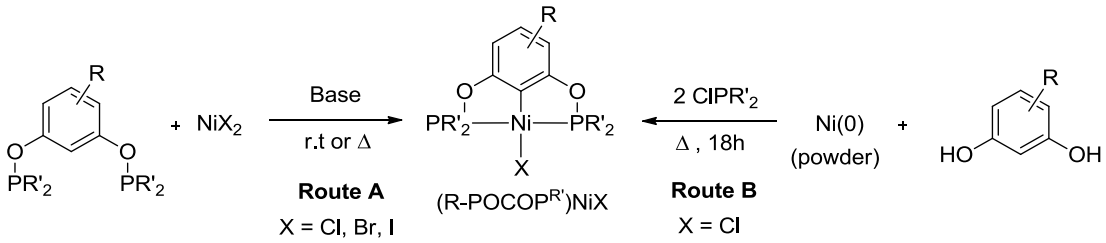

Scheme 5.1 Synthetic routes for ^{R}(POCOP)NiX complexes.

In analogy with the previously reported syntheses of (PCP)NiF via halide exchange between the chloro or bromo precursors and TlF[30] or AgF,[22] we examined salt metathesis reactions between the bromo precursor (POCOP)NiBr and fluoride salts such as CsF, KF, and AgF. The effectiveness of this approach proved to be highly dependent on the source of F^- and the reaction conditions, giving the target fluoride complex in moderate yields (with AgF) or not at all (with CsF and KF). The reaction solvent was also important, the metathesis with AgF taking place fairly well in THF but not at all in hexane. Optimization studies eventually allowed us to prepare (POCOP)NiF, **2**, in 80% isolated yield by reacting the bromo precursor **1a** with 5 equiv of AgF in THF at r.t. overnight (Scheme 5.2). The complexes (R-POCOP$^{i\text{-}Pr}$)$NiCF_3$, **3**, were prepared in ca. 85% yields by direct reaction of the bromo precursors **1a** or **1b** with excess CF_3SiMe_3 and AgF (Scheme 5.2).[31] The Ni-CF_3 derivatives **3** are stable in ambient air and even in wet solvents,[49] whereas the Ni-F derivative **2** appears to be hygroscopic but fairly resistant to hydrolysis under

standard conditions of room temperature and fairly dry solvents, or in the solid state. (See Supporting Information for further details.)

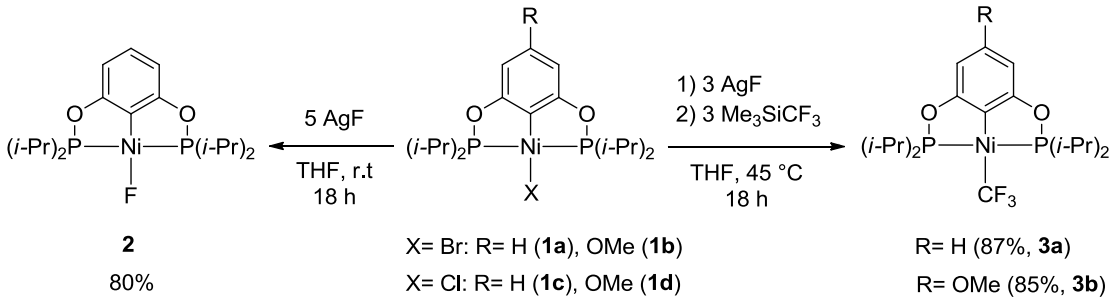

Scheme 5.2 Synthetsis of (POCOP)NiF et ^{R}(POCOP)NiCF$_3$ complexes.

Formation of the Ni-CF$_3$ complexes **3** can proceed via two pathways, namely: a step-wise pathway involving the initial formation of Ni-F intermediates from AgF, followed by Ni-F/CF$_3$SiMe$_3$ exchange; or a direct transmetallation of the Ni-Br moiety with in-situ generated "AgCF$_3$". Indeed, a number of literature reports have suggested that mixtures of AgF and CF$_3$SiMe$_3$ generate "AgCF$_3$", but the formation of this species requires highly polar *N*-donor solvents such as nitriles, DMF, pyridine, or *N*-methylimidazole,[50] and does not proceed in low-polarity solvents such as THF. Since the synthesis of the Ni-CF$_3$ complexes **3a** and **3b** were carried out in THF, it is unlikely that this reaction involves "AgCF$_3$", which suggests that the formation of **3** in our conditions proceeds in a step-wise fashion via initial formation of Ni-F derivatives from the Ni-halide/AgF exchange, followed by a second exchange step between Ni-F and CF$_3$SiMe$_3$ to generate the final Ni-CF$_3$ products. The observations described below support this scenario.

A NMR tube containing a THF suspension of **1a**, AgF, and CF_3SiMe_3 (molar ratio of 1:5:2) was initially agitated for a few min in an ultrasonic bath and subsequently subjected to periodic manual agitation over a period of one day while at room temperature; the reaction progress over this period was monitored by ^{31}P NMR spectroscopy. The spectral record showed the formation of both the fluoro complex **2** and the CF_3 derivative **3a** during the initial stages of the reaction (Figure 5.1), the latter species being a minor component of the product mixture. For instance, 30 min after the start of the reaction, ca. 32% of the bromo precursor **1a** had been converted to give an approximately 4:1 mixture of the fluoride species **2** (26 %) and the CF_3 derivative **3a** (6%). Over the following 7-8 h of the reaction, the NMR spectra revealed a steady decrease in the concentration of the Ni-Br precursor, [**1a**], accompanied by a corresponding increase in [**3a**], whereas [**2**] remained fairly constant at about 30% of all P-containing species present in the reaction mixture. The subsequent phase of the reaction (t= 8-24 h) was characterized by steady declines in [**1a**] and [**2**], and a corresponding increase in [**3a**]; significantly, conversion of the Ni-Br precursor **1a** was faster than that of the Ni-F species **2a** over this period.

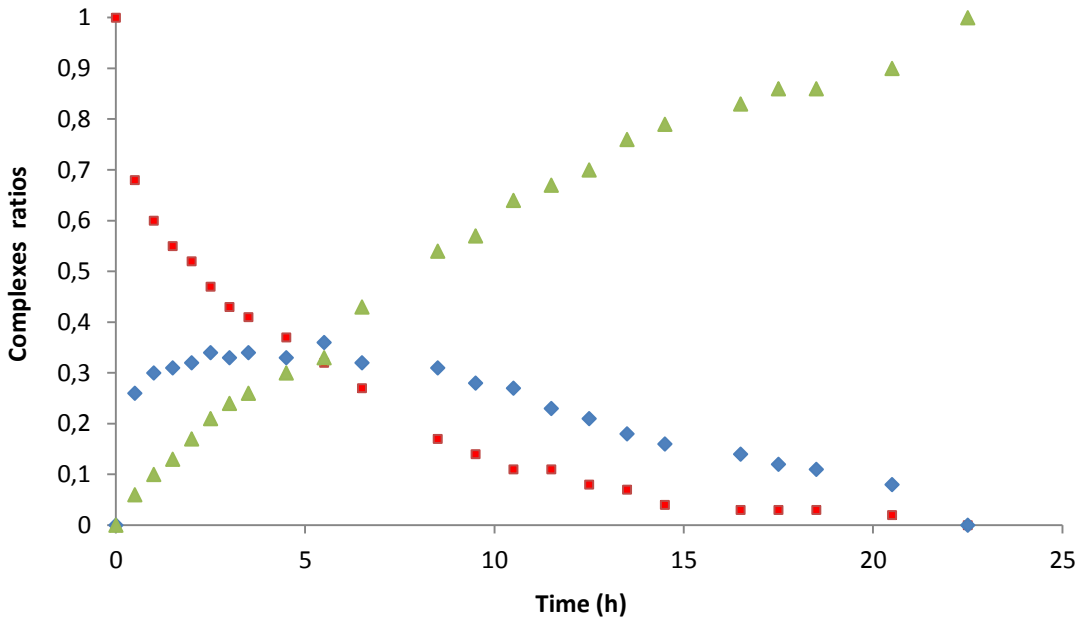

Figure 5.1: Time profiles based on ^{31}P NMR spectroscopy for the reaction of **1a** (▪) with excess AgF and CF_3SiMe_3 in THF (molar ratio of 1:3:3) giving the Ni-F complex **2** (♦) as intermediate and the Ni-CF_3 complex **3a** (▲) as final product. See the Experimental Section for details.

The above observations imply that the final product **3a** does not form via a direct reaction between (POCOP)NiBr and "$AgCF_3$" and that complex **2** is a veritable intermediate species in this reaction. This conclusion is also consistent with the following observations. First, the reaction of independently prepared Ni-F derivative **2** with CF_3SiMe_3 led to smooth conversion to **3a**, indicating that the latter can form in the absence of AgF or "$AgCF_3$" (Scheme 5.3). Second, the direct conversion of the Ni-Br precursor **1a** to the Ni-CF_3 derivative **3a** did not proceed when we used combinations of CF_3SiMe_3 and fluoride salts that are less efficient in the Ni-Br/Ni-F exchange reaction relative to AgF (e.g., CsF, KF), implying that the formation of the F derivative **2** is the key step in the formation of the target complexes **3**.[51] Finally, ^{19}F NMR monitoring of mixtures of AgF and CF_3SiMe_3 in THF have failed to detect any

new species that might be attributed to the formation of "$AgCF_3$", which is consistent with Tyrra's observation that formation of "$AgCF_3$" from AgF and CF_3SiMe_3 does not take place in *O*-donor solvents such as THF, Et_2O, glyme, etc.[50] We speculate that the F/CF_3 metathesis reaction proceeds in the absence of fluoride salts because the partially ionic character of the Ni-F bond facilitates formation of [$Me_3Si(F)(CF_3)$][(POCOP)Ni], which can collapse to give **3**. Alternatively, the Ni-F bond might be more nucleophilic toward $Me_3Si(CF_3)$ thanks to d_π-p_π repulsive interactions between F lone pairs and the filled d_{z2} orbital of this d_8 metal center (vide infra).

Scheme 3

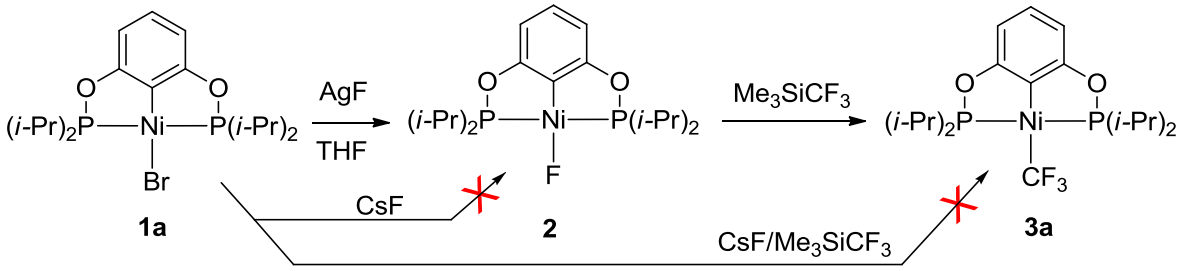

Scheme 5.3 Synthetsis of (POCOP)NiF et (POCOP)$NiCF_3$ complexes.

NMR characterization of 2, 3a, and 3b. The NMR spectra of the new complexes were in accord with the spectral patterns observed in analogous complexes (POCOP)NiX reported previously,[41a,44a,47] in particular the presence of virtual couplings that are characteristic of this family of complexes. Thus, the aliphatic region of the ^{1}H NMR spectrum of **2** showed the expected peaks for the *i*-Pr protons (1.25 and 1.39 ppm, dt^v, J_{H-H}= 7-10 Hz, $^vJ_{H-P}$= 7-7.5 Hz, 12H, Me; 2.12 ppm, dh, J_{HH}=

6.9 Hz, J_{PH}= 0.5 Hz, 4H, PC*H*), whereas the aromatic protons appeared as a doublet at 6.50 ppm (J= 8 Hz, H3 + H5) and a triplet at 6.81 ppm (J= 8 Hz, H4)..

The $^{13}C\{^{1}H\}$ NMR spectra of **3a** and **3b** also showed some characteristic features, including quartets of triplets at ca. 150 ppm for *C*F_3 ($^{1}J_{F\text{-}C}$= 354 Hz, $^{2}J_{P\text{-}C}$= 22 Hz); this region of the spectrum for **3a** is shown in Figure 5.2. The observed C-F couplings also gave rise to triplets of quartets for Ni-bonded aryl carbons (C1) in **3a** (133.35 ppm, $^{2}J_{P\text{-}C}$= 20.3 Hz, $^{3}J_{F\text{-}C}$= 11.4 Hz) and **3b** (123.0 ppm, J_{PC}= 21.6 Hz, J_{FC}= 11.7 Hz).[52] The observed 10 ppm difference in the chemical shifts of the latter signals can be attributed to the electronic effects of the C4-substituents in these complexes (H vs. OMe); curiously, these substituents had little or no effect on ^{31}P and ^{19}F NMR spectra (vide infra), but their impact on the electronics of the Ni centers is manifested in the different oxidation potentials measured for their one electron oxidation ($Ni^{II}\rightarrow Ni^{III}$, vide infra). The $^{13}C\{^{1}H\}$ NMR spectrum of the Ni-F complex **2** also showed the anticipated C-P couplings for C2 and C6 (virtual triplets at 170.06 ppm, $^{v}J_{PC}$= 10 Hz) and C1 (triplet at 119.3 ppm, J_{PC}= 22 Hz), but no C-F coupling was observed in this case; this will be rationalized below.

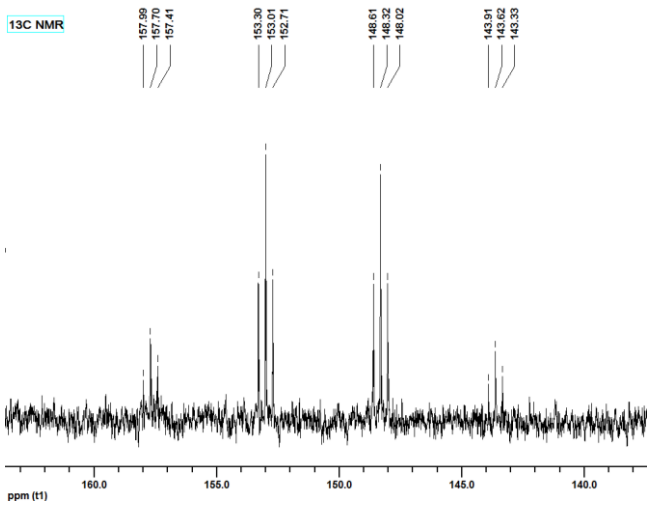

Figure 5.2 Downfield region of the $^{13}C\{^{1}H\}$ NMR spectrum (101 MHz) for a highly concentrated acetone-d_6 solution of complex **3a** showing the CF_3 resonance.

The $^{31}P\{^{1}H\}$ NMR spectra of the title complexes displayed a single resonance for the equivalent phosphinite moieties, consistent with the proposed symmetrical structure of these complexes and in accord with our previous observations for closely related (POCOP)NiX complexes.[41abc] The corresponding spectra of complexes **3a** and **3b** showed a quartet at ca. 197 ppm due to F-P coupling (J_{FP} = 15 Hz); as expected, these F-P couplings were also observed in the $^{19}F\{^{1}H\}$ NMR spectra of these complexes (triplet at 6 ppm). On the other hand, the $^{31}P\{^{1}H\}$ NMR spectrum of the Ni-F complex **2** showed a singlet resonance at 178 ppm rather than the doublet which would have been anticipated due to F-P coupling; this anomalous observation is related to the 'missing' C-F couplings noted above, and will be discussed later in the context of ^{19}F NMR spectra.

Examination of the observed δ values for the P and C_{ispo} nuclei in complex **2** and other derivatives in this series has revealed interesting trends. For instance, comparing the ^{31}P chemical shift in **2** to the corresponding values reported for

(POCOP)MX (X= Cl, Br, I; M= Ni,[41a,44] Pd[53]) confirms a previously noted trend that reveals an inverse relationship between ^{31}P chemical shifts and the electronegativity of the halogen (Figure 5.3). Assuming that a more downfield resonance indicates a greater degree of P→Ni σ–donation, the observed trend suggests that P-Ni interactions are weaker in the more electronegative halide derivatives. That the weakest σ–donor (F^-) engenders the weakest P-Ni interaction seems counter-intuitive if we consider all ligands to be in competition for binding to nickel, but two different notions might be invoked to rationalize this apparent correlation. The HSAB concept[54] can help explain how a "hard and polarizing" ligand such as F^- can undermine the interaction of "soft" P-based ligands with an otherwise "soft" Ni(II) center. Alternatively, d_π-p_π repulsive interactions between d^8 metal centers and a small, effective π–donor ligand such as F^- can modulate the electron-richness of Ni(II) and its interactions with other ligands (cis-labilizing effects).[55]

The second observed trend concerns the ^{13}C δ values of C_{ispo} carbon nucleus in (POCOP)NiX, which follow the order OTf < F < Cl < Br < CN < I < CF_3 < Et ~ CH_3 (see supporting information). Cámpora has noted a similar observation in (PCP)MX (M= Ni, Pd) and has presented a very thorough analysis of the possible factors responsible for the observed trend.[22] Briefly, the relative σ-donor strength of X (its trans influence) is sufficient for rationalizing the observed trend, but Cámpora has argued that the above-mentioned d_π-p_π interactions might also influence C-Ni interactions and ^{13}C δ values.

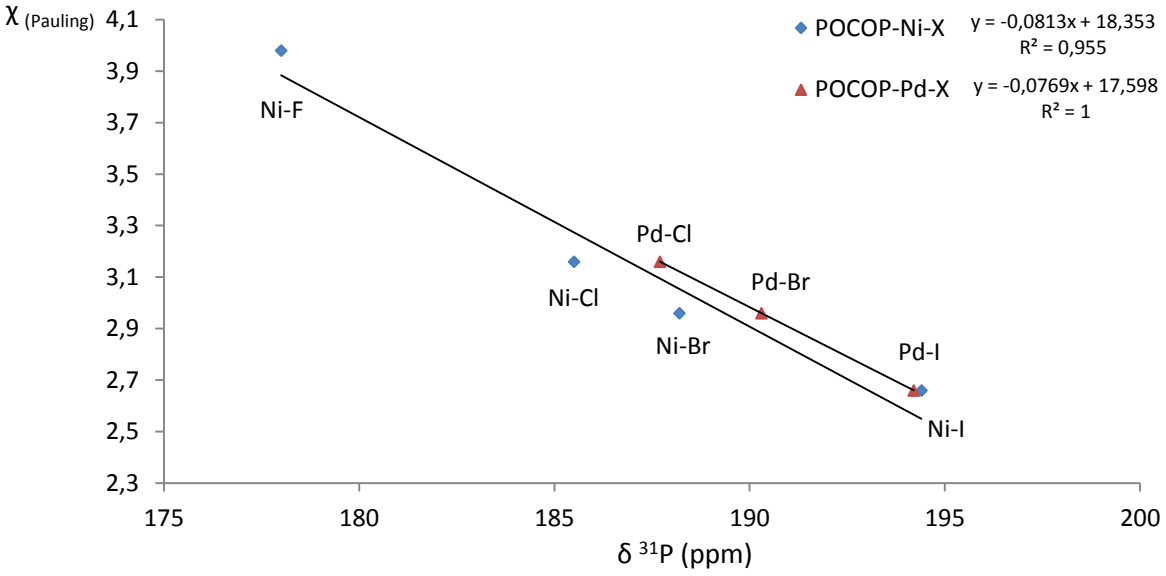

Figure 5.3 Plots of Pauling electronegativity values vs ^{31}P NMR chemical shifts of (POCOP)Ni(X) and (POCOP)Pd(X) (X = halides).

Impact of an in-situ generated HF adduct on NMR spectra of 2. As mentioned above, some anomalies were noted in the ^{13}C and ^{31}P NMR spectra of **2** due to the absence of multiplicities from anticipated C-F couplings. Similar anomalies have been reported for various transition metal-fluoro derivatives of Ni,[56] Pd,[57] Pt,[58] Rh,[59] Ru,[60] Nb,[61] Mo,[62] and W[63], and attributed to MF---HF interactions with in-situ generated H-F. A more careful analysis of complex **2** by variable temperature multinuclear NMR spectroscopy has confirmed that a similar process is occurring in our system as well. Thus, the room temperature ^{1}H NMR spectrum of **2** showed a deshielded, broad doublet (11.19 ppm ; FWHM ≈ 72 Hz) with a large coupling constant (J_{H-F} ≈ 392 Hz) characteristic of H-F protons (Figure 5.4, top trace).[64] This broad doublet transformed into a broad doublet of doublets at -68 °C (Figure 5.4, middle trace), which arises from different couplings to the two ^{19}F nuclei

in the Ni-F---H-F moiety ($J_{H-F} \approx 402$ and 42 Hz). On the other hand, this signal disappeared altogether when D_2O was added to the sample, confirming the facile exchange of the HF proton with the sample medium (Figure 5.4, bottom trace).[65] The in-situ formation of HF in mixtures of the bromo precursor **1** and AgF was also evident from the visible etching of the NMR tubes containing these samples. The coupling constants discussed above are illustrated in Figure 5.5.

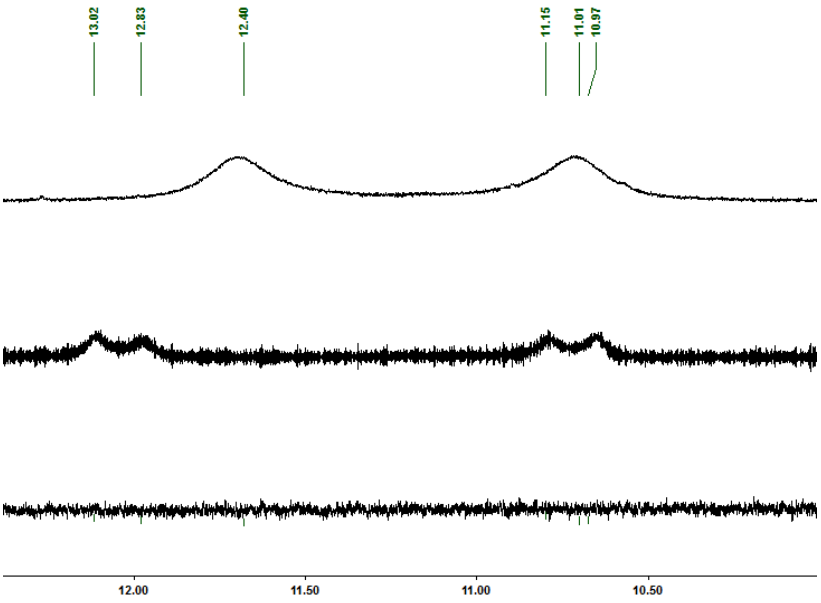

Figure 5.4 ^{1}H NMR spectra (CD_2Cl_2) of the Ni-F complex **2** at r.t. (top trace, at 400 MHz), -68 °C (middle trace, at 300 MHz), and r.t. with D_2O (bottom trace, at 400 MHz).

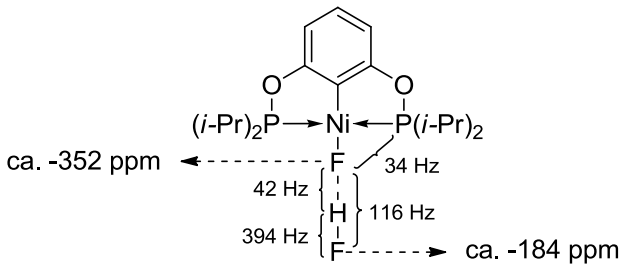

Figure 5.5 Chemical shifts and spin-spin coupling constants of (POCOP)NiF at -68 °C.

Formation of (POCOP)Ni(F---H-F) was also consistent with some distinct features seen in the ^{19}F NMR spectra of **2**. Thus, the room temperature spectrum showed a broad doublet at -184 ppm (J_{HF} = 394 Hz; FWHM ≈ 190 Hz) assigned to the terminal F in Ni-FH*F* (Figure 5.6, top trace). Suppression of the underlying exchange process at -68 °C sharpened this signal and allowed us to measure the F-F and H-F coupling constants (J_{FF} = 116 Hz). The Ni-*F* nucleus gives rise to a very broad signal (-350 to -370 ppm in CD_2Cl_2), which is barely distinguishable from the baseline at room temperature,[66] whereas at low temperature this signal appears as a broad multiplet. Indeed, the anticipated doublet of doublets of triplets appears as an overlapping doublet of quartets arising from one large coupling (J_{FF} ≈ 116 Hz) and the accidental equivalence of J_{FH} and J_{FP} coupling constants (≈ 36 Hz; see Supporting information).

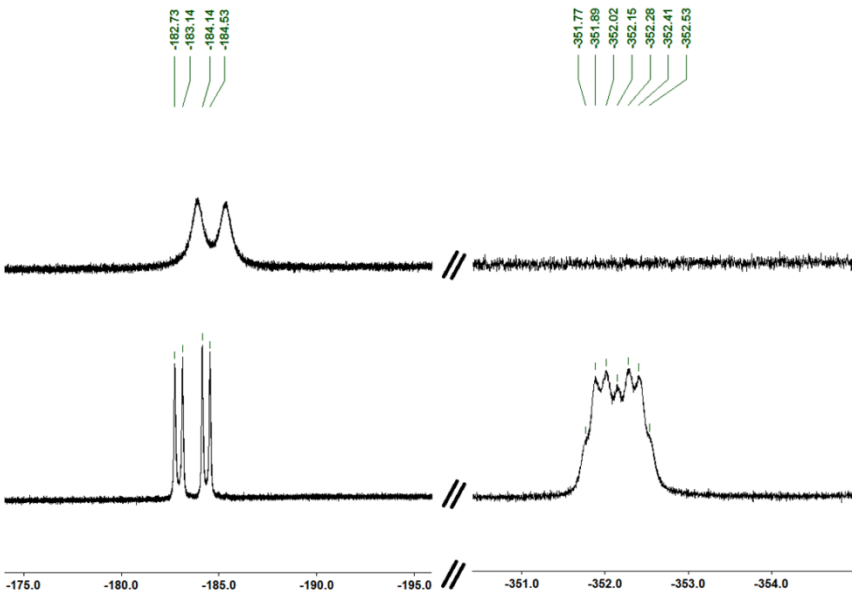

Figure 5.6 : ^{19}F NMR spectra (CD_2Cl_2; -174 to -196 ppm and -350 to -355 ppm) of complex **2** at r.t. (top trace) and -68 °C (bottom trace).

The ^{31}P NMR spectra of **2** were also in accord with the formation of (POCOP)Ni-F---H-F. Thus, the anticipated P-F coupling was absent in the room temperature spectrum (singlet at 178 ppm, Figure 5.7), whereas the -68 °C spectrum displayed a J_{PF} coupling of 34 Hz; curiously, there was not one but two doublets in this spectrum. We can rule out the possibility that these doublets represent two inequivalent phosphinite moieties arising from an off-axis orientation of the NiF---HF vector for the following reason: mutually trans, non-equivalent ^{31}P nuclei would be expected to show very large P-P couplings (> 300 Hz), which are not observed. A more plausible explanation is that the two ^{31}P doublets observed at -68 °C represent two symmetrical species detected in the slow exchange regime of the equilibrium (POCOP)NiF + HF ⇆ (POCOP)NiF(HF).

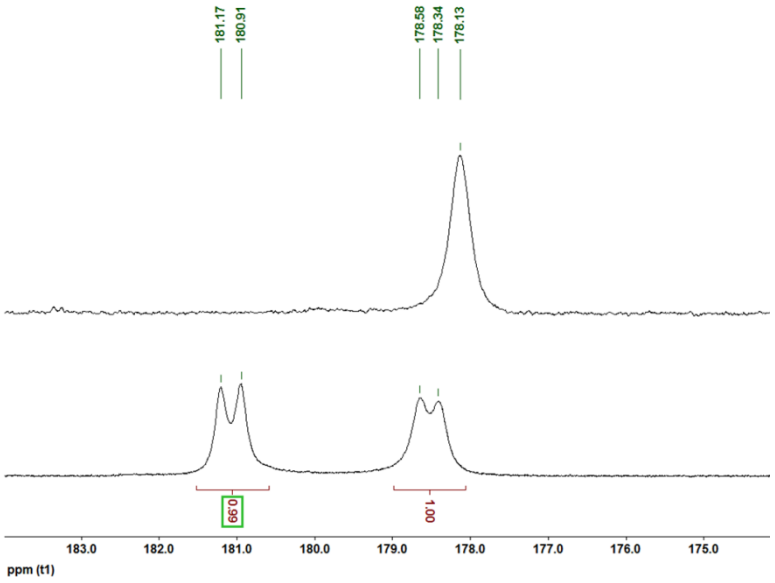

Figure 5.7 : ^{31}P NMR spectra (CD_2Cl_2) of complex **2** at r.t. (top trace) and -68°C (bottom trace).

Finally, we have studied the NMR spectra of complex **2** in the presence of NEt_3 to shed some light on the Ni-F---HF interaction. Addition of ca. 2 equiv of dry NEt_3 to a ca. 0.06 M solution of **2** in C_6D_6 (0.55 mL) changed the downfield region of the ^1H NMR spectrum as follows: the initially detected broad doublet detected at 11.19 ppm (FWHM ≈ 72 Hz, J_{H-F} ≈ 392 Hz) was replaced by a new singlet resonance at ca. 11.90 ppm (FWHM ≈ 220 Hz). The ^{19}F NMR spectrum of this sample showed the disappearance of the doublet due to HF (ca. -184 ppm) and the emergence of a better-defined broad resonance for Ni-*F* upfield of the original peak (ca. -380 ppm), whereas the ^{31}P NMR spectrum was essentially unchanged. These observations are consistent with the formation of $[HNEt_3]F$ and (POCOP)NiF.

To remove in situ generated HF, **2** is stirred on solution with CaH_2. After treatment expected NMR signals are observed : doublet in ^{31}P NMR at 175 ppm (J_{PF} = 33 Hz),

triplet in ^{19}F NMR (J_{FP} = 33 Hz) and virtual quadruplet for C_{ipso} in ^{13}C NMR at 118 ppm (21 Hz) (supporting information).

Crystallographic characterization of 2, 3a, and 3b.[67] X-ray diffraction analyses carried out on single crystals of **2**, **3a**, and **3b** showed that the Ni center in all three complexes adopts a square planar geometry characterized by the co-planar arrangement of the aromatic ring and the O atoms of the POCOP ligand as well as the significantly unequal (by ca. 13-16°) trans and cis angles (P-Ni-P < C-Ni-F; C-Ni-P < F-Ni-P). These angular distortions arise from the small bite angle of POCOP ligands and are observed commonly in (POCOP)NiX complexes. The small atomic radius of fluorine (0.5 Å)[68] results in a short Ni-F distance of ca. 1.83 Å in **2** (Figure 5.8), the shortest in the Ni-X series (X = Cl, Br, I),[41a] but the Ni-C and Ni-P distances in this complex are not influenced by this short Ni-F bond. Significantly, the solid state structure of **2** does not show any evidence of the presence of H-bonded HF, which was observed in the solution NMR spectra of this complex. For comparison, the Ni-F moiety in the closely related complex (PCP)Ni-F reported by Cámpora,[22] which is also free of the F---H-F interaction, has a similar bond length (1.84 Å), whereas a much longer Ni-F distance (1.90 Å) was reported for *trans*-[NiF(2-C_5NF_3H)(PEt_3)$_2$] which does show Ni-F--HF interaction in the solid state.[56c]

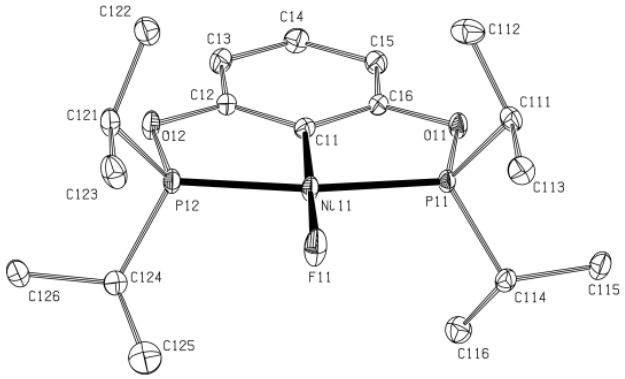

Figure 5.8. ORTEP diagram for complex **2**. Thermal ellipsoids are shown at the 30% probability level. Hydrogens are omitted for clarity. Selected bond distances (Å) and angles (°) for molecule 1: Ni11-C11= 1.875(2); Ni11-F11= 1.8346(14); Ni11-P11= 2.1615(6); Ni11-P12= 2.1572(6); C11-Ni11-F11= 179.88(10); P11-Ni11-P12= 164.69(3); C11-Ni11-P11= 82.45(7); C11-Ni11-P12= 82.34(7) F11-Ni11-P11= 97.49(5); F11-Ni11-P12= 97.72(5).

The most pertinent structural parameters in complexes **3** (Figure 5.9, Table 5.1) are the Ni-C10 bond distances of 1.93-1.94 Å, which are much shorter than the corresponding distance in (POCOP)Ni-CH_3 (1.99 Å);[41a] this observation is consistent with the anticipated greater strength of M-C bonds bearing charge-stabilizing electron-withdrawing substituents. On the other hand, a comparison of the Ni-C_{Ar} distances shows that they are nearly the same in **3** and the Ni-CH_3 analogue (1.90-1.91 Å) and shorter in the Ni-F analogue (1.88 Å), consistent with the relative trans influences of these ligands (CF_3 ~ CH_3 > F). That the Ni-P_{avg} bond distances are longer in **3** and **2** in comparison to the Ni-CH_3 analogue (ca. 2.16 vs. 2.13 Å) might be rationalized in terms of the HSAB concepts alluded to above (vide supra), CF_3 and F^- being "harder" and more polarizing than CH_3.

Curiously, the solid state structures of **3a** and **3b** do not show major differences, implying little or no structural effects resulting from the introduction of

the OMe group. In contrast, cyclic voltammetry measurements have indicated that the electrochemical potential for the one-electron oxidation of the Ni center in **3b** (831 mV, quasi-reversible) is significantly lower than that of **3a** (933 mV, irreversible), the difference being accounted for by the electron-releasing properties of the OMe substituent. The same phenomenon has been observed for the E_{ox} values of the corresponding bromo derivatives **1a** (810 mV) and **1b** (620 mV).[47c,69] It is also interesting to note that the Ni-CF_3 derivatives **3** are more difficult to oxidize than their corresponding bromo precursors.

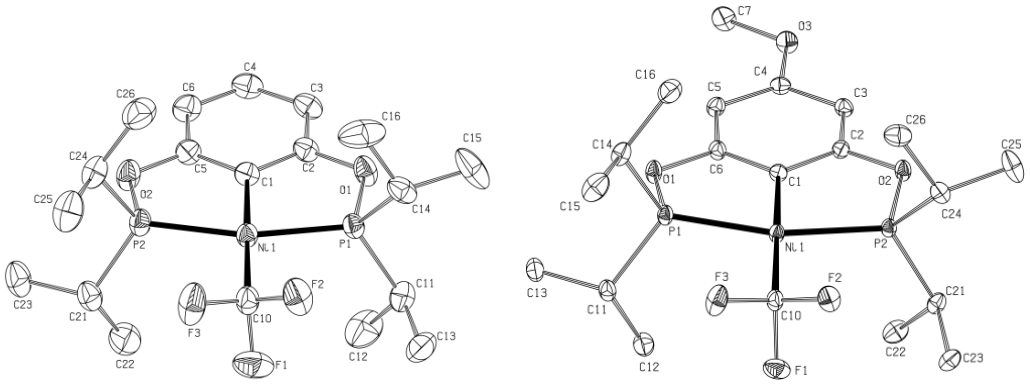

Figure 5.9 : ORTEP diagrams for **3a** (left) and **3b** (right) complexes. Thermal ellipsoids are shown at the 30% probability level. Hydrogens are omitted for clarity.

Table 5.1 : Selected bond distances (Å) and angles (°) of complexes **3a** and **3b**.

	3a	**3b**
Ni-C1	1.907(2)	1.903(2)
Ni-C10	1.928(2)	1.938(2)
Ni-P1	2.1536(5)	2.1571(5)
Ni-P2	2.1604(7)	2.1562(5)
C1-Ni-C10	177.52(9)	176.21(8)
P1-Ni-P2	163.69(2)	162.89(2)
C1-Ni1-P1	81.95(6)	81.58(6)
C1-Ni1-P2	81.83(6)	81.45(6)
C10-Ni1-P1	97.75(6)	98.64(6)
C10-Ni1-P2	98.52(6)	98.43(6)

Catalytic fluorination promoted by 2. Literature precedents on Ni-mediated fluorination reactions include electrocatalytic methodologies[70] and C-H fluorination in the presence of various sources of fluoro radicals.[71] In principle, another viable methodology for preparing fluoroorganics can involve halide exchange with haloalkanes, and such reactions should be facilitated by nickel-fluoro complexes if we assume enhanced nucleophilicity for the Ni-F moiety as a result of d_{π}-p_{π} repulsive interactions.[55] In practice, however, this approach does not seem to have been investigated extensively. Cámpora's group has reported that (PCP)NiF fluorinates dodecyl iodide into dodecyl fluoride in a stoichiometric fashion; this reaction can also be conducted in a catalytic fashion in the presence of excess AgF, but with only 2-3

catalytic turnovers.[22] Interestingly, substrate conversion is in fact more selective (in favor of halide substitution) but *slower* in the presence of (PCP)NiF, whereas the analogous Pd-F complex leads to much faster fluorination rates, better yields, and greater selectivity.[72] These literature precedents prompted us to test the reactivities of **2** to establish the effectiveness of the POCOP-Ni platform for fluorination of organyl halides.

Preliminary tests showed no reactivity with aryl halides, but benzyl halides did react with **2** to give the desired fluorinated products (Scheme 5.4). Table 2 lists the results of catalytic fluorination of $ArCH_2X$ (X= Cl, Br) conducted in dioxane at 90 °C for 48 h in the presence of **1a** (10%) and excess AgF. The crucial role of (POCOP)NiX in these reactions was established from control experiments that showed no fluorination in the absence of **1a**.[73] Another important variable is the quantity of AgF present in the reaction mixture: much higher yields are obtained with 5 equiv of AgF vs. 1.3 equiv (65% vs. 35%, entries 1 and 2), despite the limited solubility of AgF in this medium (dioxane). This finding indicates that in-situ regeneration of the Ni-F moiety is the rate limiting step of the fluorination reaction. That the fluorination under scrutiny is an S_N2-type substitution is consistent with the following observations: the catalytic fluorination is completely inhibited by residual moisture and is sensitive to nature of *para*-substituents (entries 1 vs. 3) and leaving groups (entries 1 vs. 4). Moreover, using **1b** as catalyst increases yield up to 50 % (entry 5). The same reaction under stirring condition lead to similar yields (56 % entry 6)) Analysis by ^{31}P NMR of the mixture at the end of the catalyst shows starting

catalysis **1a** (or **1b**) this proves that the catalyst does not undergo decomposition during catalysis.

Table 5.2 Fluorination of $ArCH_2X$ catalyzed by 10% (POCOP)NiBr and excess AgF

Entry	Catalyst	RX	AgF (equiv)	Yield[a]
1	**1a**	$PhCH_2Br$	1.3	35 %
2	**1a**		5.0	65%
3	**1a**	$4\text{-}NO_2\text{-}PhCH_2Br$	1.3	10 %
4	**1a**	$PhCH_2Cl$	1.3	15 %
5	**1b**	$PhCH_2Br$	1.3	50 %
6[$]	**1b**	$PhCH_2Br$	1.3	56 %

[a] Yields were calculated by integration of ^{19}F NMR signals for the products relative to an internal standard. [$] Stirred in a vial.

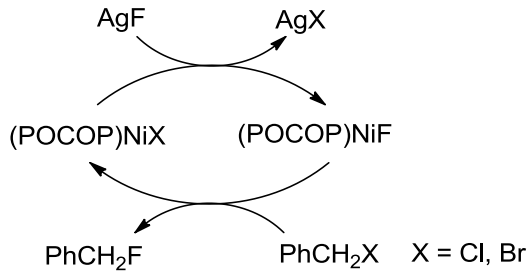

Scheme 5.4 Fluorination of benzyl halide promoted by **2**.

Stoichiometric reactivities of 3. Ni-catalyzed trifluoromethylation remains underdeveloped, presumably because the strong Ni-CF_3 bond presents an important barrier to transfer of the CF_3 moiety. Vicic has shown, for instance, that thermolysis of (dippe)Ni(CF_3)Ar gives the homocoupling products Ar-Ar and (dippe)Ni(CF_3)$_2$ instead of the desired Ar-CF_3 via reductive elimination.[74] Interestingly, the latter product does form in about 22% yield if (dippe)Ni(CF_3)Ar is heated in the presence of water.

Our initial tests of trifluoromethylation conducted under catalytic conditions (a 1:1:1 mixture of $PhCH_2Br$, CF_3SiMe_3, and AgF; 10% of **3**; dioxane; 90 °C; 18 h) gave instead $PhCH_2F$ as the major product. This observation implied that the *in-situ* generated fluoro intermediate promotes the fluorination reaction faster than it is converted to the CF_3 derivative; hence, we decided to examine the trifluoromethylation reaction in the presence of stoichiometric quantities of pre-formed **3**. Although no reactivity was evident between $PhCH_2Br$ and stoichiometric amounts of **3** in refluxing dioxane, we did observe reactivity in aromatic solvents. For instance, heating a C_6D_6 mixture of **3a** or **3b** and one equivalent of $PhCH_2Br$ at 79 °C over 18 h resulted in a color change from pale yellow to dark yellow, suggesting reactivity. Indeed, the ^{31}P NMR spectrum of the reaction mixture showed complete conversion of the Ni-CF_3 derivatives into the corresponding Ni-Br derivatives **1**. The ^1H NMR spectrum of the final mixture showed the appearance of an intense new singlet at 3.74 ppm, consistent with the formation of a new benzylic substance of formula $PhCH_2X$, but the absence of H-F coupling ruled out the formation of the anticipated organic product, $PhCH_2CF_3$. GC/MS analysis of the reaction mixture showed a new product with m/z = 173, consistent with the formation of $PhCH_2C_6D_5$. This product could be obtained reproducibly over several runs, but conversions varied (inexplicably) between 60 and 90%; these reactions also generated other, mostly volatile products that remain unidentified.

To confirm this unexpected benzylation of the reaction solvent, we repeated the reaction of **3** with $PhCH_2Br$ in toluene and toluene-d_8, *m*-xylene, and bromobenzene, and identified the corresponding products $PhCH_2$(tolyl) (m/z = 182),

$PhCH_2C_7D_7$ (m/z = 189), $PhCH_2$(xylyl) (m/z = 196), and $PhCH_2C_6H_4Br$ (m/z = 246) (Scheme 5.5).[75] The observed reactivity appeared to be limited to aromatic substrates/solvents, no reaction taking place in hexane or dioxane. Moreover, all benzylated products arose from mono-benzylation. To test whether the observed benzylation can proceed in a catalytic manner, we heated a C_6D_6 solution of $PhCH_2Br$ in the presence of 0.1 equiv of **3a**. The ^{31}P NMR spectra of this mixture showed complete conversion of **3a** to the Ni-Br derivative **1a**, and $PhCH_2C_6D_5$ was detected by GC/MS and ^1H NMR. Integration of the ^1H NMR spectrum revealed, however, that a majority of the substrate remained unreacted (ratio of $PhCH_2C_6D_5$:$PhCH_2Br$ ~1:13); therefore, the coupling appears to require stoichiometric quantities of **3a**. That the Ni-CF_3 moiety is also crucial for the coupling reaction was inferred from the observation that no coupling occurs when the Ni-Br precursors **1** are used instead of **3a**.

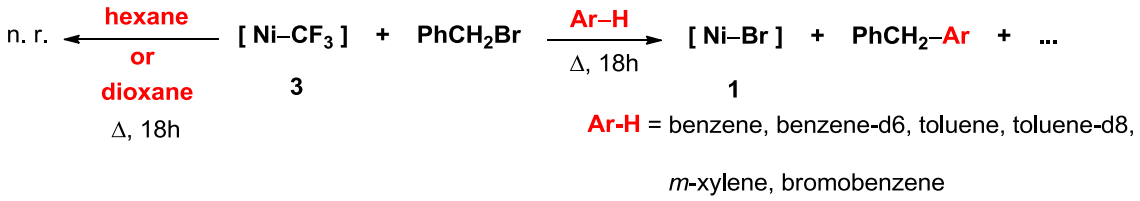

Scheme 5.5 Reactivity of **3** with benzyl bromide.

A number of tests have been conducted to gather mechanistic clues on the observed benzylation reaction. For instance, conducting the **3a**-promoted benzylation reaction in a 1:1 mixture of C_6H_6 and C_6D_6 allowed us to determine a net kinetic isotopic effect of 1.0, implying that the rate determination step does not involve C-

H/D cleavage. Another potentially significant finding was that the **3a**-promoted benzylation of C_6D_6 was completely suppressed when one equivalent of TEMPO was added to the reaction mixture or when $PhCH_2Br$ was replaced by $PhCH_2Cl$, bromobenzene, or chlorobenzene.[76] Finally, a test reaction in the presence of molecular sieves showed lower yields of $PhCH_2C_6D_5$ (ca. 20% vs. 60-90% under standard conditions), implying that residual moisture might be involved in the reaction mechanism. This finding was unexpected, because **3a** is fairly resistant to hydrolysis. Indeed, extended refluxing of a C_6D_6 mixture of **3a** containing 80 equiv of water showed that the starting material remained mostly intact (> 95% by ^{31}P NMR).

The above observations do not allow unambiguous mechanistic statements regarding the benzylation reactions observed in this study, but two different scenarios have been considered. First, a radical pathway might be implied by the inhibition of benzylation in the presence of TEMPO and the fact that the reaction works with benzyl halides but not aryl halides. Such a mechanism could be initiated by a single electron transfer (SET) from **3a** to $PhCH_2Br$ to generate a benzyl radical and a 17-electron trivalent complex such as (POCOP)Ni(CF_3)Br; the latter could undergo a unimolecular decomposition to the observed bromo derivative **1a**,[77] while the benzyl radical would generate the observed benzylation products via [$PhCH_2$-ArH]$^{\bullet}$. This scenario is conceptually analogous to SET-type mechanisms proposed for the coupling of haloarenes with unactivated arenes,[78,79,80,81] and is in line with general reactivities of pincer-Ni complexes.[82] On the other hand, a radical-based sequence of steps would be expected to generate the by-product bibenzyl, $(PhCH_2)_2$, none of which was detected in several benzylation reaction mixtures analyzed during our

studies.[83] Moreover, attempts at inducing the benzylation reaction at room temperature under irradiation for 3 h with a sun lamp (270 W) were unsuccessful,[84] confirming the importance of heating for reactivity.

A Friedel-Crafts benzylation type pathway initiated by in-situ generated HF is another distinct possibility,[85] and some of the observations presented above (and to be discussed below) are consistent with this scenario. On the other hand, the confirmed stability of the Ni-CF_3 moiety in **3a** towards hydrolysis and the absence of detectable quantities of HF in its solutions contradict this scenario. Even more importantly, a Friedel-Crafts pathway should be catalytic in nature and should proceed even if only a small quantity of HF is generated via partial hydrolysis of Ni-CF_3, whereas our experiments (vide supra) have shown clearly that the observed benzylation reaction requires stoichiometric quantities of **3a**.

It occurred to us that a Friedel-Crafts type benzylation would more likely occur in the presence of the fluoro derivative **2** that had been found to contain variable amounts of HF. Indeed, tests showed that refluxing a 10:13:1 mixture of $PhCH_2Br$, AgF, and the bromo precursor **1a** (instead of **3a**) in C_6D_6 gave the benzylated product $PhCH_2C_6D_5$, albeit in a much lower yield than obtained with **3a** (ca. 5-10%). Interestingly, this benzylation proceeds with similar yields in the presence of a slight excess of AgF only. This finding raises interesting questions about the mechanism of the benzylation reaction promoted by samples of **3a** which do not contain any AgF. The possible involvement of in-situ generated HF in the **3a**-promoted benzylation reaction cannot be ruled out, but such a scenario must be

scrutinized in light of the above-mentioned caveats regarding the requirement of a stoichiometric quantity of **3a** and the documented resistance of **3a** to hydrolysis.[49]

5.4 Conclusion

The results herein described describe the preparation, structures and reactivities of fluoro and trifluoromethyl derivatives of Ni(II) bearing a POCOP-type ligand. It was found that the exchange of bromide for fluoride required the use of AgF, other fluoride salts such as KF and CsF being completely ineffective for the synthesis of (POCOP)NiF. Similarly, the synthesis of (POCOP)NiCF_3 from the bromo precursor requires the use of AgF and CF_3SiMe_3; these reagents work in a stepwise manner, the Ni-F species forming from the bromo precursor and AgF and serving as an intermediate for the formation of the target Ni-CF_3 derivative upon treatment with CF_3SiMe_3. NMR spectroscopy helped reveal interesting structural features about these complexes, including the fact that the fluoro derivative forms an HF adduct from the interaction of the Ni-F moiety with HF, which is presumably generated in-situ from the hydrolysis of Ni-F moieties or residual Ag-F.

The reactivity of (POCOP)NiF toward $PhCH_2X$ was more or less as anticipated in that C-X bonds were displaced by the fluoride moiety, but the fairly sluggish rate of this reaction indicated that the nucelophilicity of the fluoride is not enhanced significantly as a result of the predicted d_π-p_π repulsions in (POCOP)NiF. An alternative explanation for the observed reactivity might be the hydrolytic instability of this complex. The Ni-CF_3 moiety in (POCOP)NiCF_3 showed an even

lower nucleophilicity toward $PhCH_2X$, which is consistent with the strength of the Ni-CF_3 bond. Instead, the Ni-CF_3 complex gave rise to an intriguing benzylation of arenes that appears to be stoichiometric. The various tests conducted in this study to elucidate the pathway(s) leading to the benzylated products have not provided definitive clues on the reaction mechanism. Future studies will be directed at obtaining more mechanistic information about this reaction.

5.5 Experimental section

General Procedures. Unless otherwise indicated, all manipulations were carried out under nitrogen using standard Schlenk and glove box techniques under a dry nitrogen atmosphere using solvents which were dried to water contents of less than 10-20 ppm (determined using a Mettler-Toledo C20 coulometric Karl Fischer titrator) by passing through activated aluminum oxide columns (MBraun SPS). All reagents were purchased from Aldrich and used without further purification. Published procedures were followed for synthesis of precursor complexes **1a**[44a] and **1b**[47c] see. The NMR spectra were recorded at 400 (^{1}H) and 161.9 MHz (^{31}P) using a Bruker AV400rg spectrometer, at 400 (^{1}H) and 100.56 MHz (^{13}C{^{1}H}) using a Bruker ARX400 spectrometer at 25°C. Chemical shift values are reported in ppm (δ) and referenced internally to the residual solvent signals (^{1}H and ^{13}C: 7.26 and 77.16 ppm for $CDCl_3$; 7.16 and 128.06 ppm for C_6D_6, 5.32 and 53.84 ppm for CD_2Cl_2) or externally (^{31}P, H_3PO_4 in D_2O, δ= 0). Coupling constants are reported in Hz. The elemental analyses were performed by the Laboratoire d'Analyse Élémentaire, Département de chimie, Université de Montréal.

The crystallographic data for compounds **3a** was collected on a Nonius FR591 generator (rotating anode) equipped with a Montel 200, a D8 goniometer, and a Bruker Smart 6000 area detector. The crystallographic data for compounds **2** and **3b** were collected on a Bruker APEX II equipped with a Incoatec I\muS Microsource and a Quazar MX monochromator. Cell refinement and data reduction were done using SAINT[86]. An empirical absorption correction, based on the multiple measurements of equivalent reflections, was applied using the program SADABS[87]. The space group was confirmed by XPREP routine[88] in the program SHELXTL[89]. The structures were solved by direct methods and refined by fullmatrix least-squares and difference Fourier techniques with SHELX-97[90]. All non-hydrogen atoms were refined with anisotropic displacement parameters. Hydrogen atoms were set in calculated positions and refined as riding atoms with a common thermal parameter. Complete details of the X-ray analyses reported herein have been deposited at *The Cambridge Crystallographic Data Centre* (CCDC 946259 (**2**), 946257 (**3a**), 946258 (**3b**). This data can be obtained free of charge via www.ccdc.cam.ac.uk/data_request/cif, or by emailing data_request@ccdc.cam.ac.uk, or by contacting The Cambridge Crystallographic Data Centre, 12, Union Road, Cambridge CB2 1EZ, UK; fax: +44 1223 336033.

{2,6-(*i*-Pr$_2$PO)$_2$-C$_6$H$_3$}NiF, **2.** A solution of **1a** (587 mg, 1.22 mmol) and AgF (777 mg, 6.13 mmol) was stirred overnight in THF (40 mL) at room temperature and in the dark. The final mixture was evaporated to dryness and the solid residues were extracted with hexane (50 mL) and filtered. CaH_2 power is added (21 mmol, 900 mg) and the solution is stirred for 30 min at room temperature. The solution is filtered and

evaporated to give a dark yellow powder (409 mg, 80%). Recrystallization from a saturated hexane solution cooled at -37 °C gave crystals suitable for X-ray diffraction studies. NMR ^{1}H (25°C, 400 MHz, C_6D_6): δ 1.25 (dt^{v}, J_{HH}= 7.2, $^{v}J_{HP}$= 7.0, 12H, CH_3), 1.39 (dt^{v}, J_{HH}= 8.9, $^{v}J_{H\text{-}P}$= 7.9, 12H, CH_3), 2.12 (dh, J_{HH}= 6.9, J_{PH}= 0.5, 4H, PCH(CH_3)$_2$), 6.50 (d, J_{HH}= 7.9, 2H, H_3 + H_5), 6.81 (t, J_{HH}= 7.9, 1H, H_4). NMR ^{13}C{^{1}H} (25°C, $CDCl_3$, 101 MHz): δ 16.79 (s, 4C, CH$_3$), 17.13 (vt, J_{CP} = 3.5, 4C, CH$_3$), 27.54 (vt, $^{v}J_{PC}$ = 10.1, 2C, PCH(CH_3)$_2$), 105.25 (vt, $^{v}J_{PC}$ = 5.8, 2C, C_{meta}), 118.45 (vq, J_{PC}= J_{PF} = 21.0, 1C, C_{ipso}), 128.32 (s, 1C, C_{para}), 169.44 (vt, $^{v}J_{PC}$= 10.1, 2C, C_{ortho}). NMR ^{31}P (162 MHz, 25°C, C_6D_6): δ 175.97 (d, J_{PF} = 33). NMR ^{19}F (179 MHz, 25°C, C_6D_6): δ – 377.5 (d, J_{FP} = 33), Anal. Calcd (found) for $C_{18}H_{31}FNiO_2P_2$: C, 51.59 (51.94); H, 7.46 (7.90). m.p. =105 °C.

{2,6-(*i*-Pr$_2$PO)$_2$-C$_6$H$_3$}NiCF$_3$, **3a**. To a solution of **1a** (0.5 g, 1.04 mmol) and AgF (0.4 g, 3.13 mmol) in THF (50 mL) was added Me_3SiCF_3 (1.56 mL, 3.13 mmol) and the mixture stirred in the dark at 45 °C overnight. The final mixture was evaporated, the solid residues extracted with hexane, filtered, and allowed to crystallized by slow evaporation under ambient atmosphere. Yellow crystals obtained from this step were redissolved in hexane and further purified by filtration through a plug of silica to give the product as an analytically pure solid (423 mg, 87%). NMR ^{1}H (25°C, 400 MHz, C_6D_6): δ 1.11 (dt^{v}, J_{HH}= 7.3, $^{v}J_{HP}$= 7.0, 12H, CH_3), 1.27 (dt^{v}, J_{HH}= 10.0, $^{v}J_{HP}$= 7.5, 12H, CH_3), 2.21 (dh, J_{HH}= 7.0, J_{PH}= 0.8, 4H, PCH(CH_3)$_2$), 6.66 (d, J_{HH} = 8.0, 2H, H_3 + H_5), 6.9 (t, J_{HH} = 7.6, 1H, H_4). NMR ^{13}C{^{1}H} (25°C, $(CD_3)_2CO$, 101 MHz): δ 17.25 (s, 4C, CH$_3$), 18.18 (s, 4C, CH$_3$), 29.51 (vt, $^{v}J_{PC}$= 12.0, 2C, PCH(CH_3)$_2$), 105.57 (vt, $^{v}J_{PC}$ = 6.0, 2C, C_{meta}), 131.10 (s, 1C; C_{para}), 133.35 (tq, J_{PC}= 20.3, J_{FC}=

11.4, 1C, C_{ipso}), 150.6 (qt, J_{PC}= 22.0, J_{FC}= 354.0, 1C, CF_3), 169.3 (*vt*, $^{v}J_{PC}$= 9.3, 2C, C_{ortho}). NMR ^{31}P (162 MHz, 25°C, C_6D_6): δ 196.9 (q, J_{PF} = 14.9). NMR ^{19}F (179 MHz, 25°C, C_6D_6): δ 6.4 (t, J_{FP} = 14.6), Anal. Calcd (found) for $C_{19}H_{31}F_3O_2NiP_2$: C, 48.65 (48.76); H, 6.62 (6.79). m.p. = 130 °C.

{2,6-(*i*-Pr$_2$PO)$_2$,(4-OCH$_3$)-C$_6$H$_2$}NiCF$_3$, **3b**. The procedure given above for the synthesis of **3a** was applied to furnish the desired product as yellow crystals (161 mg, 85%). NMR ^{1}H (25°C, 400 MHz, C_6D_6): δ 1.13 (dt^{v}, J_{HH}= 7.2, $^{v}J_{HP}$= 7.0, 12H, CH_3), 1.27 (dt^{v}, J_{HH}= 9.6, $^{v}J_{HP}$= 7.6, 12H, CH_3), 2.25 (dh, J_{HH}= 6.9, J_{PH}= 0.6, 4H, PCH(CH$_3$)$_2$), 3.26 (s, 3H, -OCH_3), 6.4 (s, 2H, H_3+ H_5). NMR ^{13}C{^{1}H} (25°C, ($CDCl_3$), 101 MHz): δ 16.8 (s, 4C, *C*H$_3$), 17.65 (s, 4C, *C*H$_3$), 28.68 (vt, $^{v}J_{PC}$= 11.7, 2C, P*C*H(CH$_3$)$_2$), 55.33 (s, 1C, O*C*H$_3$), 91.6 (vt, $^{v}J_{PC}$ = 6.3, 2C, C_{meta}), 123.0 (tq, J_{PC}= 21.6, J_{FC}= 11.7, 1C, C_{ipso}), 151.6 (qt, J_{PC}= 21.6, J_{FC}= 354.5, 1C, CF_3) , 162.56 (s, 1C; C_{para}OMe), 168.4 (vt, $^{v}J_{PC}$= 9.6, 2C, C_{ortho}). NMR ^{31}P (162 MHz, 25°C, C_6D_6): δ 198.25 (q, J_{PF} = 15.0). NMR ^{19}F (179 MHz, 25°C, C_6D_6): δ 6.06 (t, J_{FP} = 15.0). Anal. Calcd (found) for $C_{20}H_{33}F_3O_3NiP_2$: C, 48.14 (48.84); H, 6.62 (6.92). m.p. = 128 °C.

Kinetic monitoring of the conversion of 1a to 2 and 3a. A sealed NMR tube containing a THF mixture of **1a**, AgF, and CF_3SiMe_3 (molar ratio of ca. 1:5:2) was agitated for 5 min in an ultrasonic bath and analyzed by ^{31}P NMR over a day. The sample was agitated manually from time to time during the course of the experiment. The results are shown in Figure 5.1.

General procedure for Fluorination catalysis. A Teflon stopcock-equipped NMR tube was charged with a solution of **1a** (7 mg, 0.015 mmol), benzyl bromide (18 µL, 0.15 mmol) and 1,3-bis(trifluoromethyl)benzene (0.15 mmol 23 µL) in dioxane (0.5 mL), AgF (25 mg, 0.2 mmol). The tube is sealed and heated at 90 °C for 48 h, in the dark. Yields were determined by integration of the ^{19}F NMR signal of the product against that of 1,3-bis(trifluoromethyl)benzene, used as internal standard. Full characterization of $PhCH_2F$[91] and 4-nitrobenzylfluoride[92] have been reported.

General procedure for coupling of $PhCH_2Br$ with arenes in the presence of stoichiometric quantities of 3. A Teflon stopcock-equipped NMR tube was charged with a solution of **3a** (56 mg, 0.12 mmol) and benzyl bromide (14 µL, 0.12 mmol) in Ar-H/D as solvent (0.55 mL) and heated in an oil bath for 18h at 79 °C. The reaction mixture became dark yellow over time. The NMR tube was removed from the oil bath and allowed to cool to r.t. before opening the stopcock to allow the gaseous products to escape. The final reaction mixture was analyzed by NMR and GC-MS.

Cyclic Voltammetry Experiments. Cyclic voltammetry measurements were performed using a SP50 BioLogic Science Instrument potentiostat. A typical three-electrode system was used, consisting of a Graphite working electrode, a Pt auxiliary electrode, and a Ag/AgCl reference electrode ($E_{1/2}(FeCp_2 +/FeCp_2)$) = +0.47 V under these conditions). The experiments were carried out in dry CH_2Cl_2 at room temperature with TBAHFP as electrolyte (0.1 M), and the solutions were bubbled with nitrogen before each experiment.

5.6 Acknowledgments.

The authors are grateful to the following organizations and individuals: NSERC of Canada for a Discovery Grant to D.Z.; Université de Montréal, FQRNT of Québec, and Centre in Green Chemistry and Catalysis for graduate fellowships to B.V.; Dr. Michel Simard for his valuable assistance with crystallography; Mr. Cédric Malveau and Mr. Antoine Hamel for their valuable assistance with the recording of low temperature NMR spectra.

5.7 Supporting Information

Table 5.3 ^{31}P NMR chemical shifts of ($POC_{sp2}OP^{iPr}$)NiX complexes and Pauling electronegativity values for X

X	δ ^{31}P (ppm)	χ (Pauling)
F	178	3.98
Cl	185.5	3.16
Br	188.2	2.96
I	194.4	2.66

Table 5.4 ^{13}C NMR chemical shifts for C_{ipso} in ($POC_{sp2}OP^{iPr}$)NiX complexes.

X	δ C_{ipso} ^{13}C NMR (ppm)	Ref.
OTf	115.8	[93]
F	119.3	this work
Cl	125.2	[44a]
Br	127.9	[44a]
CN	132.0	[93]
I	132.5	[44a]
CF_3	133.3	this work
Et	139.7	[44a]
CH_3	139.8	[44a]

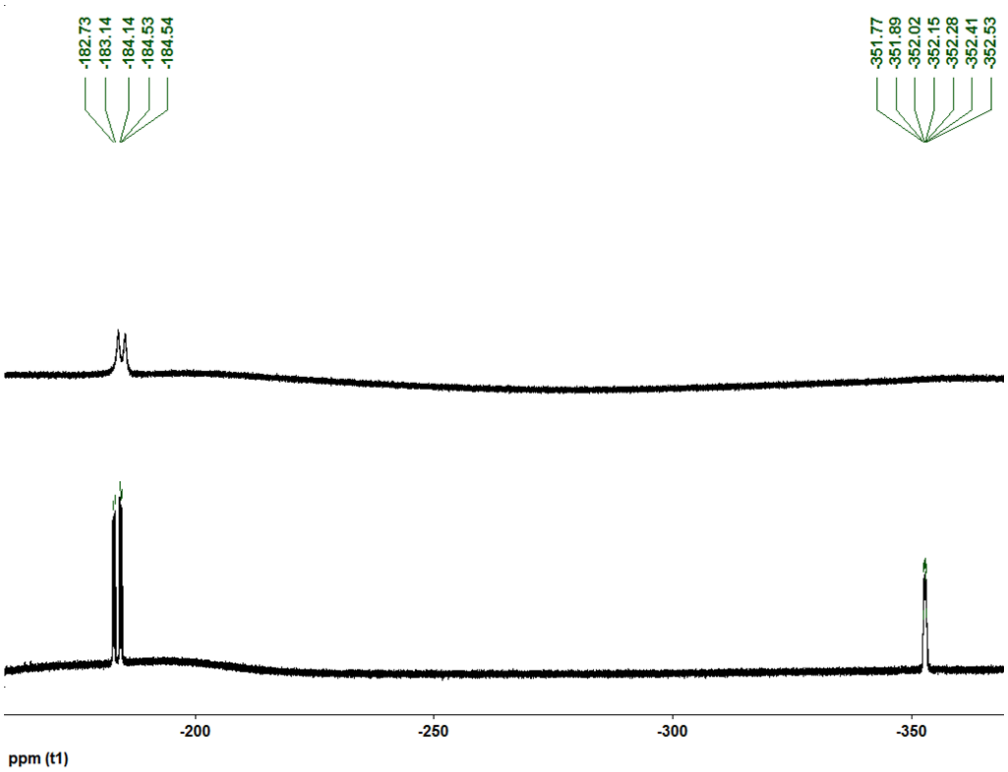

Figure 5.10 : ^{19}F NMR (280 MHz, CD_2Cl_2) spectra of complex **2** at r.t. (top) and at -68°C (bottom).

On the hydrolytic stability of ($POC_{sp2}OP^{iPr}$)NiF, 2. The Ni-F complex **2** and its HF adducts appear to be fairly stable to hydrolysis as deduced from the following observation: heating a ca. 0.1 mM C_6D_6 solution of **2**.HF containing 20-30 equivalents of water (ca. 20 μL) for two days at 80 °C showed no detectable decomposition based on ^{19}F and ^{31}P NMR spectra, shown below. (The top spectrum shows **2**.HF prior to addition of water; bottom spectrum after heating the sample for 2 days).

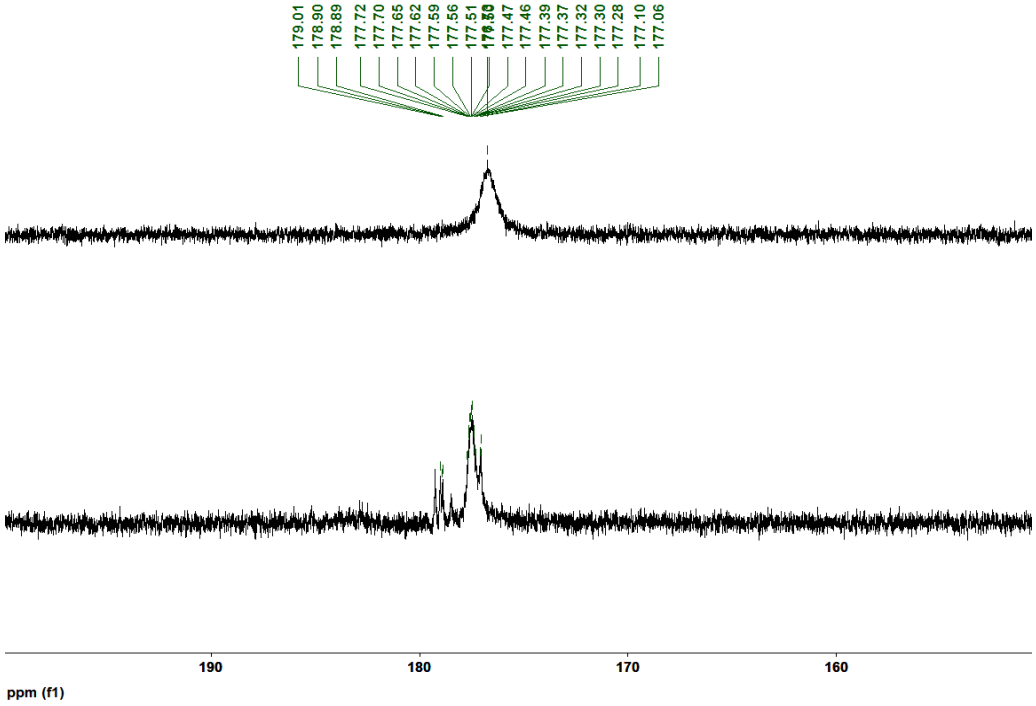

Figure 5.11: ^{31}P NMR spectra monitoring the hydrolytic stability of ($POC_{sp2}OP^{iPr}$)NiF, 2.

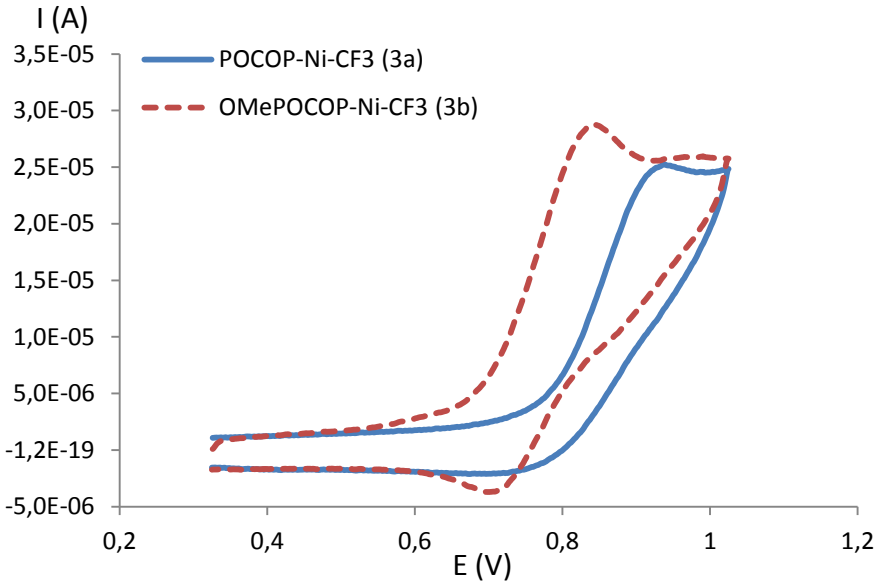

Figure 5.12. Cyclic voltammograms of ($POC_{sp2}OP^{i\text{-}Pr}$)$NiCF_3$, **3a**, and *p*-OMe($POC_{sp2}OP^{i\text{-}Pr}$)$NiCF_3$, **3b**, in CH_2Cl_2 (1 mM solutions) measured at 298 K with 0.1 M of tetrabutylammonium hexafluorophosphate as electrolyte (scan rate 100 mV. s^{-1}, *E*(V) vs Fc/Fc^+).

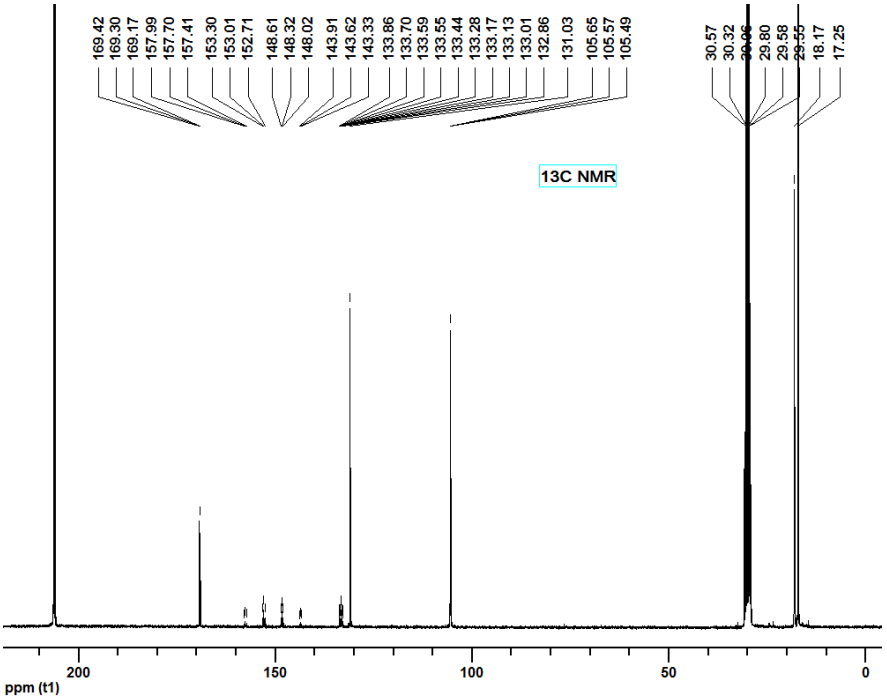

Figure 5.13 : $^{13}C\{^{1}H\}$ NMR (101 MHz) of complex **3a** in a highly concentrated $(CD_3)_2CO$ solution.

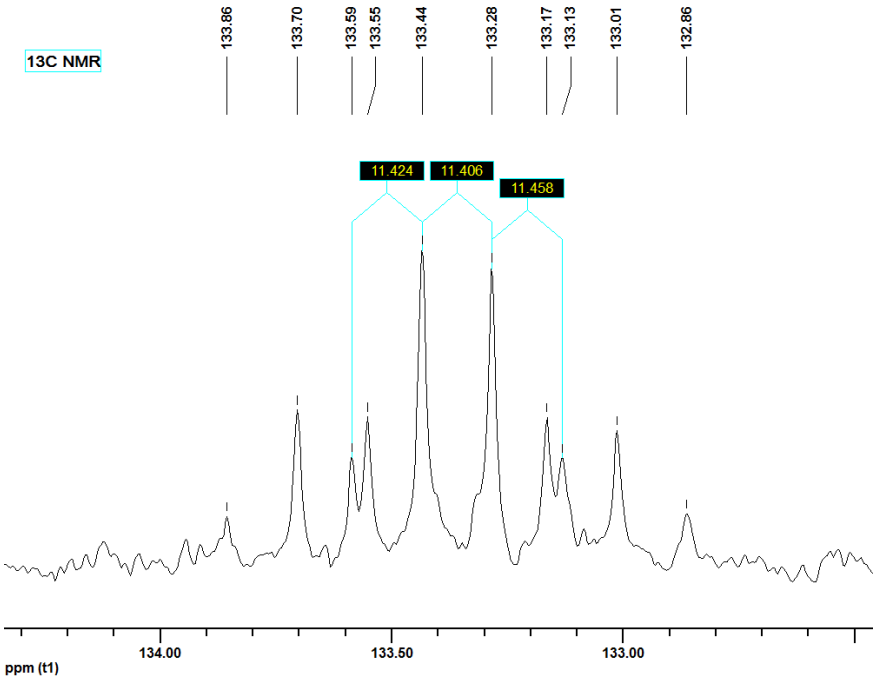

Figure 5.14 : $^{13}C\{^{1}H\}$ NMR (101 MHz) of C_{ispo} signal (triplet of quadruplets) in a highly concentrated $(CD_3)_2CO$ solution of complex **3a**.

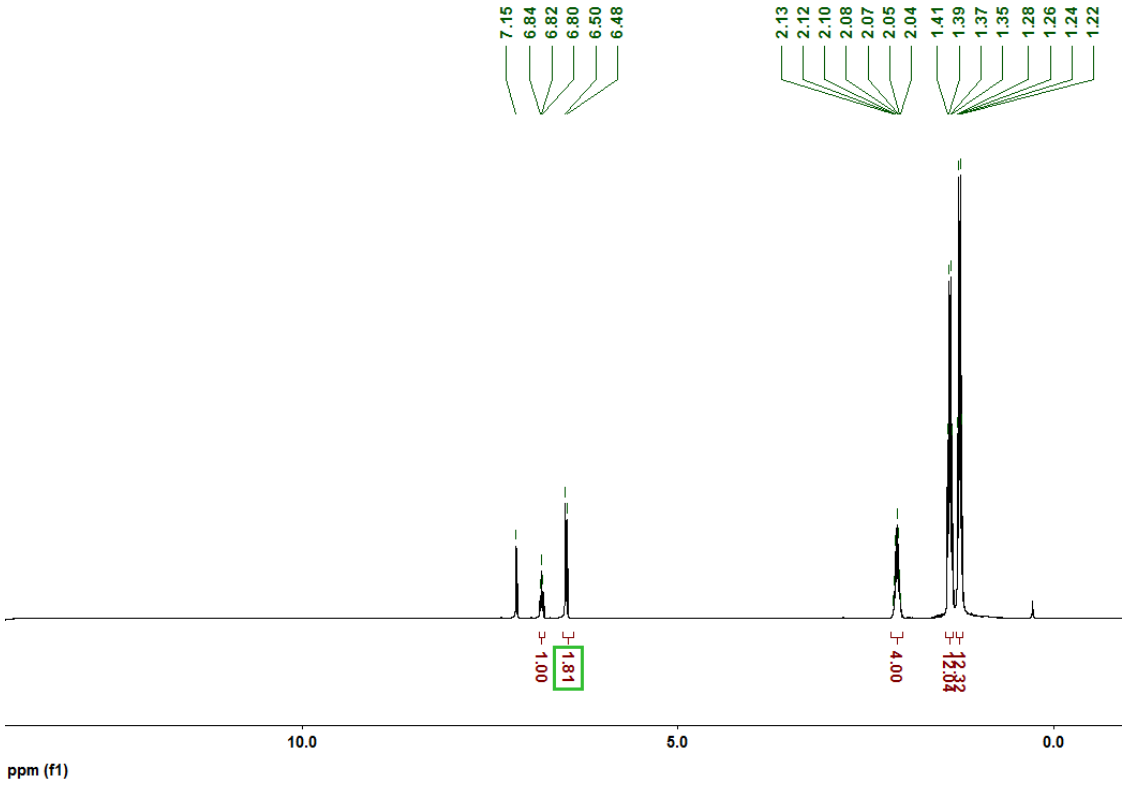

Figures 5.15 ^{1}H NMR (400 MHz, C_6D_6) spectra of complex **2**

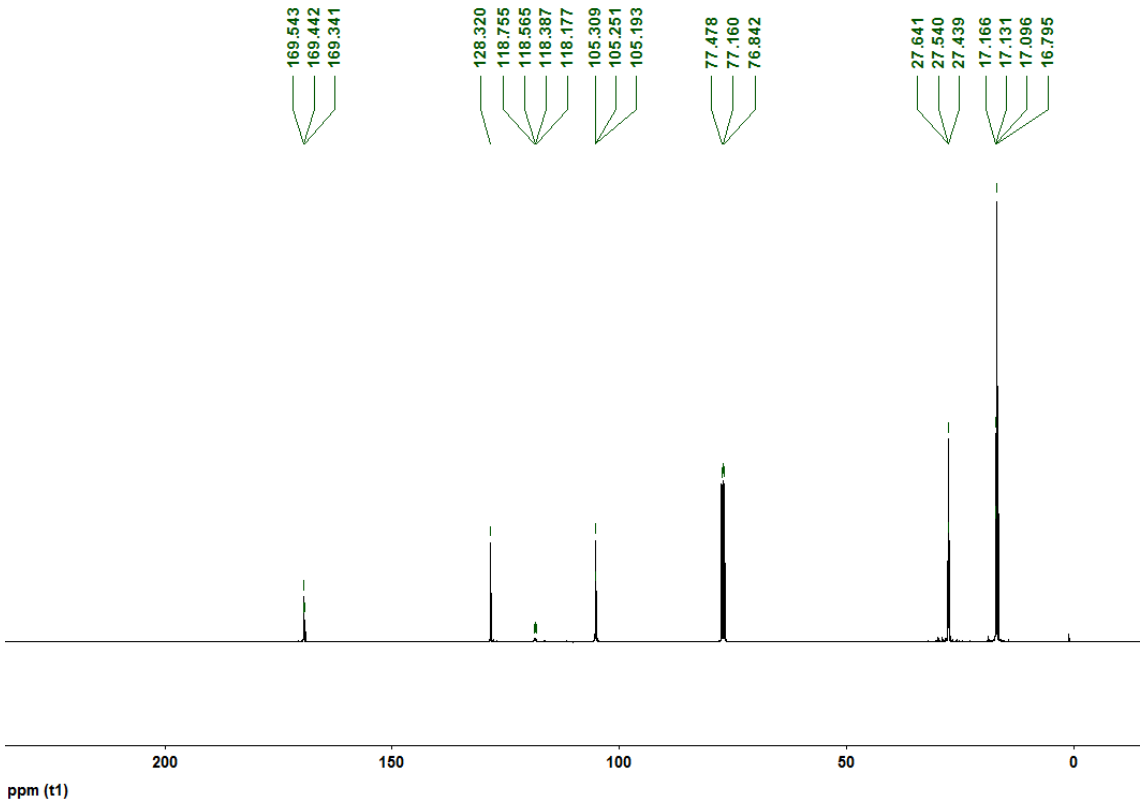

Figures 5.16 $^{13}C\{^{1}H\}$ NMR (101 MHz, $CDCl_3$) spectra of complex **2**.

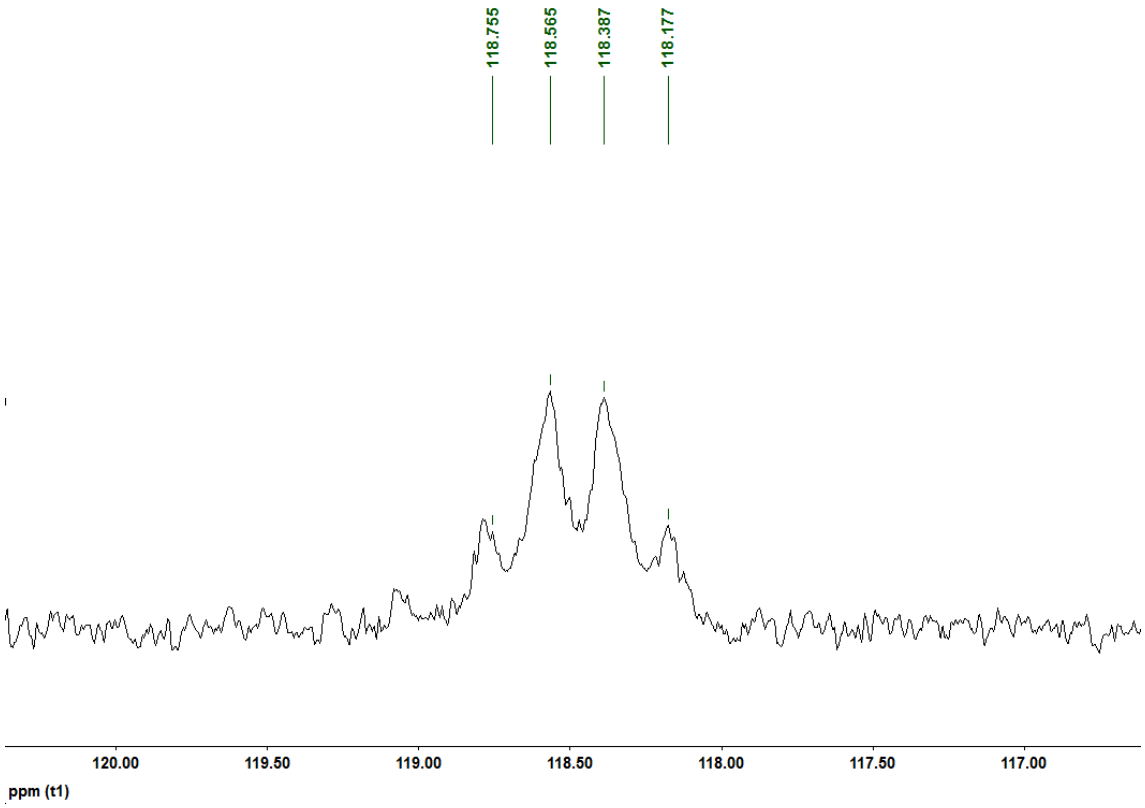

Figure 5.17 $^{13}C\{^{1}H\}$ NMR (101 MHz, $CDCl_3$) of C_{ispo} signal (virtual quadruplet) of complex **2**.

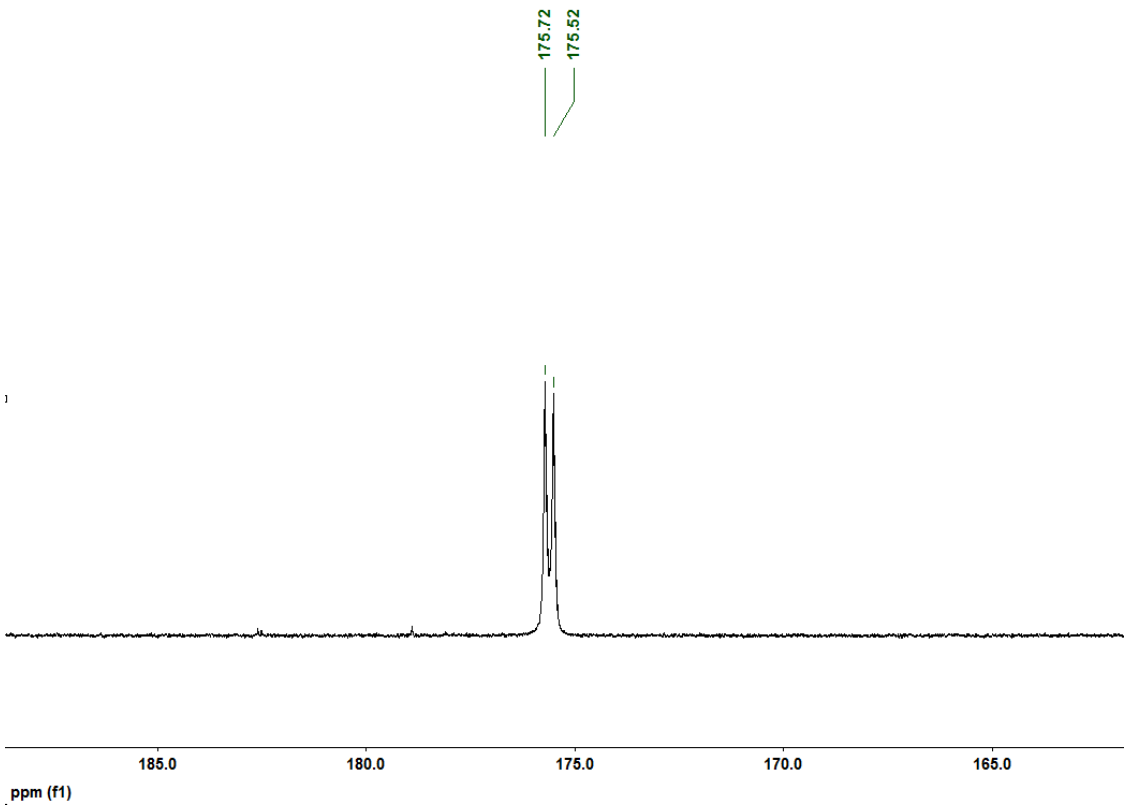

Figures 5.18 : ^{31}P NMR (162 MHz, C_6D_6) spectra of complex **2**

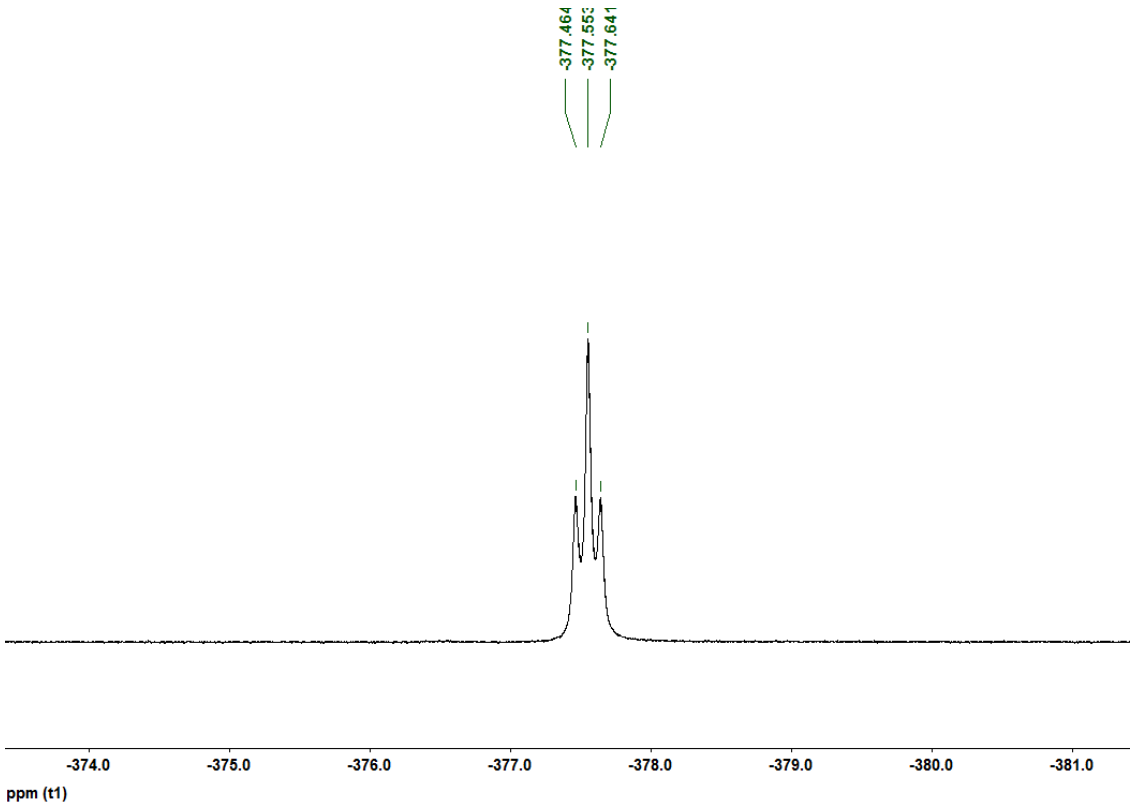

Figures 5.19 : ^{19}F NMR (179 MHz, C_6D_6) spectra of complex **2**

Table 5.5 : Crystal Data Collection and Refinement Parameters for Complexes: **3a**, **3b** and **2**

Compound	**3a**	**3b**	**2**
chemical formula	$C_{19}H_{31}F_3NiO_2P_2$	$C_{20}H_{33}F_3NiO_3P_2$	$C_{18}H_{31}FNiO_2P_2$
Fw	469.09	499.11	419.08
T (K)	200(2)	100(2)	100(2)
wavelength (Å)	1.54178	1.54178	1.54178
space group	P-1	P-1	P-1
a (Å)	8.27790(10)	8.1809(3)	7.74844(8)
b (Å)	10.5347(2)	10.7324(4)	14.85172(14)
c (Å)	13.2607(2)	13.5388(5)	18.48092(17)
β (deg)	81.8130(10)	84.1390(10)	105.4580(5)
α (deg)	81.4950(10)	88.8320(10)	90.0162(5)
γ (deg)	88.1600(10)	86.4580(10)	94.4874(5)
Z	2	2	4
V (Å^3)	1131.96(3)	1180.12(8)	2043.02(4)
ρcalcd (g cm^{-3})	1.376	1.405	1.362
μ (mm^{-1})	2.889	2.838	2.989
θ range (deg)	3.40 − 72.53	3.28 − 70.96	2.48 to 62.41
R_1[a] [I > 2ó(I)]	0.0497	0.0298	0.0345
wR_2[b] [I > 2ó(I)]	0.1254	0.0852	0.0957
R_1 [all data]	0.0503	0.0309	0.0377
wR_2 [all data]	0.1261	0.0858	0.0990
GOF	1.085	1.150	1.023

[a] $R_1=\Sigma(||Fo|-|Fc||)/\Sigma|Fo|$ [b] $wR_2=\{\Sigma[w(Fo^2-Fc^2)^2]/\Sigma[w(Fo^2)^2]\}^{1/2}$

5.8 References

[1] Jeschke, P. *ChemBioChem* **2004**, 5, 570.

[2] (a) D. Cartwright, in *Organofluorine Chemistry*, R. E. Banks, B. E. Smart, J. C. Tatlow, Eds. (Plenum, New York, 1994), pp. 237–262 (b) P. Kirsch, *Modern Fluoroorganic Chemistry* (Wiley-VCH, Weinheim, Germany, 2004) (c) Muller, K.; Faeh, C.; Diederich, F. *Science* **2007**, *317*, 1881.

[3] Patterson, J. C., II & Mosley, M. L. *Mol. Imaging Biol.* **2005**, *7*, 197.

[4] Hougham, G.; Cassidy, P. E.; Johns, K.; Davidson, T. *Fluoropolymers 1: Synthesis*; Springer US: Boston, MA, 2002.

[5] István T. Horváth *Fluorous chemistry*; Topics in current chemistry 308; Springer: Heidelberg ; New York, 2012.

[6] Middleton W. J. *J. Org. Chem.* **1975** *40,* 574.

[7] Hayashi, H.; Sonoda, H.; Fukumura, K.; Nagata, T. *Chem. Commun.* **2002,** *2002,* 1618.

[8] (a) Lal, G. S.*; Pez, G. P.; Pesaresi, R. J.; Prozonic, F. M.; Cheng, H. J. Org. Chem.* **1999***, 64,* 7048. *(b) Takaoka, A.; Iwakiri, H.; Ishikawa, N. Bull. Chem. Soc. Jpn* ***1979****, 52. 3377. (c)* Tang, P.; Wang, W.; Ritter, T. *J. Am. Chem. Soc.* **2011**, *133*, 11482..

[9] (a) For a recent review on monofluorination methodologies see: Landelle, G.; Bergeron, M.; Turcotte-Savard, M.-O.; Paquin, J.-F. *Chem. Soc. Rev.* **2011**, *40*, 2867. (b) For *N*-fluoropyridinium triflate and derivatives see: Umemoto, T.; Kawada, K.; Tomita, K. *Tetrahedron Lett.* **1986**, *24*, 4465.

[10] (a) Hudlicky, M. *Org. React.* **1988**, *35*, 513. (b) Singh, R. P.; Shreeve, J. M. *Synthesis* **2002**, 2561. (c Singh, R. P.; Meshri, D. T.; Shreeve, J. M. In Advances in Organic Synthesis: Modern Organofluorine Chemistry; Synthetic Aspects; Atta-Ur-Rahman, Laali, K. K., Eds.; Bentham Science Publishers Ltd.: Hilversum, The Netherlands, 2006; Vol. 2, pp 291-326.

[11] For recent reviews on this topic see : (a) Shibata, N.; Matsnev, A.; Cahard, D. *Beilstein J. Org. Chem.* **2010**, *6*, 65. (b) Dilman, A. D.; Levin, V. V. *Eur. J. Org. Chem.* **2011**, 831. (c) Ma, J.-A.; Cahard, D. *J. Fluorine Chem.* **2007**, *128*, 975. (d)

Prakash, G. K. S.; Yudin, A. K. *Chem. Rev.* **1997**, *97*, 757. (e) Wang, J.; Sánchez-Roselló, M.; Aceña, J. L.; del Pozo, C.; Sorochinsky, A. E.; Fustero, S.; Soloshonok, V. A.; Liu, H. *Chem. Rev.* **2014**, *214*, 2432.

[12] Joubert, J.; Roussel, S.; Christophe, C.; Billard, T.; Langlois, B. R.; Vidal, T*, Angew. Chem. Int. Ed.* **2003**, *42,* 3133.

[13] For recent review on fluorinations see: (a) Liang, T.; Neumann, C. N.; Ritter, T. *Angew. Chem. Int. Ed.* **2013**, *52*, 8214. (b) Grushin, V. V. *Acc. Chem. Res.* **2010**, *43*, 160

[14] For Cu-based methodologies see: (a) Subramanian, M. A. ; Manzer, L. E. A *Science* **2002**, *297*, 1665. (b) Fier, P. S.; Hartwig, J. F. *J. Am. Chem. Soc.* **2012**, *134*, 10795. (c) Truong, T.; Klimovica, K.; Daugulis, O. *J. Am. Chem. Soc.* **2013**, *135*, 9342. (d) Ye, Y.; Sanford, M. S. *J. Am. Chem. Soc.* **2013**, *135*, 4648. (e) Mu, X.; Zhang, H.; Chen, P.; Liu, G. *Chem. Sci.* **2014**, *5*, 275. (f) Fier, P. S.; Luo, J.; Hartwig, J. F. *J. Am. Chem. Soc.***2013**, *135*, 2552. (g) Zhang, Z.; Wang, F.; Mu, X.; Chen, P.; Liu, G. *Angew. Chem.Int. Ed.* **2013**, *52*, 7549

[15] For Ag-based methodologies see: (a) Fier, P. S.; Hartwig, J. F. *Science* **2013**, *342*, 956. (b) Wang, K.-P.; Yun, S. Y.; Mamidipalli, P.; Lee, D. *Chem. Sci.* **2013**, *4*, 3205. (c) Yin, F.; Wang, Z.; Li, Z.; Li, C. *J. Am. Chem. Soc.* **2012**, *134*, 10401. (d) Tang, P.; Furuya, T.; Ritter, T. *J. Am. Chem. Soc.* **2010**, *132*, 12150.

[16] For Rh-based methodologies see: (a) Zhu, J.; Tsui, G. C.; Lautens, M. *Angew. Chem. Int. Ed.* **2012**, *51*, 12353. (b) Evans, P. A.; Uraguchi, D. *J. Am. Chem. Soc.* **2003**, *125*, 715.

[17] (a) For an Ir-based methodolgoy see: Topczewski, J. J.; Tewson, T. J.; Nguyen, H. M. *J. Am. Chem. Soc.* **2011**, *133*, 19318. (b) For a Pd-based methodology see: Watson, D. A.; Su, M.; Teverovskiy, G.; Zhang, Y.; García-Fortanet, J.; Kinzel, T.; Buchwald, S. L. *Science* **2009**, *325*, 1661.

[18] Levin, V. V.; Zemtsov, A. A.; Struchkova, M. I.; Dilman, A. D. *Org. Lett.* **2013**, *15*, 917.

[19] For recent reviews see: (a) Studer, A. *Angew. Chem., Int. Ed.* **2012**, *51*, 8950. (b) Furuya, T.; Kamlet, A. S.; Ritter, T. *Nature* **2011**, *473*, 470. (c) Tomashenko, O. A.; Grushin, V. V. *Chem. Rev.* **2011**, *111*, 4475. (d) Liu, T.; Shen, Q. *Eur. J. Org. Chem.* **2012**, 6679.

[20] Huacuja, R.; Herbert, D. E.; Fafard, C. M.; Ozerov, O. V. *J. Fluorine Chem.* **2010**, *131*, 1257.

[21] Ball, N. D.; Kampf, J. W.; Sanford, M. S. *Dalton Trans.* **2010**, *39*, 632.

[22] Martínez-Prieto, L. M.; Melero, C.; del Río, D.; Palma, P.; Cámpora, J.; Álvarez, E. *Organometallics* **2012**, *31*, 1425.

[23] Andrew, R. E.; Chaplin, A. B. *Dalton Trans.* **2014**, *43*, 1413.

[24] (a) Lundgren, R. J.; Stradiotto, M. *Angew. Chem. Int. Ed.* **2010**, *49*, 9322 (b) , N. D.; Kampf, J. W.; Sanford, M. S. *J. Am. Chem. Soc.* **2010**, *132*, 2878 (c) Kitazume, T.; Ishikawa, N. *Chem. Lett.* **1982**, 137 (d) Wang, X.; Truesdale, L.; Yu, J.-Q. *J. Am. Chem. Soc.* **2010**, *132*, 3648 (e) Zhang, L.-S.; Chen, K.; Chen, G.; Li, B.-J.; Luo, S.; Guo, Q.-Y.; Wei, J.-B.; Shi, Z.-J. *Org. Lett.* **2013**, *15*, 10 (f) Grushin, V. V.; Marshall, W. J. *J. Am. Chem. Soc.* **2006**, *128*, 4632 (g) Grushin, V. V.; Marshall, W. *J. Am. Chem. Soc.* **2006**, *128*, 12644 (h) Cho, E. J.; Senecal, T. D.; Kinzel, T.; Zhang, Y.;

Watson, D. A.; Buchwald, S. L. *Science* **2010**, *328*, 1679 (i) Mu, X.; Chen, S.; Zhen, X.; Liu, G. *Chem. Eur. J.* **2011**, *17*, 6039 (j) Samant, B. S.; Kabalka, G. W. *Chem. Commun.* **2011**, *47*, 7236 (k) Cho, E. J.; Buchwald, S. L. *Organic Letters* **2011**, *13*, 6552 (l) Mu, X.; Wu, T.; Wang, H.; Guo, Y.; Liu, G. *J. Am. Chem. Soc.* **2012**, *134*, 878 (m) Zhang, X.-G.; Dai, H.-X.; Wasa, M.; Yu, J.-Q. *J. Am. Chem. Soc.* **2012**, *134*, 11948 (n) Ye, Y.; Ball, N. D.; Kampf, J. W.; Sanford, M. S. *J. Am. Chem. Soc.* **2010**, *132*, 14682 (o) Takemoto, S.; Grushin, V. V. *J. Am. Chem. Soc.* **2013**, *135*, 16837

[25] For a report describing the use of "thermodynamically unstable" Ni-fluorides in fluorination reactions see: Bartlett, N.; Chambers, R. D.; Roche, A. J.; Spink, R. C. H.; Chacon, L.; Whalen, J. M. *Chem. Commun.* **1996**, 1049.

[26] (a) Shibata, N.; Ishimaru, T.; Nagai, T.; Kohno, J.; Toru, T. *Synlett* **2004**, 1703. (b) Shibata, N.; Kohno, J.; Takai, K.; Ishimaru, T.; Nakamura, S.; Toru, T.; Kanemasa, S. *Angew. Chem. Int. Ed.* **2005**, *44*, 4204. (c) Shibatomi, K.; Tsuzuki, Y.; Iwasa, S. *Chem. Lett.* **2008**, *37*, 1098. (d) Paull, D. H.; Scerba, M. T.; Alden-Danforth, E.; Widger, L. R.; Lectka, T. *J. Am. Chem. Soc.* **2008**, *130*, 17260.

[27] As a typical example, see the following recent report Perutz' group and the references therein: T. Beweries, L. Brammer, N. A. Jasim, J. E. McGrady, R. N. Perutz, A. C. Whitwood, *J. Am. Chem. Soc.* **2011**, *133*, 14338.

[28] Lee, E.; Hooker, J. M.; Ritter, T. *J. Am. Chem. Soc.* **2012**, *134*, 17456.

[29] See the following reports on $(MeCN)_2Ni(CF_3)_2$ and (dippe)Ni(CF_3)Ar and references therein: (a) Zhang, C.-P.; Wang, H.; Klein, A.; Biewer, C.; Stirnat, K.; Yamaguchi, Y.; Xu, L.; Gomez-Benitez, V.; Vicic, D. A. *J. Am. Chem. Soc.* **2013**,

135, 8141. (b) Dubinina, G. G.; Brennessel, W. W.; Miller, J. L.; Vicic, D. A. *Organometallics* **2008**, *27*, 3933.

[30] Rossin A., Peruzzini M., Zanobini F., *Dalton Trans.* **2011,** *40,* 4447.

[31] (a) Kieltsch, I.; Dubinina, G. G.; Hamacher, C.; Kaiser, A.; Torres-Nieto, J.; Hutchison, J. M.; Klein, A.; Budnikova, Y.; Vicic, D. A. *Organometallics* **2010**, *29*, 1451. (b) Madhira, V. N.; Ren, P.; Vechorkin, O.; Hu, X.; Vicic, D. A. *Dalton Trans.* **2012**, *41*, 7915. (c) Klein, A.; Vicic, D. A.; Biewer, C.; Kieltsch, I.; Stirnat, K.; Hamacher, C. *Organometallics* **2012**, *31*, 5334.

[32] Chakraborty, S.; Patel, Y. J.; Krause, J. A.; Guan, H. *Angew. Chem. Int. Ed.* **2013**, *52*, 7523.

[33] Chakraborty S., Krause J. A., Guan H., **2009**, *Organometallics*, *28*, 582.

[34] (a) Chakraborty, S.; Zhang, J.; Patel, Y. J.; Krause, J. A.; Guan, H. *Inorg. Chem.* **2013**, *52*, 37 (b) Chakraborty, S.; Patel, Y. J.; Krause, J. A.; Guan, H. *Polyhedron* **2012**, *32*, 30 (c) Suh, H.-W.; Schmeier, T. J.; Hazari, N.; Kemp, R. A.; Takase, M. K. *Organometallics* **2012**, *31*, 8225 (d) Chakraborty, S.; Zhang, J.; Krause, J. A.; Guan, H. *J. Am. Chem. Soc.* **2010**, *132*, 8872.

[35] (a) Liang, L.-C.; Lee, W.-Y.; Hung, Y.-T.; Hsiao, Y.-C.; Cheng, L.-C.; Chen, W.-C. *Dalton Trans.* **2012**, *41*, 1381 (b) Wang, Z.-X.; Liu, N. *Eur. J. Inorg. Chem.* **2012**, *2012*, 901.

[36] Estudiante-Negrete, F.; Hernández-Ortega, S.; Morales-Morales, D. *Inorg. Chim. Acta* **2012**, *387*, 58

[37] Mitsudo, K.; Imura, T.; Yamaguchi, T.; Tanaka, H. *Tetrahedron Lett.* **2008**, *49*, 7287.

[38] Chen, T.; Yang, L.; Li, L.; Huang, K.-W. *Tetrahedron* **2012**, *68*, 6152.

[39] Luca, O. R.; Blakemore, J. D.; Konezny, S. J.; Praetorius, J. M.; Schmeier, T. J.; Hunsinger, G. B.; Batista, V. S.; Brudvig, G. W.; Hazari, N.; Crabtree, R. H. *Inorg. Chem.* **2012**, *51*, 8704.

[40] Hurtado, J.; Ibañez, A.; Rojas, R.; Valderrama, M.; Fröhlich, R. *J. Braz. Chem. Soc.* **2011**, *22*, 1750.

[41] (a) V. Pandarus and D. Zargarian, *Organometallics*, **2007**, *26*, 4321 (b) X. Lefèvre, G. Durieux, S. Lesturgez and D. Zargarian, *J. Mol. Catal. A.*, **2010**, 335(1–2), 1–7 (c) Salah A., Offenstein C., Zargarian D., **2011**, *Organometallics 30*, 5352. (d) Castonguay, A.; Spasyuk, D. M.; Madern, N.; Beauchamp, A. L.; Zargarian, D. *Organometallics* **2009**, *28*, 2134.

[42] Spasyuk, D. M.; Zargarian, D.; *Inorg. Chem.*, **2010**, *49*, 6203.

[43] Fossey, J. S.; Richards, C. J. *J. Organomet. Chem.* **2004**, *689*, 3056.

[44] (a) Pandarus, V.; Zargarian, D. *Chem. Commun.* **2007**, 978. (b) Van de Kuil, L. A.; Grove, D. M.; Gossage, R. A.; Zwikker, J. W.; Jenneskens, L. W.; Drenth, W.; van Koten, G. *Organometallics* **1997**, *16*, 4985 (c) Gossage, R. A.; van de Kuil, L. A.; van Koten, G. *Acc. Chem. Res.* **1998**, *31*, 423.

[45] (a) Zargarian, D.; Castonguay, A.; Spasyuk, D. M. in "ECE-Type Pincer Complexes of Nicekl" in Organometallic Pincer Chemistry, ed. G. van Koten and D. Milstein, Top. Organomet. Chem. (2013) 40: 131–174; Springer-Verlag Berlin Heidelberg 2013; DOI: 10.1007/978-3-642-31081-2_5. (b) The chemistry of pincer

compounds; Morales-Morales, D.; Jensen, C, 1st ed.; Elsevier: Amsterdam ; Boston, 2007, ISBN 0444531386.

[46] The direct nickelation of POC(H)OP ligands is thought to proceed via an electrophilic substitution type mechanism: Vabre, B.; Lambert, M. L.; Petit, A.; Ess, D. H.; Zargarian, D. *Organometallics* **2012**, *31*, 6041.

[47] (a) Gómez-Benítez, V.; Baldovino-Pantaleón, O.; Herrera-Álvarez, C.; Toscano, R. A.; Morales-Morales, D. *Tet. Lett.* **2006**, *47*, 5059 (b) Salah, A. B.; Zargarian, D. *Dalton Trans.* **2011**, *40*, 8977 (c) Vabre, B.; Spasyuk, D. M.; Zargarian, D. *Organometallics* **2012**, *31*, 8561.

[48] Vabre, B.; Lindeperg, F.; Zargarian, D. *Green Chem.*, **2013**, *15*, 3188.

[49] Although we are not aware of any precedent for the hydrolysis of a Ni-CF_3 moiety, there are many precedents for the hydrolytic instability of other M-CF_3 complexes. In some cases, such decomposition proceeds via α-elimination to F-M=CF_2 followed by hydrolysis to generate 2 HF and [M-CO][F]. (See the report by Caulton cited in ref. [51] and the following reviews: (a) Brothers, P. J.; Roper, W. R. *Chem. Rev.* **1988**, *88*, 1293. (c) Doherty, N. M.; Hoffman, N. W. *Chem. Rev.* **1991**, *91*, 553. (b) Morrison, J. A. *Adv. Organomet. Chem.* **1993**, *35*, 211. (d) Hughes, R. *Eur. J. Inorg. Chem.* **2009**, 4591.)

[50] For reports on the generation of $Ag^{I}[Ag^{III}(CF_3)_4]$, $Ag^{I}[Ag^{I}(CF_3)_2]$ and similar species from mixtures of AgF and CF_3SiMe_3 in RCN, DMF, pyridine, or *N*-methylimidazole see : (a) Tyrra, W.; Naumann, D. *J. Fluorine Chem.* **2004**, *125*, 823 (b) Tyrra, W. *J. Fluorine Chem.* **2001**, *112*, 149 (c) Tyrra, W. *Heteroat. Chem.* **2002**, *13*, 561.

[51] For one of the earliest reports on the use of CF_3SiMe_3 for preparation of transition metal derivatives see: Huang, D.; Caulton, K. G. *J. Am. Chem. Soc.* **1997**, *119*, 3185-3186. It should be noted that the Ru-CF_3 presented in this reported is prepared from the reaction of a Ru-F precursor with CF_3SiMe_3 in the presence of CsF.

[52] Spectra shown in Supporting Information.

[53] (a) Morales-Morales, D.; Grause, C.; Kasaoka, K.; Redón, R.; Cramer, R. E.; Jensen, C. M. *Inorganica Chimica Acta* **2000**, *300-302*, 958–963. (b) Wang, Z.; Eberhard, M. R.; Jensen, C. M.; Matsukawa, S.; Yamamoto, Y. *J. Organomet. Chem.* **2003**, *681*, 189.

[54] Chemical Hardness. R. G. Pearson Copyright© 1997 WILEY-VCH Verlag GmbH, Weinheim ISBN: 3-527-29482-1.

[55] Caulton, K. G. *New J. Chem.* **1994**, *18*, 25.

[56] (a) Braun, T.; Perutz, R. N. *Chem. Commun.* **2002**, 2749 (b) Archibald, S. J.; Braun, T.; Gaunt, J. A.; Hobson, J. E.; Perutz, R. N. *J. Chem. Soc., Dalton Trans.* **2000**, 2013 (c) Braun, T.; Foxon, S. P.; Perutz, R. N.; Walton, P. H. *Angew. Chem. Int. Ed.* **1999**, *38*, 3326.

[57] (a) Roe, D. C.; Marshall, W. J.; Davidson, F.; Soper, P. D.; Grushin, V. V. *Organometallics* **2000**, *19*, 4575 (b) Pilon, M. C.; Grushin, V. V. *Organometallics* **1998**, *17*, 1774.

[58]Jasim, N. A.; Perutz, R. N. *J. Am. Chem. Soc.* **2000**, *122*, 8685.

[59] Gil-Rubio, J.; Weberndörfer, B.; Werner, H. *J. Chem. Soc., Dalton Trans.* **1999**, 1437.

[60] (a) Jasim, N. A.; Perutz, R. N.; Foxon, S. P.; Walton, P. H. *J. Chem. Soc., Dalton Trans.* **2001**, 1676 (b) Whittlesey, M. K.; Perutz, R. N.; Greener, B.; Moore, M. H. *Chem. Commun.* **1997**, 187.

[61] Roesky, H. W.; Sotoodeh, M.; Xu, Y. M.; Schrumpf, F.; Noltemeyer, M. *Z. Anorg. Allg. Chem.* **1990**, *580*, 131.

[62] Murphy, V. J.; Hascall, T.; Chen, J. Y.; Parkin, G. *J. Am. Chem. Soc.* **1996**, *118*, 7428.

[63] Murphy, V. J.; Rabinovich, D.; Hascall, T.; Klooster, W. T.; Koetzle, T. F.; Parkin, G. *J. Am. Chem. Soc.* **1998**, *120*, 4372.

[64] Martin, J. S.; Fujiwara, F. Y. *J. Am. Chem. Soc.* **1974**, *96*, 7632.

[65] As mentioned earlier, the Ni-F complex **2** and its HF adduct appear to be only moderately sensitive to hydrolysis, as deduced from ^{31}P NMR spectra of solutions containing excess water. See Supporting Information.

[66] It should be noted that the broadness of this peak can vary greatly as a function of the solvent and its residual moisture content. In dry C_6D_6, for instance, the peak appears much narrower.

[67] Measurements conducted using a crystal of POCOP-Ni-F that contained crystallization solvent have yielded a structure that is somewhat different than the one discussed in this report. For details on this structure see: B. Mougang-Soume, P. Petiot, D. Zargarian, Private communication to the Cambridge Structural Database, 2013, deposition number CCDC 948456.

[68] Slater, J. C. *J. Chem. Phys.* **1964**, *41*, 3199.

[69] All E_{ox} potentials are referenced with respect to the Cp_2Fe/Cp_2Fe^+ couple measured under the same conditions as the complexes under study. See Supporting Information for the voltammograms.

[70] Drakesmith, F. G.; Hughes, D. A. *J. Fluorine Chem.* **1986**, *32*, 103.

[71] Suzuki, T.; Hamashima, Y.; Sodeoka, M. *Angew. Chemie Int. Ed.* **2007**, *46*, 5435.

[72] Recent studies have also shown that Pd-F complexes promote allylic fluorination reactions. For representative examples see the following report and the references cited therein: Katcher, M. H.; Sha, A.; Doyle, A. G. *J. Am. Chem. Sco.* **2011**, *133*, 15902.

[73] According to Cámpora's report (ref. [22]), AgF does react with dodecyl iodide *in the absence of* Ni-F or Pd-F to generate a variety of products, including dodecyl alcohol and various olefins. Other groups have also reported non-catalyzed, AgF-induced halide exchange in iodoalkanes and gem-disubstituted chlorides/bromides: (a) Wei, Z.-L.; Xiao, Y.; Yuan, H.; Baydyuk, M.; Petukhov, P. A.; Musachio, J. A.; Kellar, K. J.; Kozikowski, A. P. *J. Med. Chem.* **2005**, *48,* 1721. (b) Filippo, Jr., J. S.; Romano, L. J. *J. Org. Chem.* **1975**, *40,* 782. (c) Šilhár, P.; Pohl, R.; Votruba, I.; Hocek, M. *Org. Biomol.Chem.* **2005**, *3*, 3001. (d) Pretze, M.; Wuest, F.; Peppel, T.; Köckerling, M.; Mamat, C. *Tetrahedron Lett.* **2010**, *51*, 6410.

[74] Dubinina, G. G.; Brennessel, W. W.; Miller, J. L.; Vicic, D. A. *Organometallics* **2008**, *27*, 3933.

[75] The GC/MS analysis also revealed the formation of a mixture of regioisomers.

[76] It should be noted that the bromobenzene reaction induced color changes to green (with **3a**) or brown (with **3b**), but the nature of these reactivities could not be deciphered.

[77] Homolytic generation of $CF_3^{\cdot}$ from trivalent Ni species of the type $[(pincer)Ni(CF_3)]^{+\cdot}$ has been reported recently: Klein, A.; Vicic, D. A.; Biewer, C.; Kieltsch, I.; Stirnat, K.; Hamacher, C. *Organometallics* **2012**, *31*, 5334.

[78] Yanagisawa, S.; Ueda, K.; Taniguchi, T.; Itami, K. *Org. Lett.* **2008**, *10*, 4673.

[79] Liu, W.; Cao, H.; Zhang, H.; Zhang, H.; Chung, K. H.; He, C.; Wang, H.; Kwong, F. Y.; Lei, A. *J. Am. Chem. Soc.* **2010**, *132*, 16737.

[80] Sun, C.-L.; Li, H.; Yu, D.-G.; Yu, M.; Zhou, X.; Lu, X.-Y.; Huang, K.; Zheng, S.-F.; Li, B.-J.; Shi, Z.-J. *Nat. Chem.* **2010**, *2*, 1044.

[81] Dewanji, A.; Murarka, S.; Curran, D. P.; Studer, A. *Org. Lett.* **2013**, *15*, 6102.

[82] It should be noted that Vicic has recently reported evidence for the formation of trivalent nickel species bearing trifluoromethyl moieties.[29] Although no trivalent species based on a $POC_{sp2}OP$-type ligand has been reported to date, we have reported the preparation, isolation, and complete characterization of a few 17-electron $(pincer)Ni^{III}X_2$ complexes with $PC_{sp3}P$-, $POC_{sp3}OP$-, and POCN-type ligands. For structural information on such trivalent species see references [41a], [44a], and the following reports: a) Castonguay, A.; Beauchamp, A. L.; Zargarian, D. *Organometallics* **2008**, *27*, 5723; b) Spasyuk, D. M.; Zargarian, D.; Van der Est, A. *Organometallics* **2009,** *28,* 6531; c) Spasyuk, D. M.; Gorelsky, S. I.; Van der Est, A.; Zargarian, D. *Inorg. Chem.* **2011**, *50*, 2661.

[83] Note, however, that benzyl radicals might be stabilized in the solvent cage. For instance, van Koten has shown that (NCN)NiCl can react with halides such as CCl_4 to generate paramagnetic (NCN)$NiCl_2$ and CCl_3 radicals that appear to be stabilized in the solvent cage, initiating a Kharasch addition with excess of olefinic substrates as opposed to dimerizing. Our group has also reported the promotion of Kharasch addition by ($POC_{sp3}OP$)NiBr complexes (ref. [41]a).

[84] It is worth noting in this context that photoredox catalysis has been shown recently to be an effective approach for direct trifluoromethylation of heteroarenes in the presence of a photosensitizer such as $[Ru(phen)_3]^{2+}$ that can generate $CF_3^{\cdot}$ from triflyl chloride via a single electron transfer (SET) reaction: Nagib, D. A.; MacMillan, D. W. C. *Nature* **2011**, *480*, 224.

[85] The authors wish to thank an anonymous reviewer for pointing out a literature precedent (Bernstein, J.; Roth, J. S.; Miller, W. T. *J. Am. Chem. Soc.* **1948**, *70*, 2310) that describes benzylation reactions promoted by HgF_2 or HF generated in-situ during the distillation of $ArCH_2F$.

[86] *SAINT*, *Release 6.06; Integration Software for Single Crystal Data*; Bruker AXS Inc.: Madison, WI, 1999.

[87] Sheldrick, G. M. *SADABS, Bruker Area Detector Absorption Corrections;* Bruker AXS Inc., Madison, WI, 1999.

[88] *XPREP, Release 5.10; X-ray Data Preparation and Reciprocal Space Exploration Program*; Bruker AXS Inc.: Madison, WI, 1997.

[89] *SHELXTL, Release 5.10; The Complete Software Package for Single Crystal Structure Determination*; Bruker AXS Inc.: Madison, WI, 1997.

[90] (a) Sheldrick, G. M. *SHELXS97, Program for the Solution of Crystal Structures*; Univ. of Gottingen: Germany, 1997. (b) Sheldrick, G. M. *SHELXL97, Program for the Refinement of Crystal Structures*; University of Gottingen: Germany, 1997.

[91] Takaoka A., Iwakiri H., Ishikawa N. *Bull. Chem. Soc. Japan*, **1979**, *52*, 3377.

[92] (a) A. Takadate, T. Tahara, S. Goya, *Synthesis*, **1983**, *10*, 806; (b) G. Blessley, P. Holden, M. Walker, J. M. Brown, V. Gouverneur, *Org. Lett.* **2012**, *14*, 2754.

[93] X. Lefèvre, D. M. Spasyuk, D. Zargarian, *J. .Organomet. Chem.* **2011**, *696*, 864.

Chapitre 5

Chapitre 6 : Nickel(II) Complexes of the New Pincer-Type Unsymmetrical Ligands PIMCOP, PIMIOCOP, and NHCCOP: Versatile Binding Motifs

Article 5

Boris Vabre,[a] Yves Canac,[b] Carine Duhayon,[b] Remi Chauvin,[b] and Davit Zargarian[a]

[a] *Département de chimie, Université de Montréal, C. P. 6128, succursale Centre-ville, Montréal, Québec, Canada, H3C 3J7.*

[b] *Laboratoire de Chimie de Coordination (LCC), CNRS, 205 Route de Narbonne, 31077 Toulouse (France), and Université de Toulouse, UPS, INP, LCC, 31077 Toulouse (France).*

Chemical Communications **2012**, *48*, 10446-10448.

Chapitre 6

6.1 Abstract

Chelation/nickellation of an unsymmetrical *meta*-phenylene-based ligand featuring phosphinite and imidazolophosphine functionalities gives the corresponding pincer complex. *N*-Methylation of the latter generates a new complex featuring the ternary NHC→Ph_2P^+→Ni moiety, which can be converted subsequently into a binary NHC→Ni moiety by extrusion of Ph_2P^+, thus allowing a sequential synthesis of pincer complexes displaying varying degrees of dipolar character.

6.2 Introduction

Pincer ligands stand out among a large variety of multidentate ligands for their ability to bestow high thermal stability and enhanced reactivities to many transition metal complexes.[1] Thanks to the increasing attention paid to pincer chemistry over the past three decades, pincer-type complexes now constitute a diverse class of compounds that are well-suited for practical applications ranging from catalysis to functional materials.[2] In addition, many pincer complexes display rare or unprecedented structural features that continue to challenge our fundamental notions of metal-ligand bonding.[3]

The individual M-ligand interactions arising from a classical pincer motif (monoanionic, *mer*-terdentate) can correlate in different ways, competing with or synergistically reinforcing one another depending on the respective character of the coordinating moieties. For instance, the strongly σ-donating central aryl moiety in a *meta*-phenylene-based PCP-type pincer complex may compete with or reinforce M-

P interactions depending on whether the phosphanyl moieties are primarily σ-donating or π-accepting. Therefore, judicious selection of *P*-substituents can provide a degree of control over the electronic character of the phosphanyl functionality (σ-donating *vs* π-accepting), which can in turn help modulate the dipolar nature of the PCP-M ensemble.

We were attracted by the prospects of designing PCP-type ligands featuring electrophilic extremities in order to accentuate the dipolar character of the resulting pincer complexes (figure 6.1). Since cationic extremities would be ideally suited for this purpose, it was decided to incorporate cationic phosphenium[4] groups in the architecture of the target ligands. The choice of a specific type of phosphenium group was influenced by our recent investigations of the coordination chemistry of *ortho*-phenylene-based bidentate ligands featuring cationic imidazoliophosphine functionalities.[5] Structural studies on Rh(I) and Pd(II) complexes of these ligands have revealed that the imidazoliophosphine functionalities can be described as carbene-stabilized phosphenium adducts, such that their complexes can be viewed as possessing ternary coordination moieties of the type NHC→R_2P^+→M.[5a,b]

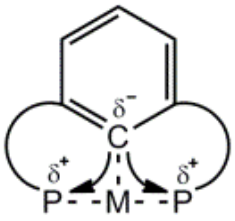

Figure 6.1 Schematic diagram showing the dipolar character of a PCP-type pincer complex arising from σ-donating and π-accepting properties of the C- and P-based functionalities.

The above finding inspired us to prepare pincer systems featuring cationic imidazoliophosphine extremities. An attempt to prepare the first symmetrical P^+CP^+-type pincer complex featuring two NHC→R_2P^+→Rh(I) ternary moieties proved unsuccessful.[6] Given our long-standing interest in the preparation of pincer complexes of Ni(II) and Ni(III) featuring symmetrical PCP[7] and POCOP[8] ligands, as well as unsymmetrical amine-phosphinite donor motifs (POCN),[9] we set out to test the feasibility of making the target pincer systems with nickel. Herein we describe the challenge of developing a practical synthesis for an unsymmetrical P^+COP-type pincer complex of Ni(II) bearing one cationic Ph_2P^+ moiety and a charge-neutral but π-accepting diphenylphosphinite, i.e., NHC→Ph_2P^+→Ni←PPh_2(OAr).

6.3 Results and discussion

The PIMCOP ligand **2** was obtained as a beige solid in *ca.* 80% yield by reacting ligand precursor **1**[10] with two equiv. of *n*-BuLi, followed by addition of two equiv. of $ClPPh_2$. (See ESI for details of all experimental work.) The ambient temperature reaction of **2** with a slight excess of $\{(i\text{-PrCN})NiBr_2\}_n$ and NEt_3 led to direct nickellation of the central C-H bond and gave the new pincer complex (PIMCOP)NiBr (**3**) as a yellow solid in 78% yield (Scheme 6.1). The metallated *mer,trans* structure proposed for **3** was deduced from the following NMR data: (i) ^{31}P doublets displaying a large coupling constant ($^2J_{P\text{-}P}$= 358 Hz) characteristic of inequivalent, *trans*-disposed P nuclei; (ii) a chemical shift for the O*P*Ph_2 moiety (*ca.* 146 ppm) that is significantly downfield of the corresponding signal in the ligand **2**

(112 ppm) and in the same range as the pincer complexes (POCOP)NiBr (146-147 ppm);[8f] (iii) a ^{13}C dd signal for C1 ($^{2}J_{P\text{-}C}$ ~ 22 and 25 Hz). The proposed structure for **3** was confirmed by high resolution mass spectroscopy, elemental analysis, and X-ray diffraction studies (Figure 6.1).

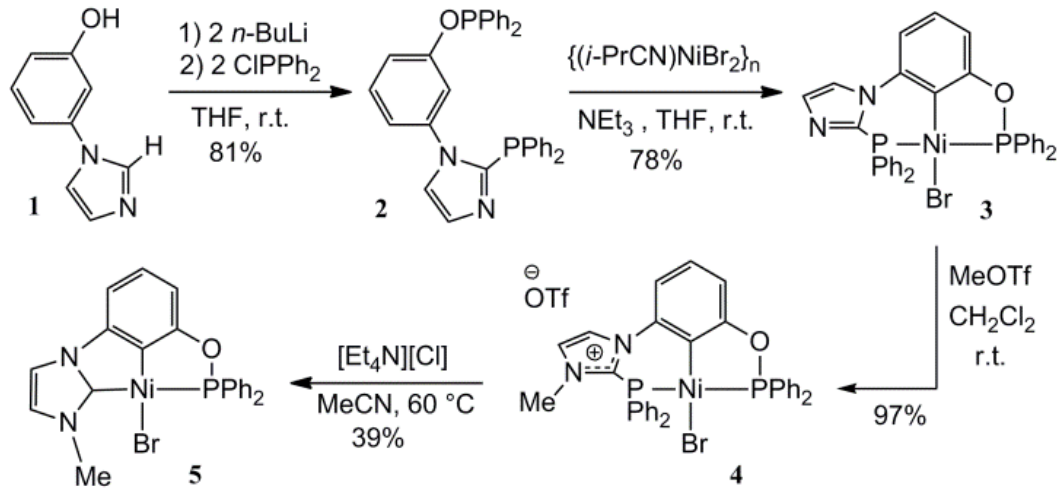

Scheme 6.1. Synthesis of (PIMCOP)NiBr (**3**), (PIMIOCOP)NiBr (**4**), and (NHCCOP)NiBr (**5**) complexes.

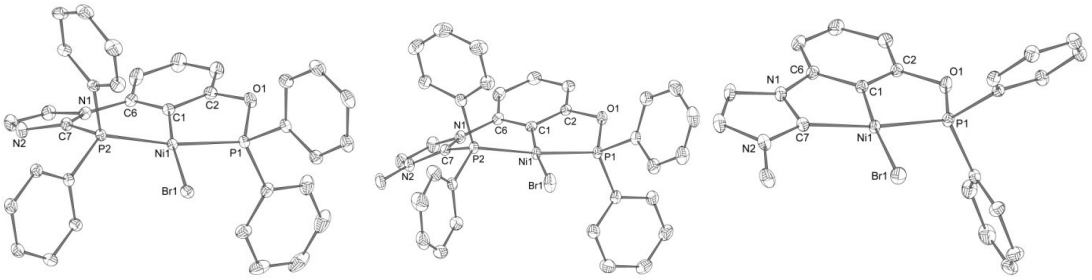

Figure 6.2 Molecular views of complexes 3 (left), 4 (middle), and 5 (right). Selected bond distances (Å) and angles (°): Ni-C1= 1.945(2) (**3**), 1.932(2) (**4**), 1.875(2) (**5**); Ni-P1= 2.1322(5) (**3**), 2.1331(6) (**4**), 2.1451(5) (**5**); Ni-P2= 2.1692(5) (**3**), 2.1762(6) (**4**) ; Ni-C7 (**5**)=1.946(2); Ni-Br= 2.3345(3) (**3**), 2.3123(3) (**4**), 2.3521(3) (**5**); P2-C7= 1.788(2) (**3**), 1.813(2) (**4**). C1-Ni-Br= 170.68(5) (**3**), 173.11(6) (**4**), 174.82(6) (**5**); P1-Ni-P2= 170.30(2) (**3**), 174.09(3) (**4**); C7-Ni-P1 (**5**)= 161.21(6). For complete details

of diffraction studies, see ESI.

With the target complex in hand, we turned our attention to transformation of the imidazolophosphine moiety. Previous studies had shown that *N*-alkylation of a *free* imidazolophosphine led to its electron-deficient imidazoliophosphine homologue that could be coordinated to Pd(II) subsequently. The resulting imidazoliophosphine-Pd species could then be converted into the corresponding NHC carbene derivative by nucleophile-induced extrusion of the phosphenium moiety (Scheme 6.2),[11] but attempts to carry out the alkylation/extrusion sequence on the coordinated imidazolophosphine failed. These findings prompted us to determine if this sequence of transformations might proceed *directly* on the Ni-bound imidazolophosphine moiety in **3**.

We were gratified to find that reaction with MeOTf led to an efficient *N*-methylation of **3**, giving an orange solid identified as the new pincer complex (PIMIOCOP)NiBr (**4**) featuring an imidazoliophosphine functionality (Scheme 6.1). Moreover, **4** was readily converted to the NHC-bearing complex (NHCCOP)NiBr (**5**) upon heating with a weak nucleophile such as the Cl anion in $[Et_4N][Cl]$.

The transformation of **3** into **4** and **5** is manifested in the NMR spectra, solid state structures, and electrochemical properties of the new complexes. For instance, *N*-methylation of the imidazolophosphine moiety in **3** caused a downfield shift of its ^{31}P signal, from *ca.* 3 to 11 ppm, and increased the value of $^{2}J_{P\text{-}P}$ from *ca.* 358 to 367 Hz. These changes are consistent with somewhat stronger Ni-P interactions, which arise presumably as a result of the stronger and synergistic donor→acceptor

interactions C→Ni and P←Ni→P present in **4** (*Cf.* figure 6.1). Methylation of the imidazole nitrogen is also evident from new singlet resonances emerging in the ^{1}H and ^{13}C NMR spectra (*ca.* 3.2 and 39 ppm, respectively), whereas the cationic nature of this species is reflected in its limited solubility in nonpolar solvents.

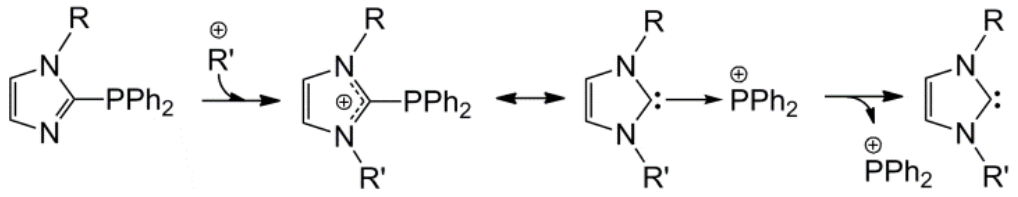

Scheme 6.2. Chemoselective *N*-alkylation of an imidazolo-phosphine, and nucleophilic displacement of the Ph_2P^+ moiety from the resulting NHC→Ph_2P^+ adduct.

Formation of **5** is implied by the appearance in the $^{13}C\{^{1}H\}$ NMR spectrum of a new doublet at *ca*. 174 ppm ($^{2}J_{P\text{-}C}$ = 112 Hz), typical of Ni-bound NHC carbene ligands.[12] The more shielded resonance for the O*P*Ph_2 signal in **5** *vs.* **4** (145 *vs.* 147 ppm) is consistent with a stronger *trans* influence of the carbene moiety. The metallated carbon nucleus C1 in **5** appears as a doublet (*ca.* 135 ppm, $^{2}J_{P\text{-}C}$ = 31 Hz) in contrast to a doublet of doublets in **3** (*ca.* 126 ppm, $^{2}J_{P\text{-}C}$ = 22 and 25 Hz) and a pseudo-triplet in **4** (*ca.* 127 ppm, $^{2}J_{P\text{-}C}$ ~ 23 Hz).

Comparison of the solid state structural parameters for the three new complexes **3**-**5** (Figure 1) has established the following important observations. First, the much longer Ni-P1 distance in **5** relative to **3** and **4** (*ca.* 2.145 *vs.* 2.132 and 2.133 Å) reflects the much stronger *trans* influence of the NHC moiety as well as the smaller bite angle in **5** (C7-Ni-P1~ 161°) *vs.* **3** and **4** (P1-Ni-P2 ~ 170° and 174°, respectively). The smaller bite angle in **5** also explains the much shorter Ni-C1

distance in **5** relative to **3** and **4** (*ca.* 1.88 *vs.* 1.94 and 1.93 Å), which in turn explains why the Ni-Br distances increase significantly in the order **4** (*ca.* 2.31 Å) < **3** (*ca.* 2.33 Å) < **5** (*ca.* 2.35 Å). Finally, the P2-C7 distance is somewhat longer in **4** than in **3** (*ca.* 1.81 *vs.* 1.79 Å), consistent with the non-negligible contribution to the resonance structure of the imidazoliophosphine moiety by the NHC-phosphenium canonical form involving a NHC→Ph_2P^+ dative bond (Scheme 6.2).

Solid samples of complexes **3**-**5** are air-stable, as are solutions of **3** and **5** over several days at ambient temperature, but solutions of **4** undergo a gradual aerobic decomposition. Cyclic voltammetry measurements conducted on complexes **3-5** have furnished electrochemical oxidation potentials that allow a comparison of the electronic properties of the three new pincer ligands under discussion. Thus, the observed order of the oxidation potentials, *cf* **5** (+0.50 V; quasi-reversible) < **3** (+0.82 V; irreversible) < **4** (+1.12 V; irreversible),[‡] reflects the electron density on the Ni centre which is anticipated to be greatest in the complex featuring the NHC moiety, followed by the charge-neutral and cationic complexes featuring imidazolophosphine and imidazoliophosphine functionalities, respectively. Comparison to previously studied (pincer)Ni(II)Br complexes featuring *meta*-phenylene-based ligands shows that the oxidation potentials increase in the order NCN < PCP < **5** < POCN < **3** ~ POCOP < **4**.[8b,c,f; 9a,b] It appears, therefore, that the new pincer ligands **3**-**5** carve a unique niche in the range of ligand donor properties observed to date.

6.4 Conclusions

The new pincer complexes reported here represent the first of the kind bearing an imidazolo-phosphine (**3**) or an imidazolio-phosphine (**4**) functionality, and a rare pincer complex of Ni featuring an NHC donor moiety (**5**).[13] These pincer systems feature functionalities of different donor-acceptor character that together create an unsymmetrical coordination environment around the Ni atom. The modular synthesis of the ligand systems described here should facilitate the preparation of a variety of interesting complexes. Particularly noteworthy is the unprecedented and facile on-the-metal derivatization route involving an efficient and regioselective *N*-methylation of the imidazole moiety and the subsequent extrusion of the *in-situ* generated Ph_2P^+ moiety. That this sequence of transformations is not supported by the previously examined symmetrical, bidentate *ortho*-bis(imidazolo)phenylene ligand[5] is a testimony to the important advantages of the pincer framework. These attractive characteristics augur well for exploration of catalytic reactivities with these families of pincer complexes, an effort that is currently underway in our laboratories.

6.5 Acknowledgments

The authors are grateful to the following organisms for financial support of this study: the French Ministère de l'Enseignement Supérieur de la Recherche et de la Technologie, Centre National de la Recherche Scientifique (CNRS), ANR program (ANR-08-JCJC-0137-01), NSERC of Canada (Discovery grants to DZ), and Centre in Green Chemistry and Catalysis (scholarships to BV). Direction des Relations

Internationales of Université de Montréal and Université Paul Sabatier are gratefully acknowledged for the travel grants that made this collaborative project possible.

6.6 Supporting Information

General Comments. Unless otherwise indicated, all manipulations were carried out using standard Schlenk and glove box techniques under nitrogen atmosphere. All solvents used for experiments were dried to water contents of less than 10 ppm (determined using a Mettler Toledo C20 coulometricKarl Fischer titrator) by passage through activated aluminum oxide columns (MBraun SPS) and freeze–thaw-degassed. All starting materials, including 3-bromoanisol, CuBr, imidazole, methyl trifluoromethanesulfonate, BuLi, Ph_2PCl, were purchased from Aldrich and used without further purification. Previous reports have described the syntheses of 3-methoxyphenyl-imidazole[14] and $NiBr_2(NC^iPr)$.[15] NMR chemical shift values are reported in ppm (δ) and referenced internally to the residual solvent signals (^1H and ^{13}C: 7.26 and 77.16 ppm for $CDCl_3$; 7.16 and 128.06 ppm for C_6D_6) or externally (^{31}P, H_3PO_4 in D_2O, $\delta = 0$). Coupling constants are reported in Hz. High Resolution Mass Spectroscopy analyses were performed by the Centre Regional de Spectroscopie de Masse – Université de Montréal, and the Laboratoire de Chimie de Coordination du CNRS – Toulouse. The elemental analyses were performed by the Laboratoire de Chimie de Coordination du CNRS – Toulouse.

Synthetic Procedures. Details of the synthesis and characterization of the new compounds reported in the accompanying communication are provided below. All

compounds are identified by their respective IUPAC names as well as the acronyms used to refer to them in the communication. In addition, we have provided a line-drawing for each compound to facilitate spectral assignments. It should be noted that the numbering scheme used in these drawings are consistent with that used in the molecular views of the solid structures of complexes **3-5** (Figure 1 in the manuscript).

3-[2-(Diphenylphosphanyl)-1H-imidazol-1-yl]phenyldiphenylphosphinite, PIMC^{H}OP (2):

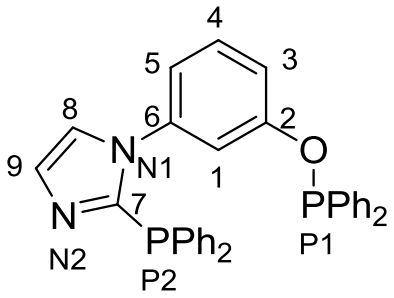

Drop-wise addition of BuLi (5.0 mL of a 2 M solution in cyclohexane, 10 mmol) to a solution of 3-hydroxyphenyl-imidazole **1** (800 mg, 5.0 mmol) in THF (75 mL) at –78 °C gave a pink suspension, which was allowed to warm to room temperature before adding $ClPPh_2$ (1.80 mL, 10.0 mmol). The resulting yellow solution was stirred for 10 min and then placed under vacuum to remove the volatiles. Extraction of the remaining solid residues with toluene (50 mL), followed by filtration and evaporation, gave the desired product as a beige solid (2.14 g, 81 %). ^{1}H NMR (CD_2Cl_2, 25 °C): δ 7.64-7.71 (m, 4H, H_{Ar}), 7.49-7.57 (m, 10H, H_{Ar}), 7.26-7.42 (m, 10H, H_{Ar}), 7.03 (m, 2H, H8 & H9). ^{13}C NMR ($CDCl_3$, 25 °C): δ 157.7 (d, J_{CP}= 9.6, C2), 140.4 (d, J_{CP}= 17.0, *i*-C_{Ph}), 139.0 (d, J_{CP}= 4.5, C6), 135.6 (d, J_{CP}= 6.8, C7), 134.1 (d, J_{CP}= 20.0, *i*-C_{Ph}), 134.0 (d, J_{CP}= 20.7, CH_{ar}), 131.4 (d, J_{CP}= 7.5, CH_{ar}),

130.7 (d, J_{CP}= 22.7, CH_{ar}), 130.1 (s, CH_{ar}), 129.9 (s, CH_{ar}), 123.8 (s, CH_{ar}), 129.1 (s, CH_{ar}), 128.7 (d, J_{CP}= 7.5, CH_{ar}), 128.6 (d, J_{CP}= 8.4, CH_{ar}), 120.4 (d, J_{CP}= 6.5, CH_{ar}), 118.8 (d, J_{CP}= 13.0, CH_{ar}), 117.1 (dd, J_{CP}= 4.5 and 10.8, C1). $^{31}P\{^{1}H\}$ NMR (CD_2Cl_2, 25 °C): δ –29.2 (s, P2), +112.3 (s, P1). MS DCI-NH_3 *m/z* 529.1 $[MH]^+$. HRMS Calcd for $C_{33}H_{27}N_2OP_2^+$: 529.15917 found 529.15931.

8-Bromo-7,7,9,9-tetraphenyl-10-oxa-2,5-diaza-7λ^5,9λ^5-diphospha-8-nickelatetracyclo[6.6.1.0^{2,6}.0^{11,15}]pentadeca-1(14),3,5,11(15),12-pentaene-7,9-bis(ylium), (PIMCOP)NiBr (3):

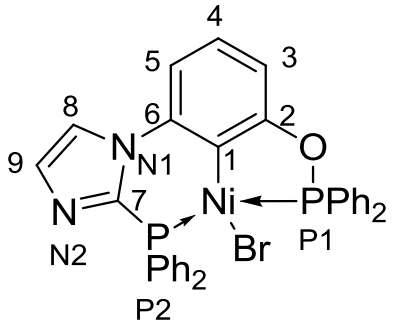

Stirring a mixture of **2** (1.72 g, 3.26 mmol), (*i*-PrCN)$NiBr_2$ (1.12 g, 3.91 mmol), and NEt_3 (4.86 mmol, 680 µL) in THF (50 mL) for 2 h at r.t. gave an orange suspension. Evaporation of the volatiles under vacuum, followed by extraction of the solid residues with toluene (75 mL), filtration, and evaporation of the filtrate, gave the crude product as a yellow solid. Slow evaporation of a saturated Et_2O solution of this solid gave analytically pure crystals of the desired product (1.70 g, 78 %). ^{1}H NMR ($CDCl_3$, 25 °C): δ 7.93-7.98 (m, 4H, H_{Ar}), 7.60-7.65 (m, 5H, H_{Ar}), 7.52-7.56 (m, 2H, H_{Ar}), 7.42-7.50 (m, 7H, H_{Ar}), 7.35-7.39 (m, 4H, H_{Ar}), 7.10 (td, J_{HH}= 7.9, J_{HP} = 1.4,

1H, H_{Ar}), 6.89 (d, J_{HH}= 7.9, 1H, H_{Ar}), 6.86 (d, J_{HH}= 8.1, 1H, H_{Ar}). ^{13}C NMR ($CDCl_3$, 25 °C): δ 167.8 (dd, J_{CP}= 5.0 and 17.5, C2), 143.7 (d, J_{CP}= 7.0, C6), 134.3 (d, J_{CP}= 11.2, CH_{Ar}), 133.3 (d, J_{CP}= 9.2, CH_{Ar}), 132.6 (d, J_{CP}= 11.9, CH_{Ar}), 132.3 (d, J_{CP}= 20.0, CH_{Ar}), 132.0 (d, $J_{CP=}$ 3.9, *i*-C_{Ph}), 131.8 (d, J_{CP}= 1.6, CH_{Ar}), 130.9 (d, J_{CP}= 1.8, CH_{Ar}), 128.6 (d, J_{CP}= 11.1, CH_{Ar}), 128.4 (d, J_{CP}= 11.8, CH_{Ar}), 128.1 (d, J_{CP} = 57.6, C7), 125.8 (dd, J_{CP}= 21.5 and 24.9, C1), 122.2 (s, CH_{Ar}), 114.6 (s, CH_{Ar}), 111.6 (d, J_{CP} = 14.1, CH_{Ar}). $^{31}P\{^1H\}$ NMR ($CDCl_3$, 25 °C): δ +3.2 (d, J_{PP}= 358.0, P2), +145.7 (d, J_{PP}= 358.0, P1). HRMS Calcd for $C_{33}H_{26}N_2OP_2NiBr^+$: 665.0038 found 665.0057. Anal. Calcd. for $C_{33}H_{25}BrN_2NiOP_2$ (666,11): C, 59.60 ; H, 3.78 ; N, 4.21. Found: C, 59.62 ; H, 3.77 ; N, 4.21.

8-Bromo-5-methyl-7,7,9,9-tetraphenyl-10-oxa-2,5-diaza-7λ^5,9λ^5-diphospha-8-nickelatetracyclo[6.6.1.0^{2,6}.0^{11,15}]pentadeca-1(14),3,5,11(15),12-pentaen-5-ium-7,9-bis(ylium), (PIMIOCOP)NiBr (4):

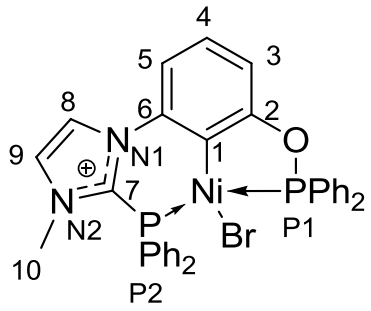

Methyl trifluoromethanesulfonate (79.0 µL, 0.72 mmol) was added to a solution of **3** (0.48 g, 0.72 mmol) in CH_2Cl_2 (30 mL) cooled to –78 °C. The mixture was then allowed to warm to r. t. and stirred for 2 h. Evaporation of the volatiles under

vacuum, followed by washing of the solid residues with Et_2O (40 mL) afforded **4** as an orange solid (0.58 g, 97 %). Recrystallization at –20 °C from THF gave analytically pure **4** as orange crystals (m.p. 133-135 °C). ^{1}H NMR (CD_2Cl_2, 25 °C): δ 8.12 (br s, 1H, H_{Ar}), 7.97-7.90 (m, 4H, H_{Ar}), 7.76-7.57 (m, 17H, H_{Ar}), 7.27 (t, J_{HH}= 7.5, 1H, H_{Ar}), 7.06 (d, J_{HH}= 7.8, 2H, H_{Ar}), 3.21 (s, 3H, CH_3). ^{13}C NMR (CD_2Cl_2, 25 °C): δ 167.3 (dd, $J_{CP=}$ 5.4 and 17.6, C2), 141.5 (d, J_{CP}= 8.8, C6), 133.7 (d, J_{CP}= 11.3, CH_{Ar}), 133.0 (s, CH_{Ar}), 132.6 (d, J_{CP}= 11.3 Hz, CH_{Ar}), 132.5 (s, CH_{Ar}), 131.6 (d, J_{CP}= 26.4, *i*-C_{Ph}), 131.1 (d, J_{CP}= 49.1, *i*-C_{Ph}), 131.0 (s, CH_{Ar}), 130.1 (d, J_{CP}= 11.3, CH_{Ar}), 130.0 (s, CH_{Ar}), 128.8 (d, J_{CP}= 11.3, CH_{Ar}), 126.9 (pst, J_{CP}= 22.6 and 22.9, C1), 125.5 (s, CH_{Ar}), 122.9 (d, J_{CP} = 50.3 Hz, C7), 120.5 (q, J_{CF}= 320.0, $CF_3SO_3^-$), 116.8 (s, CH_{Ar}), 114.5 (d, J_{CP}= 15.1, CH_{ar}), 39.2 (s, CH_3). ^{31}P NMR (CD_2Cl_2, 25 °C): δ +147.0 (d, J_{PP}= 366.6, P1), +11.1 (d, J_{PP}= 366.6, P2). MS (ES): *m/z*: 679.0 $[M]^+$. HRMS (ES): calcd for $C_{34}H_{28}N_2OBrP_2Ni$ 679.0214; found, 679.0190

1-Bromo-12-methyl-2,2-diphenyl-3-oxa-9,12-diaza-2λ^{5}phospha-1-nickelatetracyclo[6.5.1.0^{4,14}.0^{9,13}] tetradeca-1(13),4(14),5,7,10-pentaen-2-ylium, (NHCCOP)NiBr (5):

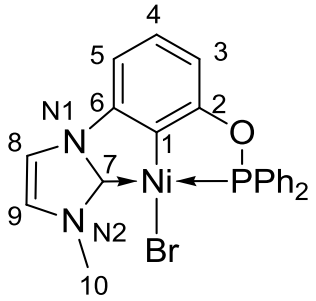

Tetra(ethyl)ammonium chloride (0.22 g, 1.33 mmol) and **4** (0.74 g, 0.89 mmol) were dissolved in CH_3CN (20 mL) and stirred at 60 °C for 24 h. Evaporation of the

solution to dryness followed by purification of the remaining solid residues by flash chromatography on silica gel (CH_2Cl_2/hexane) gave a yellow solid that turned out to be a 1:2 mixture of the desired product and its Ni-Cl analogue, respectively. Treatment of this mixture with tetra(butyl)ammonium bromide (0.29 g, 0.89 mmol) in CH_3CN (10 ml), followed by filtration on silica gel (CH_2Cl_2), gave **5** as a yellow solid (0.17 g, 39 %). Recrystallization of the crude product at –20 °C from a THF/pentane mixture gave yellow crystals (m.p. 270-272 °C). ^{1}H NMR ($CDCl_3$, 25 °C): δ 8.06-8.02 (m, 4H, H_{Ar}), 7.52-7.46 (m, 6H, H_{Ar}), 7.23 (d, J = 1.9, 1H, H_{Ar}), 7.08 (t, J = 7.8, 1H, H_{Ar}), 6.80 (t, J = 1.9, 1H, H_{Ar}), 6.68 (dd, J = 3.5 and 7.8, 2H, H_{Ar}), 4.16 (s, CH_3). $^{13}C\{^1H\}$ NMR ($CDCl_3$, 25 °C): δ 173.8 (d, J_{CP} = 112.0, C7), 166.1 (d, J_{CP}= 16.3, C2), 148.2 (s, C6), 135.4 (d, J_{CP}= 31.4, C1), 132.6 (d, J_{CP}= 44.0, *i*-C_{Ph}), 132.4 (d, J_{CP} = 12.6, CH_{Ar}), 131.5 (s, CH_{Ar}), 128.5 (d, J_{CP} = 11.3, CH_{Ar}), 127.5 (s, CH_{Ar}), 122.8 (d, J_{CP} = 5.0 Hz, CH_{Ar}), 113.4 (s, CH_{Ar}), 109.2 (d, J_{CP} = 13.8, CH_{Ar}), 105.1 (s, CH_{Ar}), 38.2 (s, CH_3). $^{31}P\{^1H\}$ NMR ($CDCl_3$, 25 °C): δ = +144.9 ppm. MS (ES): *m/z*: 415.1 $[M - Br]^+$. HRMS (ES): calcd for $C_{22}H_{18}N_2OPNi$ 415.0510; found, 415.0510.

Procedure for electrochemical measurements. Cyclic voltammetry measurements were carried out with a potentiostat Autolab PGSTAT100. Experiments were performed at room temperature in an homemade airtight three–electrode cell connected to a vacuum/argon line. The reference electrode consisted of a saturated calomel electrode (SCE) separated from the solution by a bridge compartment. The counter electrode was a platinum wire of *ca* 1.0 cm^2 apparent surface. The working electrode was a glassy carbon microdisk (1.0 mm diameter).

Voltammograms were recorded in dry CH_2Cl_2 solution (*ca* 3 x 10^{-3} M) in the presence of 0.1 M *n*-tetrabutylammonium hexafluorophosphate as the supporting electrolyte, under argon at 25°C. In these conditions, the redox couple $FeCp_2^+/FeCp_2$ was found at 0.44 V/SCE. All oxidation potentials reported are referenced to the $FeCp_2^+/FeCp_2$ redox couple.

Procedure for crystal structure determinations. Intensity data were collected at 180K on a Bruker Apex2 diffractometer. Structures were solved by direct methods using SIR92[16] or SHELXS,[17] and refined by full-matrix least-squares procedures using the program CRYSTALS.[18] Atomic scattering factors were taken from the International tables for X-ray Crystallography.[19] All non-hydrogen atoms were refined anisotropically. Hydrogen atoms were refined using a riding model. Absorption corrections were introduced using the program MULTISCAN.[20]

Crystal data for **3**. $C_{37}H_{35}BrN_2NiO_2P_2$, M = 740.26 g.mol^{-1}, Triclinic, a = 10.8276(8), b = 12.6576(9), c = 14.1398(10) Å, α = 89.271(4), β = 69.270(4), γ = 67.245(4), V = 1653.9(2) Å^3, space group P -1, Z = 2, μ(Mo-Ka) = 1.928 mm^{-1}, 45525 reflections measured, 12897 unique (Rint = 0.023), 9265 reflections used in the calculations [I > 3σ(I)], 382 parameters, R1 = 0.0378, wR2 = 0.0475.

Crystal data for **4**. $C_{39}H_{36}BrF_3N_2NiO_5P_2S$, M = 902.35 g.mol^{-1}, Triclinic, a = 10.3522(6), b = 15.0431(9), c = 16.8048(9) Å, α = 91.599(3), β = 98.038(3), γ = 92.758(3), V = 2586.7(3) Å^3, space group P -1, Z = 2, μ(Mo-Ka) = 1.295 mm^{-1}, 53685 reflections measured, 10359 unique (Rint = 0.026), 7411 reflections used in the calculations [I > 3σ(I)], 523 parameters, R1 = 0.0312, wR2 = 0.0323.

Crystal data for **5**. $C_{26}H_{26}BrN_2NiO_2P$, M = 568.09 g.mol^{-1}, Triclinic, a = 9.8280(4), b = 11.2069(5), c = 13.2269(6) Å, α = 65.649(2), β = 69.724(2), γ = 68.158(2), V = 1199.39(9) Å^3, space group P -1, Z = 2, μ(Mo-Ka) = 2.568 mm^{-1}, 27313 reflections measured, 7770 unique (Rint = 0.027), 5414 reflections used in the calculations [I > 3σ(I)], 298 parameters, R1 = 0.0321, wR2 = 0.0326

6.7 References

[1] Pincer ligands and complexes were first introduced in the 1970's by the groups of Shaw and van Koten: (a) C.J. Moulton and B.L. Shaw, *Dalton Trans*, 1976, 1020. (b) G. van Koten, K. Timmer, J.G. Noltes, A.L. Spek, *J. Chem. Soc., Chem. Commun*., 1978, 250.

[2] For a few reviews on pincer complexes and their applications see: (a) M. Albrecht and G. van Koten, *Angew. Chem., Int. Ed.* 2001, **40**, 375. (b) M.E. van der Boom and D. Milstein, *Chem. Rev*., 2003, **103**, 1759. (c) J.T. Singleton *Tetrahedron*, 2003, **59**, 1837. (d) M.Q. Slagt, D.A.P. van Zwieten, A.J.C.M. Moerkerk, R.J.M.K. Gebbink and G. van Koten, *Coord. Chem. Rev.*, 2004, **248**, 2275. (e) L.-C. Liang, *Coord. Chem. Rev*. 2006, **250**, 1152. (f) H. Nishiyama, *Chem. Soc. Rev.* 2007, **36**, 1133. (g) W. Leis, H.A. Mayer, and W.C. Kaska, *Coord. Chem. Rev.*, 2008, **252**, 1787. (h) N. Selander and K.J. Szabó, *Chem. Rev.*, 2011, **111**, 2048.

[3] (a) M. Gozin, A. Weisman, Y. Ben-David, and D. Milstein, *Nature*, 1993, **364**, 699. (b) M. Gozin, M. Aizenberg, S.-Y. Liou, A. Weisman, Y. Ben-David and D. Milstein, D. *Nature*, 1994, **370**, 42. (c) M.A. McLoughlin, R.J. Flesher, W.C. Kaska and H.A.

Mayer, *Organometallics*, 1994, **13**, 3816. (d) V.F. Kuznetsov, A.J. Lough and D.G. Gusev, *Chem. Comm.*, 2002, 2432. (e) D.G. Gusev and A.J. Lough, *Organometallics*, 2002, **21**, 2601. (f) D.G. Gusev, F.-G. Fontaine, A.J. Lough and D. Zargarian, *Angew. Chem. Int. Ed*., 2003, **42**, 216. (g) J. Zhao, A.S. Goldman and J.F. Hartwig, *Science*, 2005, **307**, 1080.

[4] (a) N. Kuhn, J. Fahl, D. Bläser, R. Boese, *Z. Anorg. All. Chem*. 1999, **625**, 729. (b) M. Azouri, J. Andrieu, M. Picquet, P. Richard, B. Hanquet, I. Tkatchenko, *Eur. J. Inorg. Chem.,* 2007, 4877. (c) N. Debono, Y. Canac, C. Duhayon, R. Chauvin, *Eur. J. Inorg. Chem*., 2008, 2991. (d) J. Petuskova, H. Bruns, M. Alcarazo, *Angew. Chem., Int. Ed.* 2011, **50**, 3799.

[5] (a) Y. Canac, N. Debono, L. Vendier, R. Chauvin, *Inorg. Chem*. 2009, **48**, 5562. (b) Y. Canac, N. Debono, C. Lepetit, C. Duhayon, R. Chauvin, *Inorg. Chem*., 2011, **50**, 10810. (c) Y. Canac, C. Maaliki, I. Abdellah, R. Chauvin, *New. J. Chem*., 2012, **36**, 17.

[6] C. Barthes, C. Lepetit, Y. Canac, C. Duhayon, D. Zargarian and R. Chauvin, *Inorg. Chem.* 2013, **52**, 48.

[7] (a) L.F.Groux, F. Bélanger-Gariépy and D. Zargarian, *Can. J. Chem.* 2005, **83**, 634. (b) A. Castonguay, C. Sui-Seng, D. Zargarian and A. L. Beauchamp, *Organometallics*, 2006, **25**, 602. (c) A. Castonguay, A.L. Beauchamp and D. Zargarian, *Organometallics,* 2008, **27**, 5723. (d) A. Castonguay, A.L. Beauchamp and D. Zargarian, *Inorg. Chem.* 2009, **48**, 3177.

[8] (a) V. Pandarus and D. Zargarian, *Chem. Commun*., 2007, 978. (b) V. Pandarus and D. Zargarian, *Organometallics*, 2007, **26**, 4321. (c) A. Castonguay, D.M. Spasyuk,

N. Madern, A.L. Beauchamp, A. L. and D. Zargarian, *Organometallics*, 2009, **28**, 2134. (d) X. Lefèvre, G. Durieux, S. Lesturgez and D. Zargarian, *J. Mol. Catal. A*., 2011, **335** 1. (e) X. Lefèvre, D.M. Spasyuk and D. Zargarian, *J. Organomet. Chem*., 2011, **696**, 864. (f) A. Salah and D. Zargarian, *Dalton Trans.* 2011, **40, 8977. (g)** A. Salah, C. Offenstein and D. Zargarian, *Organometallics*, 2011, **30***,* 5352.

[9] (a) D.M. Spasyuk, D. Zargarian, and A. van der Est, *Organometallics*, 2009, **28**, 6531. (b) D.M. Spasyuk, D. Zargarian, *Inorg. Chem*., 2010, **49**, 6203. (c) D.M. Spasyuk, S.I. Gorelsky, A. van der Est and D. Zargarian, *Inorg. Chem*., 2011, **50**, 2661.

[10] D.A. Pratt, R.P. Pesavento, W.A. van der Donk, *Org. Lett.*, 2005, **7**, 2735.

[11] (a) I. Abdellah, C. Lepetit, Y. Canac, C. Duhayon, R. Chauvin, *Chem. Eur. J*., 2010, **16**, 13095. (b) I. Abdellah, M. Boggio-Pasqua, Y. Canac, C. Lepetit, C. Duhayon, R. Chauvin, *Chem. Eur. J*., 2011, **17**, 5110. (c) C. Maaliki, C. Lepetit, Y. Canac, C. Bijani, C. Duhayon, R. Chauvin, *Chem. Eur. J*., 2012, **18**, 7705.

[12] The carbenic C atoms in [(CCC)Ni(NCMe)]PF_6 resonate at *ca.* 170 and 173 ppm: A. Liu, X. Zhang, and W. Chen, *Organometallics*, 2009, **28**, 4868.

[13] To our knowledge, the CCC-type complexes reported in ref. 12 are the only other pincer complexes of Ni bearing an NHC donor moiety.

[14] D. A. Pratt, R. P. Pesavento, W. A. van der Donk, *Org. Lett.*, 2005, **7**, 2735.

[15] Vabre, B.; Spasyuk, D. M.; Zargarian, D. *Organometallics* **2012**, *31*, 8561.

[16] A. Altomare, G. Cascarano, C. Giacovazzo, A. Guagliardi, M. C. Burla, G. Polidori, M. Camalli, *J. Appl. Cryst*. **1994**, *27*, 435.

[17] G. M. Sheldrick, *Acta Cryst.* 2008, **A64**, 112.

[18] P. W. Betteridge, J. R. Carruthers, R. I. Cooper, K. Prout, D. J. Watkin, *J. Appl. Cryst.* 2003, **36**, 1487.

[19] International Tables for X-ray Crystallography, vol. IV, Kynoch Press, Birmingham, England, 1974.

[20] R. H. Blessing, *Acta Crystallogr. Sect A* 1995, **51**, 33.

Chapitre 7 : Neutral and Cationic Ni(II) Complexes of the PIMCOP, PIMIOCOP and NHCCOP Pincer Ligands : Synthesis, Characterization and Reactivities.

Article 6

Boris Vabre,[a] *Yves Canac,**[bc] *Christine Lepetit,**[bc] *Carine Duhayon,*[bc] *Remi Chauvin,**[bc] *and Davit Zargarian**[a]

[a] Département de chimie, Université de Montréal, Montréal (Québec), Canada

[b] Laboratoire de Chimie de Coordination (LCC), CNRS, 205 Route de Narbonne, 31077 Toulouse, France

[c] Université de Toulouse, UPS, INP, LCC, 31077 Toulouse, France

Chapitre 7

7.1 Abstract

The synthesis and characterization of a new family of pincer-type ligands, PIMCOP, PIMIOCOP and NHCCOP, and their corresponding charge neutral and cationic Ni(II) complexes are here reported. PIMCOP ligands were isolated in good yields (70-72 %) after deprotonation of 3-methoxyphenyl-imidazole precursor by *n*-BuLi followed by addition of $ClPR_2$ (R= -*i*-Pr, Ph). Treating the PIMCOP ligands at room temperature with $\{(^{i}PrCN)NiBr_2\}_n$ in the presence of NEt_3 facilitated the C-H activation to afford the corresponding nickellated complexes (^{R}PIMCOP$^{R'}$)NiBr (^{R}PIMCOP$^{R'}$ = $\kappa^P,\kappa^C,\kappa^P$-{2-(R'$_2$PO)-6-(R$_2PC_3H_2N_2$)-C$_6H_3$}; R = *i*Pr; R' = Ph, *i*-Pr) (45-84 %). Treatment of (^{iPr}PIMCOP^{iPr})NiBr with MeOTf led to *N*-methylation at the imine moiety of the imidazole ring to give the corresponding complex (^{iPr}PIMIOCOP^{iPr})NiBr (^{iPr}PIMIOCOP^{iPr} = $\kappa^P,\kappa^C,\kappa^P$-[2-(*i*-Pr$_2$PO)-6-{(*i*-Pr$_2$P)(*N*-Me-C$_3H_2N_2$)}-C$_6H_3$][OTf] (89 %). Reacting the latter with NaOEt as nucleophile led to the new complex (NHCCOP^{iPr})NiBr (NHCCOP= $\kappa^P,\kappa^C,\kappa^C$-{2-(*i*-Pr$_2P_2$PO)-6-(*N*-Me-C$_3H_2N_2$)-C$_6H_3$}; (47 %). Cationic acetonitrile adducts of the new Ni(II) complexes were obtained by bromide abstraction using a Ag(I) salt to give in 79-90 % isolated yields (^{R}PIMCOP$^{R'}$)Ni(NCCH$_3$)(OTf), (^{R}PIMIOCOP^{R})Ni(NCCH$_3$)(OTf) and (NHCCOP^{R})Ni(NCCH$_3$)(OTf) (R = Ph, *i*-Pr). The catalytic activities of the latter cationic species were evaluated for the transformation of nitriles to amidines.

7.2 Introduction

Nickel pincer complexes are increasingly studied because of their robustness, low cost and interesting catalytic properties. The large variety of new pincer ligands

introduced over the last few decades (e.g., NCN, POCOP, PCP, POCN, PCN, etc.) have enabled a broad modulation of the structural, spectroscopic, electrochemical and catalytic properties of pincer-type complexes of Ni (Figure 7.1).[1] Cationic derivatives of these complexes are useful for promotion of Michael-type additions including hydroamination and hydroalkoxylation. For the latter transformation, it has been demonstrated that improved catalytic activities result from specific modifications of pincer architecture that render these ligands more electron-poor.[2]

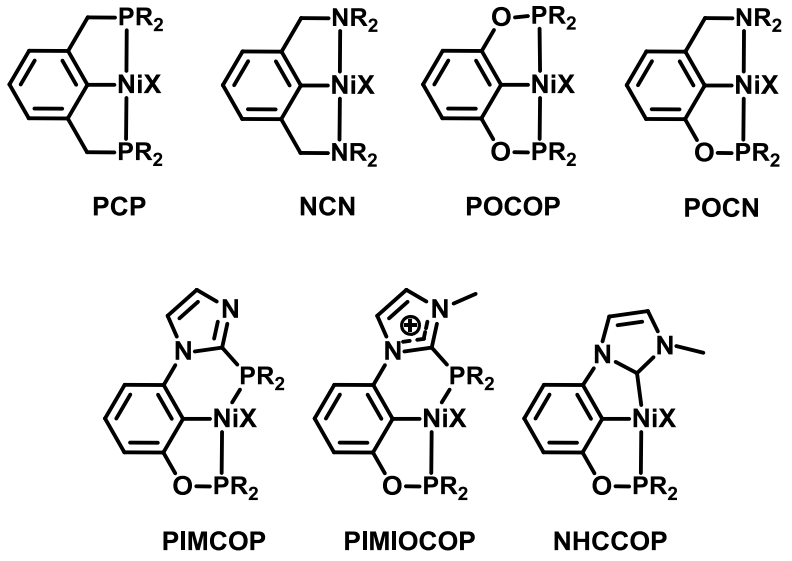

Figure 7.1. Schematic representation of known Ni(II) pincer complexes.

During our on-going investigations on development of new pincer-type complexes of Ni, we set out to introduce new donor moieties that would modulate the overall electron donation to the metal center. Inspired by recent reports on the versatility of imidazole- and imidazoliophosphine in different contexts,[3] we have introduced[4] new families of unsymmetrical pincer complexes of Ni bearing phosphinite- and imidazolophosphine-derived ligands, namely: (PIMCOP)NiBr,

[(PIMIOCOP)NiBr][OTf], and (NHCCOP)NiBr (Figure 7.1). As continuation of this initial study, we have investigated the chemistry of Ni complexes based on new ^{R}PIMCOP$^{R'}$ ligands. Application of post-derivatization strategies to the latter complexes has allowed us to prepare new derivatives featuring either a more electrophilic imidazoliophosphine moiety [(PIMIOCOP)NiBr][OTf] or a more nucleophilic NHC-carbene ((NHCCOP)NiBr). The present report describes the preparation and the characterization of these bromo complexes and related cationic acetonitrile adducts [(^{R}PIMCOP^{R})Ni(NCMe)][OTf], [(^{R}PIMIOCOP^{R})Ni(NCMe)][OTf], and [(NHCCOP^{R})Ni(NCMe)][OTf] (R = Ph, *i*-Pr). We have also investigated the catalytic activities of these cationic species in the conversion of nitriles to amidines.

7.3 Results and discussion

Synthesis and Reactivity. The preparation of PIMCOP ligands starts from readily available 3-methoxyphenyl-imidazole **1**.[5] As similarly reported for ^{Ph}PIMCOP^{Ph} ligand **2** in the aryl series,[4] double deprotonation of **1** by *n*-BuLi at –78°C in THF, followed by addition of two equivalents of ClP^{i}Pr$_2$ afforded the 'alkylated analogue' ^{iPr}PIMCOP^{iPr} ligand **3** in 70% yield. Resulting of a sequential strategy, *ca* adding first one equivalent of ClP^{i}Pr$_2$ and then a stoichiometric amount of ClPPh$_2$, the mixed ^{iPr}PIMCOP^{Ph} ligand **4** was obtained in 72% yield. The latter demonstrated that the first phosphinylation takes place at the most nucleophilic lithiated carbon atom, *ca* at the N*CH*N fragment of the N-imidazole ring (Scheme 7.1). (PIMCOP)NiBr complexes **6-7** were then obtained *via* direct nickellation of the central C-H bond by treating PIMCOP ligands **3-4** with a slight excess of {(^{i}PrCN)NiBr$_2$}$_n$ in presence of

NEt_3.[6] The lower yield obtained for (^{iPr}PIMCOP^{Ph})NiBr **7** (*ca*, in 45% yield) with respect to analogues **5-6** (*ca*, in 84-89 % yield) might be due to the presence of two electronically different phosphorus coordinating ends. As previously reported,[4] to reach cationic analogues, neutral (^{iPr}PIMCOP^{iPr})NiBr complex **6** was thus treated with an equivalent of MeOTf giving the corresponding *N*-methylated (^{iPr}PIMIOCOP^{iPr})NiBr complex **9** in 89% yield. Then by addition of a stochiometric amount of a nucleophile such as EtONa, (NHCCOP^{iPr})NiBr complex **13** was isolated in 45% yield. The formation of the latter results of the formal expulsion of the phosphenium [$^{i}Pr_2P$:]$^+$ which in presence of EtONa led to the corresponding phosphinite $^{i}Pr_2POEt$. It is Noteworthy that [Et_4N][Cl] was previously used as nucleophile to prepare the related (NHCCOP^{Ph})NiBr complex **12**.[4] All Ni(II) complexes were finally converted to their cationic counterparts by abstraction of the bromide co-ligand using a slight excess of AgOTf. Thus, cationic (PIMCOP)Ni(NCMe)(OTf) **16-17**, (NHCCOP)Ni(NCMe)(OTf) **12-13** and dicationic (PIMIOCOP)Ni(NCMe)(OTf) **10-11** complexes were isolated and fully characterized by classical methods (Scheme 7.1 and Table 7.1).

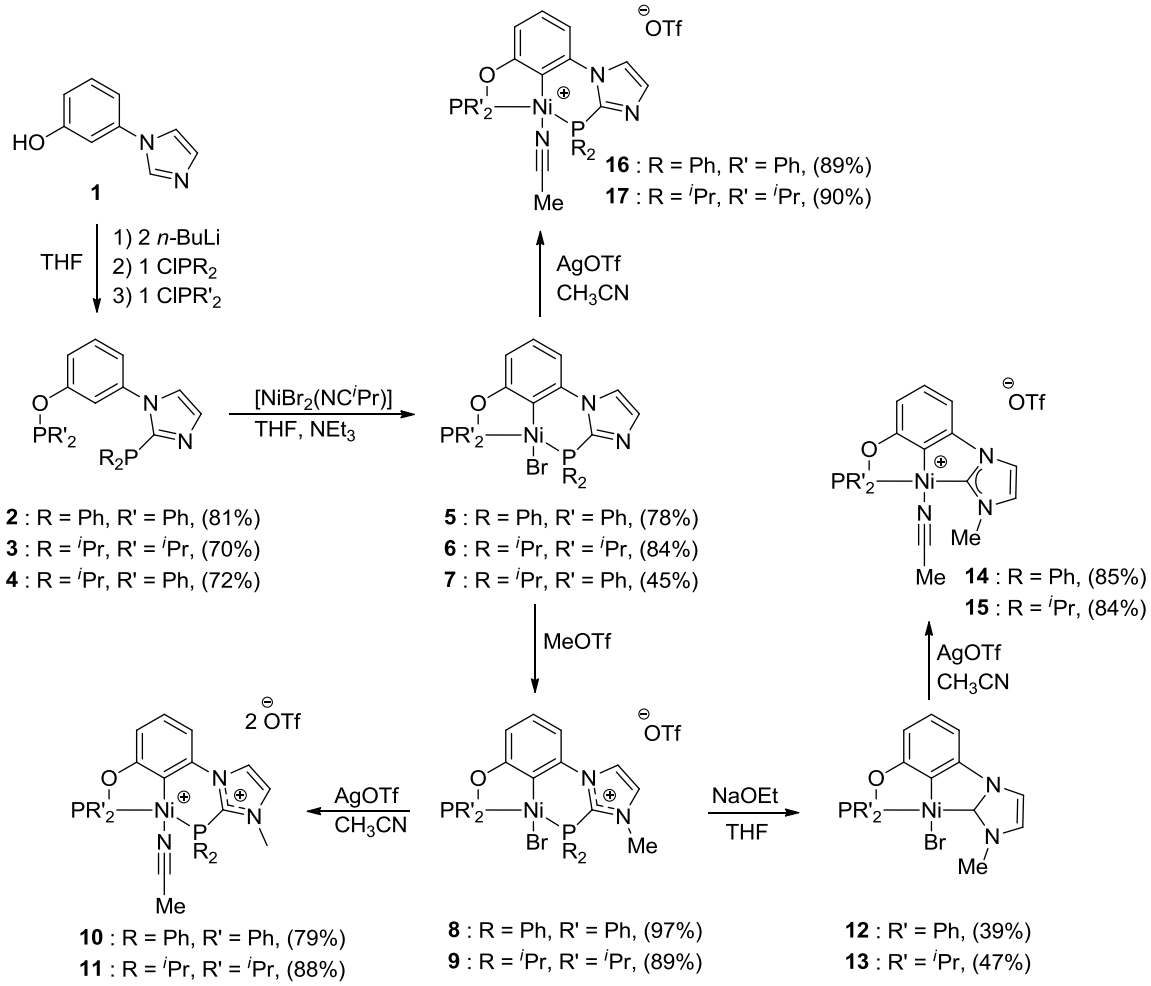

Scheme 7.1. Synthesis of (PIMCOP)-, (PIMIOCOP)- and (NHCCOP)NiX [X = Br, (NCMe)(OTf)] complexes from 3-methoxyphenyl-imidazole **1**.

To emphasize the difference of reactivity between cationic (PIMIOCOP)NiBr complexes bearing either PPh_2 (**8)** or P^iPr_2 (**9)** donor extremities, a competitive reaction was attempted (Scheme 7.2). For this purpose, in a NMR tube, **8** and **9** were mixed in an equimolar amount, in THF, and then treated with an equivalent of EtONa. After heating the mixture at 50 °C for one hour, ^{31}P NMR spectrum indicated the total convertion of **8** [δ_p = +11.1 (d); +147.0 (d) ppm] into the corresponding ($NHCCOP^{Ph}$) complex **12** [s, δ_p = +144 ppm (s)], while **9** remained unreacted [δ_p =

+4.3 (d); +149.7 (d) ppm].[7] The greater reactivity of (^{Ph}PIMIOCOP^{Ph})NiBr complex **8** toward a nucleophile with respect to its alkykated analogue **9** is in good agreement with the higher electrophilicity of the diphenylphosphenium [$Ph_2P{:}^+$] *vs.* [$^i Pr_2P{:}^+$] (Scheme 7.2).

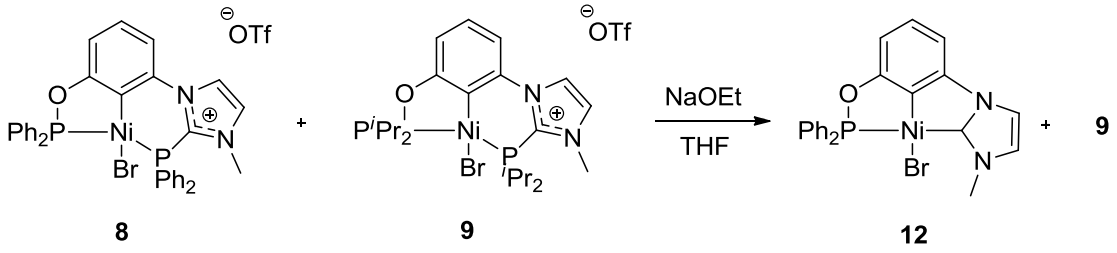

Scheme 7.2. Competitive reaction between (PIMIOCOP)NiBr pincer complexes **8** and **9** in presence of the nucleophile EtONa.

Spectroscopic Characterization. The NMR data of all new compounds are consistent with those of the previously reported derivatives (Table 7.1).[2] In the ^{31}P NMR spectra, two single resonances are observed for PIMCOP ligands **3-4**, with the O*P*R$_2$ moiety [+151.9 ppm (O*P*^{i}Pr$_2$); +113.6 ppm (O*P*Ph$_2$)] being significantly deshielded than the Im*P*^{i}Pr$_2$ fragment (*ca*. –14-15 ppm). After nickellation, (PIMCOP)NiBr complexes **6-7** display two ^{31}P doublets that are downfield [+183.9 ppm (O*P*^{i}Pr$_2$); +142.0 ppm (O*P*Ph$_2$); +12.5-15.4 ppm (Im*P*^{i}Pr$_2$)] of the signal of the corresponding precursor ligands **3-4**, with a large coupling constant ($^2J_{PP} \approx$ 305-330 Hz) characteristic of inequivalent, *trans*-located P-atoms. Quaternization of the *N*-imidazole ring resulted of a downfield shift of the ^{31}P signal of 21 ppm on the ImP^{i}Pr$_2$ moiety (from **6** to **9**). Noteworthy, only a deshielding of 8 ppm was observed on the ImP^{i}Ph$_2$ moiety (from **5** to **8**). Moreover, no significant difference on δ ^{31}P chemical shift values was observed between Ni(Br) complexes and their corresponding MeCN

adducts (Table 7.1). More generally, the impact of the presence of phenyl *vs.* isopropyl substituents R on δ^{31}P chemical shifts was found to be more effective on OPR_2 than on $ImPR_2$ moieties (the average of the difference of δ^{31}P values between ^{i}Pr and Ph substituents is indeed about 40 ppm for OPR_2 for only 16 ppm for $ImPR_2$).

Table 7.1. Yields (%) and δ^{31}P NMR chemical shifts (ppm) of ligands and complexes.

N°	Yield (%)	δ^{31}P NMR	N°	Yield (%)	δ^{31}P NMR
2	81[4]	–29 (s); 112 (s)	**10**	79	4 (d); 150 (d)
3	70	–14 (s); 151 (s)	**11**	88	31 (d); 194 (d)
4	72	–14 (s); 113 (s)	**12**	39[4]	145 (s)
5	78[4]	3 (d); 156 (d)	**13**	47	192 (s)
6	84	12 (d); 184 (d)	**14**	85	151 (s)
7	45	15 (d); 142 (d)	**15**	84	195 (s)
8	97[4]	11 (d); 147 (d)	**16**	89	1 (d); 149 (d)
9	89	33 (d); 185 (d)	**17**	90	17 (d); 193 (d)

In the ^{1}H NMR spectra, while all H-atoms appear in the aromatic regions for compounds of the phenyl series, isopropyl based-derivatives are clearly evidenced by the existence of a typical doublet of septet at $\delta_H \approx$ +2.5-3.0 ppm [$P(CHMe_2)_2$]. For (PIMIOCOP)NiX complexes, the presence of the *N*-CH_3 substituent is indicated by a single resonance at $\delta_H \approx$ +3.2 ppm. In the ^{13}C NMR spectra for ligands **2-3**, the C1 carbon atom which will be subsequently metallated, appears as a doublet of doublet at $\delta_C \approx$ +117-118 ppm. In contrast for (PIMCOP)- and (PIMIOCOP)NiBr complexes, the C1 carbon atom resonates at lower field as a pseudo-triplet (*ca*. +125-130 ppm).

The formation of NHCCOP complexes **13-15** is apparent by the presence of a doublet at *ca*. 172-175 ppm ($^2J_{PC} \approx$ 90-110 Hz), typical of Ni-bound NHC ligands.

IR data of acetonitrile adducts can offer an opportunity to estimate the overall donor character (σ-donor *vs*. π-accepting properties) of the pincer ligands. In all cases, $\nu_{(C\equiv N)}$ values of acetonitrile coordinated to cationic Ni(II) center appeared to be higher than that of the free molecule of about 37 cm^{-1} in average (Table 7.2). These values indicate that in all studied complexes ligand-to-metal σ-donation is more important than metal-to-ligand π-backbonding, confirming the electrophilicity of the Ni(II) center.[2c] Moreover, the $\nu_{(C\equiv N)}$ values found for complexes bearing -PPh_2 ends (**10**, **14** and **16**) higher than those of their analogues bearing -P^iPr_2 moieties (**11**, **15** and **17**) are in agreement with the more electron-donating character of the ^{i}Pr substituent relative to the Ph one. It is noteworthy that, the same trend was observed for previously reported (POCOP)Ni(NCMe)(OTf) complexes,[2c] however, direct comparison of the $\nu_{(C\equiv N)}$ values between (PIMCOP)-, (PIMIOCOP)- and (NHCCOP)Ni(NCMe) complexes tend to demonstrate that electronic factors can not alone explain these results, and that different steric requirement of PIMCOP, PIMIOCOP and NHCCOP backbones have to be also considered. Indeed, the ideal position of coordinated MeCN, *a priori* in trans to the phenylene ring (with C1–Ni–N ~ 180°) can be disturbed by the steric hindrance of the pincer ligand. Consequently, depending on the C1–Ni–N angle values (see Table 7.5), orbital overlap between MeCN and the Ni center would be more or less effective, affecting therefore the σ-donation of MeCN ligand, and the IR $\nu_{(C\equiv N)}$ values.

Table 7.2. IR data for complexes **10-11** and **14-17** and related compounds.

Complexes	ν (C≡N) (cm^{-1})	Δν (C≡N) (cm^{-1})
(^{Ph}PIMIOCOP^{Ph})Ni(NCMe) **10**	2291	38
(^{iPr}PIMIOCOP^{iPr})Ni(NCMe) **11**	2284	31
(NHCCOP^{Ph})Ni(NCMe) **14**	2299	46
(NHCCOP^{iPr})Ni(NCMe) **15**	2296	43
(^{Ph}PIMCOP^{Ph})Ni(NCMe) **16**	2287	34
(^{iPr}PIMCOP^{iPr})Ni(NCMe) **17**	2284	31
(^{Ph}POCOP^{Ph})Ni(NCMe) [2c]	2297	44
(^{iPr}POCOP^{iPr})Ni(NCMe) [2c]	2292	39
NCMe	2253	0

Electrochemical Measurements. As the oxidation potential (E_{ox}) of a complex can *a priori* reflect the electronic endowment of the corresponding ligand, all prepared Ni(II) pincer complexes were then investigated by cyclic voltammetry (Table 7.3). Thus, the observed order of the oxidation potentiels respect the expected trend *ca.* E_{ox} (NHCCOP)NiBr (~ +0.5 V) < (PIMCOP)NiBr (~ +0.8 V) < (PIMIOCOP)NiBr (~ +1.0 V). Moreover in all cases, the transformation of a neutral NiBr pincer complex to its cationic Ni(MeCN)(OTf) analogue resulted of an increase of the oxidation potential value of about +0.1 V. The oxidation potential values (~ +1.2 V) for (PIMIOCOP)Ni(NCMe)(OTf) complexes **10-11** which are dicationic in nature, demonstrate therefore the high electron deficiency on the Ni(II) center, presuming that they should be able to act as strong Lewis acids (Table 7.3). It is

noteworthy that direct comparison between Ni pincer complexes bearing PPh_2 and P^iPr_2 donor moieties indicate that the oxidation potential values do no depend only on the electronic factors of the P-substituent, but they can be also connected to steric considerations. Indeed, the expectation of P^iPr_2- representatives to be easily oxidized is not necessarily respected.

Table 7.3. Oxidation potentials (*vs*. $FeCp_2$) of Ni(II) pincer complexes **5-17.**

Complexes	E_{ox} (mV)	Reversibility
(^{Ph}PIMCOP^{Ph})NiBr **5**	820	No
(^{iPr}PIMCOP^{iPr})NiBr **6**	862	No
(^{iPr}PIMCOP^{Ph})NiBr **7**	834	No
(^{Ph}PIMIOCOP^{Ph})NiBr **8**	1120	No
(^{iPr}PIMIOCOP^{iPr})NiBr **9**	1001	No
(^{Ph}PIMIOCOP^{Ph})Ni(NCMe) **10**	1220	quasi
(^{iPr}PIMIOCOP^{iPr})Ni(NCMe) **11**	1195	No
(NHCCOP^{Ph})Ni(Br) **12**	500	quasi
(NHCCOP^{iPr})NiBr **13**	547	quasi
(NHCCOP^{Ph})Ni(NCMe) **14**	530	No
(NHCCOP^{iPr})Ni(NCMe) **15**	618	No
(^{Ph}PIMCOP^{Ph})Ni(NCMe) **16**	1020	No
(^{iPr}PIMCOP^{iPr})Ni(NCMe) **17**	966	No

Solid State Characterization.

Single crystals were grown for (PIMCOP)NiBr complexes **6-7**, and (NHCCOP)NiBr complex **13**, and their solid state structures were compared to those of the previously reported (PIMCOP)NiBr complex **5** and (NHCCOP)NiBr **12**, respectively (Figure 7.2 and Table 7.4).[8] In (PIMCOP)NiBr complexes **5-7**, the Ni(II) atom is located at the center of a distorted square-planar environment ($\Sigma° \approx 359\text{-}360°$) with the two P- centers being in mutual *trans*-position (Figure 7.2). It is noteworthy that for complexes **6-7** bearing bulkier ImP^iPr_2 donor extremities, the P1–Ni–P2 angle appeared to be significantly wider (*ca*. +5-6°). Otherwise, bonds length values are generally weakly influenced by the nature of the substituents, and only in **7**, the presence of the ImP^iPr_2 moiety results in the lengthening of the related Ni–P^iPr_2Im bond distance (*ca*. +0.03 Å) with respect to **5** bearing ImPPh_2 fragment. (NHCCOP)NiBr complexes **12-13** present also a distorted square-planar geometry ($\Sigma° \approx 359\text{-}360°$) with minimal structural variations according to the nature of the substituent. The longer Ni–P1 distance in NHCCOP derivatives **12-13** relative to PIMCOP representatives **5** and **7** (*ca*. 2.1451 and 2.1478 *vs*. 2.1322, 2.1339 and 2.1383) reflects the stronger *trans* influence of the NHC fragment (Table 7.4). The smaller bite angle P–Ni–C7 associated with the shorter Ni–C1 distance in NHC complexes **12-13** by contrast to PIMCOP analogues **5-7** results of the presence of a five membered structure in the carbene series.

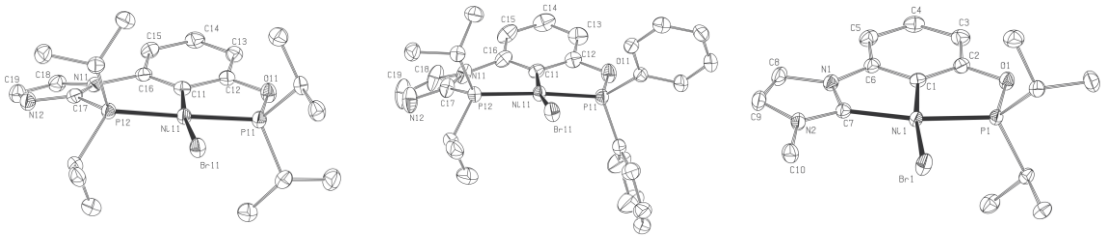

Figure 7.2. Molecular views of the X-ray crystal structures of neutral Ni(II) pincer complexes **6**, **7** and **13** with thermals ellipsoids drawn at the 50 % probability level (for clarity, hydrogen atoms are omitted).

Molecular structures of cationic pincer complexes **14** and **17**, revealed also a distorted square plane geometry (Σ° ≈ 359-360°) around the Ni center (Figure 7.3 and Table 7.5), with the acetonitrile ligand located in *trans* position to the central phenylene ring [**14**: C1–Ni–N = 177.5(2)°, Ni–N–C = 177.3(4)°; **17**: C1–Ni–N = 168.92(7)°, Ni–N–C = 172.4(2)°]. The strong distortion observed along the C1–Ni–N axis, especially in the cationic (^{iPr}PIMCOP^{iPr}) complex **17** (C1–Ni–N = 168.92(7)°) can explain the IR ν_{CN} values (see Table 7.2). Indeed, the weaker distortion observed in the NHC complex **14** (C1–Ni–N = 177.5(2)°) should induce a better orbital overlap between the cationic Ni center and the MeCN ligand, resulting in a better σ-donation of the latter. As previously, the Ni–P1 bond in the (NHCCOP)Ni(NCMe)(OTf) complex **14** (2.166(2) Å) is greater than that of the (POCOP)Ni(NCMe)(OTf) complex **17** (2.1572(5) Å) due to the stronger *trans* influence of the NHC moiety (Table 7.5). It is noteworthy that the general tendency of an acute bite angle P–Ni–C7 along with a short Ni–C1 bond in NHC complexes is also verified in the present case.

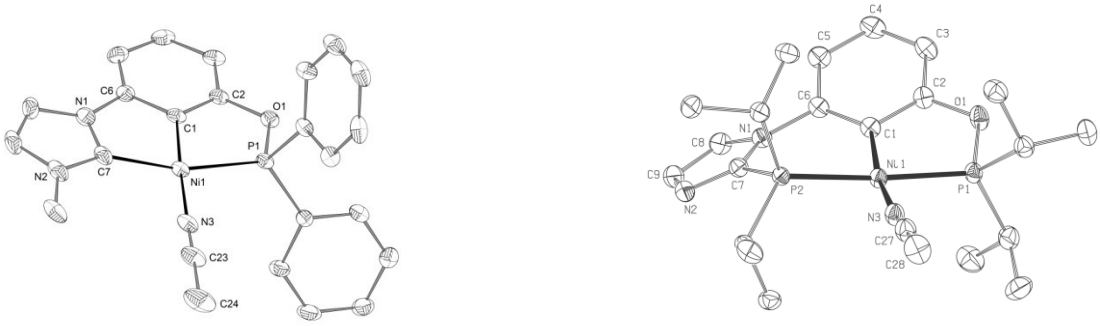

Figure 7.3. Molecular views of the X-ray crystal structures of cationic Ni(II) pincer complexes **14** (*left*) and **17** (*right*) with thermals ellipsoids at the 50 % probability level (for clarity, hydrogen atoms and triflate anion are omitted).

Table 7.4. Selected crystallographic data, bond lengths [Å] and bond angles [°] from X-ray diffraction studies of neutral Ni(II) complexes **5**, **6**, **7**, **12** and **13**.

	Ni–C1 *Ni-C11*	Ni–Br	Ni–P1	Ni–P2 *Ni–C7*	P1–Ni–P2 *P1–Ni–C7*	C1–Ni–Br
5	1.945(2)	2.3345(3)	2.1322(5)	2.169(2)	170.30(2)	170.68(5)
6	*1.939(3)*	2.3414(5)	2.1339(8)	2.1682(8)	176.60(3)	172.06(8)
7	*1.943(2)*	2.3404(5)	2.1383(7)	2.1985(7)	175.90(3)	169.54(8)
12	1.875(2)	2.3521(3)	2.1451(5)	*1.946(2)*	*161.21(6)*	174.82(6)
13	1.870(2)	2.3464(3)	2.1478(5)	*1.951(2)*	*162.31(6)*	173.14(6)

Table 7.5. Selected crystallographic data, bond lengths [Å] and bond angles [°] from X-ray diffraction studies of cationic Ni(II) complexes **14** and **17**.

	Ni–C1	Ni–N	Ni–P1	*Ni–C1* Ni–P2	*P1–Ni–C7* P1–Ni–P2	C1–Ni–N	Ni–N–C
14	1.876(4)	1.888(4)	2.166(2)	*1.943(5)*	*161.0(2)*	177.5(2)	177.3(4)
17	1.944(2)	1.882(2)	2.1572(5)	2.2005(5)	175.70(2)	168.92(7)	172.48(15)

Amidine Synthesis. Prepared cationic Ni(II) pincer complexes and the previously described (^{Ph}POCOP^{Ph})NiNCMe(OTf)[2c] were first investigated for the catalytic hydroamination of acrylonitrile (supporting information). Noteworthy, related cationic Ni(II) pincer complexes based on PCP- and POCOP backbones have been already reported to behave as pre-catalysts for the addition of aliphatic amines and aniline to activated acrylonitrile and its derivatives.[2]

Then, cationic Ni(II) pincer complexes were considered for the catalytic preparation of amidines by nucleophilic attack of amines at the nitrile moiety (Scheme 7.3). Amidines which represent formally the dinitrogen analogs of carboxylic acids and esters, display strong basicity, biological activity, and can be used as intermediates in the synthesis of functionalized heterocycles.[9] While different routes provide access to amidines,[10] reaction between a nitrile and an amine represent *a priori* the most straightforward strategy. It is noteworthy that only lanthanide complexes were shown to catalyze efficiently the formation of amidines from such simple precursors.[11] Otherwise, Lewis acids have to be used in a stoichiometric amount with the need of harsh conditions.[12] In the nickel series, an example of cationic pincer (POCOP)Ni(NCMe)(OTf)2[b] and a "pincer like" complex ($PN_{sp3}P$)Ni]$(BF_4)_2$[13] have

been recently evidenced to act as pre-catalysts for the nucleophilic addition of amines to nitriles. In the first case, morpholine was reacted to different cyano-olefins while in the second case the nucleophilic addition of piperidine to acetonitrile produced $HN=C(CH_3)NC_5H_{10}$. However, these encouraging results are very preliminary, and further study undoubtedly deserves to be undertaken. In a first time, catalytic experiments were realized in order to determine the most active cationic Ni(II) pincer complex for the addition of piperidine to benzonitrile. At 50 °C after 67 h of reaction, using an equimolar amount of reactants, with 1.0 % of pre-catalyst, and in solvent free condition, the (^{iPr}PIMIOCOP$^{iPr)}$Ni(NCMe)(OTf) complex **11** (entry 2, Table 7.6) was found to be the most active pre-catalyst (TON up to 30). Other pincer complexes bearing PIMCOP (**16-17**) and POCOP ligands were shown to present lower reactivity (entries 3-5, Table 7.6).

Table 7.6. Catalytic addition of piperidine to benzonitrile using different cationic Ni(II) pincer complexes.

Catalyst	Entry	Amine	TON
10	1	piperidine	13
11	2	piperidine	30
17	3	piperidine	8
16	4	piperidine	0
(^{Ph}POCOP^{Ph})NiNCMe	5	piperidine	2
No catalyst	6	piperidine	0

Reaction conditions: 1.0 % of catalyst, 50 °C, 67 h, 1 equiv. of benzonitrile, solvent free. Yields are determined by GC-MS with $C_{12}H_{26}$ as internal standard. Chemicals are used without any further purification.

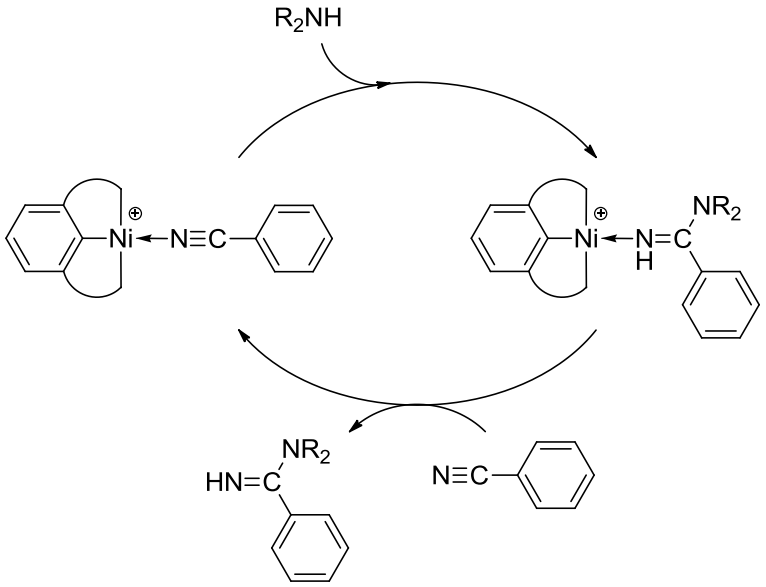

Scheme 7.3. Proposed catalytic cycle of the formation of amidines by addition of secondary amines to benzonitrile.

In a second time, optimization of the condition reactions was attempted by using the selected pre-catalyst **11**. While with a piperidine : benzonitrile ratio of 1:1, at 80 °C for 3 h with 1.0 % of **11**, the reaction yield remained poor (entry 1, Table 7.7), by increasing the reaction time to 21 h, the yield was improved to 49 % (entry 2). The use of 2 equiv. of piperidine relative to benzonitrile resulted in an improvement of the reaction yield (*ca*. 68 %) (entry 3). Moreover, by increasing the temperature reaction up to 100 °C, the piperidinobenzamidine was obtained in 72 % yield (entry 4). The best result was finally observed by using a higher catalytic loading of **11** (*ca*. 5 %, entry 5, Table 7.7) which allowed the isolation of the amidine product in 80 % yield.

Table 7.7. Optimization conditions for the synthesis of piperidinobenzamidine by using the cationic Ni(II) pincer complex **11**.

Entry	Catalyst (%)	Temperature (°C)	Time (h)	benzonitrile / piperidine	Yield	TON
1	1	80	3	1 : 1	13	13
2	1	80	21	1 : 1	49	49
3	1	80	21	1 : 2	68	68
4	1	100	21	1 : 2	72	72
5	5	80	21	1 : 2	80	16
6	10	80	21	1 : 2	68	14

Reaction Conditions: Pre-catalyst **11**, solvent free. Yields are determined by GC-MS with $C_{12}H_{26}$ as internal standard. Chemicals are used without any further purification.

The scope of the reaction was then investigated over a set of amine substrates (Table 7.8). As shown in Table 7.8, the nucleophilicity of the amine appeared to be the determinant factor for the formation of amidine products. Indeed, using the less nucleophilic morpholine resulted in a decrease of the yield (from 49 to 33 %, entries 1-2). Moreover, aromatic amines as aniline and diphenylamine were completely inert toward benzonitrile (entries 4-5). Despite the strong nucleophilicity of diisopropylamine, its steric hindrance prevented any coupling reaction (entry 3). Finally, primary amines such as *n*-hexylamine and cyclohexylamine were found to afford corresponding amidines in 33 % (entry 4) and 55% (entry 7) yield, respectively. In the latter case, the formation of *N,N'*-disubstituted amidines identified by GC-MS (*m/z*: 288 for *n*-hexylamine and *m/z*: 284 for cyclohexylamine) was

attributed to the second alkylation of benzamidine product followed by the elimination of ammonia. [11a]

Table 7.8. Screening of amidine synthesis from benzonitrile and various amines.

Entry	Amidine	Yield	Entry	Amidine	Yield
1	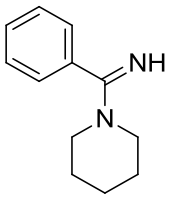	49	5	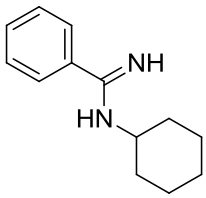	55[a]
2	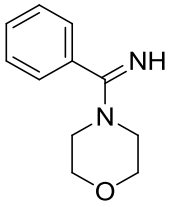	33	6	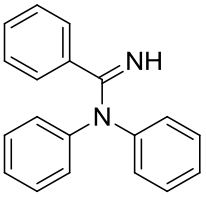	0
3	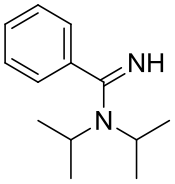	0	7	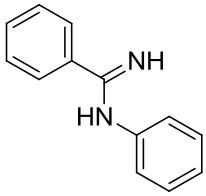	0
4	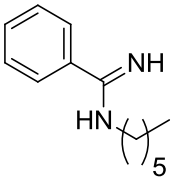	33[a]			

Reaction conditions: 1.0 % of pre-catalyst **11**, 80 °C, 21 h, 1 equiv. of benzonitrile, solvent free. Yields are determined by GC-MS with $C_{12}H_{26}$ as internal standard. [a] formation of *N,N′*-dialkylated amidine by-product. Chemicals are used without any further purification.

It is noteworthy that replacing benzonitrile by an unactivated nitrile such as acetonitrile resulted in a decrease of reactivity. Indeed, with a piperidine:acetonitrile

ratio of 1:1, at 80 °C for 48 h, with 1.0 % of **11**, only 3 % yield of amidine product was observed (after 5 days, yield was improved up to 10 %).

To determine the mechanism of amidine formation, the stability of the pre-catalyst **11** was first considered. For this purpose, **11** was dissolved in wet benzonitrile and 4 equiv. of piperidine were then added (Scheme 7.4). After 5 min. at room temperature, ^{31}P NMR spectrum indicated the desappearance of **11** [+194.2 ppm (O*P*iPr_2); +31.2 ppm (Im*P*iPr_2)] and the formation of two new compounds at δ_P = +187.0 (br s) and +54.1 ppm (s) attributed respectively to a cationic species **18** of general formula (NHCCOP^{iPr})NiL and [$^{i}Pr_2$P(O)H] corresponding to the oxidized form of the released diisopropylphosphenium. The presence of the NHCCOP backbone in **18** was also confirmed by ^{13}C NMR spectroscopy with the existence of a characteristic signal at δ_C = +173.9 ppm (J_{CP} = 99.5 Hz) for the Ni bonded carbenic center. The thermal stability of (NHCCOP^{iPr})NiL complex **18** was demonstrated by the persistence of the δ ^{31}P NMR signal after heating at 80 °C for 20 min. Moreover, monitoring by ^{31}P NMR spectroscopy, the addition of an excess of piperidine to the cationic (NHCCOP^{iPr})Ni(NCMe)(OTf) complex **15** in wet acetonitrile indicated the transformation of the sharp singlet of **15** (δ_P = +195.3 ppm) into the same previously observed singlet at δ_P = +187.0 ppm. Finally, **18** was tentatively attributed to the (NHCCOP^{iPr})Ni[HNC(Ph)N$(CH_2)_5$] complex. The same broad NMR signal was also observed when the previously prepared [HNC(Ph)N$(CH_2)_5$] amidine was added to the (NHCCOP^{iPr})Ni(NCMe)(OTf) complex **15** (Scheme 7.4). This proposal was confirmed by the observation of similar catalytic activity of complexes **11** and **15** for amidine synthesis [**11**: 49 % (entry 2, Table 7.8); **15**: 55 %].

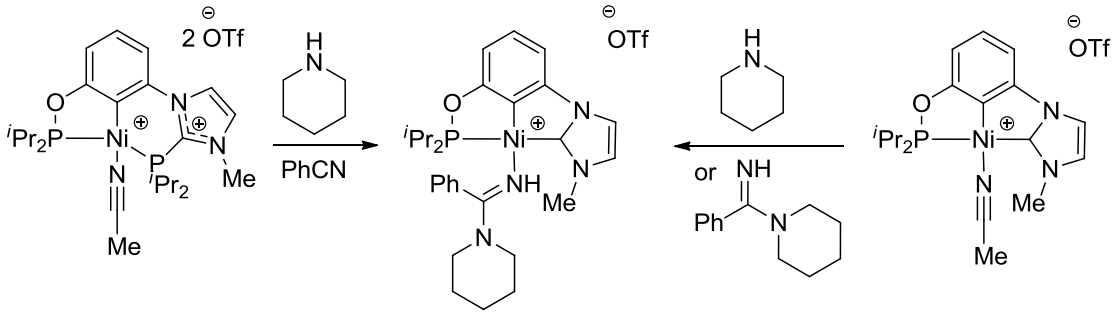

Scheme 7.4. Formation of (NHCCOP^{iPr})Ni[HNC(Ph)N(CH$_2$)$_5$] **18** from (PIMIOCOP)- and (NHCCOP)- pincer Ni(II) complexes **11** and **15**, respectively.

Rapid formation of the catalytic active species **18** was confirmed by a GC-MS monitoring where no induction period was observed for the catalyzed *N*-piperidino-benzamidine formation (Figure 7.4).

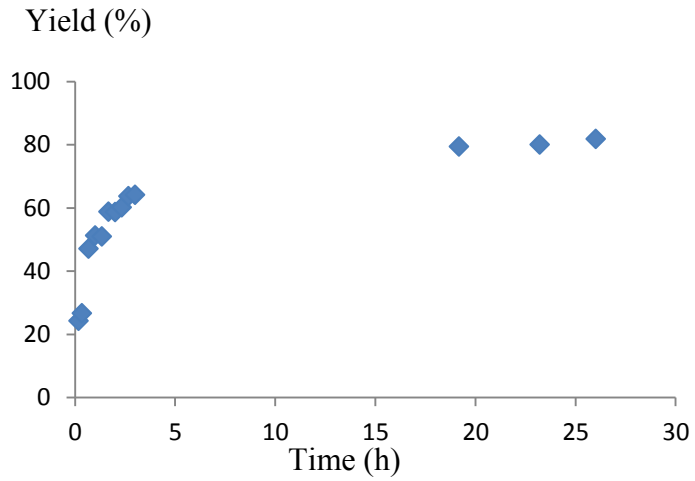

Figure 7.4. Formation of *N*-piperidino-benzamidine *vs*. time. Reaction conditions: 1.0 % of pre-catalyst, 2eq. of piperidine, 80 °C, solvent free. Yields are determined by GC-MS with $C_{12}H_{26}$ as internal standard.

7.4 Conclusion

The results described in the present study serve to highlight the differences in structural and spectroscopic properties of PIMCOP, PIMIOCOP and NHCCOP complexes of Ni(II) and the reactivities of their cationic derivatives in the amidination of nitriles. For instance, IR spectroscopic analysis based on of $\nu_{C\equiv N}$ values of the cations has demonstrated that PPh_2-based complexes show higher stretching frequencies relative to their P^iPr_2 analogues, this difference arising from the greater N→Ni σ-donation for the more electrophilic PPh_2 complexes. The greater electrophilicity of the latter derivatives also reflected in the more facile transformation of [(PIMIOCOP)NiBr][OTf] into (NHCCOP)NiBr. On the other hand, investigation of the catalytic amidination reactions using the cationic acetonitrile adducts has shown that the more electrophilic PPh_2 complexes are in fact less active than their *i*-Pr_2P counterparts. Another curious observation touches on the absence of a linear correlation between the oxidation potential E_{ox} of both charge-neutral bromo derivatives and cationic adducts, which varied in the order in order PIMIOCOP> PIMCOP> NHCCOP, versus the $\nu_{C\equiv N}$ values, which follow the order NHCCOP> PIMIOCOP > PIMCOP. In the case of [(PIMCOP)Ni($NCCH_3$)][OTf] for which a solid state structure was obtained, this counter-intuitive observation is attributed to a distortion of the C-N-Ni angle (169°) that likely decreases the extent of σ-donation by acetonitrile.

In terms of their catalytic activities in amidination of benzonitrile, the cationic pre-catalysts [(PIMIOCOP)Ni($NCCH_3$)][$OTf]_2$ proved to be significantly more active than their POCOP and PIMCOP analogues. Interestingly, it was found that these

PIMIOCOP complexes are readily converted into NHCCOP analogues during the catalysis, and it is the latter that appear to be the active catalysts in the presence of substrate (piperidine). The superior catalytic activities of the *in situ* generated NHCCOP cationic species can be attributed to their greater stability provided by the presence of NHC moiety. Optimization studies have allowed the formation of *N*-piperidino-benzamidine in 80% yield, but the range of amine substrates active in this reaction remains quite limited. Thus, diispropylamine and aromatic amines are unreactive, whereas primary amines lead to *N,N*-diamino products, the latter result being potentially interesting for opening the way for the development of catalytic synthesis of triazines.

7.5 Experimental Section

Unless otherwise indicated, all manipulations were carried out under nitrogen atmosphere using standard Schlenk and glove box techniques. All solvents were dried by passage through activated aluminum oxide columns (MBraun SPS) and freeze thaw-degassed. NEt_3 was dried by distillation over CaH_2. The reagents $ClP(i\text{-}Pr)_2$, $ClP(Ph)_2$, AgOTf, NaOEt and MeOTf, were purchased from Sigma-Aldrich and used without further purification. NMR spectra were recorded at 400 MHz (^1H) and 161.9 MHz (^{31}P) using a Bruker AV400rg spectrometer, or at 400 MHz (^1H) and 100.56 MHz ($^{13}C\{^1H\}$) using a Bruker ARX400 spectrometer. Chemical shift values are reported in ppm (δ) and referenced internally to the residual solvent signals (^1H and ^{13}C: 7.26 and 77.16 ppm for $CDCl_3$; 7.16 and 128.06 ppm for C_6D_6) or externally (^{31}P, H_3PO_4 in D_2O, $\delta = 0$). Coupling constants are reported in Hz. High Resolution

Mass Spectroscopy analyses were performed by the Centre Regional de Spectroscopie de Masse – Université de Montréal, and the Laboratoire de Chimie de Coordination du CNRS – Toulouse. The IR spectra were recorded on Bruker Alpha-P FTIR (4000-400 cm^{-1}). The elemental analyses were performed by the Laboratoire d'Analyse Elémentaire – Université de Montréal.

3-[2-(Diisopropylphosphanyl)-1H-imidazol-1-yl]phenyl diisopropylphosphinite, $P^{iPr}IMC^{H}OP^{iPr}$ (3): Drop-wise addition of *n*-BuLi (3.2 mL of a 2 M solution in cyclohexane, 6.4 mmol) to a solution of **1** (510 mg, 3.19 mmol) in THF (40 mL) at -78 °C gave a suspension, which was allowed to warm to room temperature for 1 h. After addition of $ClP(^{i}Pr)_2$ (1.15 mL, 7.02 mmol) at -78 °C, the solution was slowly warmed to room temperature. After evaporation of the solvent under vacuum, the crude residue was extracted with hexane (50 mL). Filtration and evaporation of the solvent under vacuum afforded the desired product as an orange oil (880 mg, 70%). ^{1}H NMR (C_6D_6, 25 °C): δ 0.95 (dd, J_{HH} = 7.2, J_{HP} = 15.9, 6H, CH_3), 1.00 (dd, J_{HH} = 6.8, J_{HP} = 15.3, 6H, CH_3), 1.10 (dd, J_{HH} = 7.0, J_{HP} = 10.6, 6H, CH_3), 1.16 (dd, J_{HH} = 6.9, J_{HP} = 12.0, 6H, CH_3), 1.73 (hd, J_{HH} = 2.8 and 7.1, 2H, CH), 2.44 (h, J_{HH} = 7.0, 2H, CH), 6.8 (dm, J_{HH} = 7.9, 1H, H_{Ar}), 6.85 (m, 1H, H_{Ar}), 6.98 (t, J_{HH} = 8.1, 1H, H_{Ar}), 7.13 (dm, J_{HH} = 8.3, 1H, H_{Ar}), 7.38 (d, J_{HH} = 0.9, 1H, H_{Ar}), 7.42 (m, 1H, H_{Ar}). ^{13}C NMR (C_6D_6, 25 °C): δ 17.7 (d, J_{CP} = 8.6, 2C, CH_3), 20.5 (d, J_{CP} = 18.4, 2C, CH_3), 20.4 (d, J_{CP} = 9.4, 2C, CH_3), 20.7 (d, J_{CP} = 18.5, 2C, CH_3), 25.7 (d, J_{CP} = 9.3, 2C, CH), 29.2 (d, J_{CP} = 18.5, 2C, CH), 118.8 (dd, J_{CP} = 4.8 and 7.1, 1C, CH_{Ar}), 119.0 (d, J_{CP} = 10.1, 1C, CH_{Ar}), 121.2 (d, J_{CP} = 3.9, 1C, CH_{Ar}), 123.7 (s, 1C, CH_{Ar}), 130.3 (s, 1C, CH_{Ar}), 131.6 (s, 1C, CH_{Ar}), 140.7 (s, 1C, C_{Ar}), 148.4 (d, J_{CP} = 20.6, 1C, C_{Ar}),

160.6 (d, J_{CP} = 9.2, 1C, C_{Ar}). $^{31}P\{^{1}H\}$ NMR (C_6D_6, 25 °C): δ -14.3 (s, P^{i}Pr$_2$), +150.9 (s, OP^{i}Pr$_2$). HRMS Calcd for $C_{21}H_{35}N_2OP_2NiBr^+$: 393.22191 found 393.22227.

3-[2-(Diisopropylphosphanyl)-1H-imidazol-1-yl]phenyl diphenylphosphinite, P$^{i\mathrm{Pr}}$IMC$^{\mathrm{H}}$OP$^{\mathrm{Ph}}$ (4):

Drop-wise addition of *n*-BuLi (5.94 mL of a 2 M solution in cyclohexane, 11.87 mmol) to a solution of **1** (950 mg, 5.94 mmol) in THF (75 mL) at -78 °C gave a suspension, which was allowed to warm to room temperature for 1 h. After addition of ClP(^{i}Pr)$_2$ (970 µL, 5.94 mmol) at -78 °C, the solution was warmed to room temperature for 1 h, and ClP(Ph)$_2$ (1.06 mL, 5.94 mmol) was added. After evaporation of the solvent under vacuum, the crude residue was extracted with toluene (70 mL). Filtration and evaporation of the solvent under vacuum afforded the desired product as a yellow oil (1.97 g, 72%). ^{1}H NMR ($CDCl_3$, 25 °C): δ 0.99 (m, 12H, CH_3), 2.29 (hd, J_{HH} = 7.0, J_{HP} = 1.5, 2H, CH), 7.01 (dm, 1H, H_{Ar}), 7.12 (m, 1H, H_{Ar}), 7.15 (m, 1H, H_{Ar}), 7.20 (dm, 1H, H_{Ar}), 7.32-7.42 (m, 8H, H_{Ar}), 7.57-7.61 (m, 4H, H_{Ar}). ^{13}C NMR ($CDCl_3$, 25 °C): δ 19.6 (d, J_{CP} =19.6, 2C, CH_3), 19.9 (d, J_{CP} =18.0, 2C, CH_3), 24.9 (d, J_{CP} = 8.3, 2C, CH_3), 117.9 (dd, J_{CP} = 8.2 and 3.5, CH_{Ar}), 118.9 (d, J_{CP} = 10.9, CH_{Ar}), 121.5 (d, J_{CP} = 4.2, CH_{Ar}), 123.2 (s, CH_{Ar}), 128.7 (d, J_{CP} = 7.2, 4C, CH_{Ar}), 129.7 (s, CH_{Ar}), 130.1 (s, 2C, CH_{Ar}), 130.4 (s, CH_{Ar}), 130.7 (d, J_{CP} = 22.7, 4C, CH_{Ar}), 139.5 (d, J_{CP} = 1.0, C_{Ar}), 140.3 (d, J_{CP} = 1.0, C_{Ar}), 147.6 (d, J_{CP} = 20.3, C_{Ar}), 157.6 (d, J_{CP} = 10.2, 1C, C_{Ar}). $^{31}P\{^{1}H\}$ NMR ($CDCl_3$, 25 °C): δ -14.5 (s, P^{i}Pr$_2$), +113.6 (s, OPPh$_2$). HRMS Calcd for $C_{27}H_{31}N_2OP_2^+$: 461.19061 found 461.19224. Anal. Calcd. for $C_{27}H_{30}N_2OP_2$ (460.49) : C, 70.42 ; H, 6.57 ; N, 6.08. Found: C, 70.38 ; H, 6.72 ; N, 5.92.

8-Bromo-7,7,9,9-tetraisopropyl-10-oxa-2,5-diaza-7λ5,9λ5-diphospha-8-nickelatetracyclo[6.6.1.02,6.011,15]pentadeca-1(14),3,5,11(15),12-pentaene-7,9-bis(ylium), ($P^{iPr}IMCOP^{iPr}$)NiBr (6): To a solution of **3** (1.05 g, 2.67 mmol) in THF (50 mL), NEt_3 (560 µL, 4.01 mmol) and $[NiBr_2(NC^iPr)]_n$ (923 mg, 3.21 mmol) were added. After stirring the mixture for 1 h at 45 °C, the solvent was removed under vacuum. Extraction of the crude residue with hexane (75 mL), filtration and evaporation of the filtrate gave the product as a yellow solid. Yellow crystals were obtained from a saturated hexane solution at -15 °C (880 mg, 84%). M.p. 80 °C. ^{1}H NMR (C_6D_6, 25 °C): δ 1.15 (dd, J_{HH} = 7.0, J_{HP} = 14.3, 6H, CH_3), 1.36 (dd, J_{HH} = 7.0, J_{HP} = 14.7, 6H, CH_3), 1.41 (dd, J_{HH} = 6.9, J_{HP} = 16.8, 6H, CH_3), 1.42 (dd, J_{HH} = 7.1, J_{HP} = 17.1, 6H, CH_3), 2.43 (hd, J_{HP} = 1.9, J_{HH} = 7.0, 2H, CH), 3.04 (m, 2H, CH), 6.63 (d, J_{HH} = 7.2, 1H, H_{Ar}), 6.87 (t, J_{HH} = 8.0, 1H, H_{Ar}), 6.9 (d, J_{HH} = 7.4, 1H, H_{Ar}), 7.17 (m, 1H, H_{Ar}), 7.32 (m, 1H, H_{Ar}). ^{13}C (C_6D_6, 25 °C): δ 17.2 (s, 2C, CH_3), 18.5 (s, 2C, CH_3), 18.6 (d, J_{CP} = 3.7, 2C, CH_3), 19.6 (d, J_{CP} = 3.8, 2C, CH_3), 26.2 (d, J_{CP} = 27.1, 2C, CH), 28.9 (dd, J_{CP} = 23.4 and 2.3, 2C, CH), 110.7 (d, J_{CP} = 13.1, 1C, CH_{Ar}), 114.0 (s, 1C, CH_{Ar}), 121.7 (s, 1C, CH_{Ar}), 125.2 (vt, J_{CP} = 21.8, 1C, C_{Ar}), 128.4 (s, 1C, CH_{Ar}), 132.8 (d, J_{CP} = 7.8, 1C, CH_{Ar}), 134.1 (d, J_{CP} = 56.6, 1C, C_{Ar}), 144.9 (d, J_{CP} = 6.5, 1C, C_{Ar}), 170.3 (dd, J_{CP} = 5.0 and 10.2, 1C, C_{Ar}). ^{31}P{^{1}H} NMR (C_6D_6, 25 °C): δ +12.5 (d, J_{PP} = 305.0, P^iPr_2), +183.9 (d, J_{PP} = 305.0, OP^iPr_2). Anal. Calcd. for $C_{21}H_{33}BrN_2NiOP_2$ (530.04): C, 47.59 ; H, 6.28 ; N, 5.29. Found: C, 47.78 ; H, 6.33 ; N, 5.24.

($P^{iPr}IMCOP^{Ph}$)NiBr (7): To a solution of **4** (640 mg, 1.39 mmol) in THF (50 mL), NEt_3 (252 µL, 1.81 mmol) and $[NiBr_2(NC^iPr)]_n$ (480 mg, 1.67 mmol) were added.

After stirring the mixture for 2 h at 50 °C, the solvent was removed under vacuum. Extraction of the crude residue with toluene (50 mL), filtration and evaporation of the filtrate gave the product as a yellow solid. Yellow crystals were obtained by slow evaporation from a saturated hexane solution (370 mg, 45%). M.p. 157 °C. ^{1}H NMR ($CDCl_3$, 25 °C): δ 1.35 (dd, J_{HH} = 7.1, J_{HP} = 15.0, 6H, CH_3), 1.38 (dd, J_{HH} = 7.0, J_{HP} = 17.0, 6H, CH_3), 2.95 (m, 2H, CH), 6.91 (d, J_{HH} = 7.8, 2H, CH), 7.15 (vt, J_{HH} = 7.8, 1H, H_{Ar}), 7.39 (s, 1H, H_{Ar}), 7.45-7.53 (m, 6H, H_{Ar}), 7.59 (s, 1H, H_{Ar}), 7.93-7.97 (m, 4H, H_{Ar}). ^{13}C NMR ($CDCl_3$, 25 °C): δ 18.4 (s, 2C, CH_3), 19.3 (d, J_{CP} = 3.3, 2C, CH_3), 25.7 (d, J_{CP} = 26.9, 2C, CH), 111.2 (d, J_{CP} = 14.3, 1C, CH_{Ar}), 114.1 (s, 1C, CH_{Ar}), 121.5 (s, 1C, CH_{Ar}), 124.6 (vt, J_{CP} = 22.2, 1C, C_{Ar}), 128.4 (s, 1C, CH_{Ar}), 128.4 (d, J_{CP} = 10.3, 4C, CH_{Ar}), 131.6 (s, 2C, CH_{Ar}), 132.1 (d, J_{CP} = 3.9, 1C, CH_{Ar}), 132.2 (d, J_{CP} = 3.4, 2C, C_{Ar}), 132.5 (d, J_{CP} = 11.6, 4C, CH_{Ar}), 133.2 (d, J_{CP} = 57.5, 1C, C_{Ar}), 143.9 (d, J_{CP} = 6.3, 1C, C_{Ar}), 167.6 (dd, J_{CP} = 4.5 and 18.2, 1C, C_{Ar}). ^{31}P{^{1}H} NMR ($CDCl_3$, 25 °C): δ +15.4 (d, J_{PP} = 330.4, P^iPr_2), +142.0 (d, J_{PP} = 330.4, $OPPh_2$). Anal. Calcd. for $C_{27}H_{29}BrN_2NiOP_2$ (598,08) : C, 54.22 ; H, 4.89 ; N, 4.68. Found: C, 54.30 ; H, 5.04 ; N, 4.53.

(P^{iPr}IMIOCOP^{iPr})NiBr (9): MeOTf (239 µL, 2.11 mmol) was added to a solution of **6** (1.12 g, 2.11 mmol) in CH_2Cl_2 (20 mL) at -78 °C. The mixture was allowed to warm to room temperature and stirred for 18 h. After evaporation of the solvent under vacuum, **9** was obtained as a yellow solid (1.3 g, 89%). M.p. 185 °C. ^{1}H NMR ($CDCl_3$, 25 °C): δ 1.36 (dd, J_{HH} = 6.9, J_{HP} = 15.0, 6H, CH_3), 1.46 (dd, J_{HH} = 6.7, J_{HP} = 17.6, 6H, CH_3), 1.48 (dd, J_{HH} = 7.0, J_{HP} = 17.5, 6H, CH_3), 1.53 (dd, J_{HH} = 7.1, J_{HP} = 17.9, 6H, CH_3), 2.67 (m, 2H, CH), 3.12 (m, 2H, CH), 4.38 (s, 3H, CH_3), 6.93 (d,

J_{HH} = 7.9, 1H, H_{Ar}), 7.0 (d, J_{HH} = 8.0, 1H, H_{Ar}), 7.24 (t, J_{HH} = 8.2, 1H, H_{Ar}), 8.00 (m, 1H, H_{Ar}), 8.23 (m, 1H, H_{Ar}). ^{13}C NMR ($CDCl_3$, 25 °C): δ 17.1 (s, 2C, CH_3), 18.4 (s, 2C, CH_3), 19.9 (d, J_{CP} = 2.9, 2C, CH_3), 20.3 (s, 2C, CH_3), 27.1 (d, J_{CP} = 19.6, 2C, CH), 29.0 (dd, J_{CP} = 25.1 and 1.9, 2C, CH), 40.8 (s, 1C, CH_3), 113.2 (d, J_{CP} = 12.9, 1C, CH_{Ar}), 116.0 (s, 1C, CH_{Ar}), 124.8 (vt, J_{CP} = 21.0, 1C, C_{Ar}), 125.3 (s, 1C, CH_{Ar}), 129.5 (s, 1C, CH_{Ar}), 131.0 (m, 1C, CH_{Ar}), 134.2 (s, 1C, C_{Ar}), 142.2 (d, J_{CP} = 7.7, 1C, C_{Ar}), 168.7 (dd, J_{CP} = 5.6 and 13.1, 1C, C_{Ar}). ^{31}P{^{1}H} NMR ($CDCl_3$, 25 °C): δ +32.6 (d, J_{PP} = 309.0, P(^{i}Pr)$_2$), +184.8 (d, J_{PP} = 309.0, OP(^{i}Pr)$_2$). ^{19}F ($CDCl_3$, 25 °C): δ -78.3 (s, CF_3). HRMS Calcd for $C_{22}H_{36}BrN_2NiOP_2^+$: 543.08303 found 543.08342. Anal. Calcd. for $C_{26}H_{44}BrF_3N_2NiO_4P_2S$ (694.15) : C, 39.80 ; H, 5.23 ; N, 4.04 ; S, 4.62. Found: C, 39.99 ; H, 5.17 ; N, 3.95 ; S, 5.33.

[(P^{Ph}IMIOCOP^{Ph})NiNCCH$_3$][OTf]$_2$ (10): A solution of **8** (320 mg, 0.38 mmol) and AgOTf (108 mg, 0.42 mmol) in CH_2Cl_2 (20 mL) was stirred at room temperature for 4 h. After filtration of the precipitate, evaporation of the solvent under vacuum, afforded **9** as a red solid (273 mg, 79%). Dec.p. 148-150 °C. ^{1}H NMR (CD_3CN, 25 °C): δ 8.10 (brs, 1H, H_{Ar}), 7.94-7.85 (m, 5H, H_{Ar}), 7.82-7.62 (m, 16H, H_{Ar}), 7.22 (t, J = 7.8, 1H, H_{Ar}), 7.04 (d, J = 8.1, 1H, H_{Ar}), 6.91 (d, J = 7.5, 1H, H_{Ar}), 3.44 (s, 3H, CH_3). ^{13}C NMR (CD_3CN, 25 °C): δ 165.2 (dd, J_{CP} = 3.8 and 15.1, C_{Ar}), 140.2 (d, J_{CP} = 11.3, C_{Ar}), 134.1 (d, J_{CP} = 13.8, CH_{Ar}), 133.6 (s, CH_{Ar}), 133.3 (s, CH_{Ar}), 131.4 (d, J_{CP} = 13.8 Hz, CH_{Ar}), 131.2 (d, J_{CP} = 46.5, C_{Ar}), 131.1 (d, J_{CP} = 45.3, C_{Ar}), 130.2 (d, J_{CP} = 10.1, CH_{Ar}), 130.1 (d, J_{CP} = 10.1, CH_{Ar}), 129.9 (s, CH_{Ar}), 129.7 (d, J_{CP} = 11.3, CH_{Ar}), 124.7 (s, CH_{Ar}), 121.5 (d, J_{CP} = 45.3, C_{Ar}), 119.7 (dd, J_{CP} = 22.6 and 30.2, C_{Ar}), 118.2 (s, CH_{Ar}), 114.7 (d, J_{CP} = 15.1, CH_{Ar}), 38.7 (s, CH_3). ^{31}P NMR (CD_3CN, 25°C): δ

+149.7 (d, J_{PP} = 301.8, P1), +4.3 (d, J_{PP} = 301.8, P2). MS (ES): *m/z*: 749.1 [M + CF_3SO_3]$^+$. HRMS (ES): Calcd for $C_{35}H_{28}N_2O_4F_3P_2SNi$ 749.0551; found, 749.0571. IR (solid state, cm^{-1}): 1024, 1102, 1154, 1221, 1239, 1438, 1483, 1587, 2291.

[(P$^{i\mathrm{Pr}}$IMIOCOP$^{i\mathrm{Pr}}$)Ni(NCCH$_3$)][OTf]$_2$ (11): A solution of **9** (0.87 g, 1.25 mmol) and AgOTf (386 mg, 1.5 mmol) in CH_3CN (20 mL) was stirred at room temperature for 2 h. After filtration of the precipitate, evaporation of the solvent under vacuum, afforded **11** as a yellow powder (975 mg, 88%). Dec.p. 130 °C. ^{1}H NMR (CD_3CN, 25 °C): 1.26-1.38 (m, 12H, CH_3), 1.41-1.55 (m, 12H, CH_3), 2.47 (m, 2H, CH), 2.77 (m, 2H, CH), 4.27 (s, 3H, CH_3), 6.81 (d, J_{HH} = 7.7, 1H, H_{Ar}), 6.88 (d, J_{HH} = 8.0, 1H, H_{Ar}), 7.23 (t, J_{HH} = 7.9, 1H, H_{Ar}), 7.28 (m, 1H, H_{Ar}), 7.73 (m, 1H, H_{Ar}). ^{13}C NMR (CD_3CN, 25 °C): δ 16.5 (d, J_{HH} = 2.9, 2C, CH_3), 17.4 (d, J_{HH} = 5.1, 2C, CH_3), 18.6 (d, J_{CP} = 3.8, 2C, CH_3), 19.3 (d, J_{HH} = 1.5, 2C, CH_3), 25.3 (d, J_{CP} = 16.1, 2C, CH), 29.7 (dd, J_{CP} = 5.1 and 18.9, 2C, CH), 39.7 (s, 1C, CH_3), 114.4 (dd, J_{CP} = 1.4 and 14.4, 1C, CH_{Ar}), 117.6 (dd, J_{CP} = 23.1 and 26.5, 1C, CH_{Ar}), 118.9 (m, 1C, CH_{Ar}), 122.0 (d, 1C, J_{CP} = 321.0, C_{Ar}), 125.6 (d, 1C, J_{CP} = 1.3, CH_{Ar}) 130.6 (d, 1C, J_{CP} = 16.1, CH_{Ar}), 136.3 (dd, J_{CP} = 8.3 and 2.2, 1C, C_{Ar}), 142.0 (d, J_{CP} = 8.2 , 1C, C_{Ar}), 167.8 (dd, J_{CP} = 4.1 and 11.8, 1C, C_{Ar}). ^{31}P{^{1}H} NMR (CD_3CN, 25 °C): δ +31.2 (d, J_{PP} = 250.0, P(^{i}Pr)$_2$), +194.2 (d, J_{PP} = 250.0, OP(^{i}Pr)$_2$). ^{19}F (CD_3CN, 25 °C): δ -77.7 (s, C*F*$_3$). IR (solid state, cm^{-1}): 1026 (SO_3), 1149 (CF_3), 1242 (SO_3), 1447 (C=C_{Ar}), 1580 (C=CAr), 2284 (N≡C). HRMS (ES): Calcd for $C_{24}H_{39}N_3OP_2Ni$ 252.59554; found, 252.5967; Anal. Calcd. for $C_{26}H_{39}F_6N_3NiO_7P_2S_2$ (804.37): C, 38.82 ; H, 4.89 ; N, 5.22 ; S, 7.97. Found: C, 38.30 ; H, 4.87 ; N, 5.33 ; S, 8.09.

1-Bromo-12-methyl-2,2-diisopropyl-3-oxa-9,12-diaza-2λ5phospha-1-nickelatetracyclo[6.5.1.04,14.09,13] tetradeca-1(13),4(14),5,7,10-pentaen-2-ylium, (NHCCOP^{iPr})NiBr (13): NaOEt (92 mg, 1.35 mmol) and **9** (626 mg, 0.90 mmol) were dissolved in THF (50 mL) and stirred at 55 °C for 18 h. Evaporation of the solution to dryness followed by purification of the remaining solid by flash chromatography on silica gel (toluene) gave a yellow solid. Yellow crystals were obtained from a saturated hexane solution at -15 °C (183 mg, 47%). M.p. 181 °C. ^{1}H ($CDCl_3$, 25 °C): δ 1.33 (dd, J_{HH} = 7.0, J_{HP} = 14.0, 6H, CH_3), 1.47 (dd, J_{HH} = 7.2, J_{HP} = 17.1, 6H, CH_3), 2.46 (o, $J_{HH} = J_{HP}$ = 6.9, 2H, CH), 4.08 (s, 3H, CH_3), 6.50 (d, J_{HH} = 8.0, 1H, H_{Ar}), 6.57 (d, J_{HH} = 7.6, 1H, H_{Ar}), 6.75 (vt, J_{HH} = 1.5, 1H, H_{Ar}), 6.99 (vtd, J_{HH} = 6.9, 1H, H_{Ar}), 7.16 (d, J_{HH} = 1.6, 1H, H_{Ar}). ^{1}H {^{31}P} (25 °C, $CDCl_3$): δ 1.35 (d, J_{HH} = 7.0, 6H, CH_3), 1.48 (d, J_{HH} = 7.3, 6H, CH_3), 2.47 (h, J_{HH} = 7.1, 2H, CH), 4.10 (s, 3H, CH_3), 6.51 (d, J_{HH} = 7.8, 1H, H_{Ar}), 6.58 (d, J_{HH} = 7.6, 1H, H_{Ar}), 6.76 (d, J_{HH} = 1.8, 1H, H_{Ar}), 6.98 (vt, J_{HH} = 6.9, 1H, H_{Ar}), 7.17 (d, J_{HH} = 7.2, 1H, H_{Ar}). ^{13}C NMR ($CDCl_3$, 25 °C): δ 16.9 (s, 2C, CH_3), 18.1 (d, J_{CP} = 4.8, 2C, CH_3), 27.9 (d, J_{CP} = 19.6, 2C, CH), 37.9 (s, 1C, CH_3), 104.7 (s, 1C, CH_{Ar}), 108.5 (d, J_{CP} = 12.3, 1C, CH_{Ar}), 113.3 (s, 1C, CH_{Ar}), 122.7 (d, J_{CP} = 4.9, 1C, CH_{Ar}), 127.1 (s, 1C, CH_{Ar}), 134.7 (d, J_{CP} = 31.3, 1C, C_{Ar}), 148.2 (d, J_{CP} = 3.3, 1C, C_{Ar}), 167.7 (d, J_{CP} = 13.7, 1C, C_{Ar}), 174.9 (d, J_{CP} = 104.3, 1C, C_{Ar}). ^{31}P{^{1}H} ($CDCl_3$, 25 °C): δ +191.6 (s, OP(^{i}Pr)$_2$). Anal. Calcd. for $C_{16}H_{22}BrN_2NiOP$ (427.93): C, 44.91 ; H, 5.18 ; N, 6.55. Found: C, 45.16 ; H, 5.13 ; N, 6.48.

[(NHCCOP^{Ph})NiNCCH$_3$][OTf] (14): A solution of **12** (75 mg, 0.15 mmol) and AgOTf (43 mg, 0.16 mmol) in CH_2Cl_2 (5 mL) was stirred at room temperature for 4

h. After filtration of the precipitate, evaporation of the solvent under vacuum afforded **14** as a yellow solid (72 mg, 85%). Recrystallization in CH_3CN at -20 °C gave yellow crystals. Dec.p. 198-200 °C. ^{1}H NMR (CD_3CN, 25°C): δ 7.86-7.82 (m, 4H, H_{Ar}), 7.74-7.71 (m, 2H, H_{Ar}), 7.67-7.63 (m, 4H, H_{Ar}), 7.50 (d, J = 1.7, 1H, H_{Ar}), 7.16 (t, J = 8.4, 1H, H_{Ar}), 7.08 (t, J = 1.8, 1H, H_{Ar}), 6.89 (d, J = 7.7, 1H, H_{Ar}), 6.70 (d, J = 8.0, 1H, H_{Ar}), 3.81 (s, 3H, CH_3). ^{13}C NMR (CD_3CN, 25°C): δ 172.2 (d, J_{CP} = 101.9, C_{Ar}), 166.1 (d, J_{CP}= 16.3, C_{Ar}), 148.5 (d, J_{CP}= 2.5, C_{Ar}), 133.0 (s, CH_{Ar}), 131.5 (d, J_{CP}= 13.8, CH_{Ar}), 130.9 (d, J_{CP}= 45.3, C_{Ar}), 130.8 (d, J_{CP}= 31.4, C_{Ar}), 130.0 (s, CH_{Ar}), 129.5 (d, J_{CP} = 10.1, CH_{Ar}), 124.1 (d, J_{CP} = 3.8 Hz, CH_{Ar}), 114.9 (s, CH_{Ar}), 109.8 (d, J_{CP} = 13.8, CH_{Ar}), 106.9 (s, CH_{Ar}), 36.7 (s, CH_3). ^{31}P NMR (CD_3CN, 25°C): δ = +150.7 ppm. MS (ES): *m/z*: 415.05 $[M]^+$. HRMS (ES): Calcd for $C_{22}H_{18}N_2OPNi$ 415.0510; found, 415.0501. IR (solid state, cm^{-1}): 1030, 1109, 1154, 1260, 1475, 1577, 2299.

[(NHCCOP^{iPr})NiNCCH$_3$][OTf] (15): A solution of **13** (42 mg, 0.1 mmol) and AgOTf (28 mg, 0.11 mmol) in CH_3CN (5 mL), was stirred at room temperature for 2 h. After evaporation of the solvent under vacuum, the crude residue was extracted with CH_2Cl_2. Filtration of the precipitate and evaporation of the solvent under vacuum afforded **15** as a orange powder (45 mg, 84%). ^{1}H NMR ($CDCl_3$, 25 °C): δ 1.26 (dd, J_{HH} = 6.9, J_{HP} = 14.3, 6H, CH_3), 1.33 (dd, J_{HH} = 7.2, J_{HP} = 18.3, 6H, CH_3), 2.32 (m, 3H, $NCCH_3$,), 2.37 (m, 2H, CH), 3.77 (s, 3H, CH_3), 6.46 (d, J_{HH} = 8.1, 1H, H_{Ar}), 6.62 (d, J_{HH} = 7.6, 1H, H_{Ar}), 6.90 (s, 1H, H_{Ar}), 6.99 (vt, J_{HH} = 7.7, 1H, H_{Ar}), 7.21 (s, 1H, H_{Ar}). ^{13}C NMR ($CDCl_3$, 25 °C): δ 3.9 (bs, 1C, NC*C*H_3), 16.8 (d, J_{CP} = 1.3, 2C, CH_3), 17.6 (d, J_{CP} = 5.9, 2C, CH_3), 28.3 (d, J_{CP} = 20.5, 2C, CH), 37.3 (s, 1C, CH_3), 105.8 (s,

1C, CH_{Ar}), 109.5 (d, J_{CP} = 12.6, 1C, CH_{Ar}), 114.4 (s, 1C, CH_{Ar}), 123.8 (d, J_{CP} = 3.7, 1C, CH_{Ar}), 129.1 (d, J_{CP} = 29.1, 1C, C_{Ar}), 129.5 (s, 1C, CH_{Ar}), 148.3 (d, J_{CP} = 2.9, 1C, C_{Ar}), 168.2 (d, J_{CP} = 11.7, 1C, C_{Ar}), 172.9 (d, J_{CP} = 92.9, 1C, C_{Ar}). $^{31}P\{^{1}H\}$ ($CDCl_3$, 25 °C): δ +195.3 (s, $OP(^{i}Pr)_2$). ^{19}F NMR ($CDCl_3$, 25 °C): δ -77.0 (s, CF_3). IR (solid state, cm^{-1}): 1025 (SO_3), 1153 (CF_3), 1242 (SO_3), 1452 ($C{=}C_{Ar}$), 1593 (C=CAr), 2296 (N≡C). HRMS (ES): Calcd for $C_{18}H_{25}N_3OP_2Ni$ 388.10832; found, 388,10833.

[($P^{Ph}IMCOP^{Ph}$)NiNCCH$_3$][OTf] (16): A solution of **5** (355 mg, 0.53 mmol) and AgOTf (150 mg, 0.58 mmol) in CH_2Cl_2 (20 mL) was stirred at room temperature for 6 h. After filtration of the precipitate, evaporation of the solvent under vacuum afforded **16** as a red powder (348 mg, 89%). Dec.p. 188-190 °C. ^{1}H NMR (CD_3CN, 25 °C): δ 7.90-7.85 (m, 5H, H_{Ar}), 7.77-7.74 (m, 2H, H_{Ar}), 7.71-7.68 (m, 4H, H_{Ar}), 7.59-7.39 (m, 10H, H_{Ar}), 7.39 (s, 1H, H_{Ar}), 7.12 (t, J = 7.9, 1H, H_{Ar}), 6.90 (d, J = 7.9, 1H, H_{Ar}), 6.85 (d, J = 7.9, 1H, H_{Ar}). ^{13}C NMR (CD_3CN, 25 °C): δ 165.5 (dd, J_{CP} = 3.8 and 17.6, C_{Ar}), 141.7 (d, J_{CP} = 8.8, C_{Ar}), 133.5 (d, J_{CP} = 11.3, CH_{Ar}), 132.9 (d, J_{CP} = 1.3, CH_{Ar}), 132.4 (d, J_{CP} = 7.5, CH_{Ar}), 132.2 (d, J_{CP} = 2.5, CH_{Ar}), 131.7 (dd, J_{CP} = 43.4 and 5.7, C_{Ar}), 131.3 (d, J_{CP} = 12.6, CH_{Ar}), 130.1 (br s, C_{Ar}), 129.5 (d, J_{CP} = 11.3, CH_{Ar}), 129.4 (d, J_{CP} = 11.3, CH_{Ar}), 129.3 (s, CH_{Ar}), 125.5 (d, J_{CP} = 47.8, C_{Ar}), 123.6 (s, CH_{Ar}), 119.4 (dd, J_{CP} = 21.4 and 30.2, C_{Ar}), 116.6 (s, CH_{Ar}), 112.9 (d, J_{CP} = 13.8, CH_{Ar}). $^{31}P\{^{1}H\}$ NMR (CD_3CN, 25 °C): δ +0.6 (d, J_{PP} = 299.5, P2), +149.1 (d, J_{PP} = 299.5, P1). MS (ES): *m/z*: 585.1 $[M]^+$. HRMS Calcd for $C_{33}H_{25}N_2OP_2Ni$: 585.0796 found 585.0833. IR (solid state, cm^{-1}): 1024, 1102, 1150, 1258, 1437, 1482, 1585, 2287.

[(P^{iPr}IMCOP^{iPr})NiNCCH$_3$][OTf] (17): A solution of **6** (119 mg, 0.22 mmol) and AgOTf (63 mg, 0.25 mmol) in CH_3CN (5 mL) was stirred at room temperature for 2 h. After evaporation of the solvent under vacuum, the crude residue was extracted with CH_2Cl_2. Filtration of the precipitate and evaporation of the solvent under vacuum afforded **17** as a red powder (129 mg, 90%). M.p. 87 °C. ^{1}H NMR ($CDCl_3$, 25 °C): δ 1.20-1.29 (m, 18H, CH_3), 1.41 (dd, J_{HH} = 7.1, J_{HP} = 18.8, 6H, CH_3), 2.57 (m, 5H, CH and $NCCH_3$), 2.85 (m, 2H, CH), 6.76 (d, J_{HH} = 7.8, 1H, H_{Ar}), 6.81 (d, J_{HH} = 7.8, 1H, H_{Ar}), 7.14 (vt, J_{HH} = 7.8, 1H, H_{Ar}), 7.47 (s, 1H, H_{Ar}), 7.59 (s, 1H, H_{Ar}). ^{13}C NMR ($CDCl_3$, 25 °C): δ 16.8 (d, J_{CP} = 2.0, 2C, CH_3), 17.5 (d, J_{CP} = 4.9, 2C, CH_3), 18.7 (s, 2C, CH_3), 18.8 (d, J_{CP} = 3.6, 2C, CH_3), 25.4 (d, J_{CP} = 23.9, 2C, CH), 28.3 (dd, J_{CP} = 20.5 and 3.1, 2C, CH), 112.5 (d, J_{CP} = 13.1, 1C, CH_{Ar}), 115.8 (s, 1C, CH_{Ar}), 116.9 (dd, J_{CP} = 20.8 and 23.2, 1C, C_{Ar}), 123.3 (s, 1C, CH_{Ar}), 130.7 (s, 1C, CH_{Ar}), 131.2 (d, J_{CP} = 59.5, 1C, CH_{Ar}), 133.6 (s, 1C, C_{Ar}), 142.9 (d, J_{CP} = 7.6, 1C, C_{Ar}), 168.6 (dd, J_{CP} = 4.0 and 11.4, 1C, C_{Ar}). ^{31}P{^{1}H} NMR ($CDCl_3$, 25 °C): δ +16.6 (d, J_{PP} = 247.4, P(^{i}Pr)$_2$), +193.4 (d, J_{PP} = 247.4 , OP(^{i}Pr)$_2$). ^{19}F NMR ($CDCl_3$, 25 °C): δ -77.6 (s, CF_3). IR (solid state, cm^{-1}): 1026 (SO_3), 1149 (CF_3), 1242 (SO_3), 1447 (C=C_{Ar}), 1580 (C=C_{Ar}), 2284 (N≡C). HRMS (ES): Calcd for $C_{23}H_{36}N_3OP_2Ni$ 490.16816; found, 490.17036

Typical Procedure for Hydroamination Reactions (supporting information). In a screw-capped vial, a solution of catalyst in THF (1 mL of 0.02 M solution, 0.02 mmol), acrylonitrile (131 µL, 2 mmol), aniline (182 µL, 2 mmol) and dodecane as internal standard (45.3 µL, 0.2 mmol) was stirred at 50 °C for 3 h (all reactants were

dried before use). A sample of the solution was then analysed by GC-MS to identify the products and determine the yield using a previously prepared calibration curve.

Typical Procedure for Amidine Synthesis. In a vial, the catalyst (0.025 mmol), benzonitrile (255 µL, 2.5 mmol), piperidine (247 µL, 2.5 mmol) and dodecane as the internal standard (57 µL, 0.25 mmol) were stirred at 80 °C for 21 h (all reactants were used without further purification). A sample of the solution was then analysed by GC-MS to identify the products and determine the yield using a previously prepared calibration curve. In a higher scale (16.7 mmol of benzonitrile), the product was isolated as following: volatiles of the reaction mixture were evaporated under vacuum at room temperature. The mixture was then diluted with CH_2Cl_2 (20 mL), and washed with an aqueous solution of $NaHCO_3$ (50 mL). After washing the aqueous phase with CH_2Cl_2 (2 x 30 mL), organic phases were combined and extracted again with an aqueous solution of $NaHCO_3$ (2 x 30 mL). The combined aqueous phases were basified to pH ~ 14 by addition of a NaOH solution and then extracted with CH_2Cl_2 (3 x 60 mL). Organic phases were finally combined, dried over $MgSO_4$, filtered and evaporated, affording a pale yellow oil (1.1g, 35%). ^{1}H NMR ($CDCl_3$, 25 °C): δ 7.30 (m, 5H, H_{Ar}), 6.26 (s, 1H, NH), 3.29 (m, 4H), 1.59-1.52 (m, 6H). ^{13}C NMR ($CDCl_3$, 25 °C): δ 169.6, 138.7, 128.8, 128.4, 126.6, 46.9, 25.7, 24.6. ^{1}H and ^{13}C NMR spectra of *N*-piperidino-benzamidine are available in the supporting information.

Crystal Structure Determinations. The crystallographic datas for compounds **6**, **13** and **17** were collected on a Bruker APEX II equipped with an Incoatec I\muS Microsource and a Quazar MX monochromator. The crystallographic data for compound **7** was collected on a Bruker Microstar generator (micro source) equipped

with a Helios optics, a Kappa Nonius goniometer, and a Platinum135 detector. Cell refinement and data reduction were done using SAINT.[14] An empirical absorption correction, based on the multiple measurements of equivalent reflections, was applied using the program SADABS.[15] The space group was confirmed by XPREP routine[16] in the program SHELXTL.[17] The structures were solved by direct methods and refined by fullmatrix least-squares and difference Fourier techniques with SHELX-97.[18] All non-hydrogen atoms were refined with anisotropic displacement parameters. Hydrogen atoms were set in calculated positions and refined as riding atoms with a common thermal parameter.

Cyclic Voltammetry Experiments. Cyclic voltammetry measurements were performed using a SP50 BioLogic Science Instrument potentiostat. A typical three-electrode system consisting of a graphite working electrode, a Pt auxiliary electrode, and a Ag/AgCl reference electrode was employed. The experiments were carried out at room temperature at 100mV/s on analyte solutions prepared in dry CH_2Cl_2 containing [*n*-Bu_4N][PF_6] as electrolyte (0.1 M). The samples were bubbled with nitrogen before each experiment. Under the experimental conditions of our studies, the redox potential ($E_{1/2}$) for the Cp_2Fe^+/Cp_2Fe couple was +0.43 V.

7.6 Acknowledgments

The authors are grateful to: NSERC of Canada for a Discovery Grant to D.Z.; Université de Montréal, Centre in Green Chemistry and Catalysis (CGCC) and Fonds de recherche du Québec - Nature et technologies (FQRNT) for graduate fellowships to B.V.; Dr. Michel Simard for its valuable assistance with crystallography. The

authors thanks also the French Ministère de l'Enseignement Supérieur de la Recherche et de la Technologie, the Université Paul Sabatier in Toulouse, and the Centre National de la Recherche Scientifique (CNRS).

7.7 Supporting information

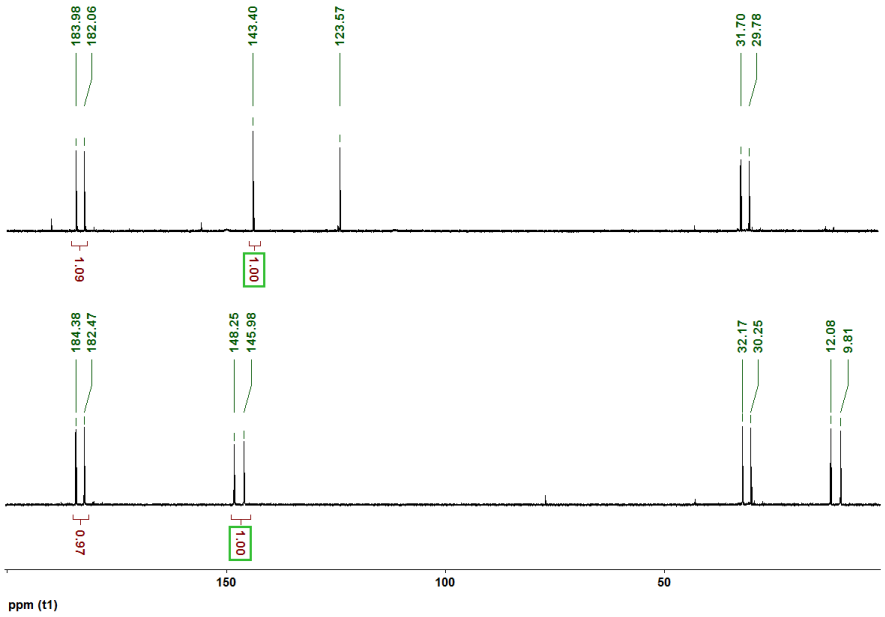

Figure 7.5. ^{31}P NMR spectra of competition reaction between a mixture of **7** and **8** (below) and after addition of NaOEt (above) in THF (162 MHz).

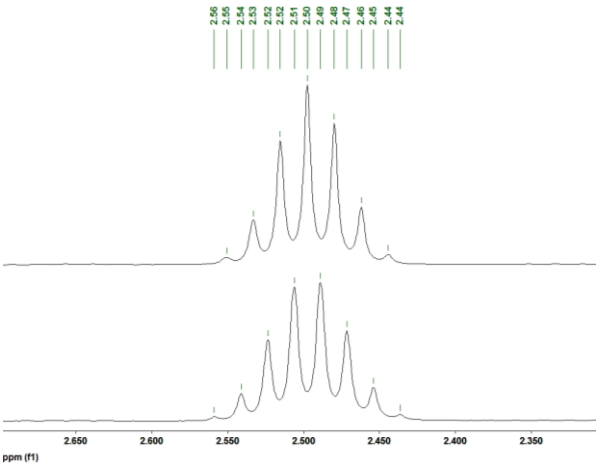

Figure 7.6. ^{1}H NMR spectra (below) and ^{1}H{^{31}P } NMR spectra (above) of Me_2CH-signal of (NHCCOP^{iPr})Ni(Br) complexe ($CDCl_3$, 400Mz).

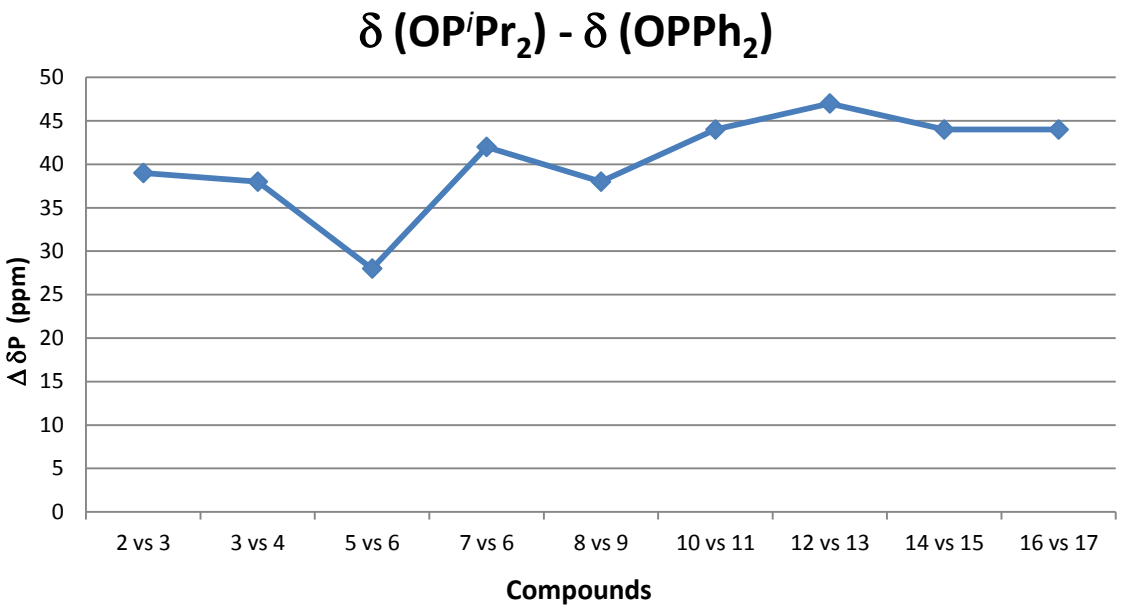

Figure 7.7 Difference of ^{31}P NMR chemical shift of ((OP^{i}Pr$_2$) - (OPPh$_2$)) moiety for various compounds.

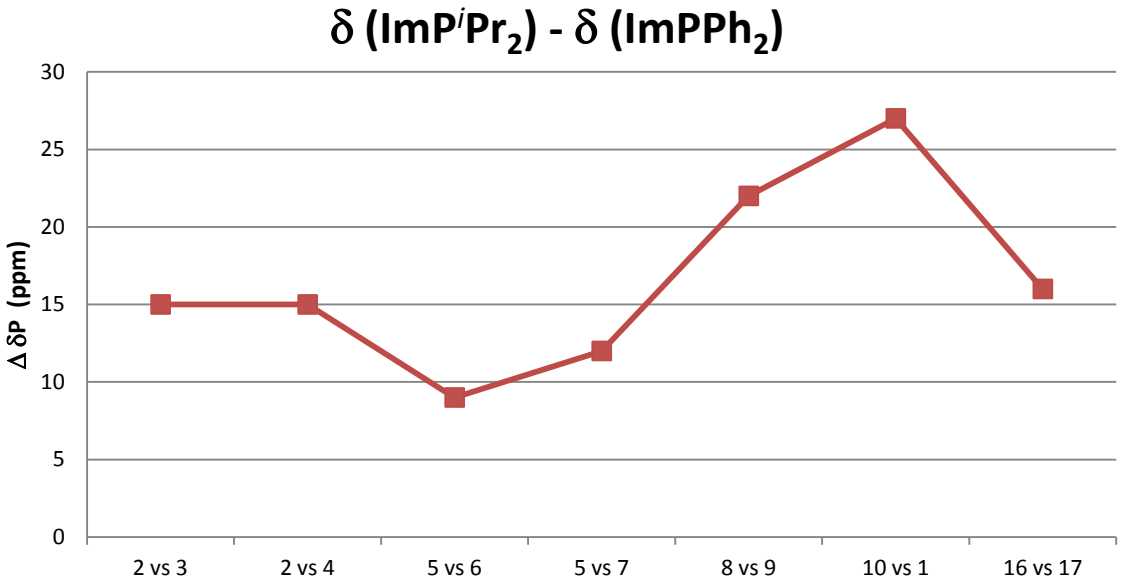

Figure 7.8 Difference of ^{31}P NMR chemical shift of ((ImP^{i}Pr$_2$) - (ImPPh$_2$)) moiety for various compounds.

Table 7.9. Catalytic addition of aniline and phenol to acrylonitrile using different cationic Ni(II) pincer complexes.

	Hydroamination[a]		
Catalyst	Entry	TON	TOF
10	4	67	22
11	3	26	9
15	5	59	20
16	2	83	28
17	1	76	25
(^{Ph}POCOP^{Ph})NiNCMe	6	53	18
No catalyst	7	0	0

[a] Reaction conditions: 1.0 % catalyst, THF, 3 h, 50 °C, yields determined by GC/MS using $C_{12}H_{26}$ as internal standard. Chemicals are dried before used.

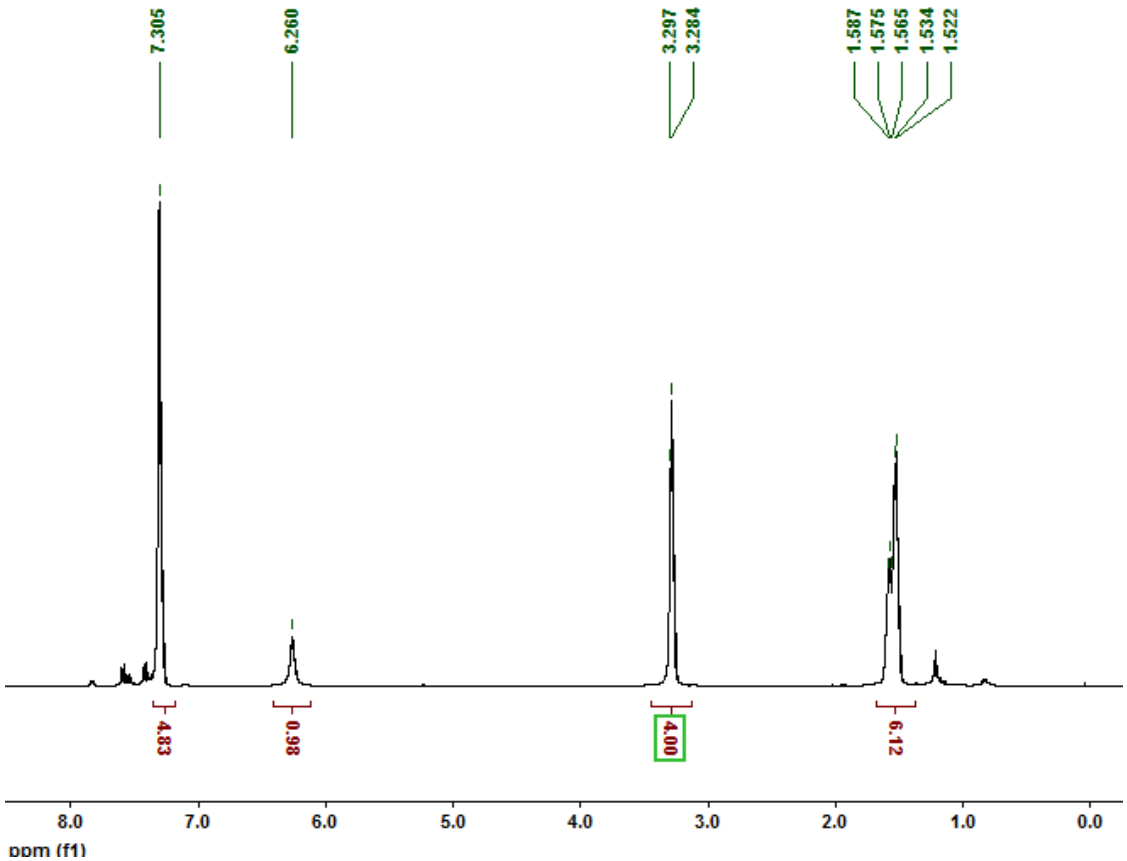

Figure 7.9. ^{1}H NMR spectra of N-Piperidino-benzamidine (400 MHz, $CDCl_3$).

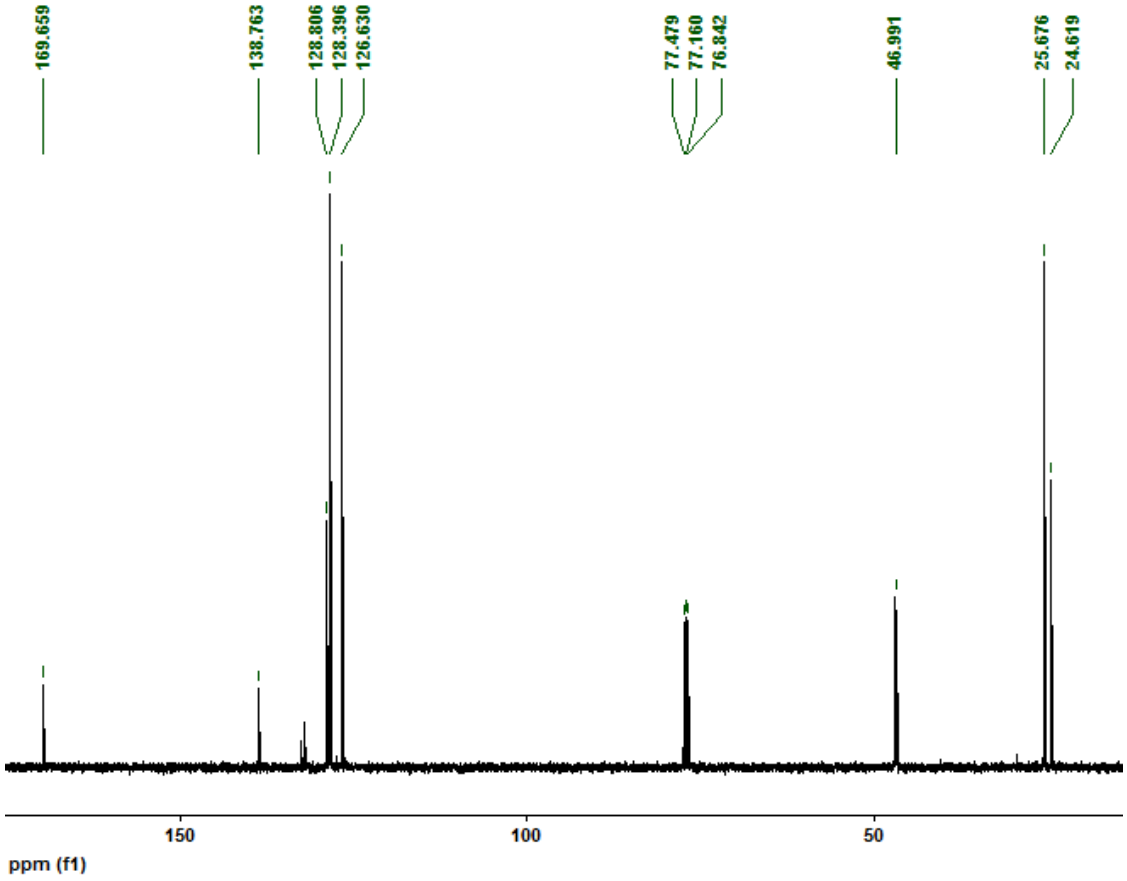

Figure 7.10. ^{13}C NMR spectra of N-Piperidino-benzamidine (100 MHz, $CDCl_3$).

Table 7.10 : Crystal Data Collection and Refinement Parameters for cationic complexes.

	[NHCCOP^{Ph} Ni-NCCH$_3$] [OTf]	[^{iPr}PIMCOP^{iPr} Ni-NCCH$_3$] [OTf]
chemical formula	$C_{24}H_{21}N_3NiOP,CF_3O_3S,0.5(C_2H_3N)$	$C_{23}H_{36}N_3NiOP_2,CF_3O_3S,CHCl_3$

crystal colour	yellow	yellow
Fw; *F*(000)	626.73; 642	759.64; 3136
T (K)	100	100
wavelength (Å)	1.54180	1.54178
space group	P-1	C2/c
a (Å)	7.9987(4)	38.7807(11)
b (Å)	12.4974(7)	8.477(2)
c (Å)	15.1117(10)	20.3341(6)
α (deg)	99.176(5)	90
β (deg)	100.800(5)	93.4154(14)
γ (deg)	107.451(5)	90
Z	2	8
V (Å^3)	1377.55(16)	6672.9(4)
ρ_{calcd} (g·cm^{-3})	1.511	1.512
μ (mm^{-1})	2.799	5.001
θ range (deg); completeness	3.810 − 61.760; 0.995	2.28 − 70.96; 0.993
R1[a]; wR2[b] [I > 2σ(I)]	0.0777; 0.0953	0.0299; 0.0813
R1; wR2 [all data]	0.0821; 0.0953	0.0326; 0.0837
GOF	1.0398	1.062
largest diff peak and hole	1.10 and -0.88	0.654 and -0.432

[a] $R_1=\Sigma(||F_o|-|F_c||)/\Sigma|F_o|$ [b] $wR_2=\{\Sigma[w(F_o^2-F_c^2)^2]/\Sigma[w(F_o^2)^2]\}^{½}$

	$P^{iPr}IMCOP^{iPr}$-Ni-Br	$P^{iPr}IMCOP^{Ph}$-Ni-Br	$NHCCOP^{iPr}$-Ni-Br
chemical formula	$C_{21}H_{33}BrN_2NiOP_2$	$C_{27}H_{29}BrN_2NiOP_2$	$C_{16}H_{22}BrN_2NiOP$
crystal colour	yellow	yellow	yellow
***Fw*; *F*(000)**	530.05; 4384	598.08; 2448	427.95; 872
***T* (K)**	100	150	100
wavelength (Å)	1.54178	1.54178	1.54178
space group	P21/c	P21/n	P21/n
***a* (Å)**	22.9260(3)	20.2217(9)	12.9699(4)
***b* (Å)**	10.5340(1)	10.2472(5)	10.1372(3)
***c* (Å)**	39.9222(6)	25.6244(11)	14.4925(4)
α (deg)	90	90	90
β (deg)	96.2182(9)	102.2225(18)	113.9721(14)
γ (deg)	90	90	90
Z	16	8	4
***V* (Å^3)**	9584.6(2)	5189.4(4)	1741.09(9)
ρ_{calcd} (g·cm^{-3})	1.469	1.531	1.633
μ (mm^{-1})	4.487	4.226	5.179
θ range (deg); completeness	1.94 − 71.19; 0.980	2.54 − 69.67; 0.996	3.86 − 71.12; 0.997
R1[a]; wR2[b] [I > 2σ(I)]	0.0412; 0.1051	0.0370; 0.1013	0.0257; 0.0697
R1; wR2 [all data]	0.0490; 0.1119	0.0384; 0.1031	0.0272; 0.0714
GOF	1.020	1.076	1.007
largest diff peak and hole	0.865 and -0.608	2.722 and -0.647	0.718 and -0.292

[a] $R_1=\Sigma(||F_o|-|F_c||)/\Sigma|F_o|$ [b] $wR_2=\{\Sigma[w(F_o^2-F_c^2)^2]/\Sigma[w(F_o^2)^2]\}^{1/2}$

Table 7.11 : Crystal Data Collection and Refinement Parameters for 'Ni-Br' Complexes

7.8 References.

[1] (a) Zargarian, D.; Castonguay, A.; Spasyuk, D. M. in "ECE-Type Pincer Complexes of Nickel" in Organometallic Pincer Chemistry, ed. G. van Koten and D. Milstein, *Top. Organomet. Chem.* (2013) 40: 131–174; Springer-Verlag Berlin Heidelberg 2013.

[2] (a) Castonguay, A.; Spasyuk, D. M.; Madern, N.; Beauchamp, A. L.; Zargarian, D. *Organometallics* **2009**, *28*, 2134. (b) Lefèvre, X.; Durieux, G.; Lesturgez, S.; Zargarian, D. *J. Mol. Catal. A: Chem.* **2011**, *335*, 1. (c) Salah, A. B.; Offenstein, C.; Zargarian, D. *Organometallics* **2011**, *30*, 5352. (d) V. Pandarus and D. Zargarian, *Organometallics*, **2007**, *26*, 4321. (e) Spasyuk, D. M.; Zargarian, D.; *Inorg. Chem.*, **2010**, *49*, 6203.

[3] (a) Kuhn, N.; Fahl, J.; Bläser, D.; Boese, R. *Z. Anorg. Allg. Chem*. **1999**, *625*, 729. (b) Azouri, M.; Andrieu, J.; Picquet, M.; Richard, P.; Hanquet, B.; Tkatchenko, I. *Eur. J. Inorg. Chem*. **2007**, 4877. (c) Debono, N.; Canac, Y.; Duhayon, C.; Chauvin, R. *Eur. J. Inorg. Chem*. **2008**, 2991. (d) Petuskova, J.; Bruns, H.; Alcarazo, M. *Angew. Chem. Int. Ed.* **2011**, *50*, 3799. (e) Digard, E.; Andrieu, J.; Cattey, H. *Inorg. Chem. Com*. **2012**, *25*, 39. (f) Maaliki, C.; Lepetit, C.; Duhayon, C.; Canac, Y.; Chauvin, R. *Chem. Eur. J.* **2012**, *18*, 16153. (g) Barthes, C.; Lepetit, C.; Canac, Y.; Duhayon, C.; Zargarian, D.; Chauvin, R. *Inorg. Chem*. **2013**, *52*, 48. (h) Maaliki, C.; Canac, Y.; Lepetit, C.; Duhayon, C.; Chauvin, R. *RSC Adv.,* **2013**, *3*, 20391. (i)

Canac, Y.; Debono, N.; Vendier, L. Chauvin, R. *Inorg. Chem*. **2009**, *48*, 5562. (j) Canac, Y.; Debono, N.; Lepetit, C.; Duhayon, C.; Chauvin, R. *Inorg. Chem*. **2011**, *50*, 10810. (k) Abdellah, I.; Lepetit, C.; Canac, Y.; Duhayon, C.; Chauvin, R. *Chem. Eur. J*. **2010**, *16*, 13095. (l) Abdellah, I.; Boggio-Pasqua, M.; Canac, Y.; Lepetit, C.; Duhayon, C.; Chauvin, R. *Chem. Eur. J*. **2011**, *17*, 5110. (m) Gaillard, S.; Renaud, J.-L. *Dalton Trans.* **2013**, *42*, 7255. (n) Canac, Y.; Maaliki, C.; Abdellah, I.; Chauvin, R. *New J. Chem.* **2012**, *36*, 17.

[4] Vabre, B.; Canac, Y.; Duhayon, C.; Chauvin, R.; Zargarian, D. *Chem. Commun.* **2012**, *48*, 10446.

[5] Pratt, D. A.; Pesavento, R. P.; van der Donk, W. A. *Org. Lett*. **2005**, *7*, 2735.

[6] This step possibly occurs via an electrophilic mechanism, see: Vabre, B.; Lambert, M. L.; Petit, A.; Ess, D. H.; Zargarian, D. *Organometallics* **2012**, *31*, 6041.

[7] In the ^{31}P NMR spectrum, a new resonance appeared at δ_P = +124 (s) ppm which was attributed to the formation of Ph_2POEt (See Supporting Information).

[8] CCDC 1012838 (**6**), CCDC 1012839 (**7**), CCDC 1012840 (**13**), CCDC (coming soon) (**14**), CCDC 1012837 (**17**) contain the supplementary crystallographic data for this paper. These data can be obtained free of charge from the Cambridge Crystallographic Data Centre via www.ccdc.cam.ac.uk/data_request/cif.

[9] (a) Pietra, F. *Chem. Biodivers.* **2012**, *9*, 331. (b) Kotthaus, J.; Steinmetzer, T.; van de Locht, A.; Clement, B. *J. Enzyme Inhib. Med. Chem.* **2011**, *26*, 115. (c) Oediger, H.; MöLler, F.; Eiter, K. *Synthesis* **1972**, *1972*, 591. (d) Taylor, J. E.; Bull, S. D.; Williams, J. M. J. *Chem. Soc. Rev.* **2012**, *41*, 2109. (e) Quek, J. Y.; Davis, T. P.; Lowe, A. B. *Chem. Soc. Rev.* **2013**, *42*, 7326.

[10] (a) Aly, A. A.; Nour-El-Din, A. M. Arkivoc **2008**, 153. (b) Partridge, M. W.; Smith, A. *J. Chem. Soc., Perkin Trans.* 1 **1973**, 453. (c) Hill, A. J.; Johnston, J. V. *J. Am. Chem. Soc.* **1954**, *76*, 920. (d) Mandel, H. G.; Hill, A. J. *J. Am. Chem. Soc.* **1954**, *76*, 3978. (e) Weintraub, L.; Oles, S. R.; Kalish, N. *J. Org. Chem.* **1968**, *33*, 1679. (f) Roger, R.; Neilson, D. G. *Chem. Rev.* **1961**, *61*, 179. (g) Schaefer, F. C.; Peters, G. A. *J. Org. Chem.* **1961**, *26*, 412. (h) Oxley, P.; Partridge, M. W.; Short, W. F. *J. Chem. Soc.* **1947**, 1110. (i) Judkins, B. D.; Allen, D. G.; Cook, T. A.; Evans, B.; Sardharwala, T. E. *Synth. Commun.* **1996**, *26*, 4351. (j) Dondoni, A.; Barbaro, G. *J. Chem. Soc., Chem. Commun.* **1975**, 761. (k) Baati, R.; Gouverneur, V.; Mioskowski, C. *Synthesis* **1999**, *6*, 927. (l) Schnur, R. C. *J. Org. Chem.* **1979**, *44*, 3726. (m) Katritzky, A. R.; Cai, C.; Singh, S. K. *J. Org. Chem.* **2006**, *71*, 3375. (n) McGowan, M. A.; McAvoy, C. Z.; Buchwald, S. L. *Org. Lett.* **2012**, *14*, 3800. (o) Sävmarker, J.; Rydfjord, J.; Gising, J.; Odell, L. R.; Larhed, M. *Org. Lett.* **2012**, *14*, 2394.

[11] (a) Forsberg, J. H.; Spaziano, V. T.; Balasubramanian, T. M.; Liu, G. K.; Kinsley, S. A.; Duckworth, C. A.; Poteruca, J. J.; Brown, P. S.; Miller, J. L. *J. Org. Chem.* **1987**, *52*, 1017. (b) Wang, J. F.; Xu, F.; Cai, T.; Shen, Q. *Org. Lett.* **2008**, *10*, 445.

[12] (a) Garigipati, R. S. *Tett. Lett.* **1990**, *31*, 1969. (b) Rousselet, G.; Capdevielle, P.; Maumy, M. *Tett. Lett.* **1993**, *34*, 6395. (c) Moss, R. A.; Ma, W.; Merrer, D. C.; Xue, S. *Tett. Lett.* **1995**, *36*, 8761.

[13] Rozenel S.S.; Kerr J. B.; Arnold J. *Dalton Trans.*, **2011**, *40*, 10397.

[14] SAINT, Release 6.06; Integration Software for Single Crystal Data; Bruker AXS Inc.: Madison, WI, 1999

[15] Sheldrick, G. M. SADABS, Bruker Area Detector Absorption Corrections; Bruker AXS Inc., Madison, WI, 1999

[16] XPREP, Release 5.10; X-ray Data Preparation and Reciprocal Space Exploration Program; Bruker AXS Inc.: Madison, WI, 1997.

[17] SHELXTL, Release 5.10; The Complete Software Package for Single Crystal Structure Determination; Bruker AXS Inc.: Madison, WI, 1997.

[18] (a) Sheldrick, G. M. SHELXS97, Program for the Solution of Crystal Structures; Univ. of Gottingen: Germany, 1997. (b) Sheldrick, G. M. SHELXL97, Program for the Refinement of Crystal Structures; University of Gottingen: Germany, 1997

Chapitre 7

Chapitre 8 : Ortho-Derivatization of Phenols Through C-H Nickelation : Synthesis, Characterization and Reactivities of Orthonickelated Complexes

Article 7

*Boris Vabre, Félix Deschamps and Davit Zargarian**

Département de chimie, Université de Montréal, Montréal (Québec),

Organometallics **2014**, *accepted*.

Chapitre 8

8.1 Abstract

Reported here are the synthesis and characterization of orthonickelated complexes derived from phosphinite ligands and investigated as model compounds in the development of C-H functionalization strategies for arenol substrates. Reaction of *i*-Pr_2POPh with 0.6 equiv of $[NiBr_2(NC^iPr)]_n$ and 0.8 equiv of NEt_3 in toluene (100 °C, 36 h) gave the yellow, monomeric cyclometalated complex *trans*-{κ^2-*P*,*C*-*i*-$Pr_2P(OC_6H_4)$}-Ni(*i*-Pr_2POPh)Br, **3a**, in 93% yield; using 2 equiv each of the Ni precursor and NEt_3 gave the closely related yellow-orange dimeric species [{κ^2-*P*,*C*-*i*-$Pr_2P(OC_6H_4)$}NiBr]$_2$, **4a**, in 70% yield. These complexes interconvert in the presence of excess ligand (**4a** → **3a**) or excess Ni precursor (**3a** → **4a**); they have been characterized fully and the cyclometalation pathway has been probed. Ambient temperature mixtures of *i*-Pr_2POPh and $[NiBr_2(NC^iPr)]_n$ lead to immediate formation of a dark-brown species that crystallizes as *trans*-(*i*-$Pr_2POPh)_2NiBr_2$, **2a**. NMR studies showed that **2a** undergoes a rapid ligand exchange at r.t., which can be slowed down at -68 °C; this fluxional process shifts in the presence of NEt_3, implying the partial formation of an amine adduct. Heating toluene mixture **2a** and NEt_3 at 90 °C for 38 h led to formation of **3a** via C-H nickelation. That phosphinite dissociation from **2a** precedes the C-H nickelation step is implied by the observation that formation of **3a** is hindered in the presence of excess *i*-Pr_2POPh. The impact of phenol ring substituents on the C-H nickelation rate was probed by preparing substituted derivatives of **2a**, *trans*-{(4-R-C_6H_4O)P(*i*-Pr_2)}$_2NiBr_2$ (R= OMe (**2b**), Me (**2c**), and COOMe (**2d**)), and measuring their relative rates of C-H nickelation; these studies showed that the formation of cyclonickelated products is favored in the order

COOMe < Me < OMe, which is consistent with an electrophilic metalation mechanism. Studying the C-H nickelation of (3-F-C_6H_4O)P(*i*-Pr_2) allowed us to establish that metalation is favored at the *para* position with respect to F (85:15). Treatment of **3a** or **4a** with benzyl bromide at 90 °C over extended periods led to benzylation of the Ni-aryl moiety in these complexes.

8.2 Introduction

Synthetic strategies based on C-H functionalization have grown in prominence and presently constitute a central part of the global drive to develop sustainable chemical processes. [1] The most facile and common strategy in the area of metal-catalyzed C-H metalation relies on the presence in substrates of nucleophilic moieties that can bind the metal atom, thereby facilitating its interaction with the C-H moiety to be activated. This type of chelation-assisted approach based on "functional directing groups" is commonly assumed to generate metallacycles as key intermediates that subsequently react with co-substrates to give the products of functionalization. Although in most cases C-H functionalization methodologies are based on one-pot approaches that bypass isolation or even detection of reaction intermediates, there are potentially significant benefits in intercepting the initial cyclometalated species and investigating the main factors influencing their formation, stability, and reactivities. Any knowledge gained from such studies should improve our understanding of the important steps involved in catalytic C-H functionalization processes and help develop more efficient methodologies.

Chapitre 8

A survey of C-H functionalization literature reveals that most of the early successes in this area hinged on the use of noble metals Ru, Rh, and Pd,[2] whereas their more abundant 3d counterparts Fe,[3] Co,[4] and Ni[5] have received increasing attention over the recent years. The use of Ni precursors in the drive toward more efficient and sustainable C-H functionalization strategies also has a historic significance since Ni was one of the earliest metals to show an aptitude in C-H metalation.[6] These considerations and our group's long-standing interest in organonickel chemistry[7] has prompted us to initiate projects aimed at developing C-H functionalization methodologies based on Ni precursors.

In light of the above-mentioned importance of metallacycles, our strategy is to prepare complexes based on nickelacycles and study their ease of formation and reactivities, their structures and reactivities as a long-term strategy aimed at developing Ni-based C-H functionalization methodologies. An initial search of the literature revealed that very few metallacyclic complexes of Ni have been reported previously, especially in comparison to the much better known metallacyclic complexes based on Pd and Pt. Moreover, of the relatively few nickellacyclic complexes, very few have been prepared via C-H nickelation. For instance, several nickellacycles based on aromatic Schiff bases and benzyl amines,[8] as well as aromatic phosphines[9] and phosphinites[10] have been synthesized by oxidative addition of C-X bonds (X = Br, Cl) to Ni(0) precursors.[11] The Ni-Ar moiety in some of these complexes undergo insertion of CO, SO_2 or alkynes,[12] or initiates polymerization of olefins.[13]

Chapitre 8

To capitalize on our previous experience in the synthesis and reactivities of POCOP-type complexes based on bis(phosphinites),[14] we have elected to begin our studies by examining the C-H functionalization of phosphinite ligands derived from phenol and its substituted derivatives. There are literature precedents for the use of phosphinites in C-H functionalization using Ru,[15] Rh,[16] and Pd,[17] but to our knowledge no such reports exist with Ni. An important advantage of a phosphinite directing group in C-H functionalization is its facile preparation from alcohols and $ClPR_2$, which would give access to a potentially wide and diverse family of substrates. In addition, a phosphinite moiety can be removed readily by a number of simple work-up strategies, thus qualifying this strategy as a so-called "traceless" functionalization.[18]

The present study describes the synthesis and full characterization of ligands R-($^{i}Pr_2PO$)-C_6H_4 (R = H (**1a**), 4-OMe (**1b**), 4-Me (**1c**), 4-CO_2Me (**1d**), 3-F (**1e**)), and their bis adducts *trans*-{*i*-$Pr_2P(4\text{-}R\text{-}OC_6H_4)\}_2$ $NiBr_2$ (R = H (**2a**), OMe (**2b**), Me (**2c**), CO_2Me (**2d**)). Cyclonickelation of **1a** gave the complexes *trans*-{κ^2-*P*,*C*-*i*-$Pr_2P(OC_6H_4)\}$(*i*-Pr_2POPh)NiBr, **3a**, and $[\{\kappa^2\text{-}P,C\text{-}i\text{-}Pr_2P(OC_6H_4)\}NiBr(\mu\text{–}Br)]_2$, **4a**, which were fully characterized and used in functionalization tests with benzylbromide to give 2-benzyl- phenol and its phosphinated derivatives. The report will also discuss the influence of aryl substituents OMe, Me, and COOMe on C-H nickelation rates and the site selectivity in the nickelation of 3-F-phenol.

8.3 Results and discussion

Synthesis and characterization of orthonickelated complexes derived from phenol. Treating phenol with *i*-Pr_2PCl and NEt_3 in THF gave the phosphinite ligand **1a** (r.t., 1h, 90 %), which was then used for the synthesis of the target cyclometallated complexes, as follows (Scheme 8.1). Heating at 100 °C a toluene mixture of **1a** containing 0.6 equiv of our Ni precursor $[(i\text{-PrCN})NiBr_2]_n$[23] and 0.8 equiv of NEt_3 gave a yellow solid identified as *trans*-{κ^2-*P*,*C*-$P(OC_6H_4)i\text{-}Pr_2$}Ni(*i*-Pr_2POPh)Br, **3a**, in 93% yield, whereas using 2 equiv each of the Ni precursor and base gave the closely related yellow-orange dimeric species [{κ^2-*P*,*C*-$P(OC_6H_4)i\text{-}Pr_2$}$NiBr]_2$, **4a**, in 70% yield. Complex **4a** reacts readily at r.t. with an equiv of **1a** to give its phosphinite adduct **3a**, whereas heating the latter in the presence of excess Ni precursor and base cleanly furnishes **4a**. This interconversion is significant for understanding the cyclometalation pathway (vide infra):

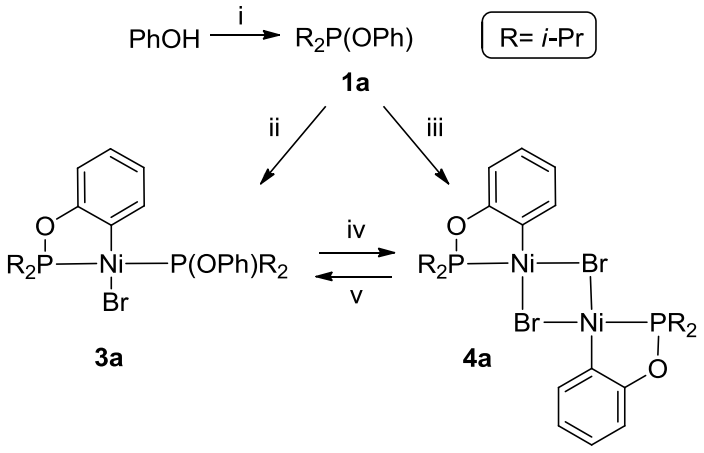

Scheme 8.1. Synthesis of cyclometallated complexes of Ni. Conditions: (i) R_2PCl, NEt_3, THF, r.t., 1 h; (ii) 0.6 $[(i\text{-PrCN})NiBr_2]_n$, 0.8 NEt_3, Toluene, 100 °C, 36 h; (iii) 2.0 $[(i\text{-PrCN})NiBr_2]_n$, 2.0 NEt_3, Toluene, 100 °C, 40 h; (iv) excess $[(i\text{-PrCN})NiBr_2]_n$, excess NEt_3, Toluene, 100 °C, 40 h; (v) 1.0 **1a**, C_6D_6, r.t., 5 min.

The phosphinite ligand **1a** has been reported previously[17] but **3a** and **4a** are new complexes, which have been characterized fully. The $^{31}P\{^{1}H\}$ NMR spectrum of **4a** shows a sharp singlet at 199 ppm, which is significantly downfield of the corresponding signal for the free ligand (149 ppm). Complex **3a** showed the anticipated AB doublets at ca. 185 and 152 ppm for the cyclometalated and non-cyclometalated phosphinite moieties, respectively; the large $^{2}J_{P\text{-}P}$ value of 325 Hz for these resonances is typical of non-equivalent phosphinites in a mutually trans position. The ^{13}C NMR resonance for C_{ipso} in **3a** appeared as a doublet of doublets at 132 ppm ($^{2}J_{C\text{-}P}$= 14 and 29 Hz), whereas a complex multiplet was observed for the corresponding signal in **4a**.

X-Ray diffraction studies crried out on single crystals of **3a** and **4a** (Figure 8.1) allowed us to confirm the solid state structures of these complexes. The Ni center in both complexes shows a square planar geometry distorted by the 5-membered metallacycle. The different steric demands of the two phosphinite ligands in **3a** also lead to structural distortions. For instance, the P atom belonging to the non-cyclometallated phosphinite moiety forms larger cis angles relative to the corresponding angles involving the P atom of the cyclometalated phosphinite moiety: 101° vs. 83° for C-Ni-P, and 92° vs. 86° for P-Ni-Br. The C-Ni-Br angle of 165° in **3a** is also much smaller than the ideal value expected for a trans angle, but the P-Ni-P angle of 173° is only marginally smaller than an analogous complex bearing two non-cyclometalated trans phosphinite ligands (vide infra).

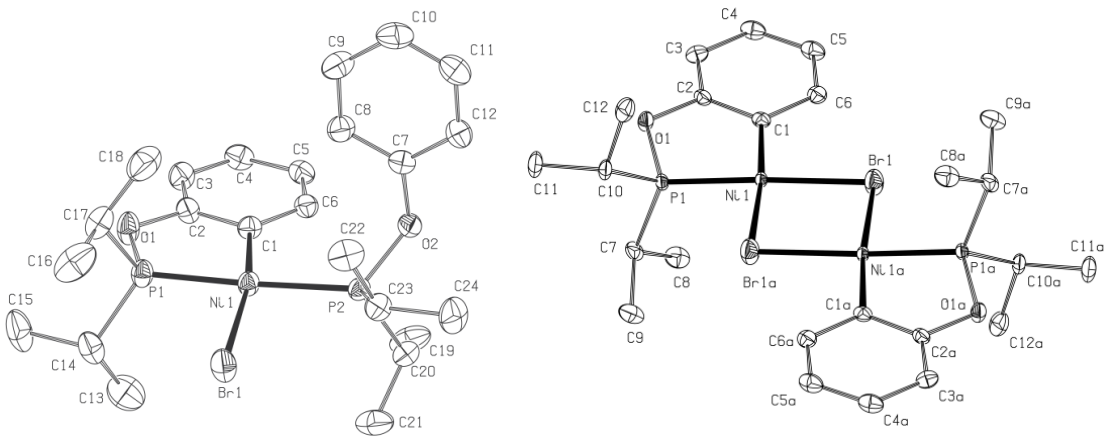

Figure 8.1. ORTEP diagrams for complexes **3a** and **4a**. Thermal ellipsoids are shown at the 50% probability level. Hydrogen atoms are omitted for clarity. Selected bond distances (Å) and angles (°): Ni-C1= 1.935(2) (**3a**), 1.914(4) (**4a**); Ni-P1= 2.1359(5) (**3a**), 2.0953(10) (**4a**); Ni-P2= 2.2510(5) (**3a**); Ni-Br1= 2.3664(3) (**3a**), 2.3641(7) (**4a**); Ni-Br1a= 2.3771(7) (**4a**); C1-Ni-Br1= 164.92(5) (**3a**), 97.61(12) (**4a**); C1-Ni-Br1a= 174.24(12) (**4a**); P-Ni-P= 172.97(2) (**3a**); C1-Ni-P1= 82.96(5) (**3a**), 82.07(12) (**4a**); C1-Ni-P2= 100.83(5) (**3a**); Br1a-Ni-P1= 92.62(3) (**4a**); Br1-Ni-P1= 85.564(15) (**3a**), 176.19(4) (**4a**); Br1-Ni-P2= 91.632(15) (**3a**); Br1-Ni-Br1a = 87.84(2) (**4a**).

The impact of cyclometalation on the solid state structure of **3a** is also evident in the shorter Ni-P distance for the chelating moiety (2.13 vs. 2.25 Å). In **4a**, the impact of cyclometalation is most evident in the cis bond angles C-Ni-Br (ca. 98°) and C-Ni-P (ca. 82°), whereas the trans angles are not affected much (174-176°). Consistent with the relative trans influences of the Br and *i*-$Pr_2P(OPh)$ ligands, the Ni-P distance in **4a** is much shorter than the corresponding distance in **3a** (2.10 vs. 2.14 Å), whereas the reason for the significantly shorter Ni-C distance in **4a** compared to **3a** (1.91 vs. 1.94 Å) is not readily evident.

Elucidation of C-H nickelation pathway. We have examined the pathway(s) leading to complexes **3a** and **4a** with the objective of detecting intermediates and

identifying the factors influencing the C-H metalation step. This examination began by attempts to intercept and characterize the species forming initially on the path to cyclometalation, as described below.

Stirring a toluene mixture of the ligand **1a** and 0.5 equiv of $[(i\text{-PrCN})NiBr_2]_n$ at r.t. led immediately to formation of a dark brown solution that displays a broad ^{31}P singlet at 136 ppm, presumably due to a fluxional process involving exchange of the phosphinite ligand. Single crystals grown at -37 °C (deep yellow, 82% yield) were subjected to X-ray diffraction studies that allowed us to identify the product as the bis(phosphinite) complex *trans*-$(i\text{-Pr}_2POPh)_2NiBr_2$, **2a**. The structural parameters for this square planar compound are unexceptional and will be discussed below along with the solid state structures of its substituted derivatives (vide infra).

To shed some light on the aforementioned fluxional process, we examined the low temperature NMR spectra of **2a** (CD_2Cl_2, Figures 8.4 and 8.5, supporting information). The broad ^{31}P singlet (FWHM ≈ 760 Hz) observed at r.t. sharpened gradually to give a fairly fine signal at -68 °C, characteristic of the analogous complexes *trans*-$(PR_3)_2NiBr_2$ (PR_3= PMe^iPr_2, PPh^iPr_2) that also undergo fast ligand exchange.[19] The $^{13}C\{^1H\}$ NMR spectrum of the sample at this temperature showed the anticipated virtual triplet for $PCH(CH_3)_2$ (29 ppm, $^{v}J_{PC=}$ 12 Hz).

With the objective of examining the above ligand exchange process under conditions relevant to the cyclometalation reaction, we prepared a toluene sample of **2a** (0.065 M) containing 1.2 equiv of NEt_3 and analyzed it by $^{31}P\{^1H\}$ NMR spectroscopy with and without heating. The predominant signal in the ambient

temperature spectrum was the original broad singlet (136 ppm), but the presence of NEt_3 gave rise to a second broad resonance at 131 ppm as well as the sharp resonance at 147 ppm attributed to free ligand **1a**; the integration ratio for these signals was approximately 20:1:1 (Figure 8.6 supporting information). We propose that the new broad singlet represents the phosphinite-depleted species $[(i\text{-}Pr_2POPh)BrNi(\mu\text{–}Br)]_2$ and its NEt_3 adduct $(i\text{-}Pr_2POPh)(NEt_3)NiBr_2$ that are in equilibrium with each other and with **2a**. Given the much weaker L→Ni binding force of NEt_3 relative to most P-based ligands, we believe it is unlikely that the substitution of the phosphinite ligand in **2a** is induced by NEt_3; instead, we postulate that NEt_3 simply captures the phosphinite-depleted intermediate generated in-situ as a result of phosphinite dissociation, as shown in Scheme 8.2.

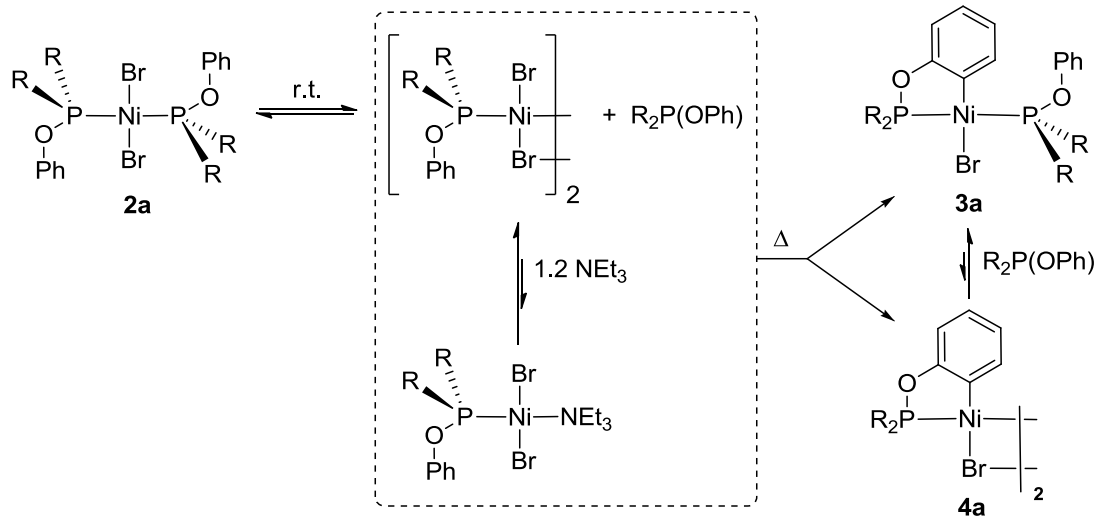

Scheme 8.2. Proposed ligand dissociation/exchange process and cyclometalation in the presence of NEt_3.

The spectrum of the above-discussed toluene sample containing **2a** and NEt_3 remained virtually unchanged after 18 h at room temperature, indicating that the

equilibrium governing the ligand exchange process is established in time of mixing, and that the cyclometallation requires higher temperatures. Heating this sample to 90 °C and monitoring by $^{31}P\{^{1}H\}$ NMR analysis allowed us to observe the gradual process of cyclometalation (Figure 8.2). The original signals arising from the above-discussed ligand exchange process were slowly replaced by the AB doublets due to the cyclometalated species **3a**, and the dark brown color of the reaction mixture faded gradually to give a light yellow mixture; the concomitant formation of $HBr.NEt_3$ was signalled by precipitation of a white solid. The sharp singlet due to the free ligand **1a** grew initially and diminished over one day, implying that the dimeric species **4a** is the initial product of cyclometalation whereas **3a** is the more stable species in the presence of excess **1a** (Scheme 8.2).

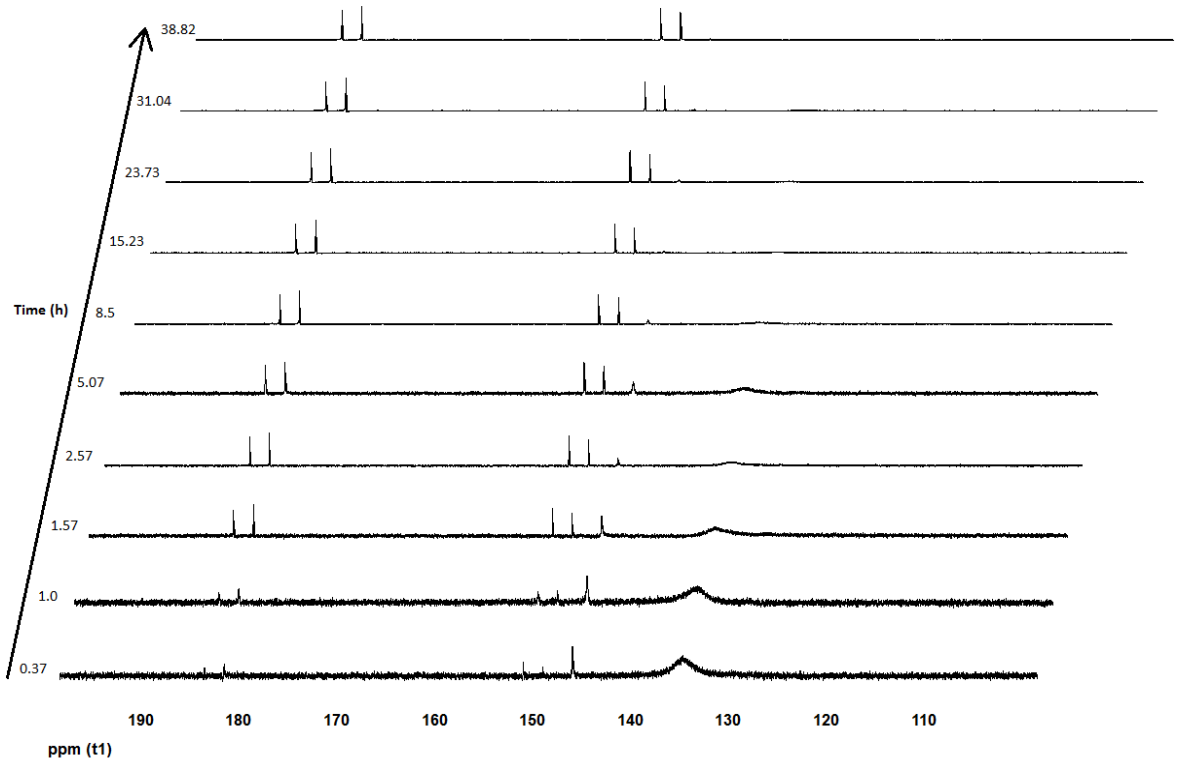

Figure 8.2. $^{31}P\{1H\}$ NMR monitoring of a solution of **2a** (50mg, 78 µmol) and NEt_3 (13 µL, 93.8 µmol) in Toluene (1.2 mL) at 90 °C over 39 h.

We also monitored by ^{31}P NMR spectroscopy the gradual formation of cyclometalated products starting from **1a**, $[(i\text{-PrCN})NiBr_2]_n$, and NEt_3 (molar ratio of 1:1:1, 90 °C, 10 days; Figure 8.10, supporting information). The predominant signal observed during the initial stages of the reaction was the broad singlet at ca. 136 ppm representing **2a**, which indicates that this bis(phosphinite) species is the main species present in the reaction mixture even when equimolar quantities of **1a** and the Ni precursor are employed. As was also established in the previous experiment discussed above, in the presence of NEt_3 **2a** is gradually converted to the cyclometalated products **3a** (AB doublets at ~185 and 152 ppm) and **4a** (a singlet at ~197 ppm). One

interesting finding revealed by monitoring the behavior of the system in the presence of only one equivalent of **1a** is that all the signals present in the spectra, including those of the cyclometalated species **3a** and **4a** emerging over time, are broad throughout the entire experiment. Indeed, the only sharp signal detected in the process is the singlet due to **4a** (198 ppm), which was observed at the very end of the experiment (after 10 days) as the sole P-bearing species. The preferential formation of **4a** over **3a** is expected because of the 1:1 ratio of **1a**:Ni employed, but the observed broadness of the signals due to **2a**, **3a**, and **4a** indicates that all of these species are in dynamic exchange as long as free **1a** is present in the reaction mixture. We conclude, therefore, that cyclometalation is the only irreversible step in this process (Scheme 8.2).

An important question that remains to answer is whether or not the cyclometalation step involves the above-postulated phosphinite-depleted intermediate species; in other words, is the observed phosphinite dissociation equilibrium required for the cyclometalation or not? We carried out the following experiments to shed some light on this issue. Four NMR tubes were charged with **2a** (89 μmol), NEt_3 (107 μmol), and 0, 4, 8 and 16 equiv of **1a** in toluene (500 μL), in addition to a sealed capillary containing a toluene solution of PPh_3 as external standard; the samples were heated to 90°C for 12.5 h and analyzed by $^{31}P\{^1H\}$ NMR spectroscopy. The results showed that the formation of **3a** diminishes in the presence of added ligand **1a** (54 %, 31 %, 19 % and 8 %, respectively), which suggests (but does not prove) that dissociation of a phosphinite from **2a** is required for the cyclonickelation step. It should be added here that previously reported studies on the orthopalladation of

closely related triaryl phosphite ligands have suggested that phosphite-depleted species analogous to the dimeric species $\{(PhOP^{i}Pr_2)NiBr_2\}_2$ postulated in Scheme 8.2 are likely involved in the C-H palladation step.[20] Indeed, dimers of the type $[(PR_3)XM(\mu–X)]_2$ are known for Pd and Pt,[21] but to our knowledge none have been reported for Ni.

Influence of aryl substituents on cyclonickelation. C-H metallation of aromatic substrates by MX_n can proceed through different mechanisms, including a process involving successive steps of oxidative addition to give hydrido(aryl) intermediates followed by reductive elimination of HX, as well as a so-called electrophilic (non-redox) process involving sequential or concerted binding of the C (or C-H) fragment and removal of H^+ by X^-. The latter process can also be considered a σ–bond metathesis if there is little or no polarization of the C-H and M-X moieties at the transition state.[22] While a redox process seems *a priori* unlikely with a Ni(II) precursor, it is difficult to rule out this scenario experimentally. On the other hand, a knowledge of the impact of electronic factors on C-H nickelation rates can help gauge the likelihood of an electrophilic mechanism. We have, thus, examined the relative rates of C-H nickelation in the context of the present system by evaluating the electronic impact of aryl substitutents on cyclometalation rates, as described below.

The arenols 4-methoxyphenol, p-cresol and methyl 4-hydroxybenzoate were used to prepare and isolate in 78-97 % yields the corresponding phosphinites *i*-$Pr_2PO(4\text{-}R\text{-}C_6H_4)$ (R= OMe (**1b**), Me (**1c**), CO_2Me (**1d**)), as described earlier for the parent ligand **1a** (THF/NEt_3, r.t., 1 h). The $^{31}P\{^1H\}$ NMR spectra of these ligands showed a singlet at ca. 150 ppm, characteristic of *i*-Pr_2POAr.[17,23] In an analogous

manner to the synthesis of **2a**, the new ligands were then treated with 0.5 equiv of [(*i*-PrCN)$NiBr_2$]$_n$ at r.t. to give the bis(phosphinite) complexes *trans*-(*i*-$Pr_2POAr)_2NiBr_2$ **2b-2d** (Scheme 8.3).

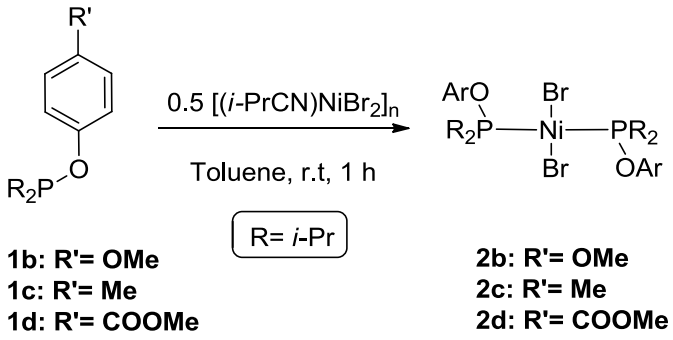

Scheme 8.3. Synthesis of **2b-d**.

Toluene solutions of **2b-2d** (0.16 mmol in 382 μL; 0.042 M) containing 10 equiv of NEt_3 were then heated at 100 °C and the formation of the corresponding cyclometalated complexes **3b-3d** was monitored by ^{31}P NMR spectroscopy.[24] The resulting spectra showed the aryl substituents' influence on nickelation: after 5.3 h, cyclometalation had progressed to a greater extent for complex **3b** (39 %) relative to **3c** (32%) and **3d** (22 %) (Figure 8.8 supporting information). These results imply an electrophilic cyclonickelation mechanism for this family of phosphinite ligands. A similar trend (OMe > Me > CO_2Me) was also found for the impact of the 4-R substituent in the nickelation of resorcinol-based bis(phosphinite) ligands to give the corresponding POCOP-type pincer complexes of Ni(II).[25]

The new complexes **2b-d** and **3b-d** generated in the course of the above study were characterized by comparing their NMR spectral patterns to those of their analogues **2a** and **3a**. For example, similarly to what was observed for **2a**, a broad ^{31}P

singlet was detected for **2b** and **2c** (136 ppm) and for **2d** (131 ppm), whereas AB doublets featuring large $^{2}J_{P\text{-}P}$ ~ 325 Hz were observed in the $^{31}P\{^{1}H\}$ NMR spectra of **3b-d** (~152 ppm and ~185 ppm). Single crystals were also grown for **2b-d** and subjected to X-Ray diffraction studies. Figure 8.3 shows ORTEP diagrams of **2a** and **2c**, and Table 8.1 lists selected structural parameters for **2a-d**. Complexes **2a** and **2b** display an inversion center at the Ni atom and a nearly ideal square planar geometry is seen for **2a**, **2b**, and **2d**, whereas **2c** shows an unexpectedly large distortion in the Br-Ni-Br angle (166°). The Ni-P and Ni-Br distances in **2a-2d**, 2.22-2.24 Å and 2.29-2.30 Å, respectively, are somewhat shorter than the corresponding distances in **3a** (2.25 Å and 2.37 Å).

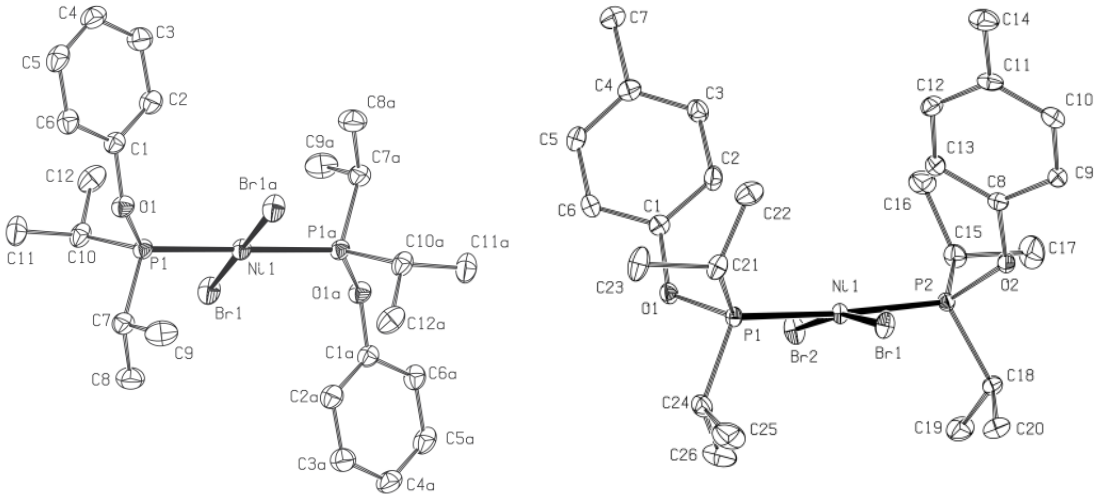

Figure 8.3. ORTEP diagrams for complexes **2a** and **2c**. Thermal ellipsoids are shown at the 50% probability level and hydrogen atoms are omitted for clarity. Selected structural parameters are listed in Table 8.1.

Table 8.1. Selected bond distances (Å) and angles (°) for complexes **2a-2d**.

Compound	Ni-P1	Ni-P2	Ni-Br1	Ni-Br2	P-Ni-P	Br-Ni-Br	P1-Ni-Br1
2a	2.243(1)		2.297(1)		180.0	180.0	88.81(1)
2b*	2.238(1)		2.298(1)		180.0	180.0	88.60(2)
2c	2.225(1)	2.240(1)	2.303(1)	2.301(1)	175.90(2)	166.63(1)	87.23(1)
2d*	2.230(1)	2.228(1)	2.290(1)	2.292(1)	179.83(2)	179.79(2)	89.16(2)

***** Values given are for molecule 1.

The question of site selectivity in cyclonickelation. The cyclometalation reactions discussed to this point have involved phosphinite ligands derived from either phenol or *para*-substituted derivatives, all of which can give only one product of monometalation. The same scenario holds for *ortho*-substituted analogues, whereas R_2POAr derived from *meta*-substituted arenols 3-R'-C_6H_4OH can, in principle, result in two different cyclonickelation products depending on which C-H is metalated, the one that is situated *ortho* to both the OPR_2 and R' or that situated *ortho* to the OPR_2 and *para* to R'. We have addressed this question briefly by studying the cyclonickelation of 3-fluorophenol, as described below. The choice of F as substituent was predicated by its similar steric properties relative to H, which should ensure that electronic effects are the dominant factor in any site selectivity.

Ligand *i*-Pr_2P(3-F-C_6H_4O), **1e**, was prepared similarly to **1a-d** described above, and was allowed to react with $[(i\text{-PrCN})NiBr_2]_n$ and NEt_3 (0.5 and 1.2 equiv, respectively) at 100 °C in toluene for 25 h (Scheme 8.4). $^{31}P\{^1H\}$ NMR analysis of the reaction mixture at t= 25 h showed the emergence of two sets of AB resonances assigned to the cyclonickelated species analogous to **3a** (Figure 8.9, supporting information). The major resonance, a pair of doublets appearing at 155.5 and 186.5 ppm (J_{PP} = 325 Hz), has been assigned to isomer **3e*p*** wherein the nickelated carbon

atom is that *para* with respect to F. The two minor AB resonances ($^2J_{P\text{-}P}$ = 341 Hz) appearing at ca. 184 ppm ($^4J_{P\text{-}F}$ = 2 Hz) and ca. 156 ppm ($^4J_{P\text{-}F}$ = 32 Hz) have been assigned to isomer **3e^o** wherein the nickelated carbon atom is that *ortho* with respect to F.

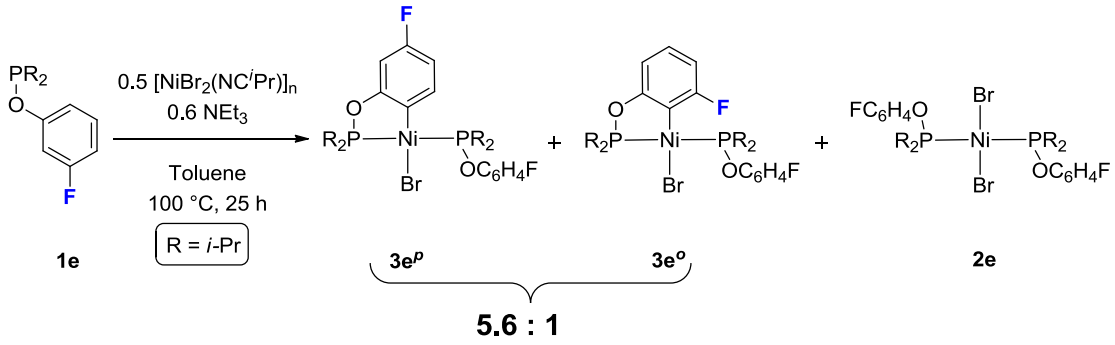

Scheme 8.4. Cyclonickelation of **1e**.

In addition to the above-noted AB resonances, the spectrum shows two broad singlets at 139 and 150 ppm assigned, respectively, to the bis(phosphinite) species *trans*-{*i*-Pr$_2$PO(3-F-C$_6$H$_4$)}$_2$NiBr$_2$, **2e**, and the free ligand **1e**; presence of these signals indicates that the reaction is incomplete. The ^{19}F NMR analysis of the final mixture confirmed the presence of four F-bearing species, and integration of ^{19}F and ^{31}P{^{1}H} signals indicated ~65 % cyclonickelation and a 5.6:1 ratio for the cyclonickelation products **3e^p**:**3e^o**. The greater preference for metallation of the C-H moiety *para* to F in 3-F-C$_6$H$_4$OP(*i*-Pr)$_2$ parallels the 6:1 selectivity reported for Pd-catalyzed acetoxylation of 2-(3-fluorophenyl)-pyridine at the position *para* to F.[26]

Ortho-functionalization. We have briefly investigated the reactivity of the newly created C-Ni bonds in the cyclometalated complexes **3a** and **4a** to establish the

feasibility of developing a viable methodology for functionalizing arenols. The first tests were done using complex **3a**, as follows. A J. Young NMR tube containing an equimolar mixture of **3a** and benzyl bromide in 0.5 mL toluene (0.08 M) was heated to 100 °C for 84 h, and the final mixture was subjected to $^{31}P\{^{1}H\}$ NMR and GC/MS analysis. The NMR analysis confirmed the complete consumption of **3a** and GC/MS showed the presence of the starting ligand **1a** (m/z = 210), its benzylated derivative **1a-Bn** (m/z = 300), and the oxidized forms of these phosphinites (m/z = 226 and 316, respectively). The ratio of combined non-benzylated species relative to combined benzylated products was about 0.8:1.0, which implies that the putative bis(phosphinite) species formed as a result of the initial benzylation reacts further to cyclometalate the monodentate phosphinite moiety, as shown in Scheme 8.5.

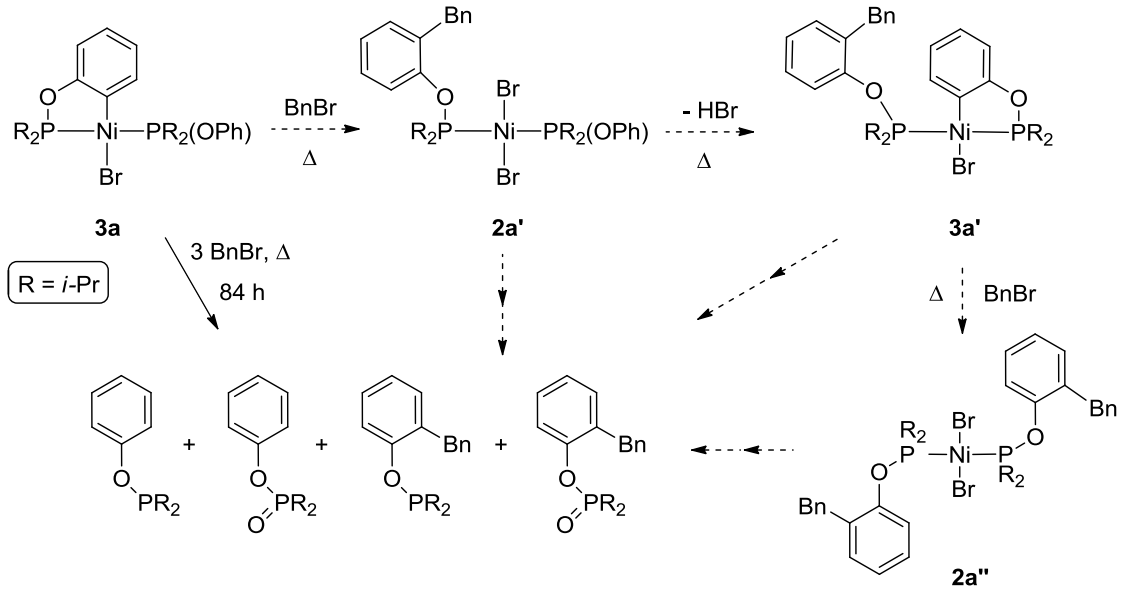

Scheme 8.5. Postulated pathway for benzylation of **3a**.

The benzylation reaction was also conducted with the dimeric species **4a** that has a 1:1 ratio of Ni:phosphinite (Scheme 8.6). Under the same conditions as the above experiment (3 equiv of benzyl bromide, toluene, 90 °C, 36 h), the 31P{^{1}H} NMR signal due to **4a** (s, 199 ppm) was replaced by two broad singlets at 134 and 133 ppm, which can be assigned to species **2a'** and **2a''** shown in Scheme 8.5, and three pairs of AB doublets ($^2J_{PP}$ = 324 Hz) at ~183 ppm and ~149-151 ppm. Of these, the more intense set of signals at 183.4 and 149.3 ppm is tentatively assigned to **3a'**, while the less intense sets are likely due to closely related products bearing different OAr moieties. It should be emphasized, however, that we have no evidence for the formation of products featuring benzylation at <u>both</u> *ortho* sites.

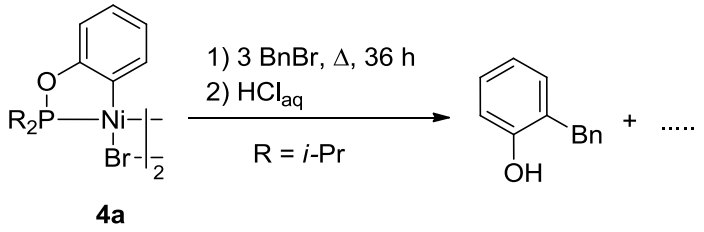

4a

Scheme 8.6. Benzylation of **4a**.

The final reaction mixture was subjected to a hydrolytic work-up in the presence of HCl_{aq} followed by column chromatography (SiO_2) to give 2-benzylphenol in 47 % isolated yield. The identity of this product was confirmed by GC/MS (mz = 184) and by ^{1}H and ^{13}C NMR (e.g., a singlet at 3.91 ppm corresponding to C*H*$_2$Ph proton and a deshielded singulet at 4.83 ppm for O*H*). These results demonstrate the feasibility of Ni-promoted orthofunctionalization of phenol through its *i*-Pr$_2$P phosphinite derivative.

8.4 Conclusion

The results reported above establish that it is feasible to orthonickelated aryl phosphinites *i*-$Pr_2P(OAr)$ using a simple Ni(II) precursor. Isolation and full characterization of the two nickellacycle compounds **3a** and **4a** has allowed us to study their structural and spectroscopic properties. We have also determined the conditions favoring the formation of one or the other of these complexes, and have investigated the importance of phosphinite dissociation and aryl substituents (OMe> Me> COOMe) on the C-H nickelation pathway. The latter studies point to an electrophilic C-H nickelation taking place with a mono(phosphinite) intermediate generated in-situ through ligand dissociation.

Orthonickelation of *i*-$Pr_2PO(3\text{-}F\text{-}C_6H_4)$ allowed us to establish that nickelation is favored at the C-H moiety *para* with respect to the fluoro substituent. Further studies are needed to determine the site selectivity of C-H nickelation with other aryl substituents. Similarly, benzylation of the nickelated carbon in **3a** and **4a** with benzyl bromide provided proof of concept for the feasibility of the envisaged areneol functionalization strategy, but much work remains to be done to expand the scope of functionalization and to identify reaction conditions under which the process can be catalytic in both Ni and chlorophosphine.

8.5 Experimental

Generalities. Unless otherwise indicated, all manipulations were carried out under a nitrogen atmosphere using standard Schlenk and glove box techniques. Solvents were

dried by passage over activated alumina contained in MBRAUN-SPS systems. Triethylamine was dried by distillation over CaH_2. The synthesis and characterization of ligands **1a** and **1c** has been reported by Bedford et al;[17] a slightly modified version of this procedure was used to prepare **1b**, **1d**, and **1e**, as described below. The preparation of the nickel precursor $[(i\text{-PrCN})NiBr_2]_n$ used throughout this study has been described previously.[23] All other reagents were purchased from Sigma-Aldrich and used without further purification.

^1H NMR spectra were recorded at 400 or 500 MHz using Bruker AV400rg Bruker, ARX400, and AV500 spectrometers; $^{13}C\{^1H\}$ NMR spectra were recorded at 100.56 MHz on ARX400, and $^{31}P\{^1H\}$ NMR spectra were recorded at 161.9 MHz on AV400rg. Chemical shift values are reported in ppm (δ), coupling constants are reported in Hz and referenced internally to the residual solvent signals (^1H and ^{13}C: 7.26 and 77.16 ppm for $CDCl_3$; 7.16 and 128.06 ppm for C_6D_6 ; 5.32 and 53.84 ppm for CD_2Cl_2) or externally (^{31}P, H_3PO_4 in D_2O, δ= 0). GC/MS measurements were made on an Agilent 6890N spectrometer. The elemental analyses were performed by the Laboratoire d'Analyse Élémentaire, Département de chimie, Université de Montréal.

(3-F-C_6H_4O)P(*i*-Pr)$_2$, 1e. Dropwise addition of $ClP(i\text{-Pr})_2$ (490 µL, 3.0 mmol) to a solution of 3-fluorophenol (271µL, 3.0 mmol) and NEt_3 (460µL, 3.5 mmol) in THF (25 mL) led to appearance of a white precipitate. The reaction mixture was stirred at r. t. for 1 h, evaporated, and the solid residues extracted with hexane (2 x 25 mL). Evaporation under vacuum gave the crude product as a colorless oil (543 mg, 78%), which was shown to be greater than 98% pure by NMR spectroscopy. This material

was used without further purification in subsequent experiments. ^{1}H NMR (400 MHz, 20 °C, C_6D_6) : δ 0.91 (dd, J_{HP} = 15.9, J_{HH} = 7.2, 6H, CH(CH_3)$_2$), 1.06 (dd, J_{HP} = 10.6, J_{HH} = 7.0, 6H, CH(CH_3)$_2$), 1.71 (hd, J_{HH} = 7.0, J_{HP} = 2.7, 2H, PCH(CH$_3$)$_2$), 6.51 (m, 1H, H$_{Ar}$), 6.85 (m, 1H, H$_{Ar}$), 6.92 (m, 1H, H$_{Ar}$), 7.03 (m, 1H, H$_{Ar}$,). ^{19}F NMR (376 MHz, 20 °C, C_6D_6): δ -111.56 (m). ^{31}P{1H} NMR (162 MHz, 20 °C, $CDCl_3$): δ 151.14 (s). ^{13}C{^{1}H} NMR (101 MHz, 20 °C, $CDCl_3$) : δ 17.03 (d, J_{CP} = 8.5, 2C, CH$_3$), 17.71 (d, J_{CP} = 20.5, 2C, CH$_3$), 28.52 (d, J_{CP} = 18.4, 2C, PCH(CH$_3$)$_2$), 106.48 (dd, J_{FC} =24.0, J_{PC} =11.5, 1C, CH_{Ar}), 108.71 (d, J_{FC} =21.2, 1C, CH_{Ar}), 114.50 (dd, J_{FC} =2.9, J_{PC} =11.0, 1C, CH_{Ar}), 130.47 (d, J_{FC} =9.9, 1C, CH_{Ar}), 161.35 (vt, J_{PC} = J_{FC} =10.4, 1C, C_{Ar}OP), 163.99 (d, J_{FC} =245.6, 1C, F-C_{Ar}). Anal. Calcd. for $C_{12}H_{18}FOP$ (228.24) : C, 63.15; H, 7.95. Found : C, 63.43; H, 8.20.

(4-OMe-C$_6$H$_4$O)P(*i*-Pr)$_2$, 1b. The procedure described above for the preparation of **1e** was used here to give **1b** as a colorless oil (1,87 g, 97%). ^{1}H NMR (400 MHz, 20 °C, $CDCl_3$) : δ 1.13 (dd, J_{HP} = 15.8, J_{HH} = 7.2, 6H, CH(CH_3)$_2$), 1.21 (dd, J_{HP} = 10.7, J_{HH} = 6.9, 6H, CH(CH_3)$_2$), 1.92 (hd, J_{HH} = 7.0, J_{HP} = 2.1, 2H, PCH(CH$_3$)$_2$), 3.74 (s, 3H, OMe), 6.81 (d, J_{HH} = 6.8, 2H, H$_{Ar}$), 7.05 (dd, J_{HH} = 8.7, J_{PH} = 1.5, 2H, H$_{Ar}$). ^{31}P{1H} NMR (162 MHz, 20 °C, $CDCl_3$): δ 150.6 (s). ^{13}C{^{1}H} NMR (101 MHz, 20 °C, $CDCl_3$) : δ 16.97 (d, J_{CP} = 8.5, 2C, CH$_3$), 17.74 (d, J_{CP} = 20.2, 2C, CH$_3$), 28.26 (d, J_{CP} = 17.8, 2C, PCH(CH$_3$)$_2$), 55.40 (s, 1C, OMe), 114.31 (s, 2C, CH$_{Ar}$), 119.25 (d, J_{PC} =9.5, 2C, CH$_{Ar}$), 153.21 (d, J_{PC} =8.8, 1C, C_{Ar}), 154.36 (s, 1C, C_{Ar}). Anal. Calcd. for $C_{13}H_{21}O_2P$ (240.28) : C, 64.98; H, 8.81. Found : C, 64.90; H, 8.94.

(4-COOMe-C$_6$H$_4$O)P(*i*-Pr)$_2$, 1d. The procedure described above for the preparation of **1e** was used here to give **1d** as a colorless oil (0.90 g, 87%). ^{1}H NMR (400 MHz,

20 °C, $CDCl_3$) : δ 1.04-1.09 (m, 6H, CH(CH_3)$_2$), 1.11-1.15 (m, 6H, CH(CH_3)$_2$), 1.92 (m, 2H, PCH(CH$_3$)$_2$), 3.85 (m, 3H, OMe), 7.13 (m, 2H, H$_{Ar}$), 7.94 (m, 2H, H$_{Ar}$). ^{31}P{1H} NMR (162 MHz, 20 °C, $CDCl_3$): δ 150.4 (s). ^{13}C{^{1}H} NMR (101 MHz, 20 °C, $CDCl_3$) : δ 17.01 (d, J_{CP} = 8.3, 2C, CH$_3$), 17.71 (d, J_{CP} = 20.2, 2C, CH$_3$), 28.37 (d, J_{CP} = 17.8, 2C, PCH(CH$_3$)$_2$), 51.90 (s, 1C, OMe), 118.15 (d, J_{PC} = 11.1 2C, CH$_{Ar}$), 123.40 (s, 1C,C$_{Ar}$), 131.5 (s, 2C, CH$_{Ar}$), 163.48 (d, J_{PC} =8.4, 1C, C=O or C_{Ar}OP), 166.84 (s, 1C, C=O or C_{Ar}OP). Anal. Calcd. for $C_{14}H_{21}O_3P$ (268.29) : C, 62.67; H, 7.89. Found : C, 62.59; H, 7.91.

***trans*-{*i*-Pr$_2$P(OPh)}$_2$NiBr$_2$, 2a.** [(*i*-PrCN)NiBr$_2$]$_n$ (1.9 mmol, 547 mg) was added to a solution of **1a** (3.81 mmol, 800 mg) in toluene (5 mL), and the resulting brown solution stirred for 2 h at r. t. Filtration and evaporation gave the target compound as a dark brown solid (995 mg, 82 %). Brown single crystals were obtained through slow crystallization in toluene (2 d at -37 °C). This complex is fairly air-stable over short periods, but aerobic decomposition sets in after a week to give an NMR-silent beige powder. ^{1}H NMR (500MHz , 20 °C, CD_2Cl_2) : δ 1.42 (d, J_{HH} = 7.1, 12H, CH(CH_3)), 1.54 (d, J_{HH} = 7.2, 12H, CH(CH_3)), 2.79 (h, J_{HH} = 7.1, 4H, CH(CH$_3$)), 7.11 (tt, J_{HH} = 7.1, J_{HH} = 1.0 2H, H$_{para}$), 7.37 (dd, J_{HH} = 8.6, J_{HH} = 7.4, 4H, H$_{meta}$), 7.66 (dm, J_{HH} = 7.6, 4H, H$_{ortho}$). ^{1}H NMR (500MHz , -68 °C, CD_2Cl_2) : δ 1.37 (dt^v, J_{HH}= 7.2, J_{HP}= 7.1, 12H, CH(CH_3)), 1.47 (dt^v, J_{HH}= 7.8, J_{HP}= 7.7, 12H, CH(CH_3)), 2.70 (m, 4H, CH(CH$_3$)), 7.10 (t, J_{HH} = 7.3, 2H, H$_{para}$), 7.37 (dd, J_{HH} = 8.3, J_{HH} = 7.6, 4H, H $_{metha}$), 7.66 (d, J_{HH} = 8.0, 4H, H$_{ortho}$). ^{13}C{1H} NMR(125 MHz , 20 °C, CD_2Cl_2) : δ 18.25 (s, 4C, CH$_3$), 19.70 (s, 4C, CH$_3$), 30.08 (s, 4C, PCH(CH$_3$)$_2$), 120.23 (s, 4C, CH$_{Ar}$), 122.96 (s, 2C, CH$_{Ar}$), 129.30 (s, 4C, CH$_{Ar}$), 155.28 (s, 2C, C_{Ar}OP). ^{13}C{1H}

NMR(125 MHz , -68 °C, CD_2Cl_2) : δ 17.6 (s, 4C, *C*H_3), 19.12 (s, 4C, *C*H_3), 29.03 (vt, J_{PC} = 11.9, 4C, P*C*H(CH_3)$_2$), 119.20 (s, 4C, *C*H_{Ar}), 122.26 (s, 2C, *C*H_{Ar}), 128.80 (s, 4C, *C*H_{Ar}), 154.26 (s, 1C, C_{Ar}OP). ^{31}P {1H} NMR (201 MHz, 20 °C, CD_2Cl_2) ; δ 136.0 (bs, 1P). ^{31}P {1H} NMR (201 MHz, -68 °C, CD_2Cl_2) ; δ 136.0 (s, 1P) Anal. Calcd. for $C_{24}H_{38}Br_2NiO_2P_2$ (639,01) : C, 45.11; H, 5.99. Found : C, 45.19; H, 5.92.

***trans*-{*i*-Pr$_2$P(4-OMe-C$_6$H$_4$O)}$_2$NiBr$_2$, 2b.** The procedure described above for the preparation of **2a** was used to give **2b** as a dark orange solid (458 mg, 80%). ^{1}H NMR (400 MHz, 20 °C, $CDCl_3$) : δ 1.42 (m, 24H, CH(C*H*$_3$)), 2.81 (m, 4H, C*H*(CH_3)), 3.82 (s, 6H, OMe), 6.88 (m, 4H, H$_{Ar}$), 7.51 (m, 4H, H$_{Ar}$). ^{13}C{1H} NMR(101 MHz , 20 °C, $CDCl_3$) : δ 18.13 (s, 4C, *C*H_3), 19.43 (s, 4C, *C*H_3), 29.73 (s, 4C, P*C*H(CH_3)$_2$), 55.63 (s, 2C, OMe), 114.02 (s, 4C, *C*H_{Ar}), 120.82 (s, 4C, *C*H_{Ar}), 148.73 (s, 2C, O*C*$_{Ar}$), 155.07 (s, 2C, C_{Ar}OP). ^{31}P {1H} NMR (162 MHz, 20 °C, $CDCl_3$) ; δ 136.0 (bs, 1P) Anal. Calcd. for $C_{26}H_{42}Br_2NiO_4P_2$ (699,06) : C, 44.67; H, 6.06. Found : C, 44.71; H, 6.14.

***trans*-{*i*-Pr$_2$P(4-Me-C$_6$H$_4$O)}$_2$NiBr$_2$, 2c.** The procedure described above for the preparation of **2a** was used to give **2c** as a dark orange solid (800 mg, 80%). ^{1}H NMR (400 MHz, 20 °C, $CDCl_3$): δ 1.40 (d, J_{HH} = 7.0, 12H, CH(C*H*$_3$)), 1.52 (d, J_{HH} = 7.1, 12H, CH(C*H*$_3$)), 2.33 (s, 6H, Me), 2.75 (h, J_{HH} = 7.1, 4H, C*H*(CH_3)), 7.11 (d, J_{HH} = 8.1, 4H, H$_{Ar}$), 7.50 (d, J_{HH} = 8.3, 4H, H$_{ortho}$). ^{31}P {1H} NMR (162 MHz, 20 °C, $CDCl_3$) ; δ 136.0 (bs, 1P) Anal. Calcd. for $C_{26}H_{42}Br_2NiO_2P_2$ (667,06) : C, 46.81; H, 6.35. Found : C, 47.08; H, 6.44.

***trans*-{*i*-$Pr_2P(4\text{-}COOMe\text{-}C_6H_4O)$}$_2NiBr_2$, 2d.** The procedure described above for the preparation of **2a** was used to give **2d** as a dark orange solid (504 mg, 91%). ^{1}H NMR (300 MHz, 20 °C, $CDCl_3$) : δ 1.40 (d, J_{HH} = 6.4, 12H, CH(CH_3)), 1.55 (d, J_{HH} = 6.4, 12H, CH(CH_3)), 2.76 (h, J_{HH} = 7.1, 4H, CH(CH_3)), 3.92 (s, 6H, OMe), 7.63 (d, J_{HH} = 7.6, 4H, H_{Ar}), 8.04 (d, J_{HH} = 8.6, 4H, H_{ortho}). ^{13}C{1H} NMR(75 MHz , 20 °C, $CDCl_3$) : δ 18.20 (s, 4C, CH$_3$), 19.70 (s, 4C, CH$_3$), 29.90 (s, 4C, PCH(CH_3)$_2$), 52.16 (s, 2C, OMe), 119.83 (s, 4C, CH$_{Ar}$), 124.76 (s, 2C, C_{Ar}), 131.09 (s, 4C, CH$_{Ar}$), 158.86 (s, 2C, C_{Ar}OP), 166.71 (s, 2C, C=O).^{31}P {1H} NMR (162 MHz, 20 °C, $CDCl_3$) ; δ 139.9 (bs, 1P) Anal. Calcd. for $C_{28}H_{42}Br_2NiO_3P_2$. C_7H_8 (847.22) : C, 49.62; H, 5.95. Found : C, 49.28; H, 5.89.

***trans*-(κ^2-*P*,*C*-*i*-Pr_2POPh)(*i*-Pr_2POPh)NiBr, 3a.** [(*i*-PrCN)$NiBr_2$]$_n$ (1.25 mmol, 360 mg) and NEt_3 (1.66 mmol, 232 µL) were added to a solution of **1a** (500 mg, 2.08 mmol) in toluene (20 mL). The resulting brown solution was stirred over 48 h at 100 °C, evaporated, and the solid residues extracted with toluene (2 x 30 mL). Evaporation of the combined extracts gave **3a** as a yellow solid (540 mg, 93%), which was found to be greater than 98% pure by NMR spectroscopy; this material was used in subsequent experiments without further purification. Single crystals were obtained from a saturated hexane solution at -37 °C. ^{1}H NMR (400 MHz, 20 °C, C_6D_6): δ 1.27 (vt, J_{HP} = J_{HH} = 6.3, 6H, CH(CH_3)$_2$), 1.30 (dd, J_{HP} = 4.5, J_{HH} = 7.0, 6H, CH(CH_3)$_2$), 1.51 (dd, J_{HP} = 16.8, J_{HH} = 7.2, 6H, CH(CH_3)$_2$), 1.56 (dd, J_{HP} = 16.0, J_{HH} = 7.3, 6H, CH(CH_3)$_2$), 2.49 (m, 2H, PCH(CH_3)$_2$), 2.81 (m, 2H, PCH(CH_3)$_2$), 6.51 (t, J_{HH} = 7.4, 1H, H_{Ar}), 6.67 (t, J_{HH} = 7.4, 1H, H_{Ar}), 6.80-6.87 (m, 2H, H_{Ar}), 6.93 (t, J_{HH} = 7.6, 2H, H_{Ar}) , 7.57 (d, J_{HH} = 8.4, 2H, H_{Ar}), 7.64 (d, J_{HH} = 7.7, 1H, H_{Ar}). ^{13}C{^{1}H}

NMR (101 MHz, 20 °C, $CDCl_3$) : δ 17.12 (s, 2C, CH_3), 17.87 (s, 2C, CH_3), 18.79 (d, J_{CP} = 3.5, 2C, CH_3), 20.52 (d, J_{CP} = 4.6, 2C, CH_3), 28.63 (dd, J_{CP}= 2.4, J_{CP}= 23.7, 2C, P$CH(CH_3)_2$), 29.94 (dd, J_{CP}= 2.8, J_{CP}= 17.6, 2C, P$CH(CH_3)_2$), 110.35 (d, J_{PC}=13.5, 1C, CH_{Ar}), 120.0 (d, J_{CP}= 6.1, 2C, CH_{Ar}), 120.55 (m, 1C, CH_{Ar}), 122.51 (s, CH_{Ar}), 126.46 (s, 1C, CH_{Ar}), 128.91 (s, 2C, CH_{Ar}), 132.0 (dd, J_{CP}= 14.3, J_{CP}= 29.3, 1C, Ni-C_{Ar}), 142.25 (d, J_{CP}= 11.0, 1C, CH_{Ar}), 154.73 (d, J_{CP}= 4.6, 1C, OC_{Ar}), 168.38 (dd, J_{CP}= 4.3, J_{CP}= 16.2, 1C, OC_{Ar}).^{31}P {1H} NMR (162 MHz, 20 °C, C_6D_6) ; δ 151.86 (d, (AB) J_{PP} = 325, 1P), 184.66 (d, (AB) J_{PP} = 325, 1P). Anal. Calcd. for $C_{24}H_{37}BrNiO_2P_2$ (558.09) : C, 51.65; H, 6.68. Found : C, 51.94; H, 6.71.

[(κ^2-*P*,*C*-*i*-Pr$_2$POPh)NiBr(μ-Br)]$_2$, 4a. $[(i\text{-PrCN})NiBr_2]_n$ (5.45 g, 19 mmol) and NEt_3 (2.64 mL, 19 mmol) were added to a solution of **1a** (2 g, 9.5 mmol) in toluene (50 mL). The resulting brown solution was stirred over 40 h at 100 °C to give a green mixture, which was evaporated and the solid residues extracted with toluene (2 x 50 mL), and washed with hexane (25 mL) to give **4a** as a yellow powder (2.3 g, 70%). Evaporation of the combined extracts gave **3a** as a yellow solid (540 mg, 93%), Single crystals were obtained from a saturated toluene/hexane solution at -37 °C. ^{1}H NMR (500MHz , 20 °C, CD_2Cl_2) : δ 1.37 (dd, J_{HH} = 6.8, J_{HP} = 14.6, 24H, CH(CH_3)), 1.57 (dd, J_{HH} = 6.0, J_{HP} = 17.3, 24H, CH(CH_3)), 2.35 (m, 4H, CH(CH_3)), 6.59 (m, 4H, H_{Ar}), 6.92 (m, 2H, H_{Ar}), 7.27 (m, 2H, H_{Ar}). ^{13}C{1H} NMR(125 MHz , 20 °C, CD_2Cl_2) : δ 16.69 (s, 4C, CH_3), 18.00 (s, 4C, CH_3), 28.90 (d, J_{CP} = 26.6, 4C, P$CH(CH_3)_2$), 110.23 (d, J_{CP} = 13.8, 2C, CH_{Ar}), 121.02 (s, 2C, CH_{Ar}), 126.95 (s, 2C, CH_{Ar}), 128.56 (bm, 2C, NiC_{Ar}), 140.71 (s, 2C, CH_{Ar}), 166.58 (d, J_{CP} = 12.0, 2C,

OC_{Ar}). ^{31}P {1H} NMR (201 MHz, 20 °C, CD_2Cl_2) ; δ 199.1 (s, 1P). Anal. Calcd. for $C_{24}H_{36}Br_2Ni_2O_2P_2$ (695.68) : C, 41.44; H, 5.22. Found : C, 42.06; H, 5.22.

Functionalization of phenol to 2-Benzylphenol. Benzyl bromide (2.84 mmol, 338 µL) was added to a solution of **4a** (0.95 mmol, 660 mg) in toluene (25 mL), and the resulting mixture was stirred for 36 h at 90°C. The final mixture was added to HCl_{aq} (100 mL, 2.5M) and extracted with CH_2Cl_2 (3 x 50 mL). The combined organic phases were dried over $MgSO_4$, filtered and evaporated under vaccum, and the residue obtained was purified on silica gel column ($CHCl_3$/Hexane = 1:1) to give 2-benzylphenol (R_f = 0.1) as a white solid (47 %, 164 mg). ^{1}H NMR (400MHz , 20 °C, $CDCl_3$) : δ 3.91 (s, 2H, CH_2), 4.83 (s, 1H, O*H*), 6.63 (d, J_{HH}= 7.8, 1H, CH_{Ar}), 6.82 (t, J_{HH}= 7.1, 1H, CH_{Ar}), 7.03 (m, 2H, CH_{Ar}), 7.14-7.21 (m, 5H, CH_{Ar}). ^{13}C NMR(125 MHz , 20 °C, $CDCl_3$) : 36.31 (s, 1C, *C*H$_2$), 115.80 (s, 1C, *C*H$_{Ar}$), 121.06 (s, 1C, *C*H$_{Ar}$), 126.38 (s, 1C, *C*H$_{Ar}$), 127.18 (s, 1C, C_q), 127.86 (s, 1C, *C*H$_{Ar}$), 128.68 (s, 2C, *C*H$_{Ar}$), 128.80 (s, 2C, *C*H$_{Ar}$), 131.04 (s, 1C, *C*H$_{Ar}$), 140.03 (s, 1C, C_q), 153.66 (s, 1C, C_q). GC-MS m/z = 184 (M^+).

Crystal Structure Determinations. The crystallographic data for compounds **2a**, **2d** and **3a** were collected on a Bruker. Microstar generator (micro source) equipped with a Helios optics, a Kappa Nonius goniometer, and a Platinum135 detector. The crystallographic data for complexes **4a**, **2c**, and **2b** were collected on a a Bruker APEX II equipped with a Incoatec I\muS Microsource and a Quazar MX monochromator. Cell refinement and data reduction were done using SAINT[27]. An empirical absorption correction, based on the multiple measurements of equivalent reflections, was applied using the program SADABS[28]. The space group was

confirmed by XPREP routine[29] in the program SHELXTL[30]. The structures were solved by direct methods and refined by fullmatrix least-squares and difference Fourier techniques with SHELX-97[31]. All non-hydrogen atoms were refined with anisotropic displacement parameters. Hydrogen atoms were set in calculated positions and refined as riding atoms with a common thermal parameter.

8.6 Acknowledgments.

The authors are grateful to: NSERC of Canada for a Discovery Grant to D.Z.; Université de Montréal, Centre in Green Chemistry and Catalysis and FQRNT for graduate fellowships to B.V. ; Dr. Michel Simard for his valuable assistance with crystallography.

8.7 Supporting Information

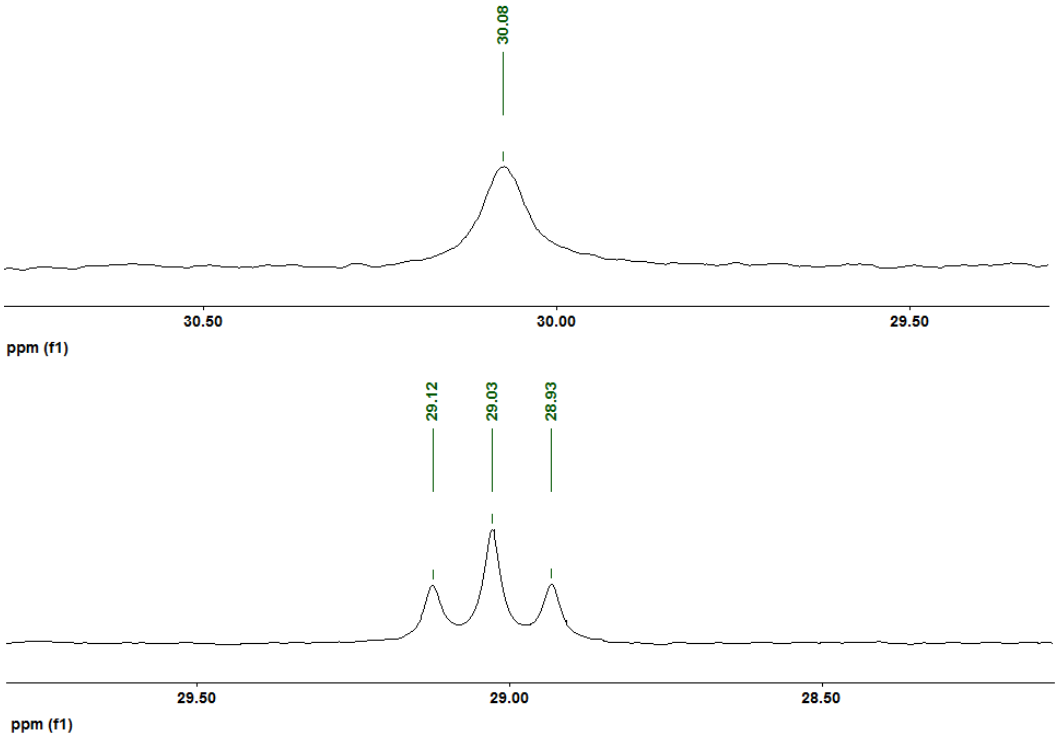

Figure 8.4 : $^{13}C\{^{1}H\}$ NMR (125 MHz) of P*C*H$(CH_3)_2$ **2a** at 20°C (top) and at -68°C (below) in CD_2Cl_2.

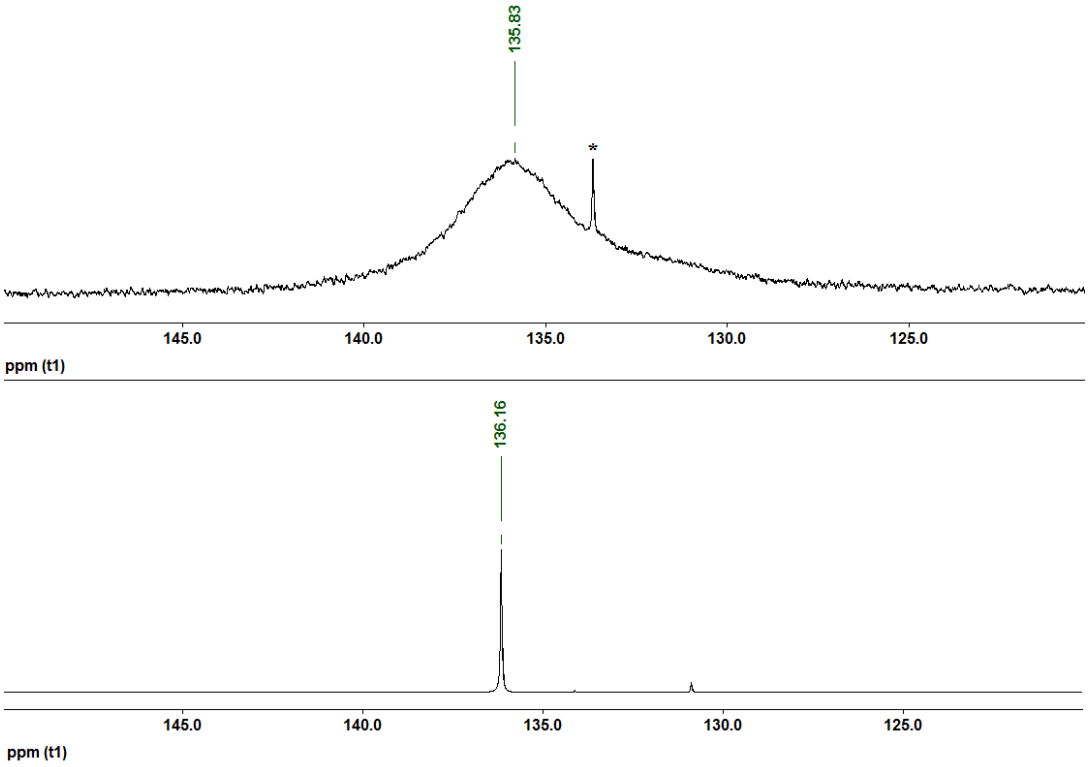

Figure 8.5 : $^{31}P\{^{1}H\}$ NMR (201 MHz) of **2a** at 20°C (top) and at -68°C (below) in CD_2Cl_2 (* = impurity).

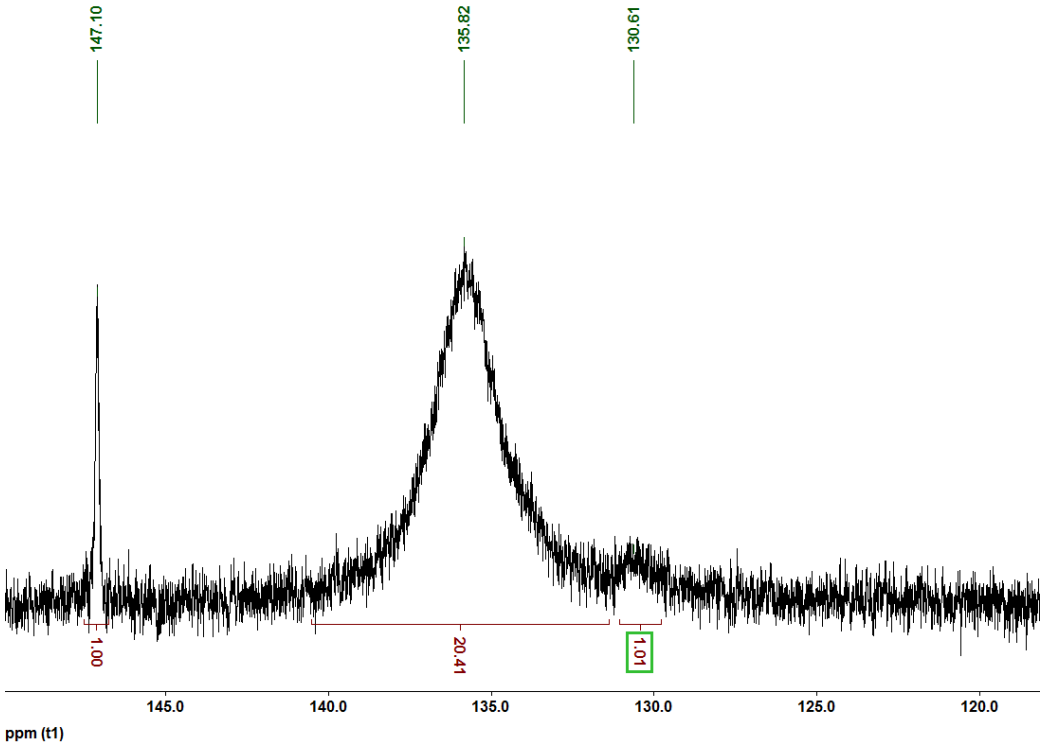

Figure 8.6 : ^{31}P NMR spectra after addition at room temperature of NEt_3 (13 µL, 93.8 µmol) to a solution of **2a** (50mg, 78.2 µmol) in Toluene (1.2 mL).

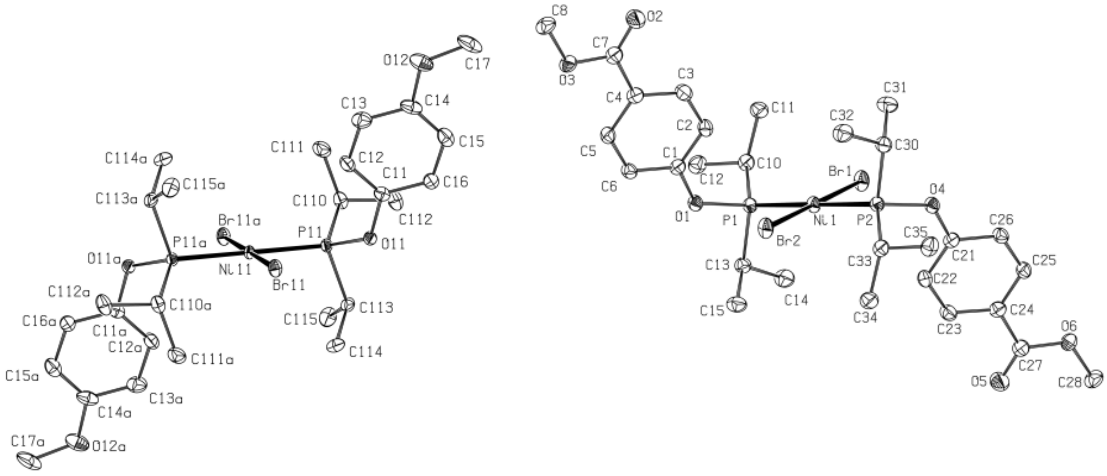

Figure 8.7. ORTEP diagrams for complexes **2b** and **2d**. Thermal ellipsoids are shown at the 50% probability level. Hydrogen atoms are omitted for clarity.

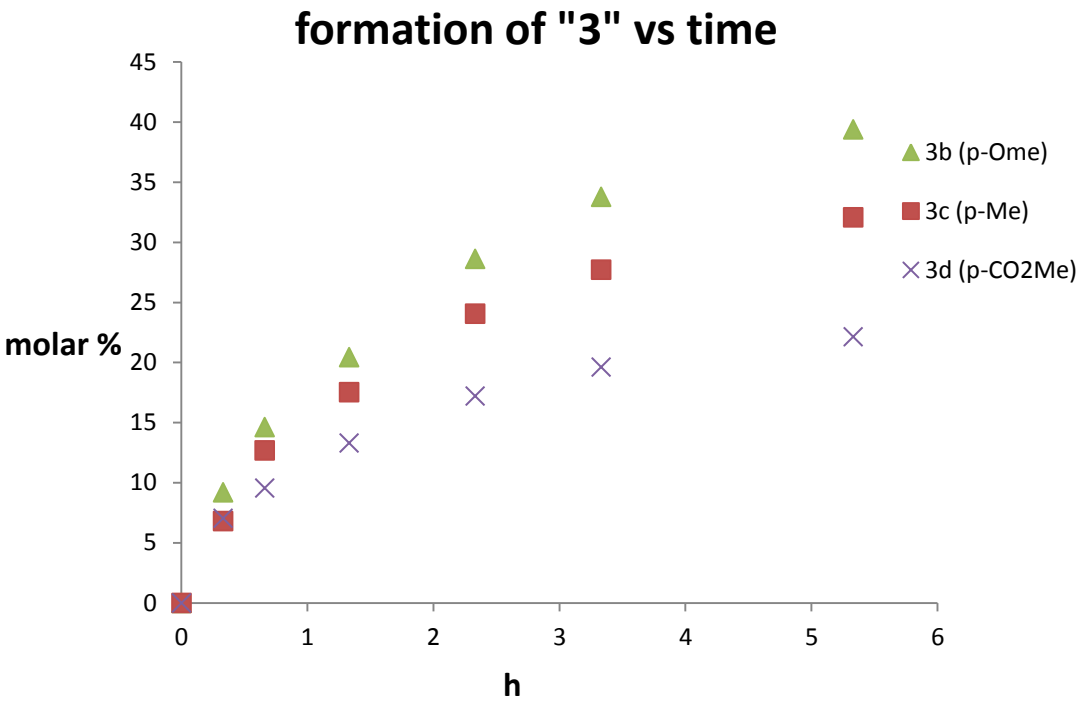

Figure 8.8 : Evolution of **3b**, **3c** and **3d** from **2b**, **2c**, **2d** (0.16 mmol) in toluene solution (382 µL) presence of NEt_3 (1.6 mmol, 218 µL) at 100°C versus time.

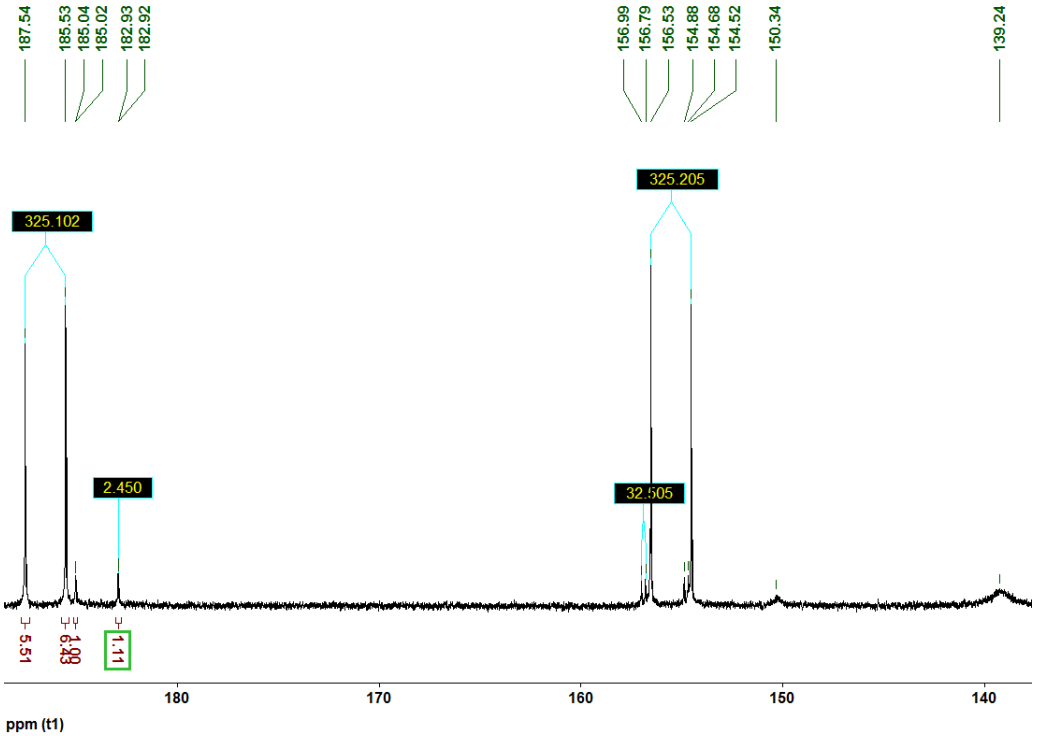

Figure 8.9 : $^{31}P\{^{1}H\}$ NMR (162 MHz) of mixture of trans-[$NiBr_2${3-F-(*i*-Pr_2PO)-C_6H_4}$_2$], of ligand 1b, and complexes 3b and 3b' in C_6D_6.

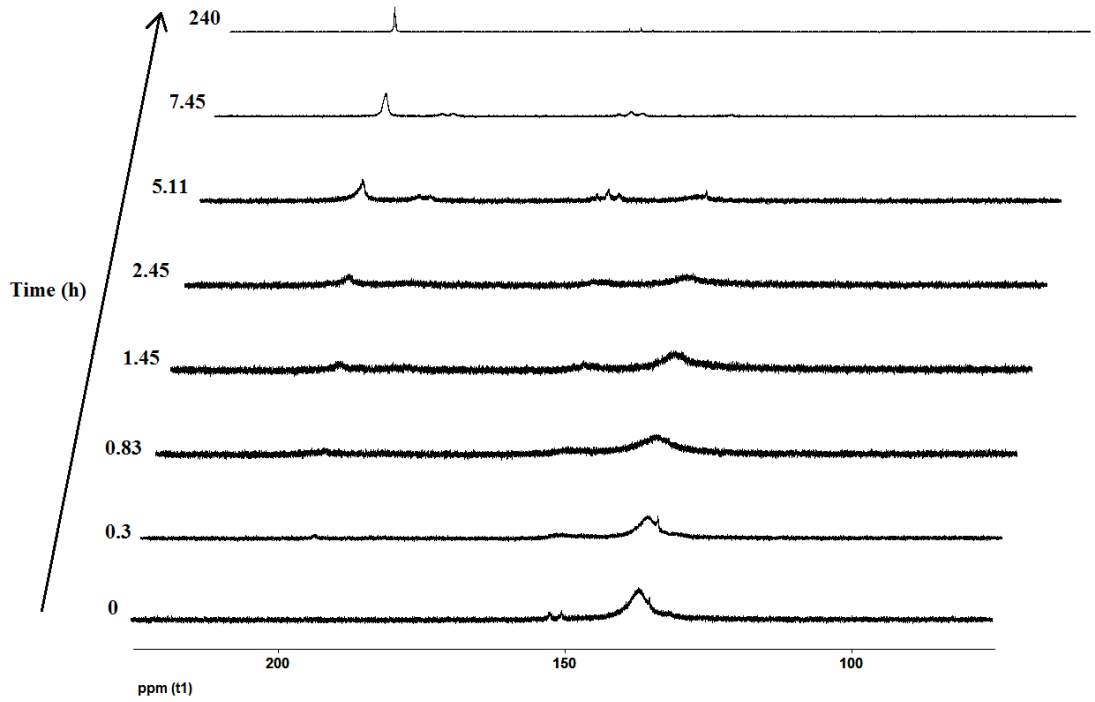

Figure 8.10 : 31P{1H} NMR monitoring of a solution of **1a** (34 mg, 0.16 mmol), NiBr2(NCiPr)]n (46 mg, 0.16 mmol) and NEt_3 (22 µL, 0.16 mmol) in Toluene (0.6 mL) at 90°C versus time.

Table 8.2. Crystal Data Collection and Refinement Parameters for Complex **2a**, **3a**, and **4a**.

	2a	**3a**	**4a**
chemical formula	$C_{24}H_{38}Br_2NiO_2P_2$	$C_{24}H_{37}BrNiO_2P_2$	$C_{24}H_{36}Br_2Ni_2O_2P$
crystal colour	red	yellow	yellow

Fw; *F*(000)	639.01; 326	558.10; 1160	695.71; 704
T (K)	150	150	100
wavelength (Å)	1.54178	1.54178	1.54178
space group	P-1	P21/n	P21/n
a (Å)	8.2865(8)	10.7627(4)	9.89710(10)
b (Å)	8.7999(8)	13.6755(5)	11.02090(10)
c (Å)	10.9270(10)	17.913(6)	12.80450(10)
α (deg)	109.64(4)	90	90
β (deg)	93.043(4)	93.7180(16)	104.5970(10)
γ (deg)	114.612(3)	90	90
Z	1	4	2
V (Å^3)	664.70(11)	2630.96(16)	1351.57(2)
ρ_{calcd} (g·cm^{-3})	1.596	1.409	1.709
μ (mm^{-1})	5.854	4.122	6.462
θ range (deg); completeness	4.41 − 69.65; 0.991	4.07 − 69.68; 0.992	6.475 − 71.018; 0.994
R1[a]; wR2[b] [I > 2σ(I)]	0.0282; 0.0748	0.0318; 0.0842	0.0408; 0.1353
R1; wR2 [all data]	0.0284; 0.0751	0.0325; 0.0849	0.0408; 0.1353
GOF	1.018	1.062	1.021
largest diff peak and hole	0.692 and -0.435	0.655 and -0.332	1.043 and -1.274

[a] $R_1=\Sigma(||F_o|-|F_c||)/\Sigma|F_o|$ [b] $wR_2=\{\Sigma[w(F_o^2-F_c^2)^2]/\Sigma[w(F_o^2)^2]\}^{½}$

Table 8.3. Crystal Data Collection and Refinement Parameters for Complexes **2b**, **2c**, and **2d**.

	2b	**2c**	**2d**
chemical formula	$C_{26}H_{42}Br_2NiO_4P_2$	$C_{26}H_{42}Br_2NiO_2P_2$	C28H42Br2NiO6P2 ,C7H8
crystal colour	red	red	yellow
Fw; *F*(000)	699.06; 716	667.06; 1368	847.22; 872
T (K)	100	100(2)	100(2)
wavelength (Å)	1.54178	1.54178	1.54178
space group	P-1	P 1 21/c 1	P-1
a (Å)	9.0321(2)	8.48140(10)	10.4323(6)
b (Å)	11.0400(3)	20.749(2)	12.5239(7)
c (Å)	15.7000(4)	17.7094(2)	15.3754(9)
α (deg)	102.066(1)	90	99.459(2)
β (deg)	96.868(1)	107.9730(10)	106.577(2)
γ (deg)	96.906(1)	90	95.334(2)
Z	2	4	2
V (Å^3)	1502.84(7)	2964.4(3)	1878.28(19)
ρ_{calcd} (g·cm^{-3})	1.545	1.495	1.498
μ (mm^{-1})	5.283	5.275	4.379
θ range (deg); completeness	2.911 − 71.175; 0.975	3.379 − 71.755; 0.997	3.061 − 69.828; 0.992
R1[a]; wR2[b] [I > 2σ(I)]	0.0403; 0.1067	0.0201; 0.0522	0.0326; 0.0910
R1; wR2 [all data]	0.0404; 0.1067	0.0202; 0.0522	0.0340; 0.0934

GOF	1.197	1.157	1.053
largest diff peak and hole	1.808 and -0.406	0.370 and -0.253	0.793 and -0.371

[a] $R_1=\Sigma(||F_o|-|F_c||)/\Sigma|F_o|$ [b] $wR_2=\{\Sigma[w(F_o^2-F_c^2)^2]/\Sigma[w(F_o^2)^2]\}^{1/2}$

8.8 References

[1] For recent review on the subject see : (a) Kakiuchi, F.; Kochi, T. *Synthesis* **2008**, *2008*, 3013. (b) Ackermann, L. *Chem. Rev.* **2011**, *111*, 1315. (c) Yamaguchi, J.; Yamaguchi, A. D.; Itami, K. *Angew. Chem. Int. Ed.* **2012**, *51*, 8960. (d) Ackermann, L. *Chem. Commun.* **2010**, *46*, 4866. (e) Chen, D. Y.-K.; Youn, S. W. *Chem. Eur. J.* **2012**, *18*, 9452.

[2] For palladium reviews see : (a) Lyons, T. W.; Sanford, M. S. *Chem. Rev.* **2010**, *110*, 1147. (b) Xu, L.-M.; Li, B.-J.; Yang, Z.; Shi, Z.-J. *Chem. Soc. Rev.* **2010**, *39*, 712. (c) Sehnal, P.; Taylor, R. J. K.; Fairlamb, I. J. S. *Chem. Rev.* **2010**, *110*, 824. (d) Dai, H.-X.; Li, G.; Zhang, X.-G.; Stepan, A. F.; Yu, J.-Q. *J. Am. Chem. Soc.* **2013**, *135*, 7567. For rhodium review see : (e) Colby, D. A.; Bergman, R. G.; Ellman, J. A. *Chem. Rev.* **2010**, *110*, 624. (f) Rouquet, G.; Chatani, N. *Angew. Chem. Int. Ed.* **2013**, *52*, 11726. For Iridium review see : (g) Klei S. R.; Tan K. L.; Golden J. T.; Yung C. M.; Thalji R. K.; Ahrendt K. A.; Ellman J. A.; Tilley T. D.; Bergman R. G. C—H Bond Activation by Iridium and Rhodium Complexes: Catalytic Hydrogen—Deuterium Exchange and C—C Bond-Forming Reactions. *In Activation and Functionalization of C-H Bonds; Goldberg, K. I.; Goldman, A. S., Eds.; ACS Symposium Series 885; American Chemical Society: Washington, DC, 2004, pp 46-55.* For ruthenium review see : (h) Arockiam, P. B.; Bruneau, C.; Dixneuf, P. H. *Chem. Rev* **2012**, *112*, 5879.

[3] (a) Yoshikai, N.; Matsumoto, A.; Norinder, J.; Nakamura, E. *Angew. Chem. Int. Ed.* **2009**, *48*, 2925. (b) Norinder, J.; Matsumoto, A.; Yoshikai, N.; Nakamura, E. *J. Am. Chem. Soc.* **2008**, *130*, 5858. (c) Wen, J.; Zhang, J.; Chen, S.-Y.; Li, J.; Yu, X.-Q. *Angew. Chem. Int. Ed.* **2008**, *47*, 8897. (d) Liu, W.; Cao, H.; Lei, A. *Angew. Chem. Int. Ed.* **2010**, *49*, 2004.

[4] (a) Yoshikai, N. *Synlett.* **2011**, *2011*, 1047. (b) Gao, K.; Yoshikai, N. *Chem. Commun.* **2012**, *48*, 4305. (b) Gao, K.; Lee, P.-S.; Fujita, T.; Yoshikai, N. *J. Am. Chem. Soc.* **2010**, *132*, 12249. (c) Lee, P.-S.; Fujita, T.; Yoshikai, N. *J. Am. Chem. Soc.* **2011**, *133*, 17283. (d) Gao, K.; Yoshikai, N. *J. Am. Chem. Soc.* **2013**, *135*, 9279. (e) Gao, K.; Yoshikai, N. *J. Am. Chem. Soc.* **2011**, *133*, 400.

[5] (a) Shacklady-McAtee, D. M.; Dasgupta, S.; Watson, M. P. *Org. Lett.* **2011**, *13*, 3490. (b) Ogata, K.; Atsuumi, Y.; Shimada, D.; Fukuzawa, S. *Angew. Chem. Int. Ed.* **2011**, *50*, 5896. (c) Shiota, H.; Ano, Y.; Aihara, Y.; Fukumoto, Y.; Chatani, N. *J. Am. Chem. Soc.* **2011**, *133*, 14952. (d) Kanyiva, K. S.; Nakao, Y.; Hiyama, T. *Angew. Chem. Int. Ed.* **2007**, *46*, 8872. (e) Nakao, Y.; Kanyiva, K. S.; Hiyama, T. *J. Am. Chem. Soc.* **2008**, *130*, 2448. (f) Tobisu, M.; Hyodo, I.; Chatani, N. *J. Am. Chem. Soc.* **2009**, *131*, 12070. (g) Aihara, Y.; Chatani, N. *J. Am. Chem. Soc.* **2013**, *135*, 5308. (h) Song, W.; Lackner, S.; Ackermann, L. *Angew. Chem. Int. Ed.* **2014**, *53*, 2477

[6] Kleiman J. P.; Dubeck M. *J. Am. Chem. Soc.*, **1963**, *85*, 1544

[7] Zargarian D. *Coord. Chem. Rev.* **2002**, *233,* 157

[8] (a) Ceder, R. M.; Granell, J.; Muller, G. *J. Chem. Soc., Dalton Trans.* **1998**, 1047. (b) Ceder, R. M.; Granell, J.; Muller, G.; Font-Bardia, M.; Solans, X.

Organometallics **1995**, *14*, 5544. (c) Ceder, R. M.; Granell, J.; Muller, G.; Font-Bardía, M.; Solans, X. *Organometallics* **1996**, *15*, 4618.

[9] (a) Muller, G.; Panyella, D.; Rocamora, M.; Sales, J.; Font-Bardía, M.; Solans, X. *J. Chem. Soc., Dalton Trans.* **1993**, 2959.

[10] Ruhland, K.; Obenhuber, A.; Hoffmann, S. D. *Organometallics* **2008**, *27*, 3482.

[11] Cámpora et al. have also reported imidoyl complexes prepared by insertion of ArNC or CO into the Ni- bimetallic species *trans*-$(Me_3P)BrNi(\mu_2\text{-}\eta^3\text{: }\eta^1\text{-}CH_2\text{-}ortho\text{-}C_6H_4)NiBr(PMe_3)_2$: (a) Campora, J.; Gutierrez, E.; Monge, A.; Poveda, M. L.; Ruiz, C.; Carmona, E. *Organometallics* **1993**, *12*, 4025. (b) Campora, J.; Gutierrez, E.; Monge, A.; Poveda, M. L.; Carmona, E. *Organometallics* **1992**, *11*, 2644.

[12] Edwards, A. J.; Macgregor, S. A.; Rae, A. D.; Wenger, E.; Willis, A. C. *Organometallics* **2001**, *20*, 2864.

[13] Nagashima, H.; Tanabiki, M. **2002** Patent Application, EP 1241175 A2

[14] (a) Pandarus, V.; Zargarian, D. *Chem. Commun.* **2007**, 978. (b) Pandarus, V.; Zargarian, D. *Organometallics* **2007**, *26*, 4321. (c) Salah, A. B.; Zargarian, D. *Dalton Trans.* **2011**, *40*, 8977. (d) Salah, A. B.; Offenstein, C.; Zargarian, D. *Organometallics* **2011**, *30*, 5352. (e) Lefèvre, X.; Spasyuk, D. M.; Zargarian, D. *J. Organomet. Chem.* **2011**, *696*, 864. (f) Lefèvre, X.; Durieux, G.; Lesturgez, S.; Zargarian, D. *J. Mol. Catal. A* **2011**, *335*, 1. (g) Vabre, B.; Lindeperg, F.; Zargarian, D. *Green Chem.* **2013**, *15*, 3188.

[15] Reaction of ethylene with Ru-phosphinite complexes obtained from C-H orthometalation provided one of the earliest examples of *ortho*-alkylation of phenol via ethylene insertion: Lewis, L. N.; Smith, J. F. *J. Am. Chem. Soc.***1986**, *108*, 2728.

[16] Bedford, R. B.; Coles, S. J.; Hursthouse, M. B.; Limmert, M. E. *Angew. Chem. Int. Ed.* **2003**, *42*, 112.

[17] Bedford, R. B.; Hazelwood (née Welch), S. L.; Horton, P. N.; Hursthouse, M. B. *Dalton Trans.* **2003**, 4164.

[18] Gulevich, A. V.; Melkonyan, F. S.; Sarkar, D.; Gevorgyan, V. *J. Am. Chem. Soc.* **2012**, *134*, 5528.

[19] Jiménez-Tenorio, M.; Puerta, M. C.; Salcedo, I.; Valerga, P.; Costa, S. I.; Silva, L. C.; Gomes, P. T. *Organometallics* **2004**, *23*, 3139.

[20] (a) Li, J.; Lutz, M.; Spek, A. L.; van Klink, G. P. M.; van Koten, G.; Klein Gebbink, R. J. M. *J. Organomet. Chem.* **2010**, *695*, 2618. (b) Bedford, R. B.; Hazelwood (néeWelch), S. L.; Limmert, M. E.; Albisson, D. A.; Draper, S. M.; Scully, P. N.; Coles, S. J.; Hursthouse, M. B. *Chem. Eur. J.* **2003**, *9*, 3216.

[21] (a) Dinger, M. B.; Scott, M. J. *Inorg. Chem.* **2001**, *40*, 856. (b) Cobley, C. J.; Ellis, D. D.; Orpen, A. G.; Pringle, P. G. *J. Chem. Soc., Dalton Trans.* **2000**, 1101.

[22] Boutadla, Y.; Davies, D. L.; Macgregor, S. A.; Poblador-Bahamonde, A. I. *Dalton Trans.* **2009**, 5820.

[23] Vabre, B.; Spasyuk, D. M.; Zargarian, D. *Organometallics* **2012**, *31*, 8561.

[24] Care was taken to ensure that all samples were treated in the same manner. The AB doublets emerging over time in the $^{31}P\{^{1}H\}$ NMR spectra and attributed to the cyclometalated complexes **3b-d** were used to estimate the extent of cyclometalation. This was done on the basis of integration against the signal for the internal standard PPh_3 contained in a carefully prepared sealed capillary that was used for all the samples.

[25] Vabre, B.; Lambert, M. L.; Petit, A.; Ess, D. H.; Zargarian, D. *Organometallics* **2012**, *31*, 6041.

[26] Kalyani, D.; Sanford, M. S. *Org. Lett.* **2005**, *7*, 4149.

[27] *SAINT*, *Release 6.06; Integration Software for Single Crystal Data*; Bruker AXS Inc.: Madison, WI, 1999

[28] Sheldrick, G. M. *SADABS, Bruker Area Detector Absorption Corrections;* Bruker AXS Inc., Madison, WI, 1999

[29] *XPREP, Release 5.10; X-ray Data Preparation and Reciprocal Space Exploration Program*; Bruker AXS Inc.: Madison, WI, 1997.

[30] *SHELXTL, Release 5.10; The Complete Software Package for Single Crystal Structure Determination*; Bruker AXS Inc.: Madison, WI, 1997.

[31] (a) Sheldrick, G. M. *SHELXS97, Program for the Solution of Crystal Structures*; Univ. of Gottingen: Germany, 1997. (b) Sheldrick, G. M. *SHELXL97, Program for the Refinement of Crystal Structures*; University of Gottingen: Germany, 1997.

Chapitre 8

Chapitre 9 : Conclusions et perspectives

Le faible coût du nickel et la synthèse facile des complexes pinces ont permis un développement considérable de cette chimie au cours de la dernière décennie. Les complexes POCOP de nickel ont montré de bonnes capacités catalytiques et ont contribué au développement d'applications remarquables. L'efficacité catalytique et la stabilité des complexes pinces dépend de leurs propriétés électroniques et stériques. La synthèse de nouveaux ligands et complexes est donc indispensable pour améliorer ces paramètres. Un autre domaine de la chimie en plein effervescence est l'activation et l'ortho-fonctionnalisation de lien C-H. L'utilisation du nickel dans ce domaine est encore sous-développée. C'est dans ce contexte que les travaux de cette thèse ont été développés. Les travaux présentés dans cette thèse concernent principalement la chimie des complexes pinces de nickel. La dernière partie ouvre une nouvelle fenêtre sur le développement de complexes cyclométallés de nickel.

Les ligands POCOP réagissent très rapidement avec $NiBr_2(NC^iPr)$ pour donner le complexe correspondant. Lors de cette synthèse, l'utilisation de précurseur de nickel fait à partir de brome et de nickel métallique dans un nitrile permet de travailler avec un précurseur de nickel soluble dans les solvants polaires (THF, nitrile (acétonitrile, propionitrile, isobutyronitrile). Une question sur la nature de ce précurseur en présence de la base se pose. Étant donné le changement de couleur lors de l'ajout de la triéthylamine (violet au bleu foncé dans le THF, bleu clair au bleu foncé dans les nitriles), il est possible qu'une substitution de ligand ait lieu pour

donner une espèce $NiBr_2(NEt_3)_n$. Une étude future UV-vis pourrait répondre à cette question.

L'utilisation de nickel métallique en poudre comme précurseur de nickel pour la synthèse des complexes reste néanmoins difficilement améliorable. Si cette nouvelle méthode de synthèse de complexe est très efficace (jusqu'à 93 % de rendement) et plus "verte", elle est optimisée avec un excès de nickel et requière des conditions plus dures (chauffage, milieu concentré et hétérogène). Cette nouvelle voie de synthèse des complexes POCOP pourrait être appliquée à d'autres métaux si le métal peut facilement être oxydé par HCl et si la métallation peut être effectuée par un précurseur métallique oxydé MCl_x.

La synthèse des ligands POCOP s'effectue à partir de résorcinol de chlorophosphine en présence de base. De nouveaux ligands R-$^{R'}$(POCOP) comportant divers substituants sur le cycle aromatique (R = 4-Me, 4-OMe, 4-COOMe, 3-OMe, 3-COOMe), ont été synthétisés avec la même méthode à partir des dérivés du résorcinol. La facilité de ces synthèses dépend principalement de la disponibilité commerciale (R = 4-Me, 4-OMe, 4-COOMe, 3-COOMe) ou de la possibilité de synthèse (R = 3-OMe) des dérivés du résorcinol. Ces facteurs s'appliquent aussi à la chlorophosphine qui détermine les substituants (R' = *i*-Pr, *t*-Bu, etc.) sur le phosphore. Les nouveaux ligands R-$^{R'}$(POCOP) et les complexes de nickel correspondants introduits au cours de nos travaux ont enrichi le catalogue des complexes POCOP de nickel (II). Malgré leurs propriétés significativement différentes, la réactivité des complexes associés ne change pas drastiquement (Figure 9.1). Cela a été observé dans le cas des (POCOP)Ni(CF_3) vs OMe-(POCOP)Ni(CF_3). Ces modifications sur le

ligand peuvent néanmoins être pratiques pour l'investigation de mécanisme réactionnel.[1] Des corrélations de Hammett peuvent notamment être effectuées, travail actuellement en cours par un membre du groupe.[2]

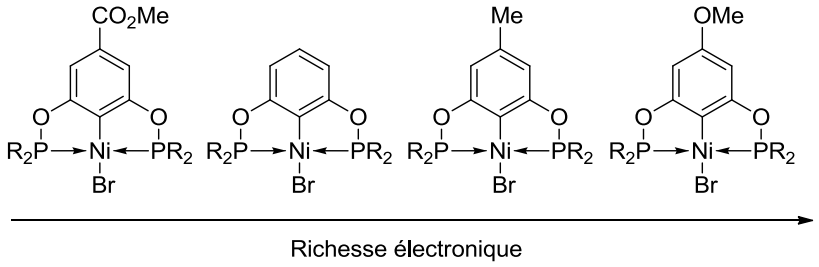

Figure 9.1 : Évolution de la richesse électronique du complexes en fonction des substituants du cycle aromatique.

Le mécanisme de synthèse de ces composés a été étudié via des réactions de compétition donnant les ratios v_1/v_2 des vitesses de nickellation de ligand 1 vs ligand 2. Les résultats montrent que les ligands plus nucléophiles $PC_{sp2}P$ et $PC_{sp3}P$ métallent mieux que leurs homologues POCOP. Cette constatation a été confirmée récemment par un autre groupe lors de la comparaison de la vitesse de métallation de composés POCOP et PCP de palladium.[3] Les ligands ^{iPr}(POCOP) substitués ont permis d'effectuer une corrélation de Hammett. La pente négative de la droite obtenue suggère un mécanisme de type électrophile où les substituants donneurs stabilisent la charge positive induite sur le carbone à l'approche du nickel lors de l'état de transition (Figure 9.2).

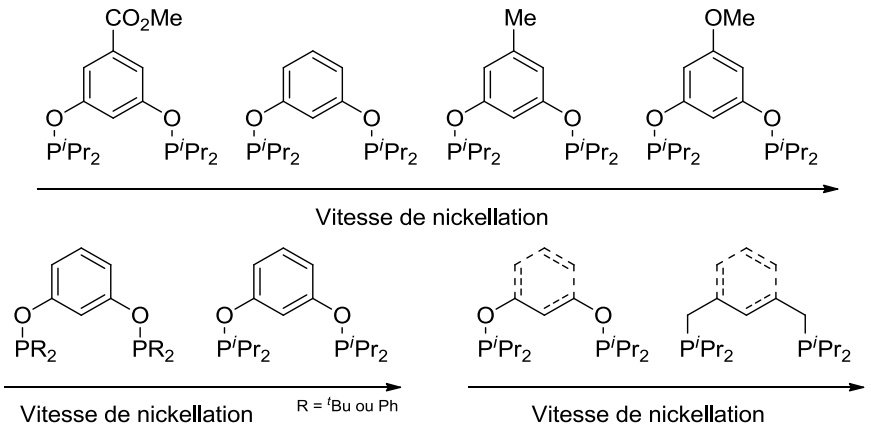

Figure 9.2 : évolution de la vitesse de nickellation en selon le ligands.

Les ligands PIMCOP possèdent des propriétés intéressantes. Tout d'abord, la dissymétrie du ligand peut être accentuée en ajoutant, après déprotonation du préligand, le 3-hydroxyphenyl-imidazole, une première phosphine sur l'imidazolate puis une seconde sur le phénolate. Ce choix de phosphine n'est pas applicable à la synthèse du ligand POCOP à partir de résorcinol, ou PCP à partir de dichlorométhaxylène. Le ligand PIMCOP est néanmoins plus long et plus couteux à synthétiser que ces ligands. En effet, à partir du 3-bromoanisole, la synthèse nécessite 3 étapes dont un couplage C-N à haute température catalysé par CuBr, et deux déprotonations par BuLi. Néanmoins le complexe PIMCOP peut subir plusieurs post dérivations pour introduire d'autres fonctions. La méthylation de l'azote donne lieu au complexe PIMIOCOP. Ce complexe phosphite-imidazoliophosphine très pauvre en électron est très fragile, car le motif phosphénium est très susceptible aux attaques nucléophiles notamment lors d'une utilisation catalytique. C'est cette constatation qui a été faite lors de son utilisation comme catalyseur pour la synthèse d'amidines. Cette caractéristique peut être utilisée pour mener facilement à la synthèse du complexe

pince de nickel de type NHCCOP comportant un carbène N-hétérocyclique. Le cation [(NHCCOP)Ni(NCCH$_3$)][OTf] synthétisé avec du triflate d'argent dans l'acétonitrile est le complexe le plus efficace pour la catalyse d'amidine. Cette bonne réactivité par rapport aux cations POCOP ou PIMCOP pourtant plus électrophiles pourrait être attribuée à une meilleure stabilité apportée par la présence du NHC (Figure 9.3).

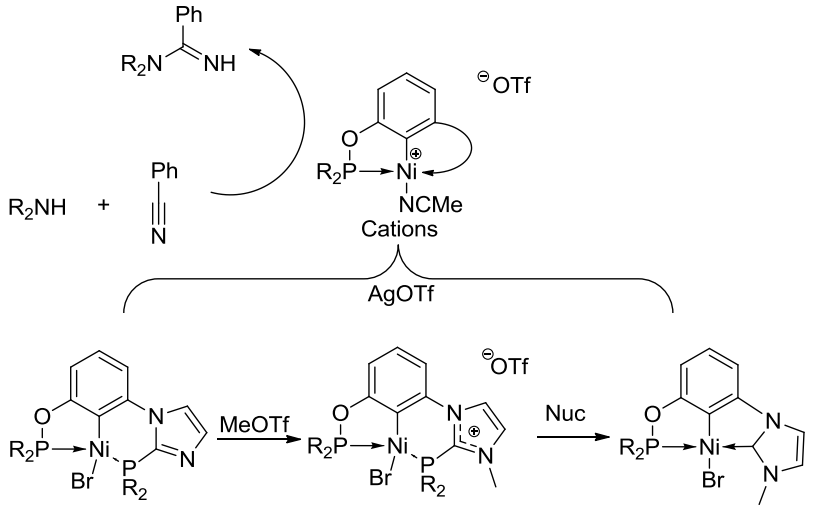

Figure 9.3 : complexes (PIMCOP)Ni(Br), (NHCCOP)Ni(Br) et (PIMIOCOP)Ni(Br) une application catalytique des cations.

Deux applications catalytiques ont été étudiées. La première concerne la fluorination à partir d'un complexe (POCOP)Ni(F) (Figure 9.4). Ce composé, qui forme facilement des liaisons hydrogène avec l'acide fluorhydrique, catalyse difficilement la fluorination du bromure de benzyle avec AgF comme source de fluorure. Il peut néanmoins réagir facilement avec le trifluorotriméthylsilane pour donner le complexe (POCOP)Ni(CF$_3$). Ce complexe réagit avec le bromure de benzyle, mais ne donne pas le trifluorométhylbenzyle espéré. À la place, un couplage entre le benzyle et des arènes non activés est observé et le complexe (POCOP)Ni(Br)

est retrouvé en fin de réaction. Plusieurs investigations ont été effectuées pour essayer de comprendre le mécanisme réactionnel. Malgré le grand intérêt de la fluorination et trifluorométhylation, le complexe POCOP n'est pas efficace pour ces réactions réputées difficiles.

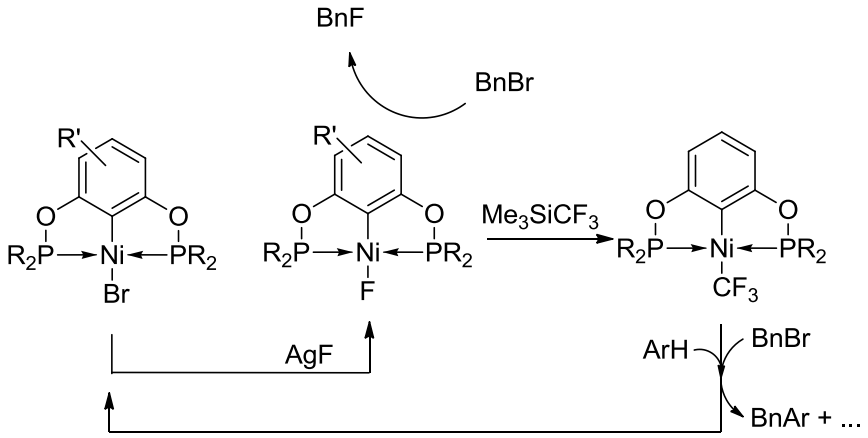

Figure 9.4 : Synthèse des complexe (POCOP)Ni(F) et (POCOP)Ni(CF_3) et réactivités avec BnBr.

La deuxième application concerne la synthèse d'amidines à partir de benzonitrile et d'amines aliphatiques (Figure 9.3). Les systèmes PIMCOP et NHCCOP développés ont démontré de meilleures performances catalytiques que le complexe POCOP. Néanmoins, les catalyseurs de nickel étudiés possèdent une réactivité limitée en comparaison des performants catalyseurs à base de lanthanides. L'utilisation de ligands plus stables et plus pauvres en électrons devraient favoriser cette réaction.

Enfin, les bonnes capacités de nickellation du précurseur $NiBr_2(NC^iPr)$ avec les ligands POCOP nous ont poussés à explorer la possibilité d'activation C-H de molécules plus petites qui possèdent un motif phosphinite. À partir de

diisopropylphénylphosphinite le chauffage du précurseur de nickel en présence de base mène à l'orthonickellation de ce ligand pour donner le dimère {Ni(μ-Br){κ^2-*P*,*C*-P^{i}Pr$_2$(OC$_6$H$_4$)}}$_2$ (Figure 9.5) L'intermédiaire *trans*-[NiBr$_2${P^{i}Pr$_2$(OC$_6$H$_5$)}$_2$] a été isolé. Le chauffer en présence de base mène à la formation du complexe cyclonickellé *trans*-Ni[(κ^2-*P*,*C*-P(OC$_6$H$_4$)-(^{i}Pr$_2$)(^{i}Pr$_2$P(OC$_6$H$_5$))]Br (Figure 9.5). Ce complexe est obtenu instantanément suite à l'addition d'un équivalent de ligand sur le dimère. On obtient le complexe dimère directement à partir du précurseur de nickel et de ligand après chauffage si le ratio (ligand) / (précurseur de nickel) ≤ 1. Si ce ratio ≥ 2 on obtiendra uniquement le complexe cyclométallé trans. Des études préliminaires ont montré que, comme il a été observé dans le cas des complexes pinces de nickel, l'étape de nickellation est favorisée avec des ligands substitués par des groupements donneurs (COOMe < Me < OMe). De plus, cette étape est défavorisée en présence d'excès de ligand. Le dimère peut réagir avec le bromure de benzyle pour mener à l'ortho-fonctionnalisation du phenol.

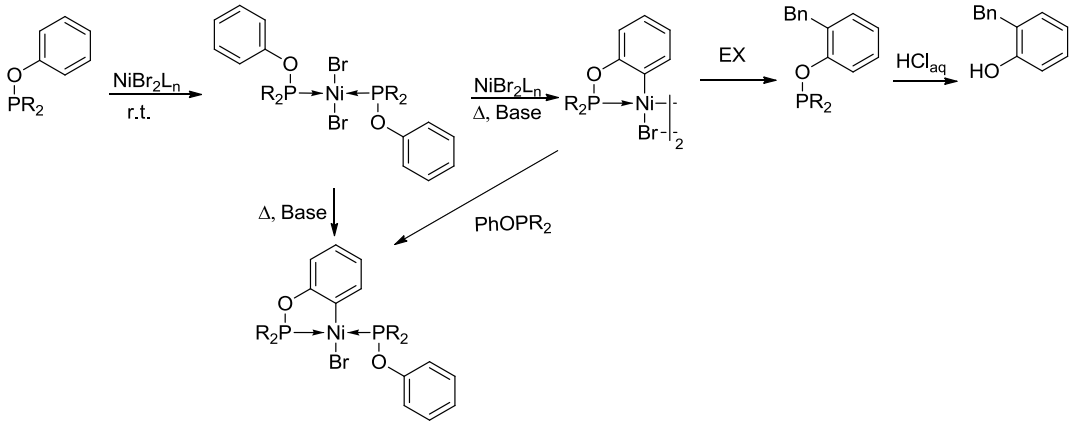

Figure 9.5 : Synthèse de complexe cyclométallés et réactivité avec le bromures de benzyle.

Ce projet possède de nombreuses perspectives. Suite à ces travaux, l'étude de nickellation par différents ligands comme $^{i}Pr_2PN(H)Ph$ a été entamée par un autre membre du groupe.[4] L'utilisation de $PhXPR_2$ (X= S, CH_2, SiR_2, etc.) comme ligand pourrait être aussi utilisée pour la suite de ce projet. Il pourrait être intéressant de métaller la 2-phénylpyridine. Les ligands comprenant un motif N-benzylimine ou benzylamine n'ont pour l'instant pas réussi à faire de cyclonickellation (Figure 9.6).[5]

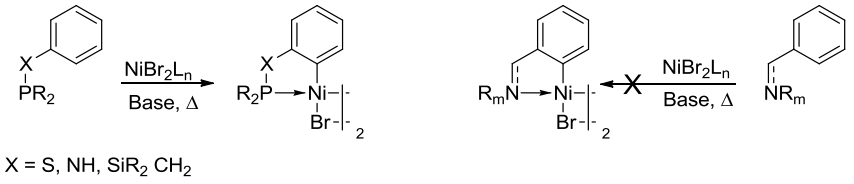

Figure 9.6 : Possibilité et échec de synthèse de complexes cyclométallés selon les ligands.

L'ortho-nickellation "one pot" à partir de nickel métallique en poudre, de phénol et de chlorodiisopropylphosphine pourrait mener à un projet futur (Figure 9.7). Plusieurs tentatives ont montré après analyse, que l'oxydation du nickel a lieu, que le ligand $P^{i}Pr_2(OC_6H_5)$ est présent en solution de même que l'intermédiaire de métallation espéré, le complexe *trans*-$[NiCl_2\{P^{i}Pr_2(OC_6H_5)\}_2]$. Ce complexe a été isolé et caractérisé par analyse élémentaire et diffraction des rayons X. Néanmoins aucune produit de cyclonickellation n'est observé. Cela pourrait être dû à la nickellation plus difficilement effectuée à partir de L_2NiCl_2. L'utilisation de $BrP^{i}Pr_2$ (éventuellement synthétisée à partir de PBr_3 et de $^{i}PrMgCl$) à la place de $ClP^{i}Pr_2$ pourrait être une solution au problème.

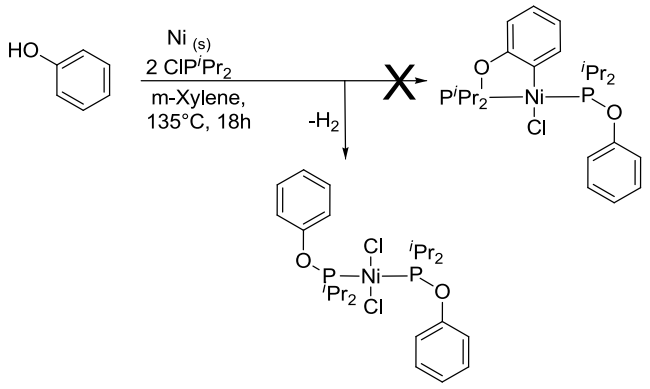

Figure 9.7 : Tentatives de cylométallation "one pot" à partir de nickel métallique.

La fonctionnalisation des ligands est très intéressante. Néanmoins, il faut savoir si cette fonctionnalisation peut être effectuée de manière catalytique à partir de ^{i}Pr$_2$POPh et d'une espèce électrophile en présence de base et de $NiBr_2L_n$ comme catalyseur (Figure 9.8). Le choix de la base s'avère crucial. En effet, elle ne doit pas réagir avec l'espèce électrophile à la température de métallation (100 °C) et ne doit pas altérer le ligand en cassant la liaison fragile P-O. Jusqu'à présent, les tentatives de fonctionnalisation catalytique ont échoué. Aucune fonctionnalisation n'a été obtenue par exemple en utilisant 10 % de $[NiBr_2(NC^iPr)]_n$ avec ^{i}Pr$_2$POPh, BnBr comme électrophile et K_2CO_3, NEt_3 ou N^{i}Pr$_2$Et (base non nucléophile) comme base dans le toluène à 100 °C pendant 17h. Une fois cette étape réussie, il faudrait pouvoir effectuer la fonctionnalisation des phénols avec une quantité catalytique de $ClPR_2$ comme cela a été fait avec l'utilisation de rhodium.[6] La fonctionnalisation catalytique utilisant des espèces électrophiles EX où X ≠ Br nécessiterait au préalable une étude sur la nickellation du ligand à partir de précurseur NiX_2 (X = Cl, I, OTf, OAc, etc.).

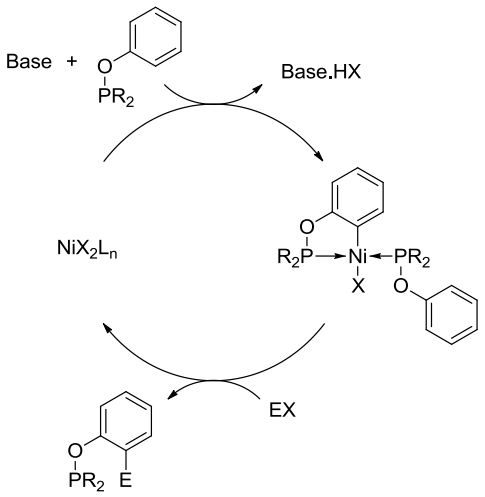

Figure 9.8 : Possibilité d'ortho-fonctionnalisation catalytique.

La littérature montre qu'il est possible d'effectuer des réactions d'insertion dans le lien C-Ni de ces complexes cyclométallés. Il est donc possible d'envisager de fonctionnaliser catalytiquement ces liens via des réactions d'insertion du CO, d'alcènes, alcynes ou autres substrats pouvant effectuer des réactions d'insertion. Le point clef de cette hypothétique catalyse serait la régénération du catalyseur.

Références

[1] Papri Bhattacharya, Jeanette A. Krause, and Hairong Guan, **2014** *communication privée*

[2] Sébastien Lapointe, **2014** *communication privée*

[3] Anderson, B. G.; Spencer, J. L. *Chem. Eur. J.* **2014**, *20*, 6421

[4] Fares Roudesly, **2014** *rapport de stage de master.*

[5] Leslie Bitard, **2013** *rapport de stage d'IUT.*

[6] Bedford, R. B.; Coles, S. J.; Hursthouse, M. B.; Limmert, M. E. *Angew. Chem. Int. Ed.* **2003**, *42*, 112